

34
S-75-14
2

US-CE-C

Property of the United States Government



TECHNICAL REPORT S-75-14

NONDESTRUCTIVE VIBRATORY TESTING OF AIRPORT PAVEMENTS

Volume I

EXPERIMENTAL TEST RESULTS AND DEVELOPMENT OF EVALUATION METHODOLOGY AND PROCEDURE

by

James L. Green and Jim W. Hall

Soils and Pavements Laboratory

U. S. Army Engineer Waterways Experiment Station

P. O. Box 631, Vicksburg, Miss. 39180

September 1975

Final Report

Approved For Public Release; Distribution Unlimited



Prepared for U. S. Department of Transportation
Federal Aviation Administration
Systems Research and Development Service
Washington, D. C. 20591

Under Inter-Agency Agreement DOT FA71WAI-218

LIBRARY BRANCH
TECHNICAL INFORMATION CENTER
US ARMY ENGINEER WATERWAYS EXPERIMENT STATION
VICKSBURG, MISSISSIPPI

| | | | |
|--|--|--|-----------|
| 1. Report No. FAA-RD-73-205-I | 2. Government Accession No. | 3. Recipient's Catalog No. | |
| 4. Title and Subtitle NONDESTRUCTIVE VIBRATORY TESTING OF AIRPORT PAVEMENTS; VOLUME I: EXPERIMENTAL TEST RESULTS AND DEVELOPMENT OF EVALUATION METHODOLOGY AND PROCEDURE | | 5. Report Date September 1975 | |
| | | 6. Performing Organization Code | |
| 7. Author(s) James L. Green, Jim W. Hall | | 8. Performing Organization Report No. Technical Report S-75-14 Volume I | |
| 9. Performing Organization Name and Address U. S. Army Engineer Waterways Experiment Station Soils and Pavements Laboratory P. O. Box 631, Vicksburg, Miss. 39180 | | 10. Work Unit No. (TRAIS) | |
| 12. Sponsoring Agency Name and Address Federal Aviation Administration Systems Research & Development Service Washington, D. C. 20591 | | 11. Contract or Grant No. DOT FA71WAI-218 | |
| | | 13. Type of Report and Period Covered Final report | |
| 14. Sponsoring Agency Code | | | |
| 15. Supplementary Notes | | | |
| 16. Abstract Conventional direct sampling methods of airport pavement evaluation interfere with aircraft operations; therefore, an evaluation procedure based on nondestructive vibratory testing was developed. The procedure considers the parameters of pavement thickness and strength, soil strength, landing gear characteristics, and load repetition through correlation of FAA direct sampling procedures with the nondestructive data form termed the dynamic stiffness modulus, which is calculated from a vibratory load-deflection graph. The results indicated the need for standardized vibratory testing equipment, and specifications for a suggested model were written. Evaluation procedures were developed for rigid and flexible pavements which consider the environmental factors of temperature and frost-thaw action, the importance of test locations and quantities, and stabilized layers. Appendix A presents results of two correlations: (a) elastic deflection and pavement performance and (b) dynamic E-modulus and CBR. Appendix B presents the nondestructive testing and performance results on U. S. Army Engineer Waterways Experiment Station test sections and the effects of bound pavement thickness on the nondestructive test results in an attempt to develop overlay design. Appendix C gives procurement specifications for recommended nondestructive test equipment. | | | |
| 17. Key Words Nondestructive testing Airport pavement evaluation Vibratory testing equipment | | 18. Distribution Statement Document is available to the public through the National Technical Information Service, Springfield, Va. 22151 | |
| 19. Security Classif. (of this report) Unclassified | 20. Security Classif. (of this page) Unclassified | 21. No. of Pages 201 | 22. Price |

W34
No. S-75-14
V. 1
Cop. 2

PREFACE .

This study was sponsored by the Federal Aviation Administration through Inter-Agency Agreement No. FA71WAI-218, "Development of Airport Pavement Criteria." This study was conducted during October 1972-November 1973 under the general supervision of Mr. James P. Sale, Chief of the Soils and Pavements Laboratory, of the U. S. Army Engineer Waterways Experiment Station (WES). This report was prepared by Messrs. James L. Green and Jim W. Hall.

Directors of WES during the conduct of the investigation and the preparation of this report were BG E. D. Peixotto, CE, and COL G. H. Hilt, CE. Technical Director was Mr. F. R. Brown.

TABLE OF CONTENTS

| | |
|--|-----|
| INTRODUCTION | 13 |
| BACKGROUND | 13 |
| PURPOSES | 17 |
| SCOPE | 18 |
| SELECTION OF EQUIPMENT | 21 |
| DESCRIPTION OF VIBRATORS | 21 |
| VIBRATOR COMPARISONS BASED ON FIELD TESTS | 30 |
| FACTORS AFFECTING VIBRATORY TESTS RESULTS | 36 |
| ACCURACY TESTS WITH 16-KIP VIBRATOR | 55 |
| RECOMMENDED NONDESTRUCTIVE TESTING EQUIPMENT | 65 |
| DEVELOPMENT OF THE EVALUATION METHODOLOGY | 67 |
| TESTS CONDUCTED | 67 |
| NONDESTRUCTIVE EVALUATION METHODOLOGY | 90 |
| NONDESTRUCTIVE EVALUATION PROCEDURE | 121 |
| NONDESTRUCTIVE TESTING EQUIPMENT | 121 |
| DATA COLLECTION | 121 |
| SELECTION OF TEST LOCATIONS | 124 |
| CORRECTIONS TO DSM VALUES | 126 |
| DETERMINATION OF ALLOWABLE AIRCRAFT LOADING | 128 |
| REDUCTION OF CAPACITY OF DISTRESSED PAVEMENTS | 135 |
| MONITORING ACCURACY OF VIBRATOR MEASUREMENTS | 138 |
| CONCLUSIONS AND RECOMMENDATIONS | 140 |
| APPENDIX A: DEFLECTION-PERFORMANCE RELATIONSHIPS AND CORRELATIONS BETWEEN DYNAMIC E-MODULUS AND CBR | 143 |
| DEFLECTION-PERFORMANCE RELATIONSHIPS | 143 |
| CORRELATIONS BETWEEN DYNAMIC E-MODULUS AND CBR | 143 |
| APPENDIX B: RELATED NONDESTRUCTIVE DATA | 148 |
| PAVEMENT PERFORMANCE STUDY | 148 |
| EFFECT OF BOUND PAVEMENT ELEMENT THICKNESS ON DSM | 150 |
| APPENDIX C: EQUIPMENT SPECIFICATIONS | 171 |
| INTRODUCTION | 171 |
| SPECIFICATIONS | 172 |
| ESTIMATED COSTS | 179 |
| SPECIFICATIONS FOR TRACTOR-TRUCK UNIT AND SEMITRAILER | 179 |
| SPECIFICATIONS FOR VIBRATION UNIT AND POWER SUPPLIES | 182 |
| SPECIFICATIONS FOR INSTRUMENTATION FOR LOAD-DEFLECTION TESTS | 189 |
| SPECIFICATIONS FOR INSTRUMENTATION FOR WAVE VELOCITY MEASUREMENTS | 199 |
| REFERENCES | 202 |

FIGURES

| | | |
|-----|--|----|
| 1. | 9-kip vibrator | 24 |
| 2. | Counterrotating masses in 9-kip vibrator | 24 |
| 3. | 16-kip vibrator | 25 |
| 4. | Electronic equipment in 16-kip vibrator | 26 |
| 5. | 50-kip vibrator | 27 |
| 6. | CERF NDPT van | 28 |
| 7. | Dynalect with cover removed | 29 |
| 8. | Model 400 Road Rater | 31 |
| 9. | Model 505 Road Rater | 31 |
| 10. | DSM of 16-kip vibrator versus DSM of 9-kip vibrator | 32 |
| 11. | DSM of 16-kip vibrator versus DSM of CERF NDPT van | 32 |
| 12. | DSM of 16-kip vibrator versus DSM of Dynalect | 33 |
| 13. | DSM of 16-kip vibrator versus DSM of Model 505 Road Rater | 34 |
| 14. | Load versus time relationships for loading conditions beneath the 16-kip vibrator | 38 |
| 15. | DSM values versus vibrator preload (items 2-5 of flexible pavement test section) | 38 |
| 16. | Vibrator preload versus DSM expressed as a percent of DSM obtained with a 5-kip vibrator preload (items 2-5 of flexible pavement test section) | 40 |
| 17. | Deflection versus load (Philadelphia International Airport, line R7A, point No. 2) | 41 |
| 18. | Deflection versus load (Philadelphia International Airport, line R11A, point No. 1) | 42 |
| 19. | Deflection versus load (Philadelphia International Airport, line A7A, point No. 4) | 43 |
| 20. | Deflection versus load (Philadelphia International Airport, line A8A, point No. 1) | 44 |
| 21. | Deflection versus load (Philadelphia International Airport, line A8A, point No. 6) | 45 |
| 22. | Typical load-deflection curves for frequencies of 10, 15, and 40 Hz | 46 |
| 23. | Deflection versus frequency for flexible pavements | 49 |
| 24. | Deflection versus frequency for rigid pavements | 50 |
| 25. | Output versus frequency from velocity transducer No. 101 (input is a constant amplitude of deflection) | 53 |
| 26. | Load plate diameter versus DSM on WES temperature effects test section | 53 |
| 27. | Plan and section of the WES temperature effects test section | 54 |
| 28. | View of load plate, load cells, and velocity transducers of 16-kip vibrator | 56 |
| 29. | Measured peak deflection versus known input peak deflection | 60 |
| 30. | Percent error versus average deflection | 61 |
| 31. | Pavement temperatures | 71 |
| 32. | DSM versus mean pavement temperature | 72 |
| 33. | Mean flexible pavement temperatures at Washington-Baltimore International Airport, Baltimore, Md. | 73 |

FIGURES (Continued)

| | | |
|-----|---|-----|
| 34. | DSM temperature adjustment curves | 75 |
| 35. | Prediction of flexible pavement temperatures | 78 |
| 36. | DSM values versus time for five test sites at Truax Field, Madison, Wis. | 84 |
| 37. | DSM versus distance from joint for slabs N-F and N-N at NAFEC | 87 |
| 38. | DSM versus distance from joint for slabs H-1 and H-2 at Houston | 88 |
| 39. | DSM versus distance from joint for slabs J-1, J-2, J-3, and J-4 at Jackson | 89 |
| 40. | DSM versus distance from center line for old runway 9-27 and taxiway A at Philadelphia | 91 |
| 41. | DSM versus allowable single-wheel load for flexible pavement . . . | 93 |
| 42. | ESWL curves for dual-wheel aircraft on flexible pavement . . . | 94 |
| 43. | ESWL curves for dual-tandem aircraft on flexible pavement . . . | 95 |
| 44. | ESWL curves for wide-bodied jet aircraft on flexible pavement | 96 |
| 45. | Load repetition factors versus total departures | 98 |
| 46. | CBR/p versus $t/\alpha\sqrt{A}$ | 100 |
| 47. | F_t versus SSF/S_p | 103 |
| 48. | DSM versus allowable singel-wheel load on rigid pavement . . . | 111 |
| 49. | F versus l for single-wheel aircraft on rigid pavement . . . | 112 |
| 50. | F versus l for dual-wheel aircraft on rigid pavement . . . | 112 |
| 51. | F versus l for dual-tandem aircraft on rigid pavement . . . | 113 |
| 52. | F versus l for various commercial jet aircraft on rigid pavement | 113 |
| 53. | F_f versus subbase thickness and soil groups | 115 |
| 54. | Approximate interrelationships of soil classifications and bearing values | 116 |
| 55. | Effect of stabilized layer on pavement stiffness | 120 |
| 56. | Deflection versus load (sample plot) | 123 |
| 57. | Evaluation curve for flexible pavement | 130 |
| 58. | Evaluation curve for rigid pavement | 134 |
| A1. | Elastic deflection versus coverages to failure for single- and multiple-wheel loads based on combined highway and airfield data | 145 |
| A2. | Dynamic E-modulus versus CBR (WES correlation) | 147 |
| A3. | Dynamic E-modulus versus CBR (comparison of Shell and WES correlations) | 147 |
| B1. | Plan and section of WES soil stabilization test section (flexible pavement) | 161 |
| B2. | Plan and section of WES soil stabilization test section (rigid pavement) | 162 |
| B3. | DSM test locations and pavment sections for Philadelphia International Airport | 163 |

FIGURES (Continued)

| | | |
|------|--|-----|
| B4. | DSM versus bituminous pavement section thickness at Philadelphia International Airport | 164 |
| B5. | DSM versus asphaltic pavement section thickness for the WES temperature effects test section | 165 |
| B6. | Pavement cross section of taxiway T-3 at Biggs Army Airfield | 166 |
| B7. | DSM versus PCC pavement section thickness for Biggs Army Airfield | 167 |
| B8. | DSM test locations at Shreveport Regional Airport | 168 |
| B9. | Pavement sections before overlay at Shreveport Regional Airport | 169 |
| B10. | Flexible overlay thickness and plots of DSM versus time for Shreveport Regional Airport | 170 |
| C1. | Truck-trailer unit with details of actuator system | 173 |
| C2. | Block diagram of the NDT process using a dynamic load-deflection response | 176 |
| C3. | Block diagram of equipment for wave-propagation measurements | 178 |

TABLES

| | | |
|-----|--|-----|
| 1. | Vibrator Characteristics | 23 |
| 2. | Vibrator Preload (Static Weight) and DSM (50-Kip Vibrator) . . | 39 |
| 3. | Variations in Computed DSM Values | 47 |
| 4. | Physical Properties of Flexible Pavements | 51 |
| 5. | Physical Properties of Rigid Pavements | 52 |
| 6. | Accuracy Test of 16-Kip Vibrator DAS | 58 |
| 7. | Deflection Measurements with Velocity Transducers at Equal Distances from Load Plate | 59 |
| 8. | Deflection Measurements and E_{90} | 63 |
| 9. | Outline of Nondestructive Tests | 69 |
| 10. | 5-Day Mean Air Temperatures at Flexible Pavement Facilities . | 76 |
| 11. | Pavement Temperature for Flexible Pavement Facilities | 77 |
| 12. | Temperature Adjustment of DSM Data | 80 |
| 13. | Pavement and Subgrade Data at Truax Field Test Sites | 81 |
| 14. | Results of DSM Measurements on PCC Test Sites | 82 |
| 15. | Results of DSM Measurements on AC Test Sites | 83 |
| 16. | Load Repetition Factors for Flexible and Rigid Pavements . . . | 99 |
| 17. | Summary Listing of Materials and Equivalency Factors | 104 |
| 18. | Equivalent Conventional Flexible Pavement Thicknesses | 107 |
| 19. | Tabulation of DSM Values (Example), Airport, USA | 125 |
| 20. | Aircraft Tire Contact Areas and Total Number of Main Gear Wheels | 132 |
| 21. | Expected Change in DSM on or near a Distressed Area of Flexible Pavement Compared with DSM on a Similar Area in Good Condition | 136 |

TABLES (Continued)

| | | |
|-----|---|-----|
| 22. | Expected Change in DSM on Distressed Slabs of Rigid Pavement Compared with DSM on Similar Slabs in Good Condition | 137 |
| B1. | Summary of DSM Values at 15 Hz and Coverages to Failure for the Flexible Pavement Test Section | 153 |
| B2. | DSM at 15 Hz Before and After Traffic for the Flexible Pavement Test Section | 154 |
| B3. | Summary of Field Test Data on Flexible Pavement Test Section . | 155 |
| B4. | DSM Values at 15 Hz and Coverages to Failure for Rigid Pavement Test Section | 156 |
| B5. | Summary of Field Test Data on Rigid Pavement Test Section . . | 157 |
| B6. | DSM Values and Bituminous Pavement Thicknesses at Philadelphia International Airport | 158 |
| B7. | DSM Values Before and After Overlay at Shreveport Regional Airport | 159 |
| B8. | Average Thickness and DSM Values for Shreveport Regional Airport Overlay | 160 |

LIST OF ABBREVIATIONS AND SYMBOLS

| | |
|----------|---|
| A | Tire contact area, sq in. |
| C_p | Numerical constant used in computing E_{90} |
| CBR | Measurement of soil strength |
| d | Peak deflection, in. |
| DSM | Dynamic stiffness modulus: the inverse of the slope of a load versus deflection plot, kips/in. |
| E | Modulus of elasticity, psi |
| E_p | Percent error |
| E_{90} | Limiting error for 90 percent of the errors (90 percent error), in. |
| ESWL | Equivalent single-wheel load: The load on a single wheel that produces stresses or deflection equal to those produced beneath a multiple-wheel assembly |
| %ESWL | Percent ESWL for the controlling number of wheels of the aircraft for which the evaluation is being made |
| f | Vibrator frequency, Hz |
| F | Load factor |
| F_d | Vibratory load, kips |
| F_f | Foundation strength factor |
| F_s | Vibrator static weight, kips |
| F_t | Factor computed from S_p and t |
| g | Acceleration due to gravity, 32.2 ft/sec ² |
| h | Thickness of the concrete slab, in. |
| k | Modulus of subgrade reaction, pci |
| l | Radius of relative stiffness, in. |
| n | Number of measurements or errors |
| p | Single-wheel or equivalent single-wheel tire contact pressure, psi |
| P_G | Allowable gross aircraft load |
| r | Relative change in pavement stiffness |
| S_p | Pavement system strength index |

| | |
|-----------|---|
| SSF | Subgrade strength factor |
| t | Flexible pavement structure thickness above the subgrade, in. |
| v | Error in deflection (difference from the average deflection of measured deflection), in. |
| V | Wave velocity, in./sec |
| W_c | Number of controlling wheels used to determine %ESWL |
| W_m | Total number of wheels on all main gears of the aircraft for which the evaluation is being made |
| X_{p1} | Known input deflection (from the calibrated shake table), in. |
| X_{p2} | Measured deflection (from a velocity transducer), in. |
| α | Load repetition factor |
| γ | Wet density of material, pcf |
| λ | Wavelength, ft |
| ν | Poisson's ratio |
| ρ | Mass density ($\gamma \div g$) |

CONVERSION FACTORS, U. S. CUSTOMARY TO METRIC (SI)
UNITS OF MEASUREMENT

U. S. customary units of measurement used in this report can be converted to metric (SI) units as follows:

| <u>Multiply</u> | <u>By</u> | <u>To Obtain</u> |
|--------------------------------------|------------|-----------------------------------|
| inches | 2.54 | centimetres |
| feet | 0.3048 | metres |
| square inches | 6.4516 | square centimetres |
| gallons (U. S. liquid) | 3.785412 | cubic decimetres |
| gallons (U. S. liquid) per minute | 3.785412 | cubic decimetres per minute |
| ounces (mass) | 0.02834952 | kilograms |
| pounds (mass) | 0.45359237 | kilograms |
| kips (mass) | 0.45359237 | metric tons |
| pounds per cubic inch | 0.0276799 | kilograms per cubic centimetre |
| pounds per cubic foot | 16.01849 | kilograms per cubic metre |
| pounds (force) | 4.448222 | newtons |
| kips (force) | 4.448222 | kilonewtons |
| pounds per inch | 1.7512685 | newtons per centimetre |
| pound-feet | 1.355818 | newton-metres |
| kips per inch | 1.7512685 | kilonewtons per centimetre |
| pounds (force) per square inch | 0.6894757 | newtons per square centimetre |
| inches per second | 2.54 | centimetres per second |
| miles (U. S. statute) per hour | 1.609344 | kilometres per hour |
| inches per second per second | 0.0254 | metres per second per second |
| feet per second per second | 0.3048 | metres per second per second |

(Continued)

CONVERSION FACTORS, U. S. CUSTOMARY TO METRIC (SI)
UNITS OF MEASUREMENT (CONCLUDED)

| <u>Multiply</u> | <u>By</u> | <u>To Obtain</u> |
|--------------------|------------|--------------------------------|
| horsepower | 745.6999 | watts |
| degrees (angle) | 0.01745329 | radians |
| Fahrenheit degrees | 5/9 | Celsius degrees or Kelvins* |

* To obtain Celsius (C) temperature readings from Fahrenheit (F) readings, use the following formula: $C = (5/9)(F - 32)$. To obtain Kelvin (K) readings, use: $K = (5/9)(F - 32) + 273.15$.

INTRODUCTION

BACKGROUND

Currently accepted methods for evaluating the load-carrying capacity of airport pavements require direct sampling techniques that are both costly and time-consuming. Often, direct sampling requires the closing of a pavement facility to traffic operations, which in turn necessitates the rerouting and/or rescheduling of aircraft. With the rapid increases in traffic operations, closing a pavement facility, even briefly, can result in inconvenience to the traveler and higher costs to the air carrier. Also, increasing aircraft loads make accurate and frequent evaluations of pavements extremely important to the airport owner since many facilities will need strengthening or rehabilitation to meet this increased demand. These considerations dictate the need for a procedure that permits rapid evaluation with a minimum of disturbance to normal traffic operations. The use of nondestructive testing techniques to determine the pertinent characteristics of pavements offers the best promise of serving this need.

Presently, there are three basic nondestructive testing techniques under study. These are:

- a. The use of steady state vibratory loadings and wave propagation measurements to determine the thicknesses and physical constants of the pavement, which can be used in a multi-layered analysis to predict allowable loadings.
- b. The use of steady state vibratory loadings and measurements of the resulting elastic deflections to determine a dynamic stiffness modulus (DSM*) of the pavement, which can be correlated with pavement performance.
- c. The use of a theoretical approach based upon the amount of energy that a pavement can absorb versus the amount of energy imparted to the pavement by aircraft traffic.

Procedures a and b have been the subject of considerable study, whereas procedure c is a more recent development.

* For convenience, symbols and unusual abbreviations are listed and defined on page 9.

Vibratory testing of materials was begun as early as 1933 by the German Research Society for Soil Mechanics and was further developed by the Royal Dutch Shell Laboratory and the Transport and Road Research Laboratory in the United Kingdom. Most of the early vibratory equipment consisted of counterrotating eccentric masses arranged to produce vertical loadings. This equipment could be used to vary the vertical load and frequency, but these parameters could not be independently varied. More recently, electrohydraulic and electromagnetic vibrators have been developed and used, both of which can apply constant loads at variable frequencies.

The U. S. Army Engineer Waterways Experiment Station (WES) commenced vibratory testing of pavements in search of nondestructive evaluation procedures in cooperation with Shell researchers in the mid-1950's. These early tests by WES followed the procedures used by Shell researchers. The results of these early studies have been reported by Heukelom and Foster¹ and by Maxwell.^{2,3} Tests with the Shell vibrator on pavement test sections at WES and at several military airfields indicated that DSM values of the test sections determined from the load-deflection relations could be correlated with pavement performance. Meanwhile, tests to obtain wave propagation measurements in pavements were being conducted at the American Association of State Highway Officials Road Test,⁴ at Foss Field,⁵ and on several other military airfields and roadways. Data collected from these have been used to develop the correlation between modulus of elasticity E and CBR (California Bearing Ratio) shown in Appendix A. Wave propagation tests were also used to measure changes in the strength with time of lime- and cement-stabilized subgrades at Randolph Air Force Base (AFB).⁶

The use of the deflection* of a loaded pavement surface to predict performance has long been an attractive evaluation concept because

* The term "deflection" is used herein to describe the downward movement of a pavement surface as a result of vibratory loading. This movement is frequently termed "displacement," the accepted definition for which is the difference between the initial position of a body and any later position.

of the simplicity of such measurements. Surface deflection due to loading has generally been accepted as an indicator of pavement performance, particularly for flexible pavements.* However, it has been found through tests of full-scale pavement test sections that deflection is not a good indicator of the remaining life (or effects of past traffic) of either flexible or rigid pavements since there seems to be little or no increase in deflection until failure occurs. An example of the relationship between deflection and flexible pavement performance developed from various studies is presented in Appendix A.⁷ Similar relationships have been developed independently by the California Division of Highways⁸ and the Transport and Road Research Laboratory.⁹ Although these relationships have not been used directly in the development of the evaluation methodology discussed herein, they are presented to illustrate that deflection is at least an indicator of pavement performance.

A literature review of nondestructive evaluation techniques¹⁰ conducted in 1967 suggested that deflections caused by vibratory loadings on pavements could be used in an evaluation procedure if properly correlated with performance data and existing direct sampling techniques. Thus, during the WES full-scale multiple-wheel heavy gear load study conducted during 1969-1970 to validate pavement design, vibratory equipment was used to monitor the performance of the pavement test sections. Tests to determine load-deflection relations (DSM values) and wave propagation were conducted periodically during this study. An analysis of the results showed that the DSM values correlated well with the performance data. However, the wave propagation results were erratic, with the computed modulus of elasticity E of the subgrade material varying

* Pavements are categorized in three ways for this report: flexible, rigid, or composite. "Flexible" pavements are those which have layers of bituminous material (usually asphaltic concrete (AC)) overlying layers of base and subbase materials. "Rigid" pavements are those which have a layer of portland cement concrete (PCC) on a base and/or subgrade. Other pavements, such as combinations of AC and PCC or various reinforcements of the layers of either flexible or rigid pavements, are termed "composite" pavements.

apparently as a function of the overburden pressures exhibited by the different pavement thicknesses. Results of these tests were published in 1972.¹¹ The correlation between DSM values and pavement performance encouraged continued work in this area at existing military airfields.

Further studies of the correlation between DSM and pavement performance were conducted at military airfields by applying vibratory loadings and comparing the resulting DSM with allowable loadings determined using existing evaluation criteria.¹² The material properties of the pavements studied were determined either from direct sampling or from data in design and construction control records. A 9-kip* counterrotating eccentric mass vibrator developed at WES was used for these tests. (This vibrator can apply a peak vibratory loading of 8,000 lb and has a frequency range of 5 to 60 Hz.) Analysis of these results indicated that the load-deflection relations of the pavements (especially the flexible pavements) were nonlinear but tended to become more linear with increasing magnitudes of applied load. Furthermore, with the heavier applied loads, the response seemed to be indicative of the entire depth of pavement, whereas with the lighter loads the response appeared to be greatly influenced by the upper layers of generally higher quality materials. Instrumented test sections were used to record deflection and pressure at various depths to 12 ft under vibrator loadings of the 9-kip vibrator. These tests led to the conclusion that the applied vibratory loading should be greater than that produced by the 9-kip vibrator. A 16-kip vibrator was then constructed to produce peak vibratory loadings up to 15,000 lb at frequencies ranging from 5 to 100 Hz, thus producing a combined static plus peak dynamic load of 31 kips, approximately equal to one wheel load of the C-5A aircraft.

In addition to the 9- and 16-kip vibrators used by WES, other vibrators, both electrohydraulic and electromagnetic, have been developed and used by various agencies. These vibrators produce peak vibratory loads from 500 to 5000 lb. Each of these vibrators has been

* A table of factors for converting U. S. customary units of measurement to metric (SI) units is presented on page 11.

of some use in the overall attempt to develop nondestructive evaluation procedures; however, no universally accepted methodology has emerged, primarily because of the problem in correlating pavement response and pavement performance. The fact that the nonlinear load-response relations of pavements are not fully understood is probably one of the major obstacles to the development of a satisfactory nondestructive evaluation methodology.

In 1972, the Federal Aviation Administration (FAA) initiated the study reported herein to develop within 2 yr a workable nondestructive evaluation procedure for airport pavements. Based upon the available data, the use of the DSM-pavement performance method was selected as the most applicable procedure to be developed in this period, with major emphasis to be placed on improving the DSM versus allowable loading correlation. Work on the development of the other two basic approaches to nondestructive evaluation of pavements by several agencies including WES has continued; however, as yet, neither of these has been developed to an acceptable confidence level.

The DSM-pavement performance approach required direct correlation between the nondestructive DSM test results and the allowable loadings of pavements as determined by existing FAA evaluation methods.

The existing pavement design and evaluation methods for flexible and rigid pavements were developed from numerous performance tests, theories, and studies¹³⁻⁴⁰ beginning in 1926 for rigid pavements with the Westergaard analysis and in 1947 for flexible pavements with full-scale test pavements using actual aircraft loadings. The procedures that resulted from the study and interpretation of these performance tests have been used to design and evaluate several hundred military airfield pavements throughout the world and are documented in numerous reports. The evaluation results have been checked against actual performance and the procedure refined through review of continuing condition survey programs.

PURPOSES

The primary purposes of this study were to select equipment for

nondestructive testing of pavements, to develop a methodology for evaluating the load-carrying capacity of pavements using the selected equipment, and to write an evaluation procedure based on this methodology.

Specific objectives of the study were to:

- a. Study the characteristics of available nondestructive testing equipment for determining the load-deflection (DSM) relations of pavements and provide complete procurement specifications for the recommended equipment.
- b. Develop correlations between the load-deflection relations and existing pavement performance data as a basic methodology for nondestructive evaluation.
- c. Develop from this methodology a step-by-step evaluation procedure for flexible and rigid airport pavements.
- d. Generate other data, as applicable, for use in validation, refinement, and expansion of the three basic types of non-destructive data (i.e., wave propagation measurements, deflection basin measurements, and frequency responses of the pavements).

SCOPE

Maximum advantage was taken of the equipment and data generated during the several years of previous investigation. Results of previous tests indicated the need to concentrate on the concept of correlating the load-deflection relations with pavement performance as determined from accepted direct sampling evaluation procedures if a nondestructive evaluation procedure having an acceptable confidence level was to be developed in the 2-yr period. Previous results also indicated the non-linearity of the load-deflection relations and pointed to the need for standardization of both test equipment and test procedures. Thus, with experience gained in the previous studies and available equipment, it was possible to initiate the data collection phase immediately with confidence that the data collected would be useful.

The first objective of this study was to select and prepare procurement specifications for recommended nondestructive testing equipment. Because previous studies had shown that the most useful type of equipment would be that employing steady state vibratory loadings, the study was limited to an investigation of this type of equipment. Comparative

tests were performed on a range of pavements with each type of vibrator available. Since it was impractical to use each available vibrator on each test pavement for comparison, the performance of each vibrator was correlated with that of the WES 16-kip vibrator. Tests were also performed to study the effects of vibrator static weight, peak vibratory load, method of application of the vibratory load to the pavement (including load plate type and size), frequency of loading, and mobility and ease of operation of the recommended equipment. Performance requirements were selected and procurement specifications prepared based on these evaluations.

The most important phase of the study to develop the evaluation methodology and thereby the evaluation procedure was the development of correlations between the nondestructive test results and the evaluation of the load-carrying capacities of the pavement by direct sampling procedures. Available pavement performance data from full-scale accelerated traffic tests and condition surveys of airports conducted over a 30-yr period were used in this phase of the study. The correlation was made by performing both nondestructive and direct sampling tests at the same locations on several airport pavements representing a range of pavement conditions. The nondestructive test data collected included DSM values, deflections for frequency sweeps from 5 to 100 Hz, deflection basin measurements, and wave propagation data. Direct sampling data collected included the thicknesses of all layers of material comprising the pavement, foundation strength values (CBR or modulus of subgrade reaction k values), concrete flexural strengths, and material classifications. Data used in the analysis and development of the nondestructive evaluation methodology are summarized and tabulated in this report. Other data collected which were applicable to other methods of nondestructive evaluation are presented in Appendix B.

Important to any nondestructive evaluation procedure is the ability to assess adequately the various parameters which affect nondestructive test measurements. Typical parameters are: (a) temperature of bituminous materials, (b) warping or curling of concrete due to temperature or moisture gradients, (c) changes in moisture conditions in

the subgrade materials, and (d) freezing and thawing of the pavement and subgrade materials. Limited tests were conducted to demonstrate the effects of some of these parameters and to develop correction factors; however, the scope of the study was not sufficiently large to include proper assessment of the effects of all of these parameters.

Similarly, the effects of chemical stabilization of layers of materials, strengthening of existing pavements with either similar or nonsimilar materials (such as bituminous overlays of concrete pavements), and reinforcing concrete pavements by various methods were considered in the development of the methodology but could not be properly assessed within the time and funding constraints of the study.

SELECTION OF EQUIPMENT

The convenience and desirability of nondestructive pavement evaluation have led to the development of several types of nondestructive testing devices capable of measuring load-deflection responses of pavements. However, since the characteristics of these devices vary, different measurements on the same test site can be expected from each. Therefore, meeting the first objective of this study involved determining the characteristics of various available vibratory devices and performing comparison tests with each device to determine if a standard vibrator was necessary for the evaluation procedure presented in this report.

The 16-kip vibrator was selected as the standard vibrator for the comparison tests because it was readily available and it had been developed to produce a range of loadings including the largest vibratory load possible with any of the transportable equipment. A large vibratory load is preferred in nondestructive testing for two reasons: (a) the vibrator should affect the pavement layers to the same significant depth as large present-day aircraft loads, and (b) measurements of large deflections are easier and require less sensitive equipment than do measurements of small deflections. In addition, the 16-kip vibrator has independently variable load and frequency settings and is capable of making deflection basin measurements.

The comparison tests consisted primarily of load-deflection tests of existing airport pavements; however, other types of tests such as wave velocity and deflection basin measurements were made, depending upon the capability of each vibrator. A study of other variables such as the effects of vibrator static weight, peak vibratory load, method of loading (including plate size and type), and frequency of loading was also made using the 16-kip vibrator and a special 50-kip vibrator.

DESCRIPTION OF VIBRATORS

Of the six vibratory testing devices used to collect data for this study, three were built by WES. Two of these are referred to by

their static weights, 9 and 16 kips.* The third, which has negligible static weight, is referred to by the maximum preload that it can apply to a pavement, 50 kips. The Civil Engineering Research Facility (CERF) under contract to the Air Force Weapons Laboratory developed a fourth vibrator referred to as the nondestructive pavement test (NDPT) van. The other two vibrators, the Dynaflect and the Road Rater, are available commercially. There are five models of the Road Rater, but specifications and performance data from only one, the Model 505, were available for this study. Table 1 shows the maximum peak vibratory load, static weight, load plate diameter, and frequency range of operation of each vibrator. All of the vibrators are mobile except the WES 50-kip model.

9-KIP VIBRATOR

The 9-kip vibrator is a counterrotating eccentric mass machine capable of generating an 8000-lb vibratory load within a frequency range of 5 to 60 Hz. It has a 9-kip static weight and is mounted in a trailer with a gross weight of 15 kips. This vibrator is equipped with load cells and velocity transducers and applies the load with a 19-in.-diam plate. Test results can be recorded on equipment in the 16-kip vibrator van or on a portable field package that records data on light-sensitive paper, from which data must be reduced manually. The 9-kip vibrator produces load versus deflection plots at variable frequencies, i.e., the load is changed by changing the frequency. A view of this machine is shown in Figure 1. A closeup of the counterrotating masses is shown in Figure 2.

16-KIP VIBRATOR

The 16-kip vibrator, which is an experimental prototype model, operates electrohydraulically and is housed in a 36-ft semitrailer that contains supporting power supplies and automatic data recording systems.

* The term "static weight" is used in this report to denote the weight of the entire mass which is vibrated to produce a vibratory load. The term "vibratory load" denotes the dynamic load applied by the vibrator to the pavement. This vibratory load produces a "dynamic force" within the pavement system.

Table 1

Vibrator Characteristics

| Vibrator Name | Type of Operation | Maximum Peak Vibratory Load kips | Static Weight of Vibrator kips | Diameter of Load Plate in. | Frequency Range of Operation Hz |
|----------------------|-----------------------|----------------------------------|--------------------------------|--|---------------------------------|
| 9-kip | Counterrotating | 8.0* | 9.0 | 19 | 5 to 60** |
| 16-kip | Electrohydraulic | 15.0 | 16.0 | 18 | 5 to 100 |
| 50-kip | Electrohydraulic | 25.0 | --† | 18 | 1 to 200 |
| CERF NDPT van | Electromagnetic | 5.0 | 6.75 | 12 | 10 to 5000 |
| Dynalect | Counterrotating | 0.5* | 1.6†† | --‡ | 8 |
| Road Rater Model 400 | Electrohydraulic ↓ | 0.75 | 0.16 | Two rectangular steel pads, 4 by 7 in., spaced 6 in. apart. Sensor spaced between pads | 10, 20, 25, 30, 40‡‡ |
| 505 | | 0.75 | 0.16 | | 10, 20, 25, 30, 40‡‡ |
| 510 | | 1.5 | 0.32 | | 10, 20, 25, 30, 40‡‡ |
| 550§ | | -- | -- | | -- |
| 600 | | 2.5 | 2.5 | | 5 to 60 |

* The vibratory load is generated by unbalanced flywheels rotating in opposite directions. The 9-kip vibrator has two pairs of flywheels; the Dynalect has one pair.

** The vibratory load is changed by changing the frequency.

† This device has negligible static weight. It applies a preload (comparable to static weight of a vibrator) that can be varied up to 50 kips by jacking a hydraulic loading mechanism against a reaction beam.

†† Static weight of entire apparatus.

‡ Contact with ground is through two 16-in.-OD steel wheels spaced 20 in. center to center.

‡‡ This frequency range of operation is for the standard model. Vibrators can be ordered that have a variable frequency of operation.

§ This model has been discontinued.



Figure 1. 9-kip vibrator

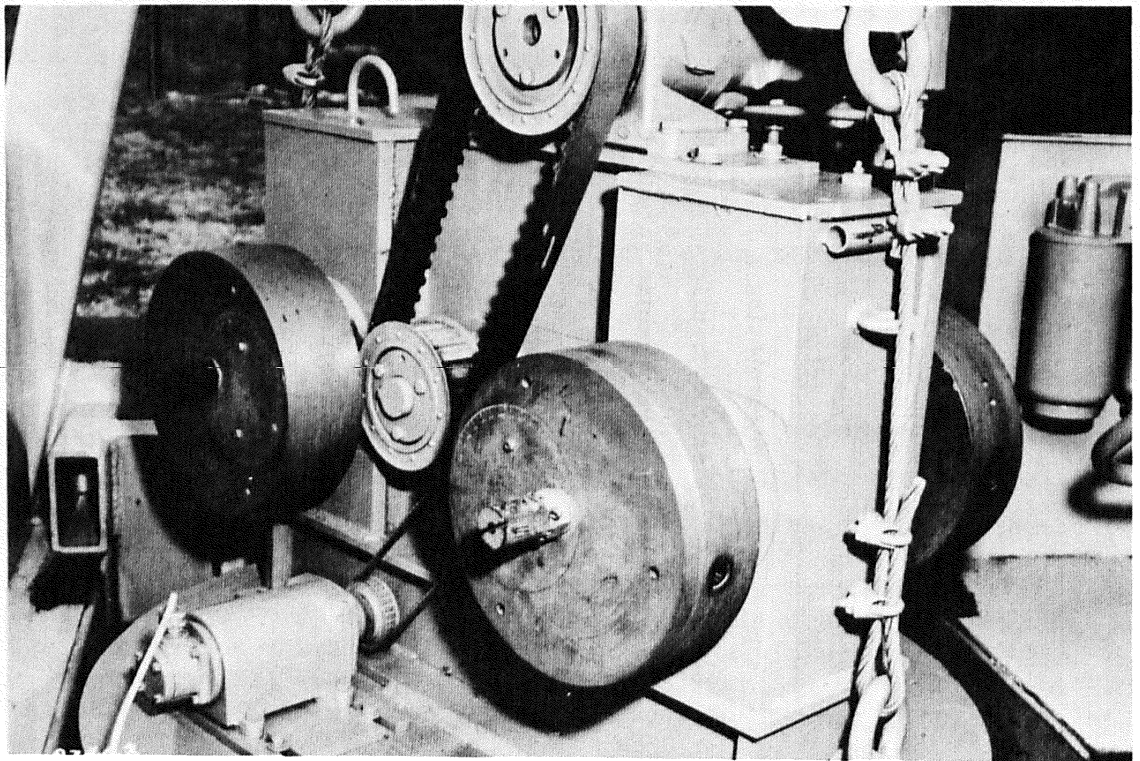


Figure 2. Counterrotating masses in 9-kip vibrator

The vibrator mass assembly consists of an electrohydraulic actuator surrounded by a 16,000-lb lead-filled steel box. The actuator uses up to a 2-in. double-amplitude stroke to produce a vibratory load ranging from 0 to 15,000 lb with a frequency range of 5 to 100 Hz for each load setting. Electric power is supplied by a 25-kw diesel-driven generator set. The hydraulic power unit is diesel-driven and has a pump which can deliver 38 gpm at 3,000 psi.

Major items of electronic equipment are a set of three load cells, which measure the load applied to the pavement; velocity transducers located on the 18-in.-diam steel load plate and at points away from the load plate, which are calibrated to measure deflections; a servomechanism, which allows variation of frequency and load; an X-Y recorder, which produces load versus deflection and frequency versus deflection curves; and a printer, which provides data in digital form. Figure 3 shows an overall view of the 16-kip vibrator, and Figure 4 is a view of the electronic equipment.

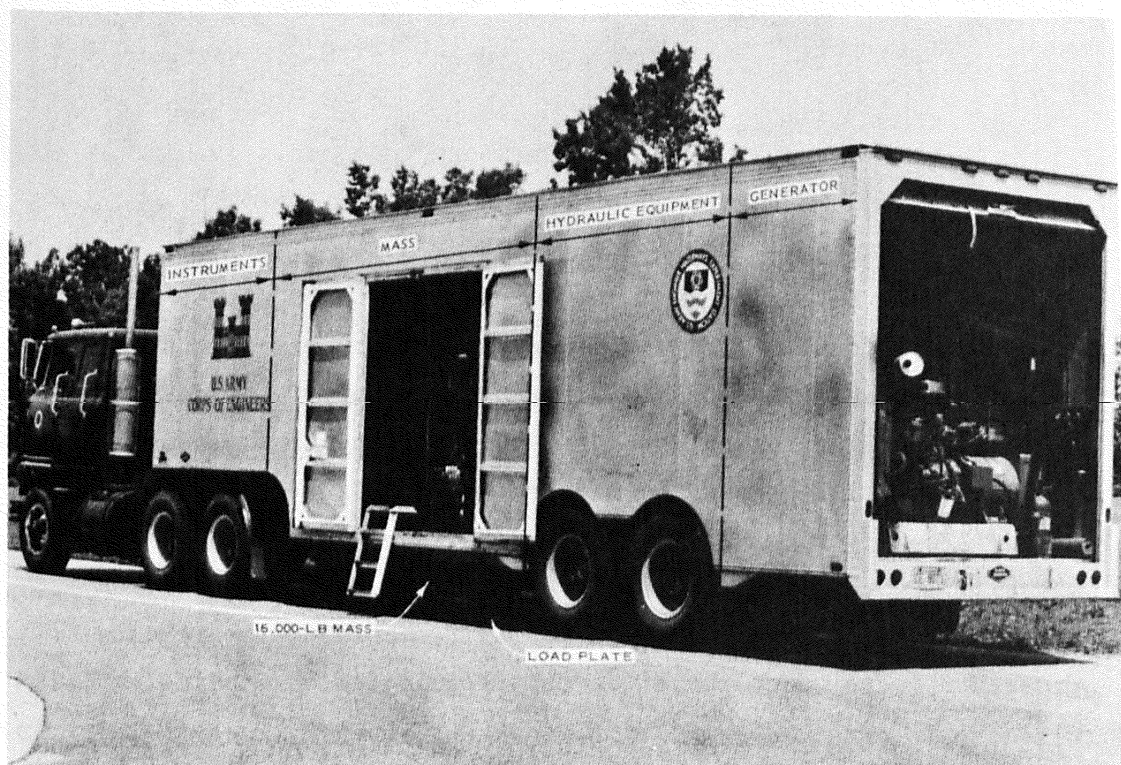


Figure 3. 16-kip vibrator

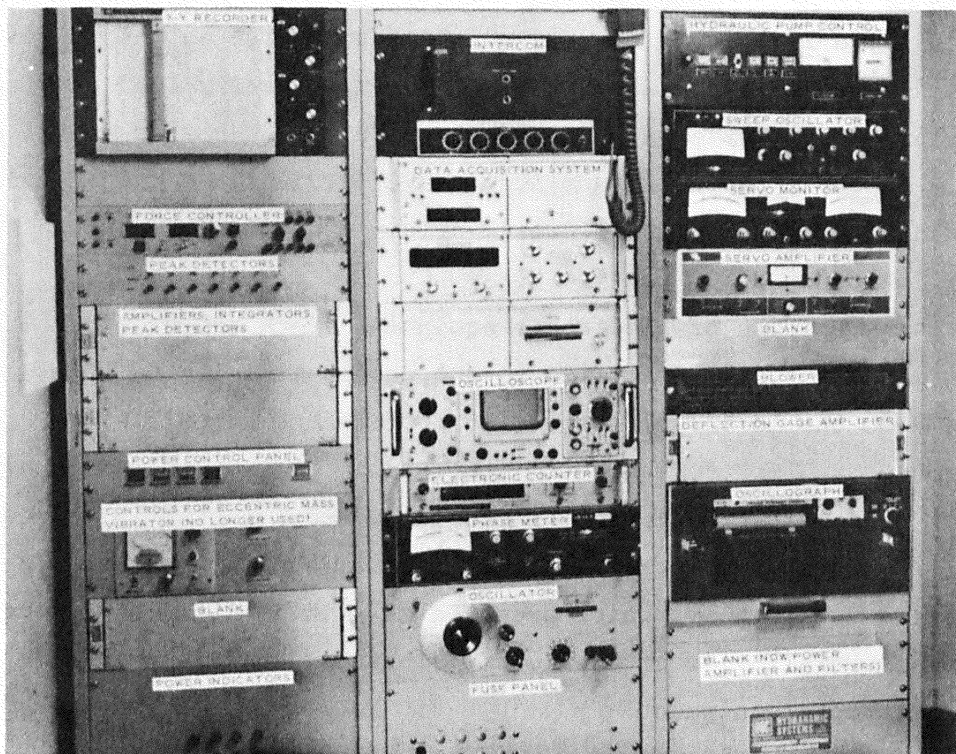


Figure 4. Electronic equipment in 16-kip vibrator

With this equipment, the vibratory load can be varied at constant frequencies and load versus deflection can be plotted. These load-deflection data are used to compute the DSM for a pavement structure. Frequency can be varied from approximately 5 to 100 Hz at constant force levels to produce the frequency response of the pavement structure. Also, at any selected load or frequency, a plot of the deflection basin shape can be drawn using data from the velocity transducers. The 16-kip vibrator can also be used to measure the velocity of shear waves propagated through various pavement layers. Wavelengths can be measured by manually moving a velocity transducer on the ground, observing the results on an oscilloscope, and manually recording the results. This procedure is repeated for different frequencies of loading, and the wave velocity is obtained by multiplying the frequency times the corresponding wavelengths as described in Appendix A.

50-KIP VIBRATOR

The 50-kip electrohydraulic vibrator (Figure 5) differs from the other five vibrators in that it is not portable and has no fixed static weight. It applies a preload that is obtained by jacking the hydraulic loading mechanism against a reaction beam. This vibrator is capable of delivering a peak vibratory load of 50,000 lb at frequencies ranging

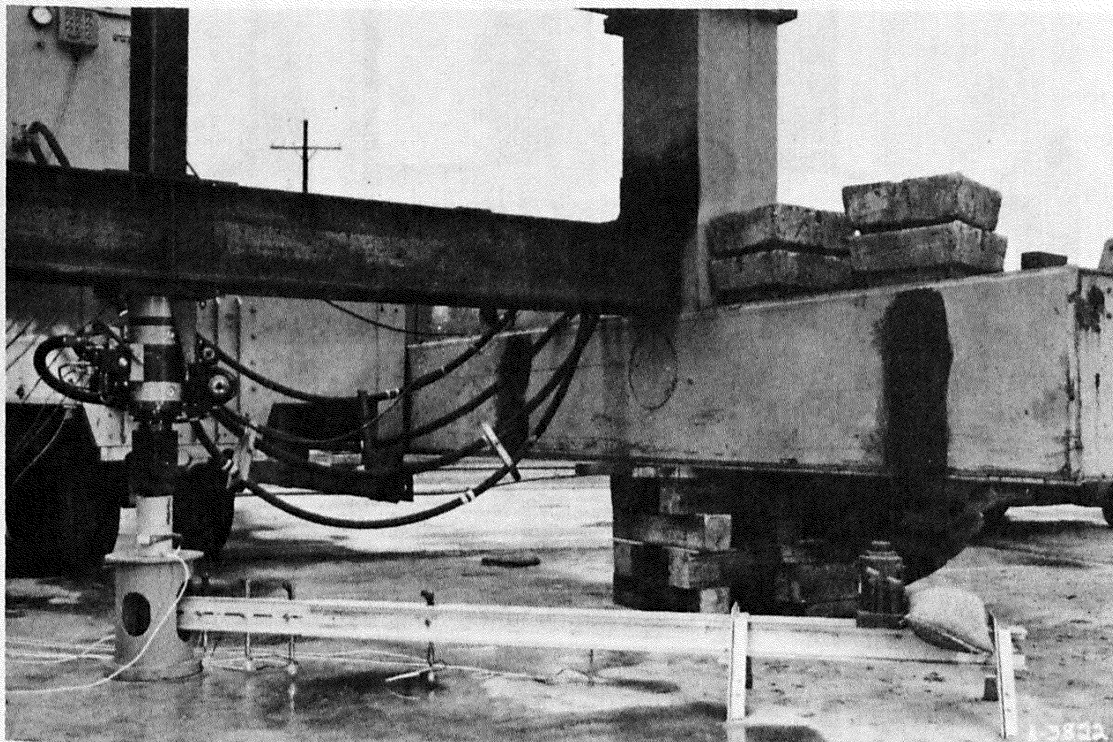


Figure 5. 50-kip vibrator

from 0 to 200 Hz and variable preloads of up to 50 kips. Although the 50-kip vibrator would not be considered as a standard test device due to its size and lack of portability, it was used in this study to determine the effect of preload (i.e., of vibrator static weight) on deflection measurements. Results of load-deflection tests were recorded on light-sensitive paper, from which data were reduced manually.

CERF NDPT VAN

The CERF NDPT van. (Figure 6) consists of a 35-ft-long trailer

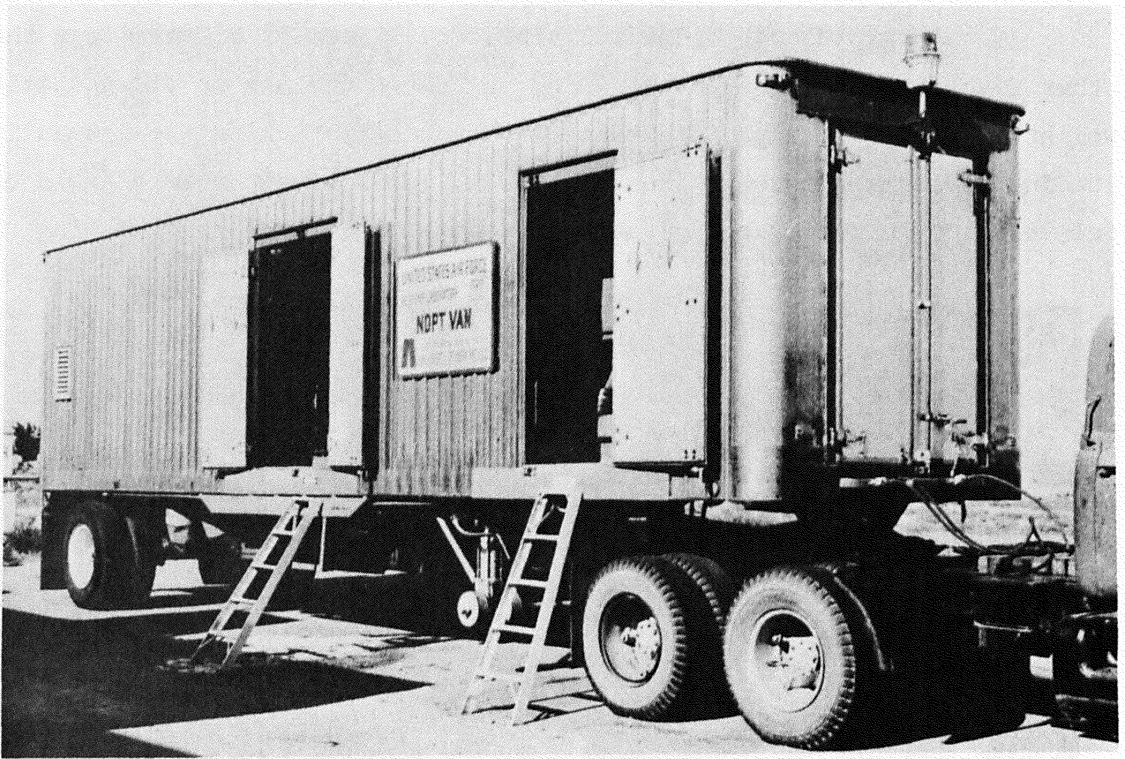


Figure 6. CERF NDPT van

that contains three compartments. The front compartment houses a 100-kw generator. The middle compartment houses a field power supply unit, transformer, vibrator, and cooling unit. The rear compartment houses the instrumentation, the principal component of which is a power amplifier console. The electromagnetic vibrator weighs 6750 lb. The vibratory load applied to the pavement is measured with three load cells mounted on a 2-in.-thick, 12-in.-diam load plate. A velocity transducer and an accelerometer are located on the 12-in. load plate. The output from the velocity transducer is integrated to obtain the displacement amplitude of the load plate. The frequency of the vibrator is controlled by a sweep oscillator. A servomechanism on the sweep oscillator is used to hold the load or acceleration at a desired level. The power amplifier provides readout units for load, displacement, and acceleration. Six panel meters on the power amplifier are used to detect malfunctions in the power amplifier unit. The instrumentation room also contains data acquisition equipment, which includes a 14-channel tape

deck, an X-Y plotter, and an oscilloscope, and digital display units for time, load, and phase angle.

DYNAFLECT

The Dynaflect is an electromechanical device (counterrotating mass) mounted on a trailer. It applies a peak vibratory load of 500 lb at a fixed frequency of 8 Hz, using the weight of the trailer as a reaction mass. The vibratory load is applied to the pavement through two 16-in.-OD steel wheels spaced 20 in. center to center. Five velocity sensors are used to measure the deflection of the pavement. One sensor is located between the steel wheels, and the other four are spaced 1, 2, 3, and 4 ft from the first one at right angles to the axis of the wheels. The Dynaflect produces numerical values of deflection at a fixed load and frequency which are recorded manually from dial gage readings. Figure 7 shows the Dynaflect with its cover removed.

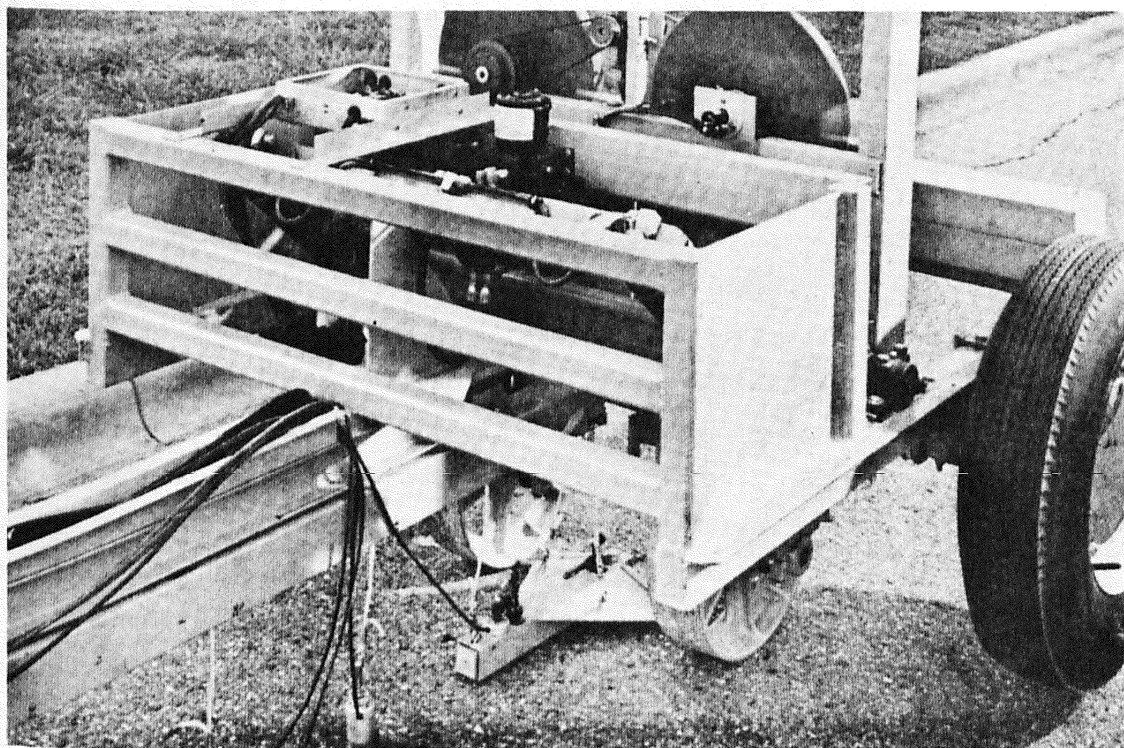


Figure 7. Dynaflect with cover removed

ROAD RATER

The Road Rater is an electrohydraulic vibratory loading device. In all models of this device except the Model 600, the actuator, or hydraulic ram, is mounted with the rod end upward (the opposite is true for the 16-kip vibrator), and a weight mounted to the rod is hydraulically oscillated to produce the vibratory load. The vibratory load is transferred to the pavement structure through two 4- by 7-in. steel pads spaced 6 in. apart. Two velocity sensors, one located between the steel loading pads and the other 1 ft away perpendicular to the axis of the pads, measure deflection of the pavement. The Road Rater produces numerical values of deflection at variable frequencies and a fixed load which are recorded manually from dial gage readings. The smallest version of this vibrator (Model 400) is mounted on the front of a truck and uses the truck as a reaction mass for stability. All other models are trailer-mounted and use the trailer weight as the reaction mass. Figure 8 shows the Model 400 truck-mounted vibrator, and Figure 9 shows the trailer-mounted Model 505.

VIBRATOR COMPARISONS BASED ON FIELD TESTS

As stated previously, the 16-kip vibrator was selected as the basic vibrator with which the other devices would be compared. DSM values were used for comparison purposes. The methods of obtaining the DSM values from the data, however, differed with each vibrator. DSM values for the 16-kip vibrator, the 9-kip vibrator, and the CERF NDPT van are obtained from the slope of the upper portion of the load-deflection data curve as described in the section on the effects of vibratory loading. The dynamic load is increased to the maximum output of each machine during a test. The 16-kip vibrator and the CERF NDPT van produce the DSM at a constant frequency, whereas the frequency is increased on the 9-kip vibrator in order to increase the dynamic load. The DSM for the other devices is the ratio of load to deflection obtained at a constant dynamic load and frequency.

Figures 10-13 are plots of DSM values obtained with the 16-kip



Figure 8. Model 400 Road Rater

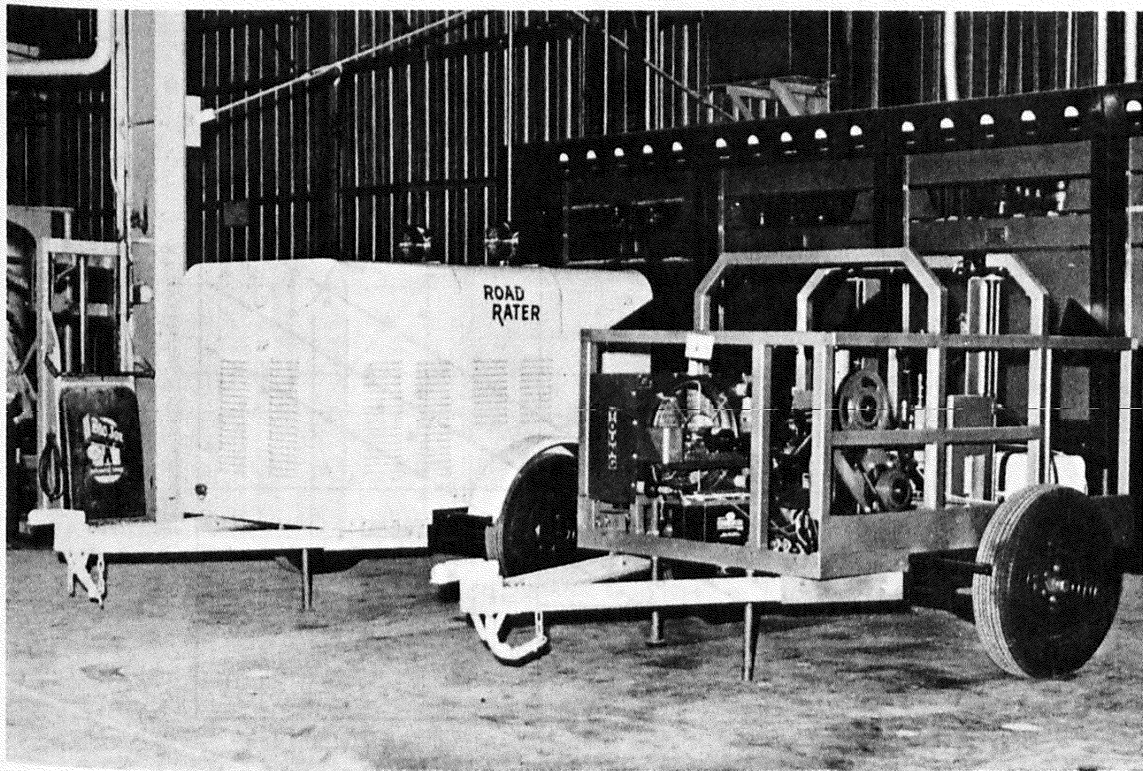


Figure 9. Model 505 Road Rater

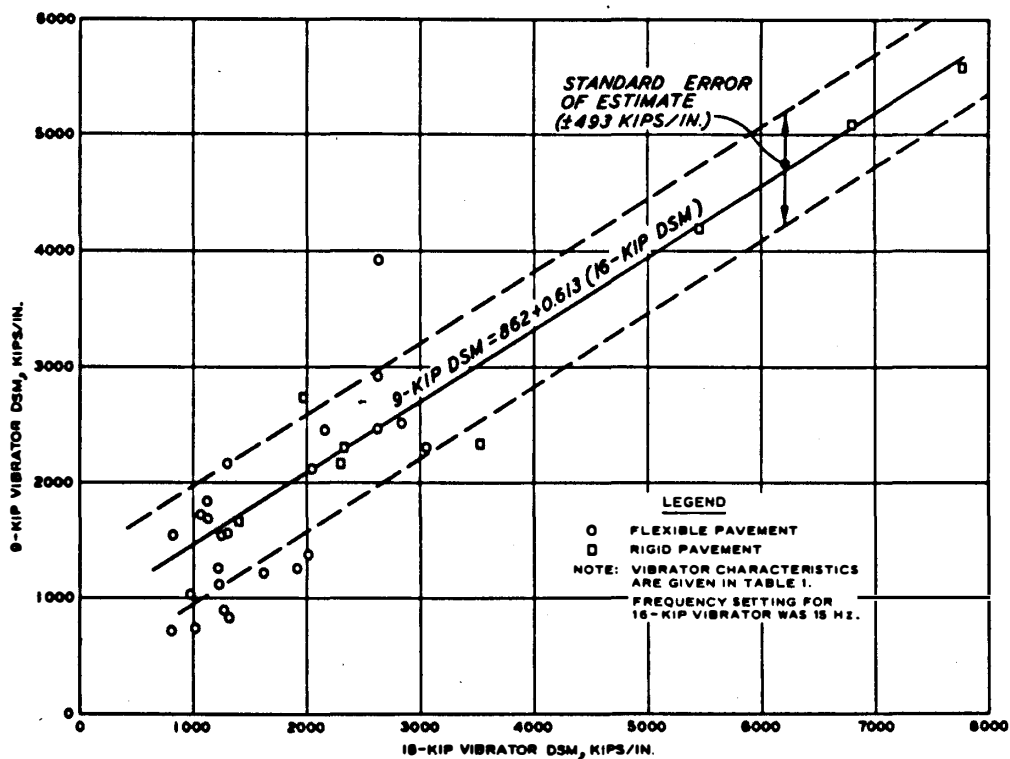


Figure 10. DSM of 16-kip vibrator versus DSM of 9-kip vibrator

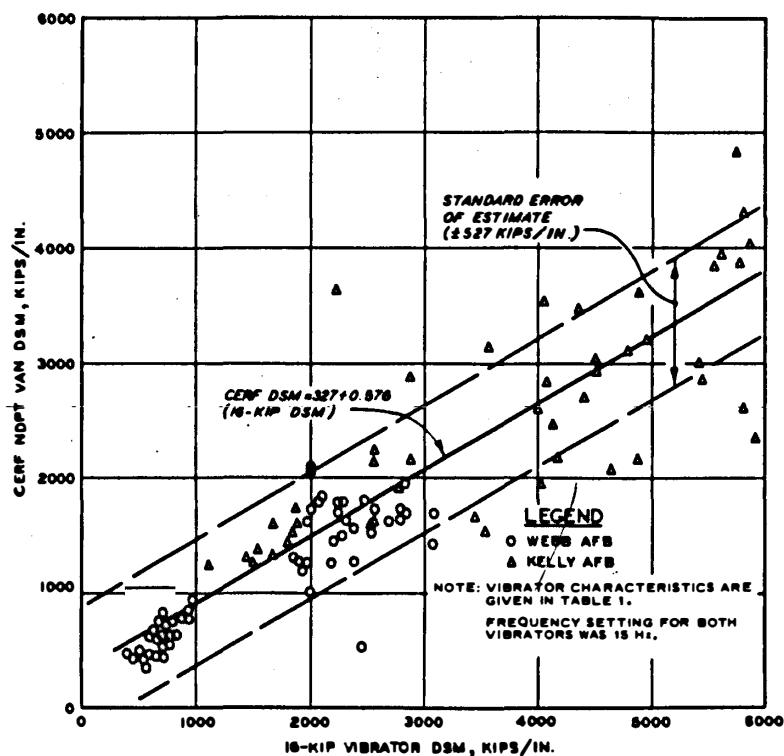


Figure 11. DSM of 16-kip vibrator versus DSM of CERF NDPT van

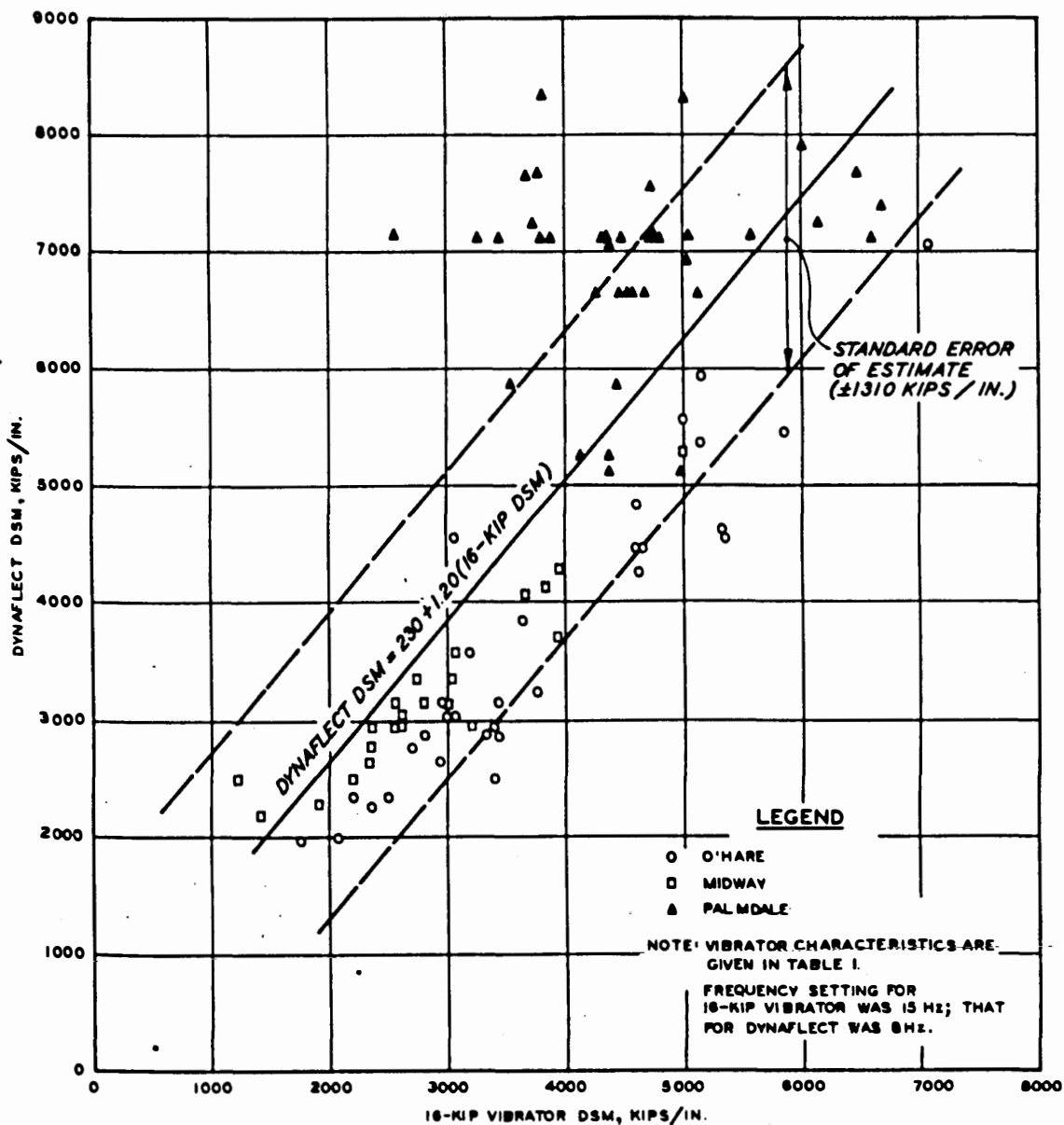
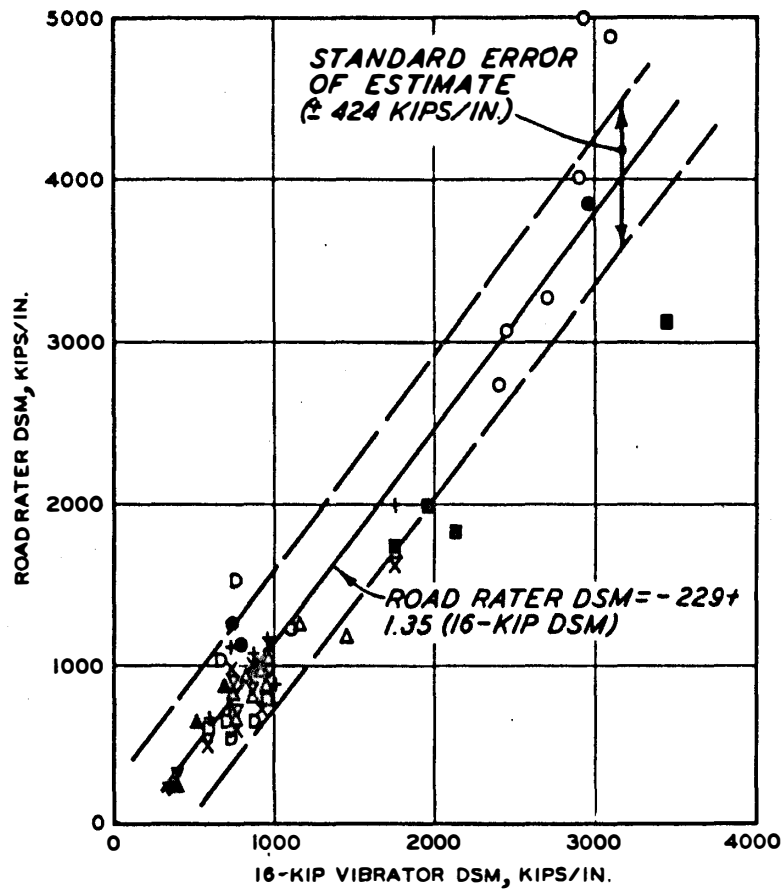


Figure 12. DSM of 16-kip vibrator versus DSM of Dynaflect



LEGEND

| SYMBOL | ROAD RATER FREQUENCY Hz | 16-KIP FREQUENCY Hz | TYPE PAVEMENT |
|---|-------------------------------|---------------------------|------------------|
| <u>NATIONAL AVIATION FACILITIES EXPERIMENTAL CENTER</u> | | | |
| O | 25 | 15 | AC |
| Δ | 25 | 15 | PCC |
| □ | 25 | 15 | AC |
| ▽ | 25 | 15 | PCC |
| X | 30 | 15 | PCC |
| + | 30 | 15 | PCC |
| <u>WES SOIL STABILIZATION TEST SECTION</u> | | | |
| D | 15 | 15 | AC |
| ● | 15 | 15 | PCC |
| <u>WES TEMPERATURE EFFECTS TEST SECTION</u> | | | |
| ▲ | 15 | 15 | AC |
| <u>JACKSON MUNICIPAL AIRPORT</u> | | | |
| ■ | 15 | 15 | PCC |
| ▼ | 15 | 15 | AC |

NOTE: VIBRATOR CHARACTERISTICS ARE GIVEN IN TABLE 1.

Figure 13. DSM of 16-kip vibrator versus DSM of Model 505 Road Rater

vibrator versus DSM values obtained with the 9-kip vibrator, the CERF NDPT van, the Dynaflect, and the Model 505 Road Rater, respectively. The comparisons discussed in the following paragraphs show the variations in data obtained with these four vibrators. Accuracy of the 16-kip vibrator will be discussed later.

Figure 10 shows a graph of the 16-kip vibrator DSM values versus the 9-kip vibrator DSM values. DSM values for the 16-kip vibrator ranged from about 800 to 7800 kips/in.; however, a significant number of data points were not obtained beyond 3500 kips/in. The line of best fit in Figure 10 shows that, up to a DSM of about 2000 kips/in., the 9-kip vibrator produces higher DSM than the 16-kip vibrator. Above a DSM of 2000 kips/in., however, the 9-kip vibrator produces lower values than the 16-kip vibrator. The standard error of estimate is ± 493 kips/in. measured along the 9-kip vibrator axis.

Figure 11 shows a graph of the 16-kip vibrator DSM values versus CERF NDPT van DSM values. DSM values for the 16-kip vibrator ranged from about 400 to 5800 kips/in. The best-fit line in Figure 11 shows that the CERF NDPT van generally yields lower DSM than the 16-kip vibrator. The standard error of estimate is ± 527 kips/in. measured along the CERF NDPT van axis.

Figure 12 shows a graph of DSM values obtained with the 16-kip vibrator versus those obtained with the Dynaflect. DSM values for the 16-kip vibrator ranged from 1200 to 7100 kips/in. The best-fit line in Figure 12 shows that the Dynaflect generally gives higher DSM values than the 16-kip vibrator. The standard error of estimate is ± 1310 kips/in. measured along the Dynaflect axis. However, it should be noted that, if the Palmdale data are not considered, the standard error of estimate is ± 415 kips/in. and the equation for the best-fit line is $\text{Dynaflect DSM} = 590 + 0.860 \times 16\text{-kip DSM}$. All the data shown in Figure 12 were collected on continuously reinforced concrete pavements, and it is not known why the data from Palmdale did not correlate well with those from Midway and O'Hare.

Figure 13 shows a graph of DSM values obtained with the 16-kip vibrator versus DSM values obtained with the Model 505 Road Rater. DSM

for the 16-kip vibrator ranged from about 400 to 3400 kips/in. The best-fit line in Figure 13 shows that the Road Rater generally gives higher DSM than the 16-kip vibrator. The standard error of estimate is +424 kips/in. measured along the Road Rater axis.

The lack of agreement between vibrator results is due to the non-linearity of pavement response and significant differences in the magnitudes of the vibratory loads, vibrator static weights, frequencies of loading, and contact areas. These results do not show that the 16-kip vibrator is the optimum size for airfield pavement testing. There is obviously a need, however, for a standardized vibrator and the 16-kip vibrator is recommended.

FACTORS AFFECTING VIBRATORY TEST RESULTS

Tests were made to evaluate the effects of such factors as vibrator static weight, vibratory load, frequency of vibration, and load plate size on load-deflection measurements.

VIBRATOR STATIC WEIGHT

The 50-kip vibrator was used to study the effects of static weight on the load-deflection measurements. The electrohydraulic system of this vibrator was used to apply a preload (comparable to static weight) to the test pavement by the hydraulic loading mechanism reacting against a load frame. The vibratory load was generated by a force applied to the preload and then released.

To demonstrate the loading conditions beneath the vibrators described in this report, a simplified load versus time relationship for the 16-kip vibrator is shown in Figure 14. This relationship is similar to those for the other vibrators except in magnitude of vibratory load. The vibrator static weight F_s is applied to the pavement surface, and then the vibratory load F_d is generated. The vibratory load can be varied but cannot exceed the static weight. The static weight of most of the vibrators is fixed, but that of the 50-kip vibrator (i.e., its preload) can be varied up to a maximum of 50 kips. Tests with the 50-kip vibrator were conducted on a flexible pavement test section at WES described in Appendix B.

Load and deflection data for items 2-5 of the WES flexible pavement test section were plotted for preloads ranging from 5 to 50 kips. The DSM value from each load-deflection plot was computed, and these values are shown in Figure 15 for the various preloads used on items 2-5. Data presented in Table 2 were also used in Figure 16 in a plot of preload versus DSM expressed as a percent of the DSM value obtained with a vibrator preload of 5 kips. This graph shows that the DSM for item 2 was increased by a factor of 3 by changing the vibrator preload from 5 to 50 kips. These results indicate the significance of varying the static weight of a vibrator.

VIBRATORY LOAD

Test results have shown that the load-deflection data are not always linear throughout the full dynamic load range of the 16-kip vibrator. Figures 17-21 illustrate a characteristic of data obtained on some pavements with the 16-kip vibrator, i.e., the load versus deflection plot tends to curve in its lower portion and then become linear in its higher portion on weak pavements. The plots in Figures 17-21 become linear at loads of 6.0, 8.6, 7.0, 4.4, and 2.4 kips, respectively. Pavements which have the same DSM values as those shown in Figures 17-21 do not always produce plots that have the same curvature, but generally, weaker flexible pavements produce load versus deflection plots which show this tendency. Rigid pavements tend to produce load-deflection plots having less curvature than those of flexible pavements.

The nonlinear load-deflection plots show that the DSM will vary when different portions of the curve or different single point loads are used to compute the DSM and all other factors are constant. This tendency is illustrated in Figure 17. The vertical arrows are drawn at loads of 0.5, 1.0, 5.0, 8.0, and 10.2 kips. For the single-point deflections at the first four of these loads, the DSM values (load divided by deflection) are 710, 770, 690, and 650 kips/in., respectively. The fifth DSM value was obtained using the inverse of the slope of the linear portion of the curve, and for this example is $4.2 \text{ kips} \div 0.0074 \text{ in.} = 570 \text{ kips/in.}$ These two methods of computing

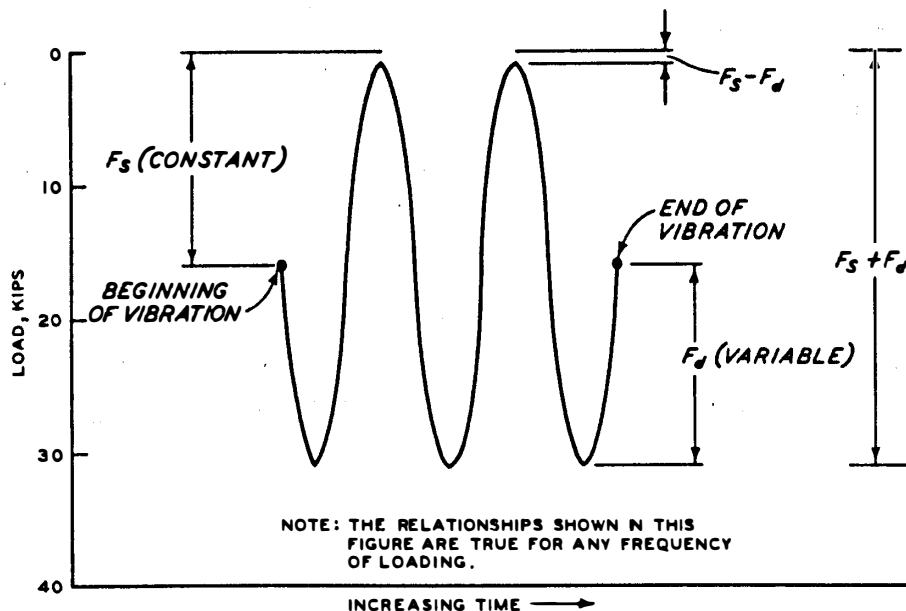
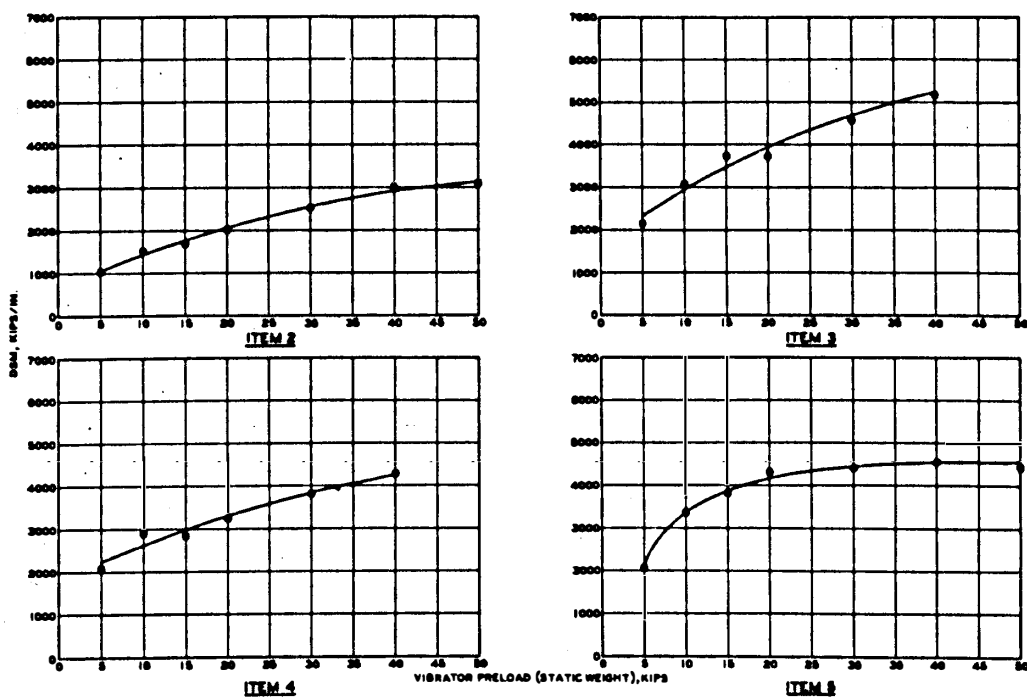


Figure 14. Load versus time relationships for loading conditions beneath the 16-kip vibrator



NOTE: PLANS AND SECTIONS OF TEST ITEMS ARE SHOWN IN FIGURE 16.
 • DATA ARE TABULATED IN TABLE 2 AND PLOTTED IN ANOTHER FORM IN FIGURE 15.
 DATA WERE OBTAINED WITH 80-KIP VIBRATOR AT A FREQUENCY OF 18 HZ.

Figure 15. DSM values versus vibrator preload (items 2-5 of flexible pavement test section)

Table 2

Vibrator Preload (Static Weight) and DSM (50-Kip Vibrator)

| Preload (Static Weight) kips | Item 2 | | | Item 3 | | | Item 4 | | | | | Item 5 | | |
|---------------------------------------|-------------|-------------------------------|---------------------------------|-------------|-------------------------------|---------------------------------|---------|-------------------------------|-----------------|----------------------------|---------------------------------|-----------------|-------------------------------|---------------------------------|
| | Maximum | Percent of 5-kip DSM | Peak Dynamic Load kips | Maximum | Percent of 5-kip DSM | Peak Dynamic Load kips | Maximum | Percent of 5-kip DSM | DSM kips/in. | Average DSM kips/in. | Peak Dynamic Load kips | Maximum | Percent of 5-kip DSM | Peak Dynamic Load kips |
| | Peak | | | Peak | | | Peak | | | | | Peak | | |
| | Load | | | Load | | | Load | | | | | Load | | |
| DSM kips/in. | DSM kips | DSM kips | DSM kips/in. | DSM kips | DSM kips/in. | Run 1 | Run 2 | Run 1 | Run 2 | Run 1 | Run 2 | DSM kips/in. | DSM kips | DSM kips/in. |
| 5 | 4.1 | 1070 | — | 5.3 | 2160 | — | 7.3 | 1940 | 2090 | 2020 | — | 6.7 | 2060 | — |
| 10 | 6.5 | 1550 | 145 | 7.5 | 3080 | 143 | 11.0 | 2620 | 2880 | 2750 | 136 | 12.1 | 3360 | 163 |
| 15 | 8.6 | 1850 | 173 | 11.9 | 3740 | 173 | 14.0 | 3150 | 2830 | 2990 | 148 | 12.9 | 3820 | 185 |
| 20 | 9.0 | 2050 | 192 | 9.9 | 3740 | 173 | 17.9 | 2980 | 3240 | 3110 | 154 | 15.9 | 4300 | 208 |
| 30 | 10.0 | 2560 | 240 | 12.5 | 4580 | 212 | 15.0 | 3340 | 3810 | 3580 | 177 | 16.4 | 4400 | 214 |
| 40 | 11.1 | 3070 | 287 | 9.9 | 5180 | 240 | 16.1 | 4000 | 4280 | 4140 | 205 | 13.3 | 4560 | 222 |
| 50 | 10.9 | 3220 | 301 | 12.0 | 5320 | 246 | 12.1 | 3800 | — | 3800 | 188 | 13.0 | 4420 | 215 |

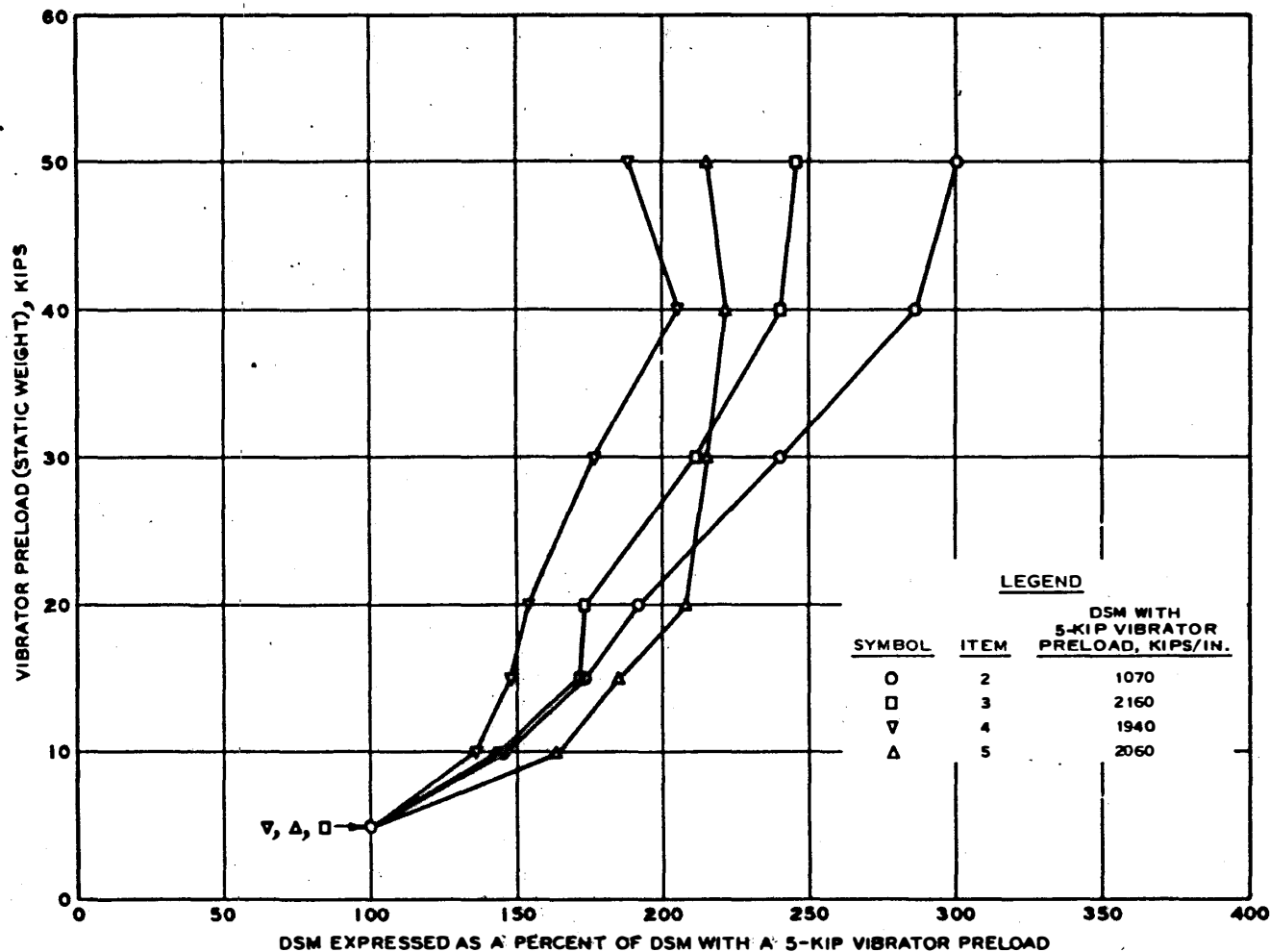


Figure 16. Vibrator preload versus DSM expressed as a percent of DSM obtained with a 5-kip vibrator preload (items 2-5 of flexible pavement test section)

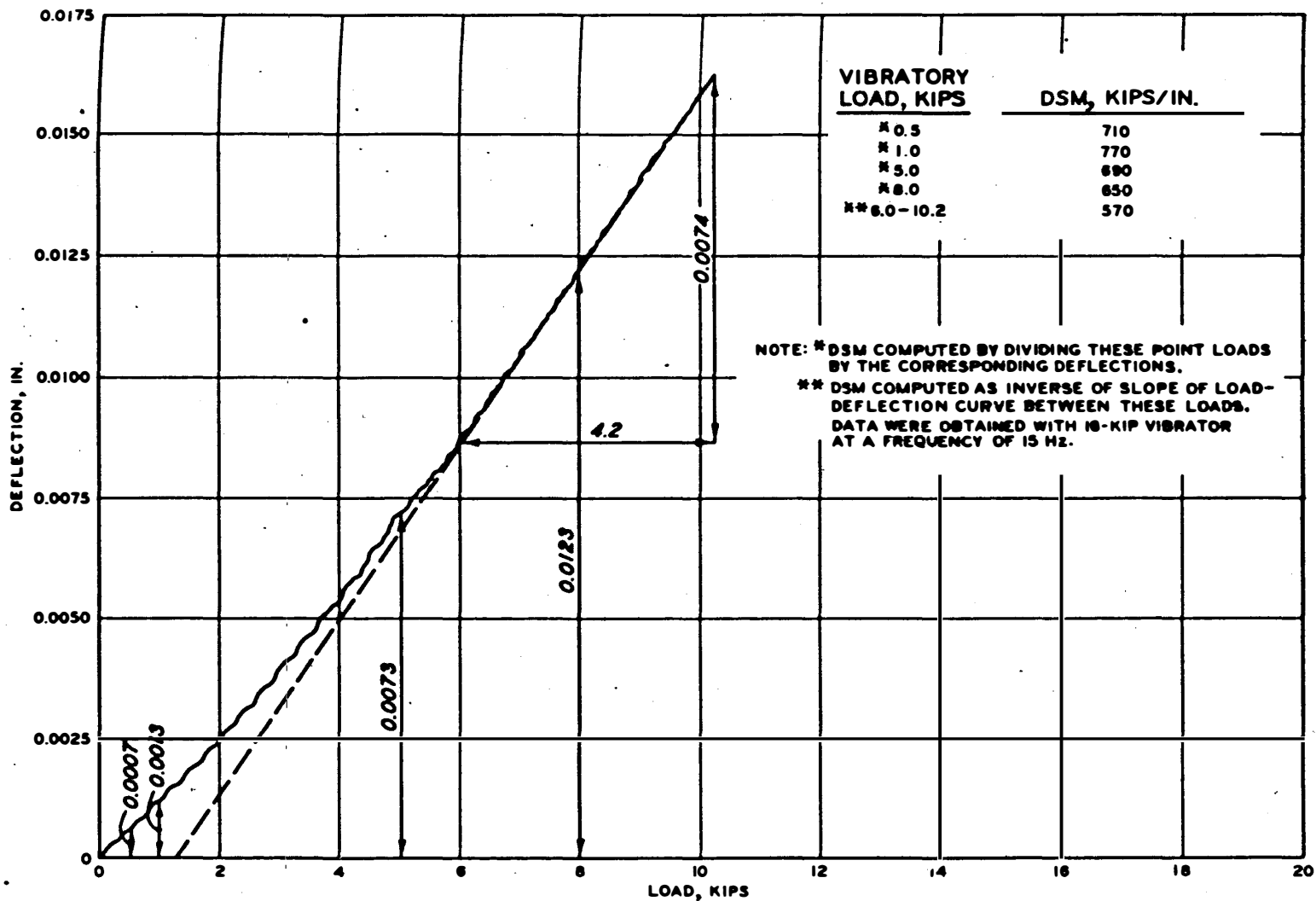


Figure 17. Deflection versus load (Philadelphia International Airport, line R7A, point No. 2)

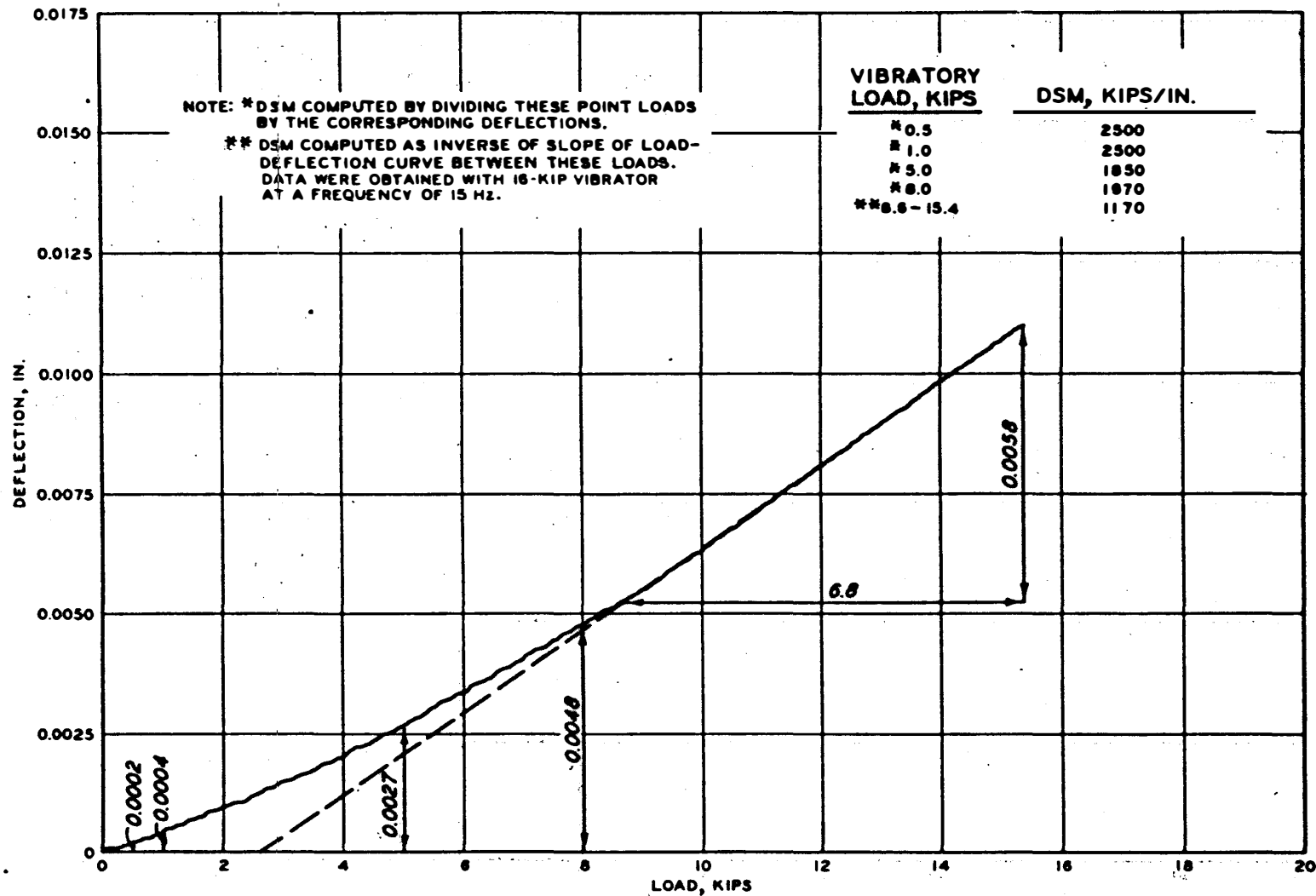


Figure 18. Deflection versus load (Philadelphia International Airport, line R11A, point No. 1)

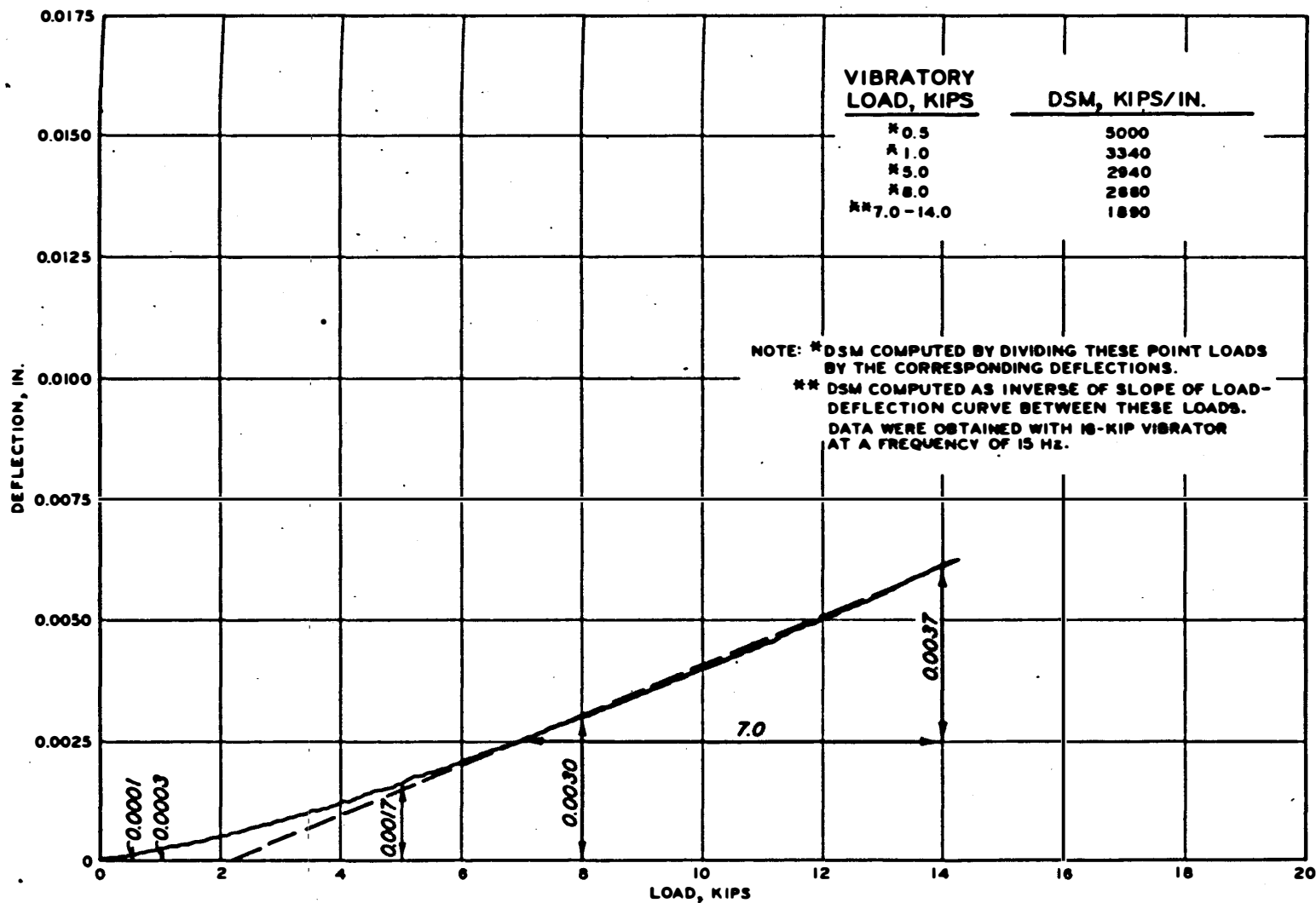


Figure 19. Deflection versus load (Philadelphia International Airport, line A7A, point No. 4)

77

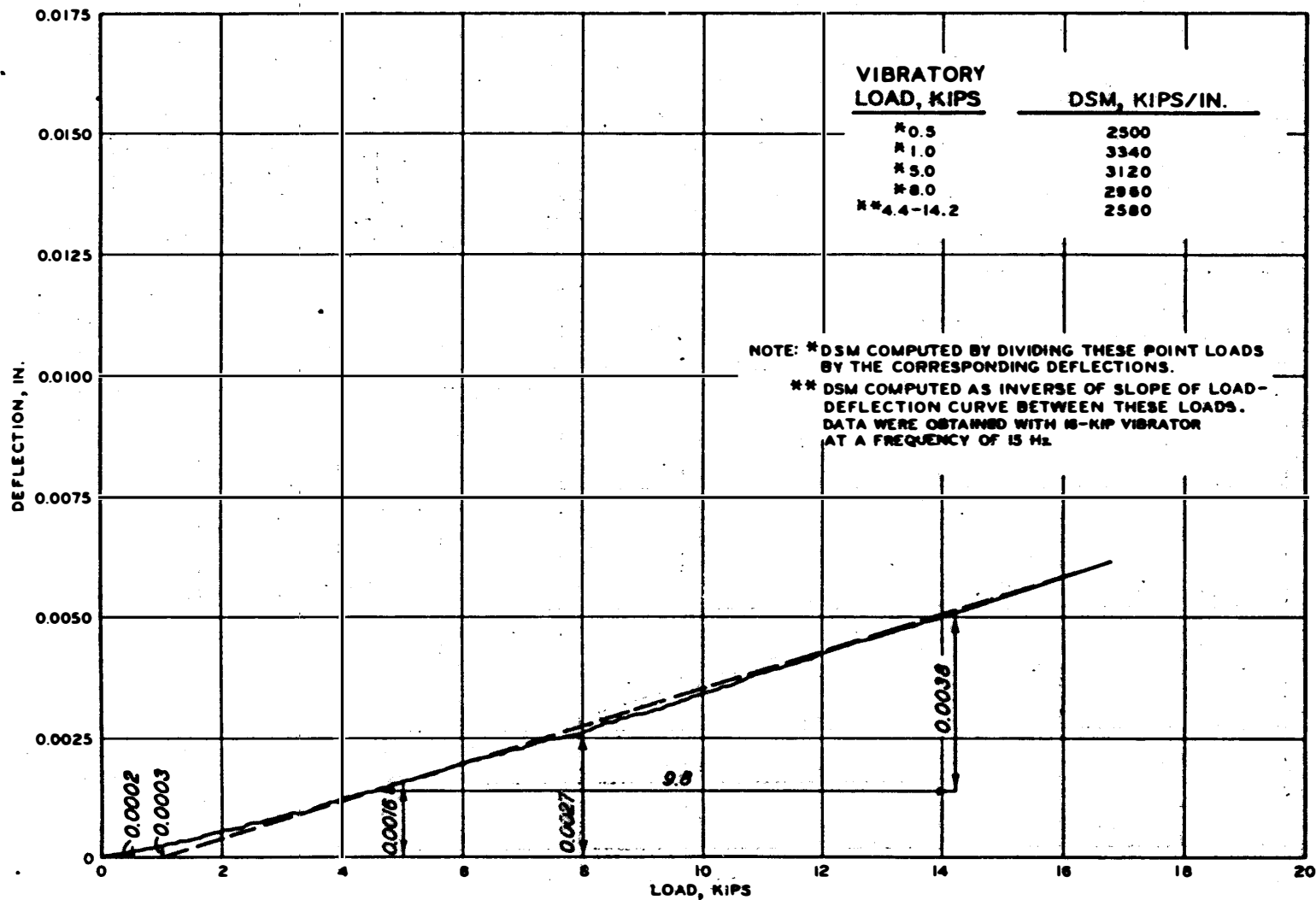


Figure 20. Deflection versus load (Philadelphia International Airport, line A8A, point No. 1)

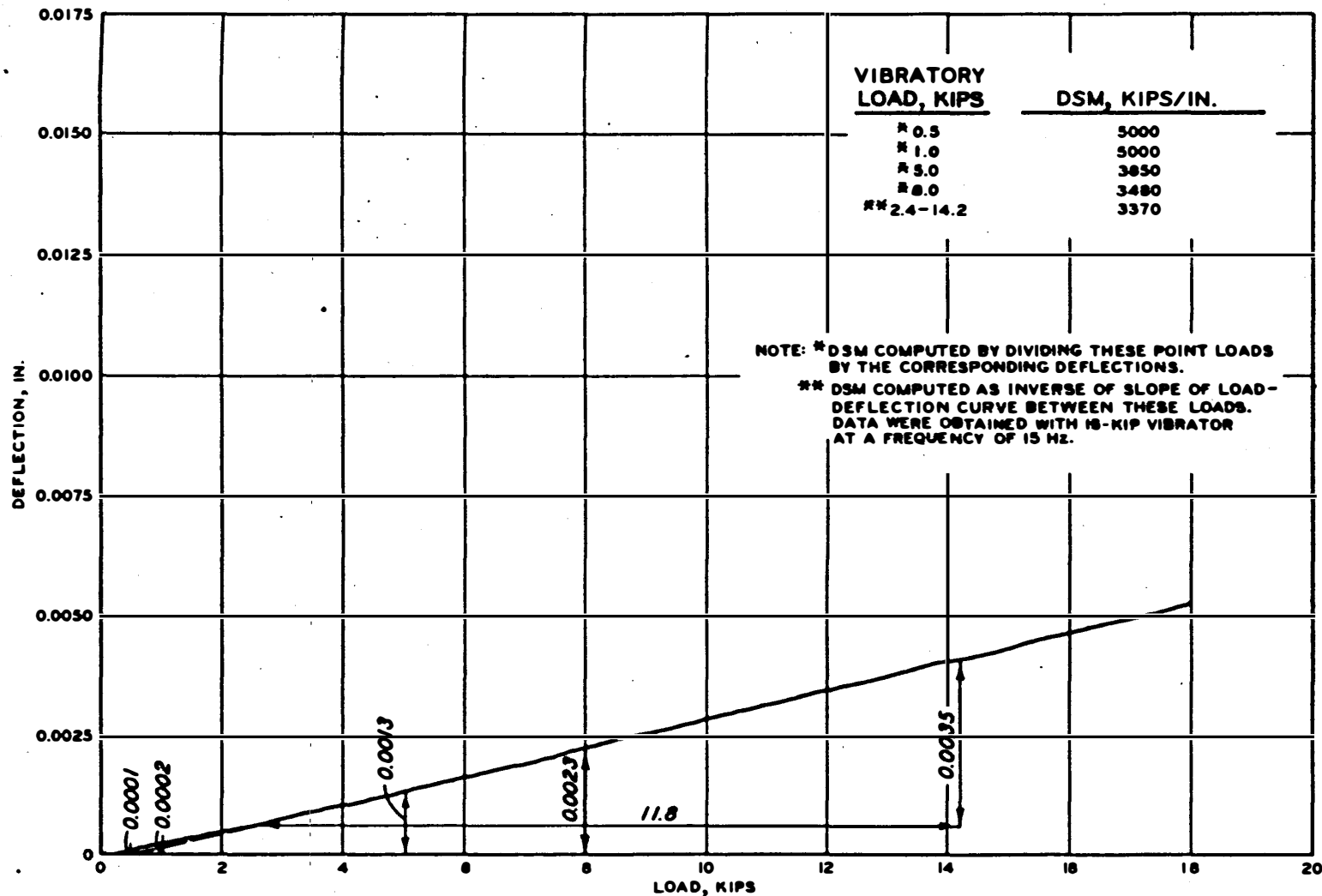


Figure 21. Deflection versus load (Philadelphia International Airport, line A8A, point No. 6)

DSM values for typical data are also used in Figures 18-21. DSM values obtained with vibratory loads of 0.5, 1.0, 5.0, and 8.0 kips ranged from 97 to 264 percent of the values obtained using the linear portion of the curve (Table 3).

This range in DSM values indicates a need either to establish a standard vibratory loading or use the slope of the linear portion of the load-deflection curve. DSM values obtained using the linear portion of the curve are lower values and are believed to represent the elastic properties of the materials of the entire pavement section and subgrade rather than those of the upper layers of higher quality materials.

FREQUENCY OF VIBRATION

Pavement response to vibratory loading varies with the frequency of vibration and pavement structure as shown in Figure 22. The load-deflection curves for constant frequency may show a nearly linear response for some pavements over a range of frequencies; however, the most linear response has generally been found, and has been indicated by theory in Volume II,⁴¹ to be at approximately 15 Hz. Earlier studies¹¹ in which the 9-kip vibrator was operated over instrumented pavements

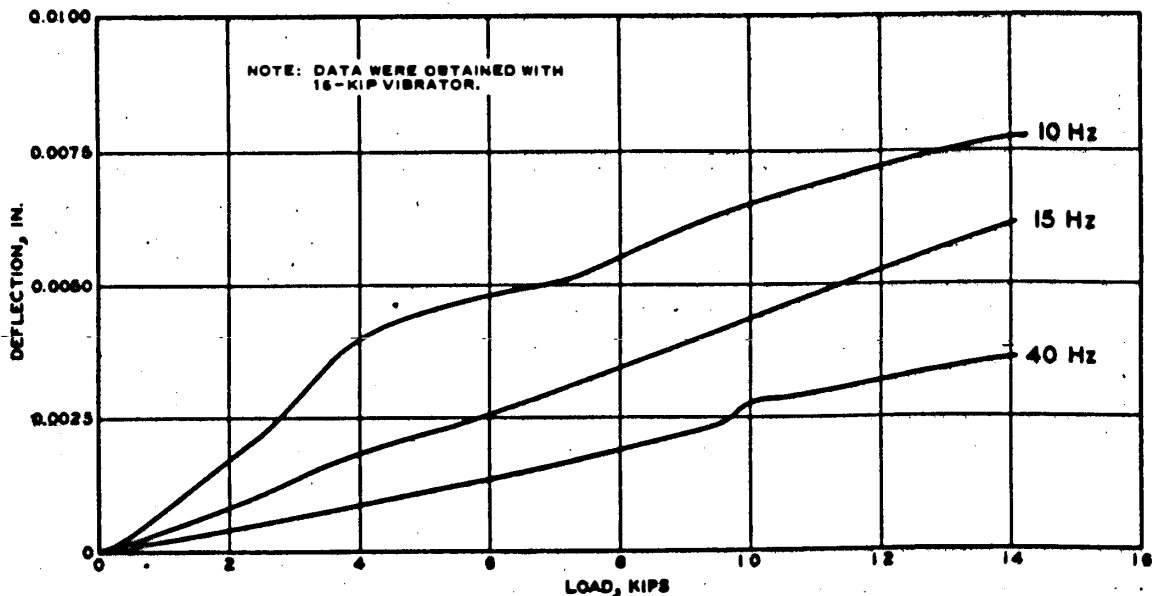


Figure 22. Typical load-deflection curves for frequencies of 10, 15, and 40 Hz

Table 3
Variations in Computed DSM Values

| Figure No. | DSM* kips/in. | DSM at 0.5-kip Load | | DSM at 1.0-kip Load | | DSM at 5.0-kip Load | | DSM at 8.0-kip Load | |
|---------------|------------------|---------------------|--------------------|---------------------|--------------------|---------------------|--------------------|---------------------|--------------------|
| | | kips/in.** | Percent of DSM* | kips/in.** | Percent of DSM* | kips/in.** | Percent of DSM* | kips/in.** | Percent of DSM* |
| 17 | 570 | 710 | 125 | 770 | 135 | 690 | 121 | 650 | 114 |
| 18 | 1170 | 2500 | 214 | 2500 | 214 | 1850 | 158 | 1670 | 143 |
| 19 | 1890 | 5000 | 264 | 3340 | 177 | 2940 | 156 | 2660 | 141 |
| 20 | 2580 | 2500 | 97 | 3340 | 129 | 3120 | 121 | 2960 | 115 |
| 21 | 3370 | 5000 | 149 | 5000 | 149 | 3850 | 114 | 3480 | 104 |

* Inverse of slope of load versus deflection plot in its linear range.

** Load divided by deflection.

indicated that 15 Hz was the optimum frequency, i.e., magnitudes of stress and deflection measurements at 15 Hz were more proportional to wheel loads throughout the range of depths considered than for measurements at other frequencies of which the vibrator was capable.

Figures 23 and 24 show the deflection at various frequencies for a constant load of 10 kips using the 16-kip vibrator. Figure 23 shows the results for 12 flexible pavement test sites, and Figure 24 shows the results for 9 rigid pavement test sites. Physical properties of pavements at these test sites are presented in Tables 4 and 5, respectively. As shown by the data in these figures, the deflection response varies appreciably with changes in frequency; therefore, the DSM is also a function of frequency.

It should be noted that the velocity transducers used with the 16-kip vibrator are always calibrated at 20 Hz. This calibration is known to be valid for frequencies of from 13 to 50 Hz (see Figure 25). There is a small error in deflections measured at frequencies below 13 Hz due to the calibration at 20 Hz. This error results in measured deflections at 5 Hz that are approximately 20 percent lower than actual values; the amount of error gradually decreases to a negligible amount at 13 Hz. Corrections for this error were not applied to the data shown in Figures 23 and 24.

It is recognized that the load-deflection relationship is dependent on the frequency of vibration and that the frequency responses of pavements can differ considerably. This research effort considered various quantities that could be obtained from the nondestructive data, and the DSM consistently proved to be the quantity that best correlated with the allowable loads obtained from existing pavement evaluation criteria. The DSM was selected as the standard measurement and a frequency of 15 Hz was selected for the reasons discussed previously.

LOAD PLATE SIZE

The load plate sizes of the vibrators evaluated in this study varied considerably (Table 1). However, the effects of contact area on test results could not be studied during the vibrator comparisons

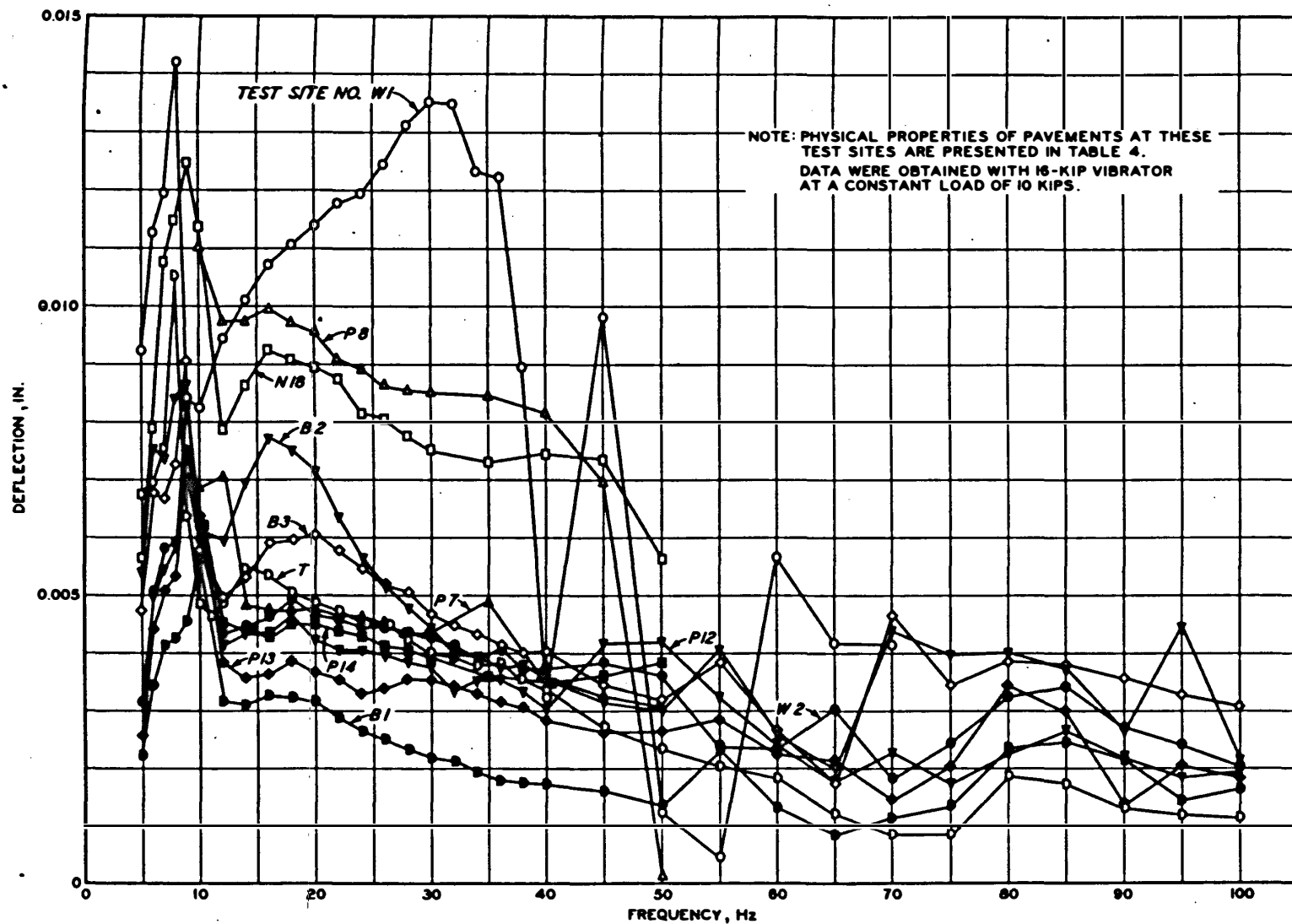


Figure 23. Deflection versus frequency for flexible pavements

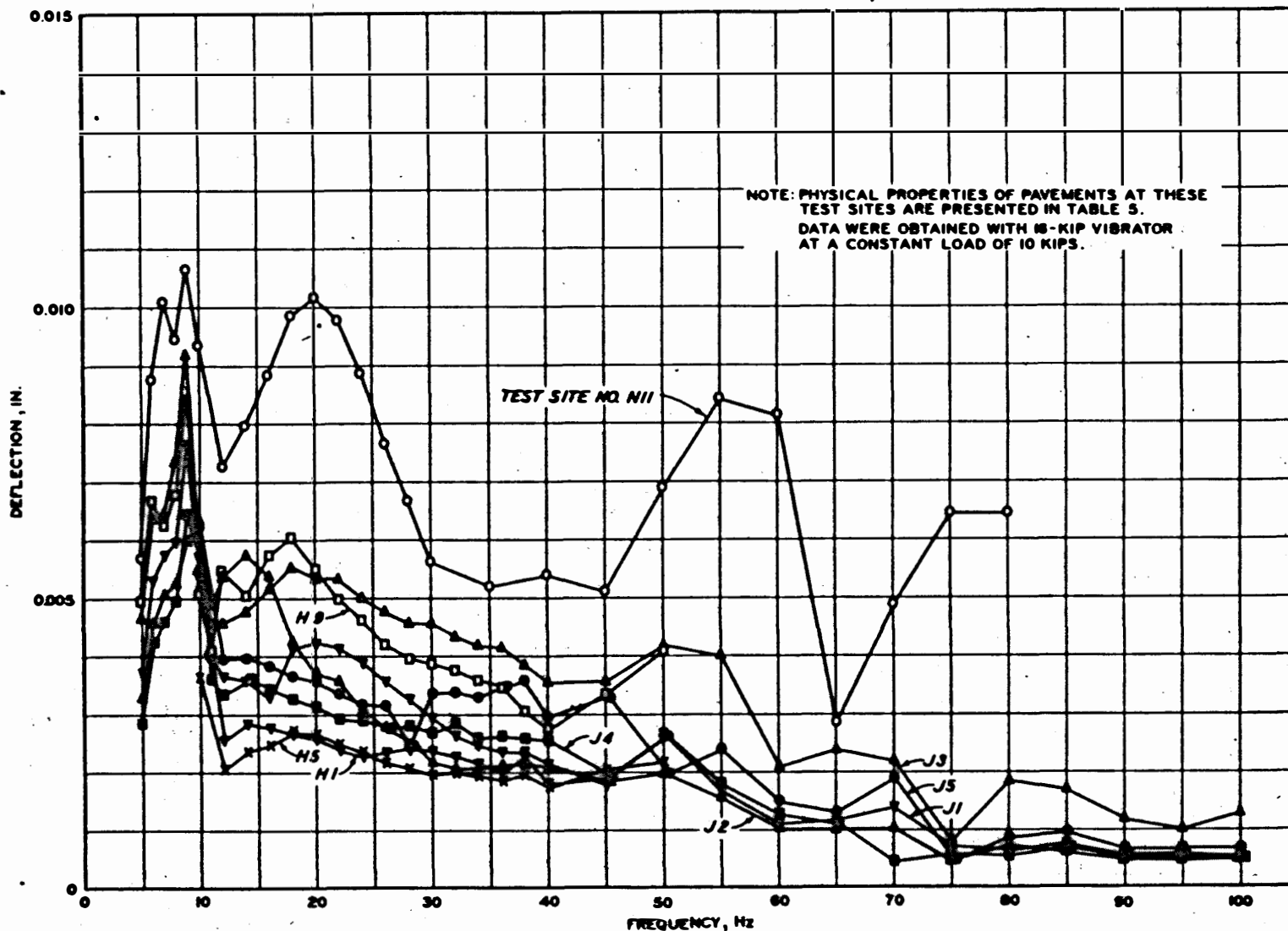


Figure 24. Deflection versus frequency for rigid pavements

Table 4
Physical Properties of Flexible Pavements

| Test Site No. | Location | Facility | AC Thickness in. | Base Course | | | Subbase | | | Subgrade | |
|---------------|--------------|---------------------------------|------------------|--|---------------|-----------|---|---------------|-----------|-------------|-----------|
| | | | | Material | Thickness in. | Field CBR | Material | Thickness in. | Field CBR | Material | Field CBR |
| W18 | NAFEC | E-W runway | 3-1/4 | E-1 (GP) | 6 | 27 | -- | -- | -- | E-2 (SM) | 18 |
| W20 | NAFEC | Taxiway A | 3 | Black base | 3 | -- | E-1 (GP) | 6 | 56 | E-2 (SM) | 18 |
| W22 | NAFEC | Taxiway A | 3 | Black base | 3 | -- | E-1 (GP) | 7 | 100+ | E-2 (SM) | 18 |
| W23 | NAFEC | Taxiway A | 3 | Black base | 3 | -- | E-1 (GP) | 7 | 100+ | E-2 (SM) | 18 |
| W1 | Wilmington | Parking apron | 9 | E-2 (GW-GM) | 5 | 100+ | -- | -- | -- | E-4 (SP-SC) | 20 |
| W2 | Wilmington | | 12 | E-2 (GW-GM) | 6 | 100+ | -- | -- | -- | E-4 (SP-SC) | 20 |
| B1 | Baltimore | | 5 | Black base | 12-1/2 | -- | E-5 (SP-SM) | 6 | 67 | E-4 (SM) | 14 |
| B2 | Baltimore | | 5 | Black base | 7 | -- | E-2 (GW-GM) | 9 | 96 | E-3 (SM-SC) | 14 |
| B3 | Baltimore | | 5 | Black base | 5-1/2 | -- | E-2 (GW-GM) | 10-1/2 | 73 | E-2 (SP-SM) | 17 |
| P1* | Philadelphia | Runway 4-22 | 4 | Black base | 6 | -- | Stone | 8 | -- | E-4 (SM) | 7 |
| P2* | | Runway 4-22 | 4 | Black base | 4-1/2 | -- | Stone | 7-1/2 | -- | E-7 (SM-SC) | 6 |
| P5* | | Taxiway U | 3 | Black base | 3 | -- | Stone | 6 | 54 | E-2 (SP) | 15 |
| P13 | | Runway 9R-27L | 15 | E-2 (GP-GC) | 5 | 83 | -- | -- | -- | E-2 (GP-GC) | 20 |
| P14 | | Runway 9R-27L | 14 | E-2 (GP-GC) | 5 | 100+ | -- | -- | -- | E-2 (GP-GC) | 20 |
| NV1* | Nashville | Taxiway 2L-20R | 5 | Black base | 8 | -- | Crushed stone | 12 | 100+ | | |
| | | | | | | | Stone | 7 | -- | E-7 (ML) | 12 |
| NV3** | | Runway 2L-20R | 3 | Black base | 5 | -- | Crushed stone | 6 | 62 | | |
| | | | | | | | Stone | 6 | -- | E-7 (ML) | 12 |
| NV4** | | Runway 2L-20R | 5 | Black base | 13 | -- | Crushed stone | 12 | 45 | E-7 (ML) | 12 |
| S81 | WES | Soil stabilization test section | 3 | Crushed stone | 6 | 100+ | GP | 33 | 56 | E-11 (CH) | 4 |
| S1 | | | 3 | Bituminous-stabilized (2.9% AC) gravelly sand with 6.5% filler | 12 | -- | -- | -- | -- | E-11 (CH) | 4 |
| S2 | | | 3 | AC | 6 | -- | AC | 6 | -- | E-11 (CH) | 4 |
| S3 | | | 3 | AC | 6 | -- | Bituminous-stabilized (2.9% AC) gravelly sand | 15 | -- | E-11 (CH) | 4 |
| S4 | | | 3 | AC | 6 | -- | Unstabilized gravelly sand | 15 | -- | E-11 (CH) | 4 |
| S5 | | | 3 | Crushed limestone | 6 | -- | Lean clay, 3.5% lime | 15 | -- | E-11 (CH) | 4 |
| S6 | | | 3 | Crushed limestone | 6 | -- | Lean clay, 10% PC | 15 | -- | E-11 (CH) | 4 |
| S7 | | | 3 | Crushed limestone | 21 | -- | -- | -- | -- | E-11 (CH) | 4 |
| S8 | | | 3 | Clayey gravelly sand with 6% PC | 21 | -- | -- | -- | -- | E-11 (CH) | 4 |
| S9 | | | 3 | Crushed limestone | 6 | -- | Lean clay, 3% lime, 2% PC, 10% fly ash | 25 | -- | E-11 (CH) | 3 |
| S10 | | | 3 | Lean clay (12%) PC | 25 | -- | -- | -- | -- | E-11 (CH) | 4 |
| S11 | | | 3 | Gravelly sand (5%) PC | 25 | -- | -- | -- | -- | E-11 (CH) | 4 |
| S12 | | | 3 | Clay sand (5%) PC | 25 | -- | -- | -- | -- | E-11 (CH) | 4 |
| S13 | | | 3 | Crushed limestone | 6 | -- | Gravelly sand | 33 | -- | E-11 (CH) | 4 |

Note: Test site locations are listed on page 67. FAA soil classifications⁴² are given first, followed by Unified Soil Classification System⁴³ groups in parentheses.

* Data furnished by Site Engineers, Inc., Cherry Hill, N. J.

** Data furnished by Brandley Engineering of Sacramento, Calif.

Table 5
Physical Properties of Rigid Pavements

| Test Site No. | Location | Facility | PCC Thickness in. | Flexural Strength psi | Base Course | | k pci | Subgrade Material | Single-Wheel Load kips |
|---------------|--------------|------------------|-------------------|-----------------------|---------------|---------------|-------|-------------------|------------------------|
| | | | | | Material | Thickness in. | | | |
| N7 | NAFEC | N-S runway | 7 | 810 | E-1 (GW) | 8 | 390 | E-4 (SP-SM) | 24.3 |
| N8 | | N-S runway | 7 | 880 | E-1 (GW) | 8 | 360 | E-4 (SP-SM) | 26.6 |
| N9 | | E-W runway | 10 | 724 | E-1 (GW) | 8 | 325 | E-4 (SP-SM) | 36.7 |
| N10 | | E-W runway | 7 | 828 | E-2 (GP) | 8 | 285 | E-4 (SP-SM) | 24.0 |
| N11 | | E-W runway | 7 | 894 | E-7 (ML-CL) | 8 | 200 | E-4 (SP-SM) | 24.4 |
| N13 | | Firehouse ramp | 7 | 910 | E-2 (GP) | 8 | 450 | E-4 (SP-SM) | 28.6 |
| N15 | | E-W runway | 10 | 864 | E-7 (ML-CL) | 9 | 100 | E-4 (SP-SM) | 37.1 |
| N16 | | NAFEC ramp | 15 | 760 | -- | -- | 370 | E-4 (GP) | 74.4 |
| N17 | | ANG ramp | 7-1/2 | 820 | -- | -- | 156 | E-6 (ML) | 23.8 |
| H1 | Houston | Taxiway K | 14 | 868 | Soil-cement | 9 | 205 | E-6 (ML) | 81.4 |
| H3 | | Taxiway K | 12 | 929 | Soil-cement | 8 | 375 | E-6 (ML) | 74.4 |
| H7 | | Taxiway B | 12 | 929 | E-5 (SP-SM) | 5-1/2 | 375 | E-6 (ML) | 64.0 |
| H9 | | Taxiway B | 12-1/2 | 891 | E-5 (SP-SM) | 11-1/2 | 425 | E-6 (ML) | 66.6 |
| H11 | | Taxiway B | 12-1/2 | 894 | E-5 (SP-SM) | 11 | 450 | E-6 (ML) | 67.4 |
| J1 | Jackson | W runway | 9-1/2 | 754 | Soil-cement | 6-1/4 | 190 | E-7 (CL) | 37.7 |
| J2 | | W runway | 11 | 724 | Soil-cement | 4 | 175 | E-7 (CL) | 40.8 |
| J3 | | Light plane ramp | 7-1/2 | 740 | Soil-cement | 4-3/4 | 230 | E-7 (CL) | 26.2 |
| J4 | | W runway | 11-1/2 | 709 | Soil-cement | 6 | 195 | E-7 (CL) | 45.2 |
| J5 | | W runway | 8-3/4 | 966 | Soil-cement | 8 | 210 | E-7 (CL) | 48.2 |
| I7 | Indianapolis | Runway 4-22 | 11-3/4 | 900 | Gravelly sand | 10-3/4 | 280 | E-4 (SP-SM) | 57.6 |
| I8 | | Runway 4-22 | 12 | 1003 | Gravelly sand | 11-1/2 | 280 | E-4 (SP-SM) | 66.3 |
| I13 | | Taxiway A | 12 | 870 | Gravelly sand | 6 | 225 | E-6 (SP-SC) | 55.8 |
| I17 | | Runway 13-31 | 11-1/2 | 970 | Gravelly sand | 10-1/2 | 275 | E-4 (SP-SM) | 59.8 |
| I20 | | Runway 13-31 | 10 | 984 | Gravelly sand | 8-1/2 | 270 | E-4 (SP-SM) | 48.6 |
| I22 | | Taxiway B | 11-1/4 | 1015 | Gravelly sand | 8-1/4 | 230 | E-5 (SM) | 99.0 |
| I35 | | Terminal ramp | 12-1/2 | 820 | Gravelly sand | 10-1/2 | 300 | E-3 (GC) | 58.4 |
| I39 | | Terminal ramp | 12 | 870 | Gravelly sand | 10 | 290 | E-1 (GW) | 57.8 |
| I40 | | Terminal ramp | 14-1/2 | 775 | Gravelly sand | 6-1/2 | 205 | E-6 (SP-SC) | 66.7 |

Note: Test site locations are listed on page 67.

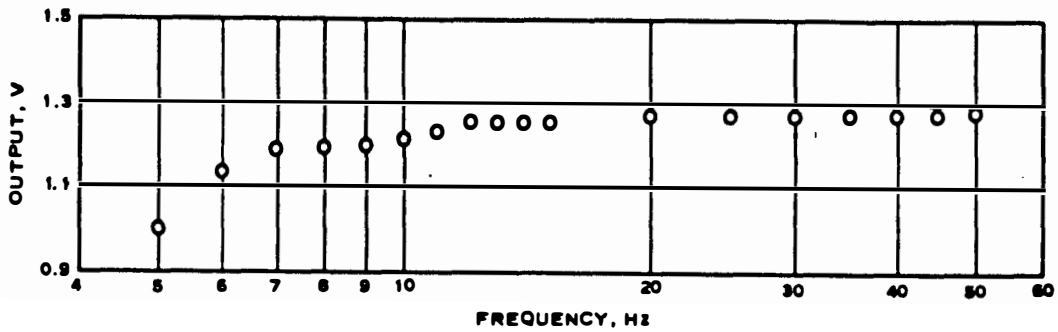


Figure 25. Output versus frequency from velocity transducer No. 101 (input is a constant amplitude of deflection)

because of the many other factors that also varied. Tests were therefore conducted with the 16-kip vibrator using 12-, 18-, and 30-in.-diam load plates. Examples of the DSM values obtained using these plate sizes are shown in Figure 26. These tests were conducted on the flexible pavement test section shown in Figure 27.

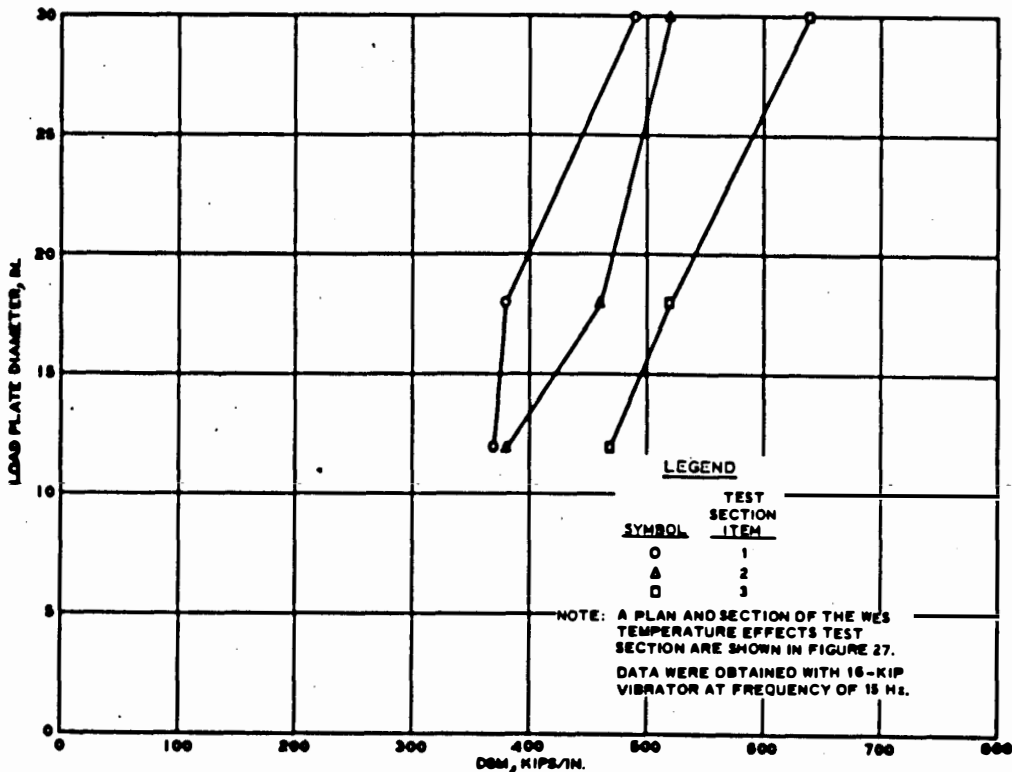


Figure 26. Load plate diameter versus DSM on WES temperature effects test section

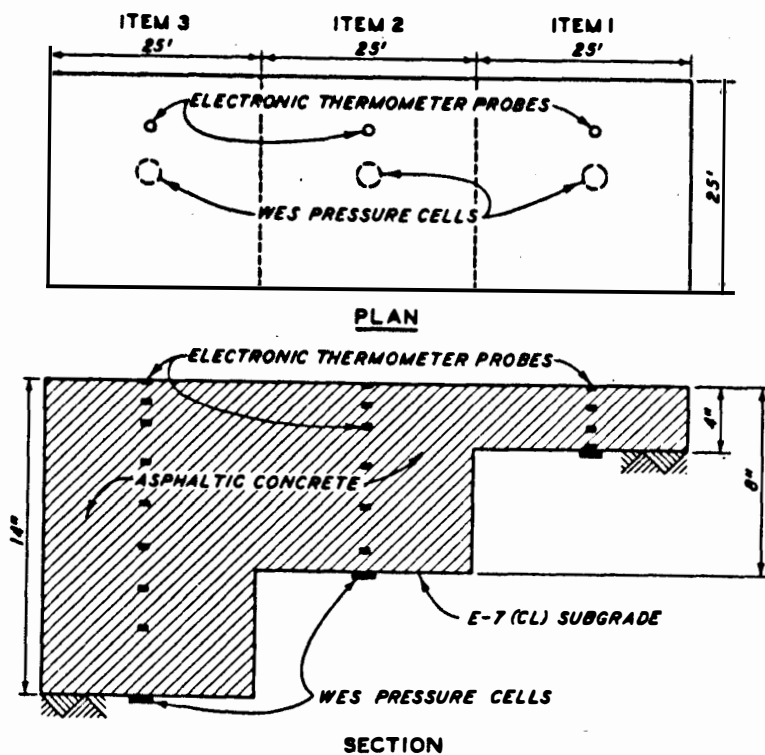


Figure 27. Plan and section of the WES temperature effects test section

The tabulation below shows the tire contact areas of several civil aircraft.

| <u>Aircraft</u> | <u>Tire Contact Area, sq in.</u> |
|-----------------|----------------------------------|
| Boeing 727 | 210 |
| DC-8-63F | 220 |
| Boeing 747 | 205 |
| DC-10-10 | 294 |
| DC-10-30 | 331 |
| L-1011 | 282 |
| Concorde | 247 |

Given the variation in DSM values obtained with the different plate sizes and the range of contact areas listed above, it was decided that a standard plate size should be selected and that it should approximate the contact areas of the tires of the above aircraft. The 18-in.-diam plate with a contact area of 254 sq in. was therefore selected.

ACCURACY TESTS WITH 16-KIP VIBRATOR

The accuracy and reproducibility of test results from the 16-kip vibrator were studied in order to determine confidence levels for the data collected. The following paragraphs present results of laboratory calibrations and checks and field tests to determine these factors.

LABORATORY CHECKS ON VELOCITY TRANSDUCERS

During field testing, five velocity transducers are calibrated to measure deflections induced by the 16-kip vibrator. One transducer is mounted to the center of the 18-in.-diam load plate, and the other four are usually spaced at distances of 6, 20, 32, and 44 in. from the edge of the load plate (Figure 28). The typical response of one of the transducers for varying frequencies is shown in Figure 25. The output of the transducers in volts is directly proportional to velocity. Deflection can be computed from velocity by

$$d = \frac{V}{4\pi f} \quad (1)$$

where

d = peak deflection, in.

V = wave velocity, in./sec

f = vibrator frequency, Hz

During the field tests, velocity is electronically integrated to provide data in terms of deflection. The transducer signal is digitized so that deflection is provided to the X-Y plotter and the digital printer in inches of peak deflection.

The transducers are less sensitive at frequencies below 13 Hz. Figure 25 shows that the typical response of the transducers is practically constant between 13 and 50 Hz.

The accuracy of the five velocity transducers was checked on a calibrated shake table in June 1972. The calibration of the shake table was based on an MB Model 124 vibration transducer (Serial No. 15939) which was calibrated by MB Electronics. The maximum percent error of the shake table was computed as 5 percent of the reading. The shake

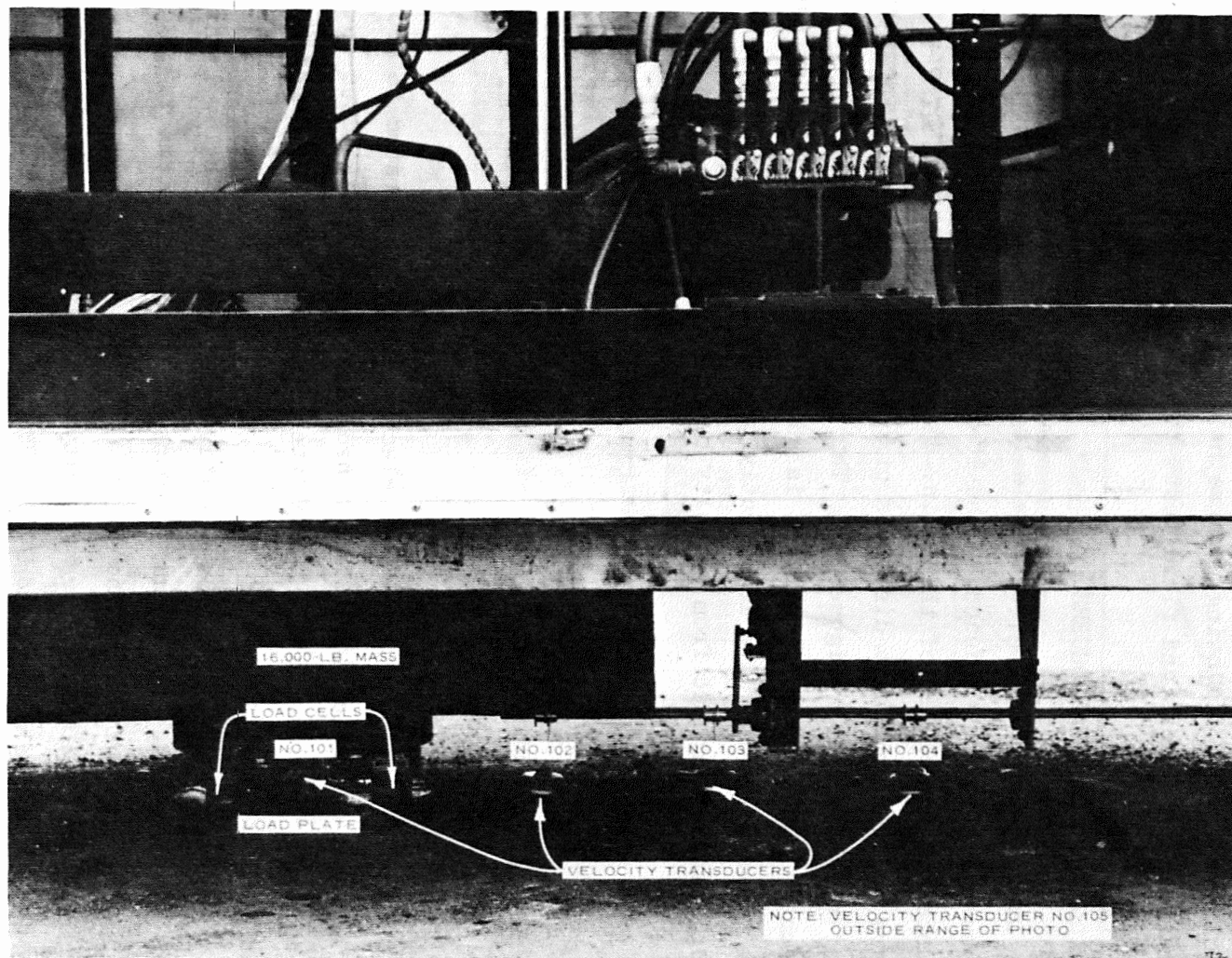


Figure 28. View of load plate, load cells, and velocity transducers of 16-kip vibrator

table had a maximum stroke of 0.5 in. Each transducer was vibrated at known deflections on the shake table, and the output signal from each transducer was recorded on the 16-kip vibrator data acquisition system (DAS). Comparisons between the known input (shake table) deflection and the measured output (transducer) deflection at a frequency of vibration of 15 Hz are shown in Table 6. The accuracy of the DAS in measuring and recording deflection is shown in Table 6 as percent error. The percent error was computed as the measured deflection X_{p2} minus the known input deflection X_{p1} divided by the known input deflection multiplied by 100. The DAS was calibrated exactly as in field operations. The known input deflection ranged from 0.5×10^{-3} to 30×10^{-3} in., which is the full scale range of the transducers. The shake table was operated at the known input deflections specified in Table 6, and the output of the velocity transducer attached to the table was electronically integrated and recorded as measured deflection through the DAS. The percent error was greater than 10 for only two measurements: one measurement gave a 17.4 percent error for velocity transducer No. 101, and one measurement gave an 11.6 percent error for velocity transducer No. 103. The larger percent errors generally occurred at lower input deflections. Measured peak deflection for velocity transducer No. 101 is shown in Figure 29.

FIELD CHECKS ON VELOCITY TRANSDUCERS

Field tests were conducted in which the velocity transducers were checked against one another by placing the four mobile transducers at equal distances from the load plate and recording the deflections at a constant load. The results of three of these tests are presented in Table 7. Also presented in Table 7 are 90 percent errors in deflection measurements for each of the three tests and the 90 percent errors expressed as percentages of the average deflections for each of the three tests.

Once a number of measurements have been made of a certain quantity, the precision of a measuring instrument can be evaluated and its accuracy estimated by computing the size of the limiting error for

Table 6
Accuracy Test of 16-Kip Vibrator DAS

| Deflection Difference | | | | Deflection Difference | | | |
|------------------------------------|----------------------|---|--|----------------------------------|----------------------|---|--|
| Deflection, 10 ⁻³ in. | | Δx_p ($x_{p2} - x_{p1}$) 10 ⁻³ in. | Percent Error ($\Delta x_p / x_{p1}$) 100 | Deflection, 10 ⁻³ in. | | Δx_p ($x_{p2} - x_{p1}$) 10 ⁻³ in. | Percent Error ($\Delta x_p / x_{p1}$) 100 |
| Known Input x_{p1} | Measured x_{p2} | | | Known Input x_{p1} | Measured x_{p2} | | |
| <u>Velocity Transducer No. 101</u> | | | | | | | |
| 0.5 | 0.413 | -0.087 | 17.4 | 4.0 | 3.897 | -0.103 | 3.2 |
| 1.0 | 0.985 | -0.015 | 1.5 | 4.5 | 4.370 | -0.130 | 2.9 |
| 1.5 | 1.435 | -0.065 | 4.3 | 5.0 | 4.872 | -0.128 | 2.6 |
| 2.0 | 1.920 | -0.080 | 4.0 | 7.5 | 7.302 | -0.693 | 9.2 |
| 2.5 | 2.424 | -0.076 | 3.0 | 10.0 | 9.963 | -0.037 | 0.4 |
| 3.0 | 2.902 | -0.098 | 3.3 | 20.0 | 19.43 | -0.570 | 2.8 |
| 3.5 | 3.413 | -0.087 | 2.5 | 30.0 | 29.10 | -0.900 | 3.0 |
| <u>Velocity Transducer No. 102</u> | | | | | | | |
| 0.5 | 0.474 | -0.026 | 5.2 | 4.0 | 4.04 | +0.04 | 1.0 |
| 1.0 | 1.075 | +0.075 | 7.5 | 4.5 | 4.51 | +0.01 | 0.2 |
| 1.5 | 1.526 | +0.026 | 1.7 | 5.0 | 5.03 | +0.03 | 0.6 |
| 2.0 | 2.01 | +0.01 | 0.5 | 7.5 | 7.52 | +0.02 | 0.3 |
| 2.5 | 2.52 | +0.02 | 0.8 | 10.0 | 10.60 | +0.60 | 6.0 |
| 3.0 | 3.02 | +0.02 | 0.7 | 20.0 | 19.99 | -0.01 | 0.0 |
| 3.5 | 3.52 | +0.02 | 0.5 | 30.0 | 30.20 | +0.20 | 0.7 |
| <u>Velocity Transducer No. 103</u> | | | | | | | |
| 0.5 | 0.452 | -0.048 | 9.6 | 4.0 | 3.81 | -0.19 | 4.8 |
| 1.0 | 1.001 | +0.001 | 0.1 | 4.5 | 4.265 | -0.235 | 5.2 |
| 1.5 | 1.455 | -0.045 | 3.0 | 5.0 | 4.76 | -0.24 | 4.8 |
| 2.0 | 1.902 | -0.098 | 4.9 | 7.5 | 7.13 | -0.87 | 11.6 |
| 2.5 | 2.37 | -0.130 | 5.2 | 10.0 | 10.09 | +0.09 | 0.9 |
| 3.0 | 2.85 | -0.15 | 5.0 | 20.0 | 18.87 | -0.13 | 0.6 |
| 3.5 | 3.31 | -0.19 | 5.4 | -- | -- | -- | -- |
| <u>Velocity Transducer No. 104</u> | | | | | | | |
| 0.5 | 0.460 | -0.040 | 8.0 | 3.5 | 3.43 | -0.07 | 2.0 |
| 1.0 | 1.02 | +0.02 | 2.0 | 4.0 | 3.91 | -0.09 | 2.2 |
| 1.5 | 1.49 | -0.01 | 0.7 | 4.5 | 4.39 | -0.11 | 2.4 |
| 2.0 | 1.96 | -0.04 | 2.0 | 5.0 | 4.95 | -0.05 | 1.0 |
| 2.5 | 2.46 | -0.04 | 1.6 | 7.5 | 7.40 | -0.10 | 1.3 |
| 3.0 | 2.95 | -0.05 | 1.7 | 10.0 | 10.45 | +0.45 | 4.5 |
| <u>Velocity Transducer No. 105</u> | | | | | | | |
| 0.5 | 0.461 | -0.039 | 7.8 | 4.0 | 4.03 | +0.03 | 0.8 |
| 1.0 | 1.02 | +0.02 | 2.0 | 4.5 | 4.50 | -- | -- |
| 1.5 | 1.51 | +0.01 | 0.7 | 5.0 | 5.02 | +0.02 | 0.4 |
| 2.0 | 2.00 | -- | -- | 7.5 | 7.50 | -- | -- |
| 2.5 | 2.53 | +0.03 | 1.2 | 10.0 | 10.61 | +0.61 | 6.1 |
| 3.0 | 3.01 | +0.01 | 0.3 | 20.0 | 19.84 | -0.16 | 0.8 |
| 3.5 | 3.52 | +0.02 | 0.5 | 30.0 | 29.81 | -0.19 | 0.6 |

Table 7

Deflection Measurements with Velocity Transducers at Equal Distances from Load Plate

| <u>Date</u> | <u>16-Kip Vibrator Recording Channel</u> | <u>Deflection, in.</u> | <u>Error v (Average - Measured Deflection), in.</u> | <u>90 Percent Error E_{90} $\left(1.6449 \sqrt{\frac{\sum v^2}{n-1}}\right)$ in.</u> | <u>E_{90}, Per- cent of Average Deflection</u> |
|-------------|--|------------------------|---|--|---|
| 25 May 1973 | 8 | 0.003467 | -0.000014 | 0.000138 | 4.00 |
| | 7 | 0.003443 | -0.000010 | | |
| | 6 | 0.003553 | +0.000100 | | |
| | 5 | 0.003348 | -0.000105 | | |
| | Average | 0.003453 | | | |
| 26 May 1973 | 8 | 0.005046 | -0.000016 | 0.000060 | 1.18 |
| | 7 | 0.005021 | -0.000041 | | |
| | 6 | 0.005079 | +0.000017 | | |
| | 5 | 0.005104 | +0.000042 | | |
| | Average | 0.005062 | | | |
| 16 Mar 1973 | 8 | 0.001516 | +0.000063 | 0.000096 | 6.61 |
| | 7 | 0.001478 | +0.000025 | | |
| | 6 | 0.001380 | -0.000073 | | |
| | 5 | 0.001438 | -0.000015 | | |
| | Average | 0.001453 | | | |

Note: 16-kip vibrator was set at a constant load of 10 kips.

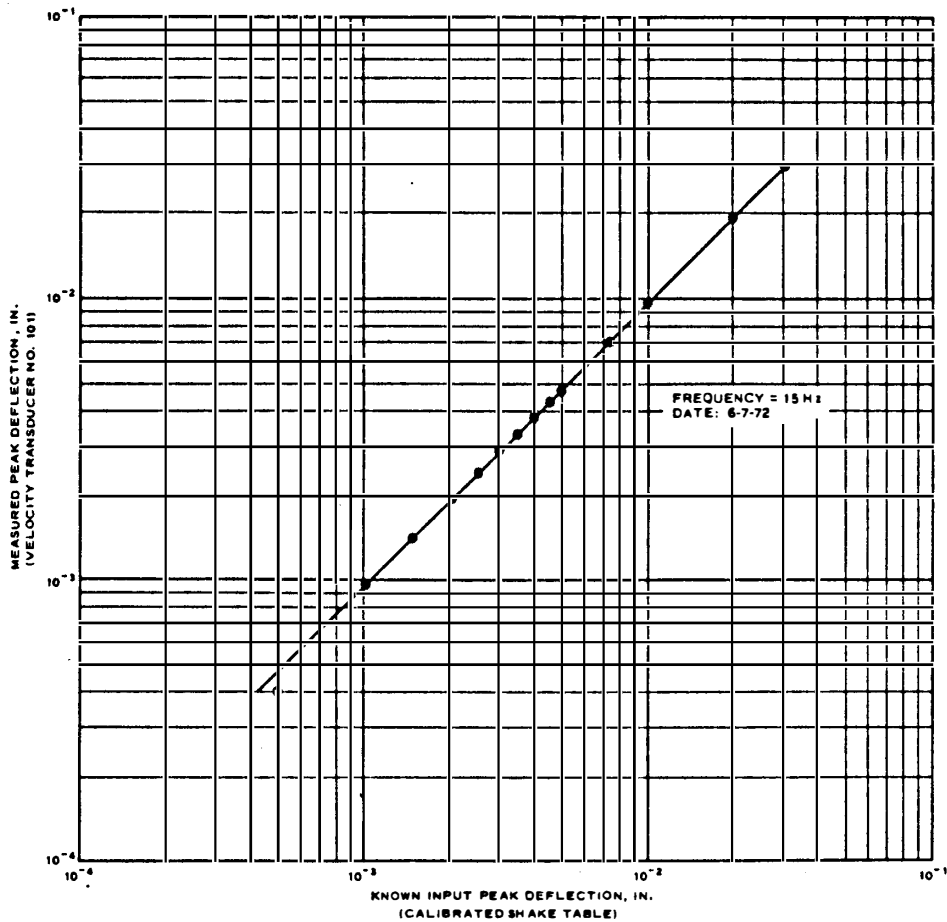


Figure 29. Measured peak deflection versus known input peak deflection

any given percentage. The limiting error for 90 percent of the errors is called the 90 percent error E_{90} . The equation for percent error can be written as

$$E_p = C_p \sqrt{\frac{\sum v^2}{n-1}} \quad (2)$$

where

E_p = percent error

C_p = numerical constant (for E_{90} , $C_p = C_{90} = 1.6449$)

$\sum v^2$ = sum of the squares of the errors, in which each error is the difference from the average deflection of the measured deflection

n = number of measurements or errors

The E_{90} values expressed as percentages of the average deflections for the three tests presented in Table 7 are plotted versus the average deflections in Figure 30.

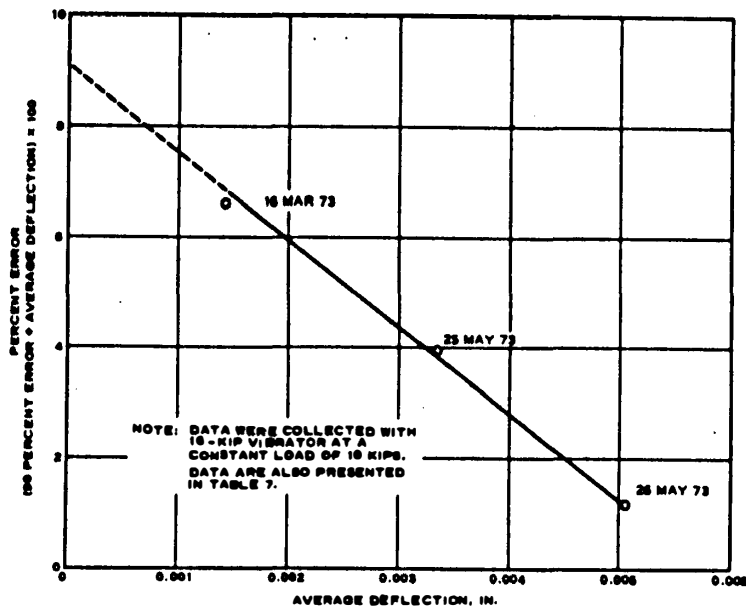


Figure 30. Percent error versus average deflection

Another means of checking velocity transducers against one another is to inspect a deflection basin plot. Maximum deflection should occur at the load plate, and minimum deflection should occur at the velocity transducer farthest from the load plate (deflection should decrease as the distance from the load plate increases). Deflections at the other three transducers should fall between the maximum and minimum deflections. This check was applied throughout the testing program as the data were collected.

FIELD CHECKS ON LOAD CELLS

Three load cells spaced near the edge of the load plate at 120-deg angles to each other are used to measure loads induced by the 16-kip vibrator. Two of these load cells are visible in Figure 28.

The load cells are 20,000-lb-capacity dynamic tension-compression cells. They have a safe overload limit of 150 percent of the rated capacity and can withstand a maximum side load, without damage, of

100 percent of the axial load capacity. The cells have a certified calibration by the manufacturer and were calibrated at WES using standardized 10,000- and 100,000-lb proving rings. The calibration accuracy of the load cells is 0.25 percent of the recorded load. Thus, for a vibratory load of 15,000 lb, the error due to the load cells would not exceed 37.5 lb. The load cells are electronically balanced and calibrated at the beginning of each day of testing and are physically checked by comparing the static weight of the vibrator recorded by the cells with the known weight.

REPRODUCIBILITY OF TEST RESULTS

The 16-kip vibrator has three methods of recording load and deflection:

- a. An X-Y plotter which automatically records load versus deflection on a continuous plot. Deflection can be scaled from this plot to four decimal places.
- b. A digital printer which prints loads and deflections to six decimal places on command.
- c. An oscillograph which records wave forms. Load and deflection can be scaled to four decimal places from the oscillograph output.

Table 8 presents data collected from 21 sites and shows comparisons between data collected using the X-Y plotter (Column 1) and data collected using the digital printer (Columns 2 and 3) for the velocity transducers on the load plate. The data in Column 3 were collected as the load versus deflection plots were being drawn. Data in Column 2 were collected in an operation independent of that used to obtain data for Columns 1 and 3, but the same electronic circuitry as that used for Column 3 was employed. Thus, the values in Columns 1-3 are independent measurements of the same quantity. Table 8 also presents the E_{90} values and E_{90} values expressed as a percent of the average of the three deflections for each of the 21 test sites. The data for test sites B2 and B3A appear to contain errors larger than those normally encountered. If these data are arbitrarily discounted, the

Table 8
Deflection Measurements and E₉₀

| Test Site No. | Date | Deflection at 10,000-lb Peak Load and 15 Hz, in. | | | Error v (Measured Deflection from Cited Column Minus Average Deflection for Three Columns), in. | | | E ₉₀ in. | E ₉₀ , Percent of Average Deflection | Average Deflection in. |
|---------------|-------------|---|---|--|---|----------|----------|---------------------|---|------------------------|
| | | Column 1 Scaled from Load Versus Deflection Plot | Column 2 From Frequency Sweep Printout | Column 3 Channel 4 of Deflection Basin Printout | Column 1 | Column 2 | Column 3 | | | |
| B1 | 25 May 1973 | 0.0030 | 0.003196 | 0.003184 | -0.0001 | +0.0001 | +0.0001 | 0.0002 | 6.45 | 0.0031 |
| B2A | 25 May 1973 | 0.0088 | 0.008150 | 0.008925 | +0.0002 | -0.0004 | +0.0003 | 0.0006 | 6.98 | 0.0086 |
| B2 | 29 May 1973 | 0.0098 | 0.007325 | 0.010007 | +0.0008 | -0.0017 | +0.0010 | 0.0025 | 27.78 | 0.0090 |
| | Difference | 0.0010 | 0.000825 | 0.001082 | -- | -- | -- | -- | -- | 0.0004 |
| B3A | 26 May 1973 | 0.0071 | 0.005879 | 0.006863 | +0.0005 | -0.0007 | +0.0003 | 0.0010 | 15.15 | 0.0066 |
| B3 | 26 May 1973 | 0.0060 | 0.005594 | 0.006069 | +0.0001 | -0.0003 | +0.0002 | 0.0004 | 6.78 | 0.0059 |
| | Difference | 0.0011 | 0.000285 | 0.000794 | -- | -- | -- | -- | -- | 0.0007 |
| W1A | 30 May 1973 | 0.0093 | 0.009197 | 0.009104 | +0.0001 | -0.0000 | -0.0001 | 0.0002 | 2.17 | 0.0092 |
| W1 | 30 May 1973 | 0.0108 | 0.010417 | 0.010409 | +0.0003 | -0.0001 | -0.0001 | 0.0004 | 3.81 | 0.0105 |
| | Difference | 0.0015 | 0.001220 | 0.001305 | -- | -- | -- | -- | -- | 0.0013 |
| W2A | 31 May 1973 | 0.0050 | 0.005308 | 0.005174 | -0.0002 | +0.0001 | -0.0000 | 0.0003 | 5.77 | 0.0052 |
| W2 | 31 May 1973 | 0.0048 | 0.004927 | 0.004996 | -0.0001 | +0.0000 | +0.0001 | 0.0002 | 4.08 | 0.0049 |
| | Difference | 0.0002 | 0.000381 | 0.000178 | -- | -- | -- | -- | -- | 0.0003 |
| F13A | 1 Jun 1973 | 0.0045 | 0.004144 | 0.004470 | +0.0001 | -0.0003 | +0.0001 | 0.0004 | 9.09 | 0.0044 |
| F13 | 1 Jun 1973 | 0.0035 | 0.003605 | 0.003723 | -0.0001 | +0.0000 | +0.0001 | 0.0002 | 5.56 | 0.0036 |
| | Difference | 0.0010 | 0.000539 | 0.000747 | -- | -- | -- | -- | -- | 0.0008 |
| F14 | 1 Jun 1973 | 0.0047 | 0.004347 | 0.004636 | +0.0001 | -0.0003 | +0.0000 | 0.0004 | 8.69 | 0.0046 |
| F14A | 1 Jun 1973 | 0.0051 | 0.004855 | 0.005113 | +0.0001 | -0.0001 | +0.0001 | 0.0002 | 4.00 | 0.0050 |
| | Difference | 0.0004 | 0.000508 | 0.000477 | -- | -- | -- | -- | -- | 0.0004 |
| J3 | 23 Jul 1973 | 0.0050 | 0.004956 | 0.005075 | 0.0000 | 0.0000 | +0.0001 | 0.0001 | 2.00 | 0.0050 |
| J3A | 23 Jul 1973 | 0.0065 | 0.006934 | 0.006666 | -0.0002 | +0.0002 | -0.0000 | 0.0003 | 4.48 | 0.0067 |
| | Difference | 0.0015 | 0.001978 | 0.001591 | -- | -- | -- | -- | -- | 0.0017 |
| J4 | 25 Jul 1973 | 0.0035 | 0.003499 | 0.003569 | +0.0000 | -0.0000 | +0.0001 | 0.0001 | 2.86 | 0.0035 |
| J4A | 25 Jul 1973 | 0.0029 | 0.003137 | 0.003099 | -0.0001 | +0.0001 | +0.0001 | 0.0002 | 6.67 | 0.0030 |
| | Difference | 0.0006 | 0.000362 | 0.000470 | -- | -- | -- | -- | -- | 0.0005 |
| J5 | 25 Jul 1973 | 0.0050 | 0.005374 | 0.005009 | -0.0001 | +0.0003 | -0.0001 | 0.0004 | 7.84 | 0.0051 |
| J5A | 30 Jul 1973 | 0.0048 | 0.004928 | 0.004828 | +0.0000 | +0.0001 | -0.0000 | 0.0001 | 2.08 | 0.0048 |
| | Difference | 0.0002 | 0.000446 | 0.000181 | -- | -- | -- | -- | -- | 0.0003 |
| J1 | 27 Jul 1973 | 0.0034 | 0.003366 | 0.003459 | 0.0000 | 0.0000 | +0.0001 | 0.0001 | 2.94 | 0.0034 |
| J2 | 27 Jul 1973 | 0.0058 | 0.005550 | 0.005786 | +0.0001 | -0.0002 | +0.0001 | 0.0003 | 5.26 | 0.0057 |

maximum E_{90} value for the other 19 test sites is 9.09 percent of the average deflection.

The data in Table 8 indicate the differences in deflection that can be obtained on similar pavements when deflection measurements are made under the same climatic conditions. Test sites with similar numbers (e.g., B2 and B2A) were made at locations a few feet apart on the same pavement. Test sites B1, B2A, B2, B3A, B3, W1A, W1, W2A, W2, P13A, P13, P14, and P14A were on AC pavements, and the others listed were on PCC pavements. The maximum differences in deflection were 0.0017 in. for two measurements on the same PCC pavement and 0.0013 in. for two measurements on the same AC pavement. In terms of DSM values, the average deflection data show that a variation of as much as 510 kips/in. was encountered on what was assumed to be the same type PCC pavement. This variation does not mean that the reliability of the equipment is within 510 kips/in. because the tests presented here as examples were run some distance apart on the same pavement.

The 16-kip vibrator records deflections to six decimal places; however, the ability of this vibrator to measure deflections accurately to six decimal places has not been proven, and no information is available on the accuracy of other vibrator recording systems. In order to illustrate the range in magnitudes of deflection measurements at different vibratory loads, data from a typical linear load-deflection test at 15 Hz are tabulated below. Deflections obtained using the lighter loads are shown as a ratio of the deflection at a 10-kip load.

| <u>Vibratory Load, kips</u> | <u>Deflection in.</u> | <u>Deflection at 10 Kips/Deflection at Vibratory Load</u> |
|-----------------------------|-----------------------|---|
| 0.5 | 0.00015 | 19.3 |
| 1.0 | 0.0003 | 9.7 |
| 5.0 | 0.0015 | 1.9 |
| 8.0 | 0.0023 | 1.3 |
| 10.0 | 0.0029 | 1.0 |

This tabulation shows that, at a vibratory load of 0.5 kip, the vibrator must have the ability to measure a deflection 19 times smaller than the deflection at a vibratory load of 10 kips. Thus, the deflection created by a vibrator can be so small that the devices which

measure deflection cannot accurately produce measurements. For example, the lower limit of the WES velocity transducer is considered to correspond to an approximate deflection of 0.0005 in. Figure 29 shows that at a deflection of 0.5×10^{-3} in. on a calibrated shake table, the deflection recorded for velocity transducer No. 101 was 0.4×10^{-3} in. or 80 percent of the shake table deflection.

RECOMMENDED NONDESTRUCTIVE TESTING EQUIPMENT

The evaluation of the vibrators shows that vibratory test results are dependent on such characteristics as vibrator static weight, vibratory load, frequency of vibration, load plate type and size, and accuracy of the recording equipment. Larger vibrators may give more accurate results on strong pavements than smaller vibrators, provided the recording equipment for both has the same limitations of accuracy, because larger vibrators create deflections larger than those created by smaller vibrators. Analytical studies of data collected with the different vibrators are under way which will provide more insight into the significance of the characteristics peculiar to a particular vibrator and the effects these characteristics have on pavement response.

From results reported in this section of the report, it is concluded that a standard vibrator must be selected for use with the non-destructive airport pavement evaluation procedure. The vibrator must have the capability to assess the strength of heavy-duty flexible and rigid pavements adequately through application of the heaviest load possible. The necessity for this type of load is described in Reference 44. Although a vibrator with a constant static weight was used to collect data for development of the evaluation methodology described in this report (the possibility of the need for variable mass was not recognized when the 16-kip vibrator was designed), it is recommended that the standard vibrator have a variable mass capability. Also, future work should relate the vibrator mass and force output to the various pertinent aircraft characteristics.

Specifications for a recommended nondestructive testing device

are given in Appendix C. The recommended device is similar to the existing 16-kip vibrator and has a vibratory load capability approaching 16 kips with a frequency range of 5 to 100 Hz, but it has a variable static weight of from 5 to 16 kips.

DEVELOPMENT OF THE EVALUATION METHODOLOGY

The development of the nondestructive evaluation methodology consisted of correlating nondestructive test results with the load-carrying capability of pavements as determined using direct sampling test procedures. The 16-kip vibrator was used to collect the nondestructive load-deflection data necessary for computing DSM values. Only the test results and analyses used in developing the methodology are presented in this section of the report; however, some of the additional data collected during the program are presented in Appendix B.

TESTS CONDUCTED

Data for this study were collected during the period November 1972-December 1973. Pavements selected for testing were free of surface defects, ranged from weak to strong in relative strength, had been subjected to negligible traffic, and were not under the influence of frost or subsequent thaw. The following tabulation lists the facilities where data were collected:

| <u>Facility and Location</u> | <u>Letter Designation Used in Figures and Tables</u> |
|---|--|
| National Aviation Facilities Experimental Center (NAFEC) Atlantic City, N. J. | N |
| Houston Intercontinental Airport, Houston, Tex. | H |
| Washington-Baltimore International Airport, Baltimore, Md. | B |
| Greater Wilmington Airport, Wilmington, Del. | W |
| Philadelphia International Airport, Philadelphia, Pa. | P |
| Jackson Municipal Airport, Jackson, Miss. | J |
| Nashville Metropolitan Airport, Nashville, Tenn. | NV |
| Weir Cook Municipal Airport, Indianapolis, Ind. | I |
| Waterways Experiment Station, Vicksburg, Miss. | S and SS |

DIRECT SAMPLING TESTING PROGRAM

The direct sampling tests consisted of determinations of conventional soil and pavement parameters through in-place tests and laboratory tests of samples of the various pavement elements. In-place tests consisted of density and moisture content determinations and foundation strength (CBR and/or plate bearing) tests on base and subgrade materials. In addition, pavement temperatures were recorded at most of the flexible pavement sites. Laboratory tests were used to determine the gradation, plasticity index, classification, and compaction characteristics of fine-grain materials and the tensile splitting and flexural strength of PCC samples. Test methods used are described in References 42 and 45. Tables 4 and 5 show the pertinent physical properties obtained for the flexible and rigid pavements, respectively.

NONDESTRUCTIVE TESTING PROGRAM

Before test pits were cut in the pavements to perform the direct sampling tests, a series of nondestructive tests was performed on each pavement, usually at two test sites in the same vicinity. An outline of the nondestructive tests which were performed at each test site when time allowed is presented in Table 9. The nondestructive tests were conducted on two test sites for each pavement in order to check the accuracy of the results; however, the test pit was placed at one of these two sites, and only the DSM value for that site was used in analysis. The load-deflection tests were conducted with the 16-kip vibrator at a frequency of 15 Hz. The load-deflection curves were adjusted for nonlinearity (as described earlier in this report) to compute the DSM values.

SPECIAL TESTING PROGRAM

In order to evaluate the effects on DSM values of temperature variations in the AC surfacing layers, joints in the PCC slabs, and freeze-thaw cycles, the following series of tests was conducted.

Effects of AC temperature. The objective of the temperature effects study was to determine if, when all other factors were held

Table 9

Outline of Nondestructive Tests

-
- I. Before start of testing each day, place velocity pickups on equal radii around load plate and check for accuracy within ± 5 percent
 - II. Tests on both AC and PCC pavements
 - A. Frequency sweeps
 - 1. Hold peak load at 10 kips
 - 2. Record frequency and deflection of load plate only
 - a. Between 0 and 40 Hz, proceed in 2-Hz intervals
 - b. Between 40 and 100 Hz, proceed in 5-Hz intervals
 - B. Load-deflection (DSM) measurements
 - 1. Vary peak load from 0 to 15 kips
 - 2. Use frequency of 15 Hz and frequencies for which peak deflections occurred during frequency sweep
 - C. Deflection basin measurements
 - 1. Measure in direction parallel to flow of aircraft traffic
 - 2. Measure at intervals of 2 kips for frequencies used during load-deflection measurements
 - D. Wave velocity measurements
 - 1. Measure in direction parallel to flow of aircraft traffic
 - 2. Measure at intervals of 10 Hz of loading frequency
 - 3. Limiting factors for maximum wavelengths
 - a. For PCC pavements, slab dimensions control
 - b. For AC pavements, length of cable or strength of signal controls
 - III. Temperature tests on AC pavements
 - A. Install electronic thermometer probes on surface of pavement and at depths of 1 and 2 in. and at 2-in. intervals below 2-in. depth
 - B. Record temperatures in 2-hr intervals during testing period
 - IV. Tests on PCC pavements
 - A. DSM profiles
 - 1. Run three profiles with peak load to 15 kips
 - 2. Begin each profile at slab center
 - 3. Measure in three directions in 2-ft intervals
 - a. Run two profiles perpendicular to adjacent slab edges
 - b. Run third profile exactly between other two
 - 4. At slab edge, perform two tests
 - a. Perform one with slab edge and load plate edge coinciding
 - b. Perform one with slab edge bisecting load plate edge
 - B. Joint efficiency determination
 - 1. Place load plate edge at slab edge
 - 2. Place two velocity pickups in line perpendicular to slab edge on opposite sides and 6 in. from edge of load plate
 - 3. Measure deflection at loads of 8,000, 10,000, and 12,000 lb
-

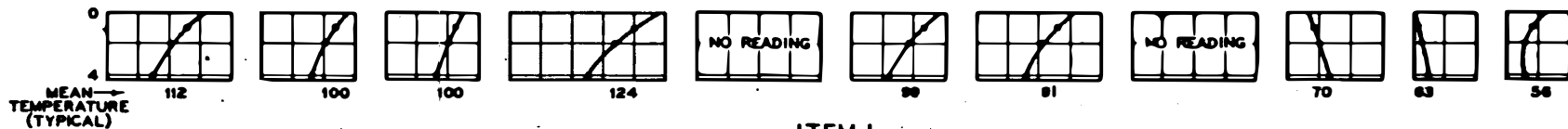
constant, variations in the temperature of the AC surfacing layer would significantly influence load-deflection measurements. If so, a temperature adjustment factor, i.e., a factor to adjust DSM results to a common temperature, would be developed.

A 25- by 75-ft test section at WES composed of AC on lean clay (E-7, ML-CL*) subgrade was used to study the effects of temperature. The test section (Figure 27) contained three 25- by 25-ft test items with AC thicknesses of approximately 4, 8, and 14 in. To limit fluctuations in the subgrade moisture to a minimum, the test section was constructed on a hilltop, ditched on three sides, and provided with paved shoulders and ditches to allow for runoff of precipitation. Pavement temperatures were recorded with electronic thermometer probes installed at the surface of each item and at depths of 1, 2, and 4 in. in item 1; at depths of 1, 2, 4, 6, and 8 in. in item 2; and at depths of 1, 2, 4, 6, 8, 10, and 11.5 in. in item 3, as shown in Figure 27.

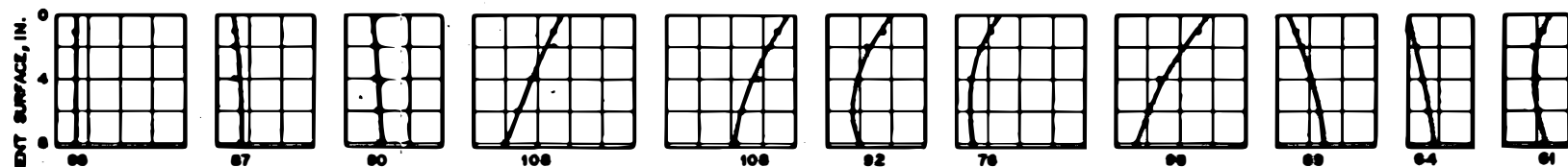
Nondestructive data for the test section were collected at 11 different times. The data collected included DSM values measured at several frequencies, deflection basin measurements, frequency sweeps with the vibratory load held constant, and wave velocity measurements; however, not all forms of nondestructive data were collected at each of the 11 test times. The discussion of temperature effects in the following paragraphs is limited to an analysis of DSM values at 15 Hz since these data were used in developing the methodology.

Temperature readings for each of the three items for the 11 test periods are shown in Figure 31. Surface temperature readings were erratic due to shadows and wind and are therefore not shown. Recorded pavement temperatures at 1 in. below the surface, at the center, and at 1 in. above the bottom of the pavement were averaged to determine the mean pavement temperatures. Mean pavement temperatures versus DSM values for each test item for each of the 11 test periods are shown in Figure 32. Mean pavement temperatures varied between 61° and 124°F,

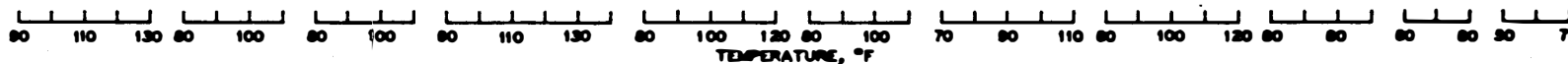
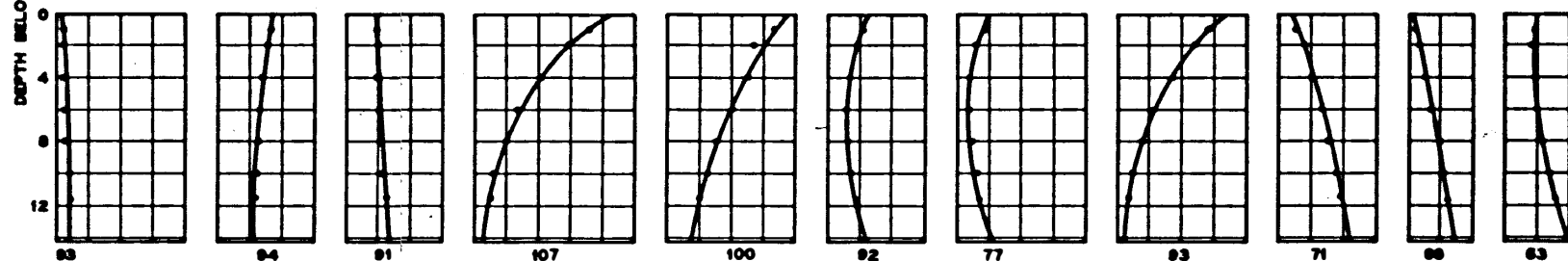
* FAA⁴² soil groups are given first, followed by the corresponding Unified Soil Classification System (USCS)⁴³ group.



ITEM 1



ITEM 2



NOTE: A PLAN AND SECTION OF THE WES TEMPERATURE EFFECTS TEST SECTION ARE SHOWN IN FIGURE 27. TEMPERATURES WERE RECORDED SEVERAL TIMES EACH DAY AND THEN PLOTTED. TEMPERATURES AT TEST TIMES SHOWN IN THIS PLOT AND IN FIGURE 32 WERE INTERPOLATED FROM THE DAILY PLOTS. SURFACE TEMPERATURES WERE ERRATIC DUE TO SHADOWS AND WIND AND WERE NOT PLOTTED.

ITEM 3

Figure 31. Pavement temperatures

with corresponding DSM variations between 1380 and 380 kips/in. The data fell into three groups according to the thicknesses of the three test items, and best-fit lines as determined by the least squares method are drawn through each of the three groups in Figure 32.

The significance of temperature in DSM measurements on the WES temperature effects test section can best be seen in Figure 32 for the 14-in. item, in which the DSM doubled from 600 to 1200 kips/in. in a mean temperature range of 105° to 65°F.

Data from Washington-Baltimore International Airport, Baltimore, Md., are shown in Figure 33 as an example of temperature variations over a short time period. It can readily be seen that daily as well as

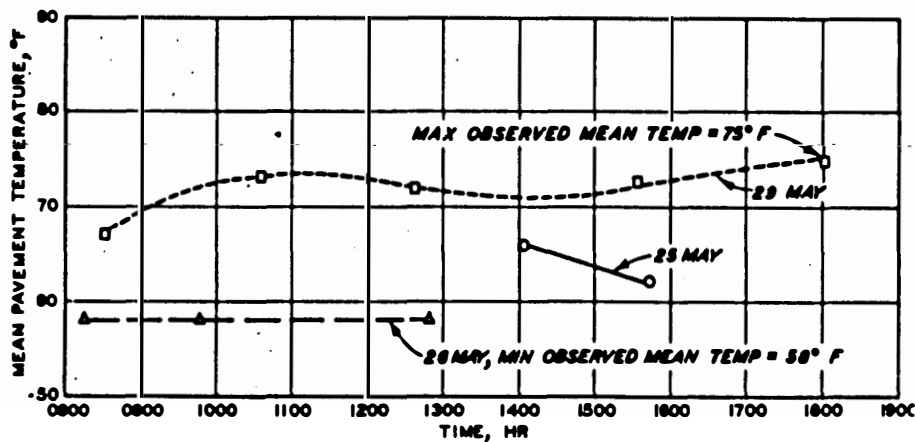
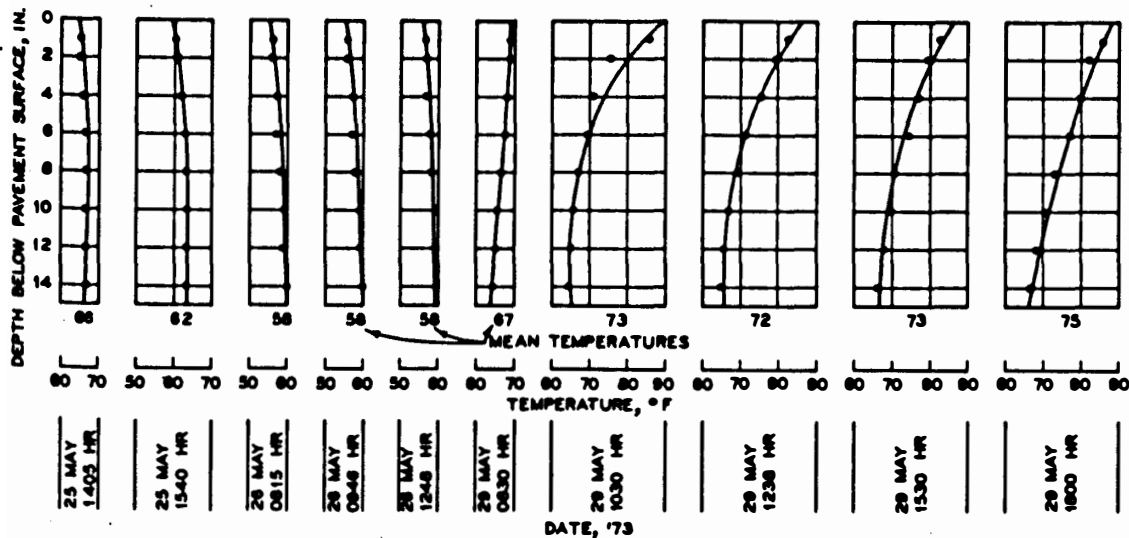


Figure 33. Mean flexible pavement temperatures at Washington-Baltimore International Airport, Baltimore, Md.

seasonal temperature variations have a significant influence on DSM results. Temperature corrections must therefore be applied in order to compare DSM measurements made at different mean pavement temperatures. Data from the temperature effects test section at WES were used to develop temperature adjustment factors shown in Figure 34. Past observations of temperature gradients in AC pavements have shown that practically no daily temperature variations occur below a depth of approximately 12 to 14 in. Therefore, computations of mean temperatures of pavements with AC thicknesses greater than 14 in. should be based on the average of the temperature at 1 in. below the surface, at the center (depth of 7 in.), and at a depth of 13 in. It has not been established that the adjustment factors discussed above are applicable to other flexible pavements in which the pavement structure may be considerably different from that of this test section.

However, the relationships shown in Figures 32 and 34 were used in adjusting the DSM values measured to derive the flexible pavement evaluation curves presented herein. It was assumed that the adjustment, even though it may not have been exact for the pavements involved, would provide a more realistic relationship between DSM values and allowable loadings.

To make the temperature adjustments to the DSM values, a mean pavement temperature was required for each test. Since temperature data were not recorded during each DSM test, an Asphalt Institute procedure⁴⁶ for predicting flexible pavement temperatures was used. This method requires the use of daily maximum and minimum air temperatures for a 5-day period preceding the test date. The 5-day mean air temperatures (Table 10) and the measured surface temperatures (Table 11) were summed and then used with Figure 35 to predict pavement temperatures at the depths shown in Table 11. These predicted pavement temperatures were then used to compute the mean temperatures for the 31 flexible pavements. Also shown in Table 11 are mean temperatures computed for seven of the test sites where the pavement temperatures were measured with thermometer installations. The column in Table 11 titled "Means of Determining Pavement Temperature" indicates whether the mean

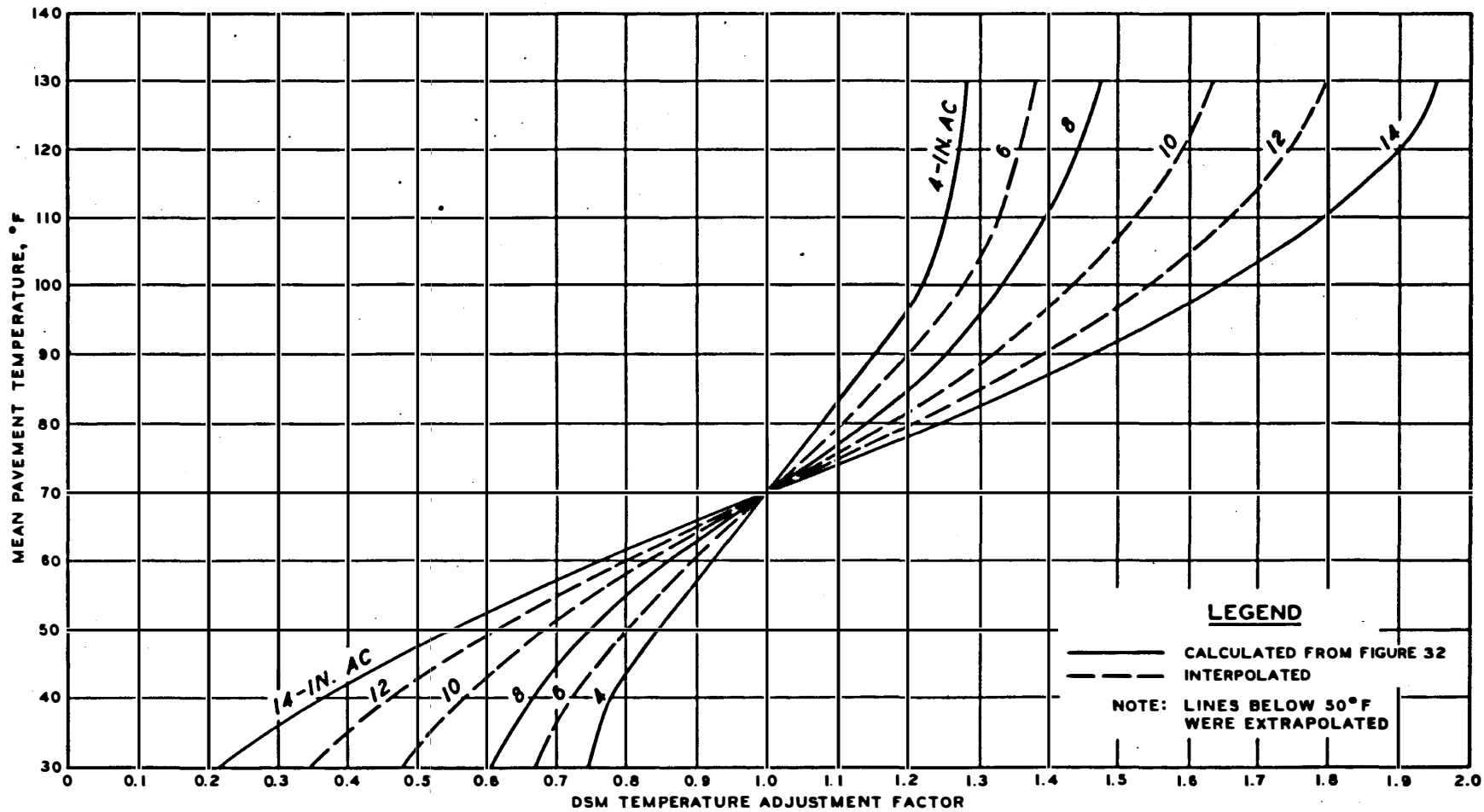


Figure 34. DSM temperature adjustment curves

Table 10

5-Day Mean Air Temperatures at Flexible Pavement Facilities

| <u>Location</u> | <u>Date</u> | <u>High Air Temp- ature, °F</u> | <u>Low Air Temp- ature, °F</u> | <u>5-Day Mean Air Temp- ature, °F</u> |
|---|-------------|-------------------------------------|------------------------------------|---|
| Philadelphia | 30 Nov 72 | 38 | 32 | |
| | 1 Dec 72 | 46 | 35 | |
| | 2 Dec 72 | 51 | 35 | |
| | 3 Dec 72 | 61 | 34 | |
| | 4 Dec 72 | 47 | 37 | 42 |
| | 27 May 73 | 55 | 50 | |
| | 28 May 73 | 81 | 55 | |
| | 29 May 73 | 81 | 65 | |
| | 30 May 73 | 84 | 59 | |
| | 31 May 73 | 77 | 61 | 67 |
| | | | | |
| NAFEC | 10 Nov 72 | 56 | 36 | |
| | 11 Nov 72 | 54 | 45 | |
| | 12 Nov 72 | 59 | 45 | |
| | 13 Nov 72 | 56 | 37 | |
| | 14 Nov 72 | 55 | 41 | 48 |
| Wilmington | 25 May 73 | 57 | 54 | |
| | 26 May 73 | 61 | 53 | |
| | 27 May 73 | 58 | 51 | |
| | 28 May 73 | 82 | 56 | |
| | 29 May 73 | 82 | 67 | 62 |
| | 30 May 73 | 82 | 58 | 65 |
| Baltimore | 20 May 73 | 62 | 54 | |
| | 21 May 73 | 67 | 51 | |
| | 22 May 73 | 78 | 48 | |
| | 23 May 73 | 63 | 55 | |
| | 24 May 73 | 61 | 52 | |
| | 25 May 73 | 55 | 51 | 59 |
| | 26 May 73 | 55 | 52 | 58 |
| | 27 May 73 | 57 | 72 | |
| | 28 May 73 | 83 | 57 | |
| | 29 May 73 | 80 | 64 | 60 |
| | | | | |
| Nashville | 31 May 73 | 75 | 59 | |
| | 1 Apr 73 | 60 | 49 | |
| | 2 Apr 73 | 69 | 48 | |
| | 3 Apr 73 | 62 | 45 | |
| | 4 Apr 73 | 52 | 44 | 56 |
| WES soil stabilization test section | 2 Sep 72 | 94 | 72 | |
| | 3 Sep 72 | 97 | 69 | |
| | 4 Sep 72 | 94 | 72 | |
| | 5 Sep 72 | 94 | 70 | |
| | 6 Sep 72 | 94 | 72 | 83 |

Table 11
Pavement Temperature for Flexible Pavement Facilities

| Test Site No. | Location | Date | AC Thickness in. | Measured Surface Temperature °F | Sum of 5-Day Mean Air Temperature* and Measured Surface Temperature, °F | Pavement Temperature, °F, at Cited Depth, in. | | | | | | | | Means of Determining Pavement Temperature | | Mean Pavement Temperature† °F |
|---------------|----------------------------|-----------|------------------|---------------------------------|---|---|-----|----|----|----|----|----|----|---|----------|-------------------------------|
| | | | | | | | | | | | | | | Predicted** | Measured | |
| | | | | | | 1 | 2 | 4 | 6 | 8 | 10 | 12 | 14 | | | |
| P1 | Philadelphia | 5 Dec 72 | 10 | 52 | 94 | 50 | 50 | 48 | 48 | 47 | | | | X | | 48 |
| P2 | | 5 Dec 72 | 6 | 52 | 94 | 50 | 50 | 48 | 48 | | | | | X | | 49 |
| P5 | | 5 Dec 72 | 3-1/2 | 52 | 94 | 50 | 50 | | | | | | | X | | 50 |
| P13 | | 1 Jun 73 | 14 | 83 | 150 | 85 | 80 | 77 | 74 | 70 | 70 | | | X | | 76 |
| | | | | | | 73 | 73 | 73 | 73 | 73 | 74 | | | | X | 73 |
| P14 | | 1 Jun 73 | 14 | 98 | 165 | 93 | 89 | 84 | 81 | 78 | 78 | | | X | | 83 |
| | | | | | | 84 | 84 | 82 | 80 | 78 | 76 | 76 | | | X | 80 |
| N18 | NAFEC | 15 Nov 72 | 3-1/4 | 29 | 77 | 39 | 39 | | | | | | | X | | 39 |
| N20 | NAFEC | 15 Nov 72 | 6 | 29 | 77 | 39 | 39 | 39 | 39 | | | | | X | | 39 |
| N22 | NAFEC | 15 Nov 72 | 6 | 41 | 89 | 47 | 47 | 44 | 44 | | | | | X | | 46 |
| N23 | NAFEC | 15 Nov 72 | 6 | 41 | 89 | 47 | 47 | 44 | 44 | | | | | X | | 46 |
| W1 | Wilmington | 30 May 73 | 9 | 99 | 161 | 91 | 89 | 83 | 79 | 76 | | | | X | | 83 |
| | | | | | | 95 | 92 | 87 | 83 | 80 | | | | | X | 87 |
| W2 | Wilmington | 31 May 73 | 12 | 81 | 146 | 81 | 79 | 75 | 70 | 69 | | | | X | | 72 |
| | | | | | | 75 | 75 | 73 | 73 | 72 | | | | | X | 73 |
| B1 | Baltimore | 25 May 73 | 17-1/2 | 57 | 116 | 65 | 62 | 58 | 56 | 56 | 56 | | | X | | 59 |
| | | | | | | 64 | 64 | 65 | 66 | 66 | 66 | 66 | 66 | | X | 65 |
| B2 | | 29 May 73 | 12 | 91 | 151 | 85 | 82 | 77 | 73 | 72 | 72 | | | X | | 77 |
| | | | | | | 84 | 81 | 78 | 76 | 71 | 70 | | | | X | 77 |
| B3 | | 26 May 73 | 10-1/2 | 56 | 114 | 62 | 60 | 58 | 56 | 56 | | | | X | | 58 |
| | | | | | | 56 | 56 | 57 | 58 | 58 | 59 | | | | X | 58 |
| NV1 | Nashville | 5 Apr 73 | 13 | 65 | 121 | 66 | 65 | 61 | 60 | 60 | 59 | | | X | | 62 |
| NV3 | Nashville | 5 Apr 73 | 8 | 65 | 121 | 66 | 65 | 61 | 60 | 60 | | | | X | | 62 |
| NV4 | Nashville | 5 Apr 73 | 18 | 65 | 121 | 66 | 65 | 61 | 60 | 60 | 59 | | | X | | 62 |
| 8S1 | WES soil | 7 Sep 72 | 3 | 107 | 190 | 107 | 103 | | | | | | | X | | 105 |
| 81 | stabilization test section | 16 Jun 70 | 15 | 100 | 183 | 104 | | | | 87 | 85 | | | X | | 92 |
| 82 | | 16 Jun 70 | 15 | 100 | 183 | 104 | | | | 87 | 85 | | | X | | 92 |
| 83 | | 16 Jun 70 | 24 | 100 | 183 | 104 | | | | | 85 | 85 | | X | | 91 |
| 84 | | 16 Jun 70 | 3 | 100 | 183 | 104 | 99 | | | | | | | X | | 101 |
| 85 | | 7 Dec 70 | 3 | 70 | 127 | 70 | 68 | | | | | | | X | | 69 |
| 86 | | 7 Dec 70 | 3 | 71 | 128 | 70 | 68 | | | | | | | X | | 69 |
| 87 | | 7 Dec 70 | 3 | 72 | 129 | 71 | 69 | | | | | | | X | | 70 |
| 88 | | 7 Dec 70 | 3 | 72 | 129 | 71 | 69 | | | | | | | X | | 70 |
| 89 | | 7 Sep 72 | 3 | 105 | 185 | 104 | 100 | | | | | | | X | | 102 |
| 810 | | 7 Sep 72 | 3 | 105 | 185 | 104 | 100 | | | | | | | X | | 102 |
| 811 | | 7 Sep 72 | 3 | 105 | 185 | 104 | 100 | | | | | | | X | | 102 |
| 812 | | 7 Sep 72 | 3 | 107 | 187 | 106 | 102 | | | | | | | X | | 104 |
| 813 | | 7 Sep 72 | 3 | 107 | 187 | 106 | 102 | | | | | | | X | | 104 |

* From Table 10.

** Temperatures were predicted using Figure 35.

† The mean pavement temperature is the average of the temperatures for 1 in. below the surface, the center, and 1 in. above the bottom of the AC layer.

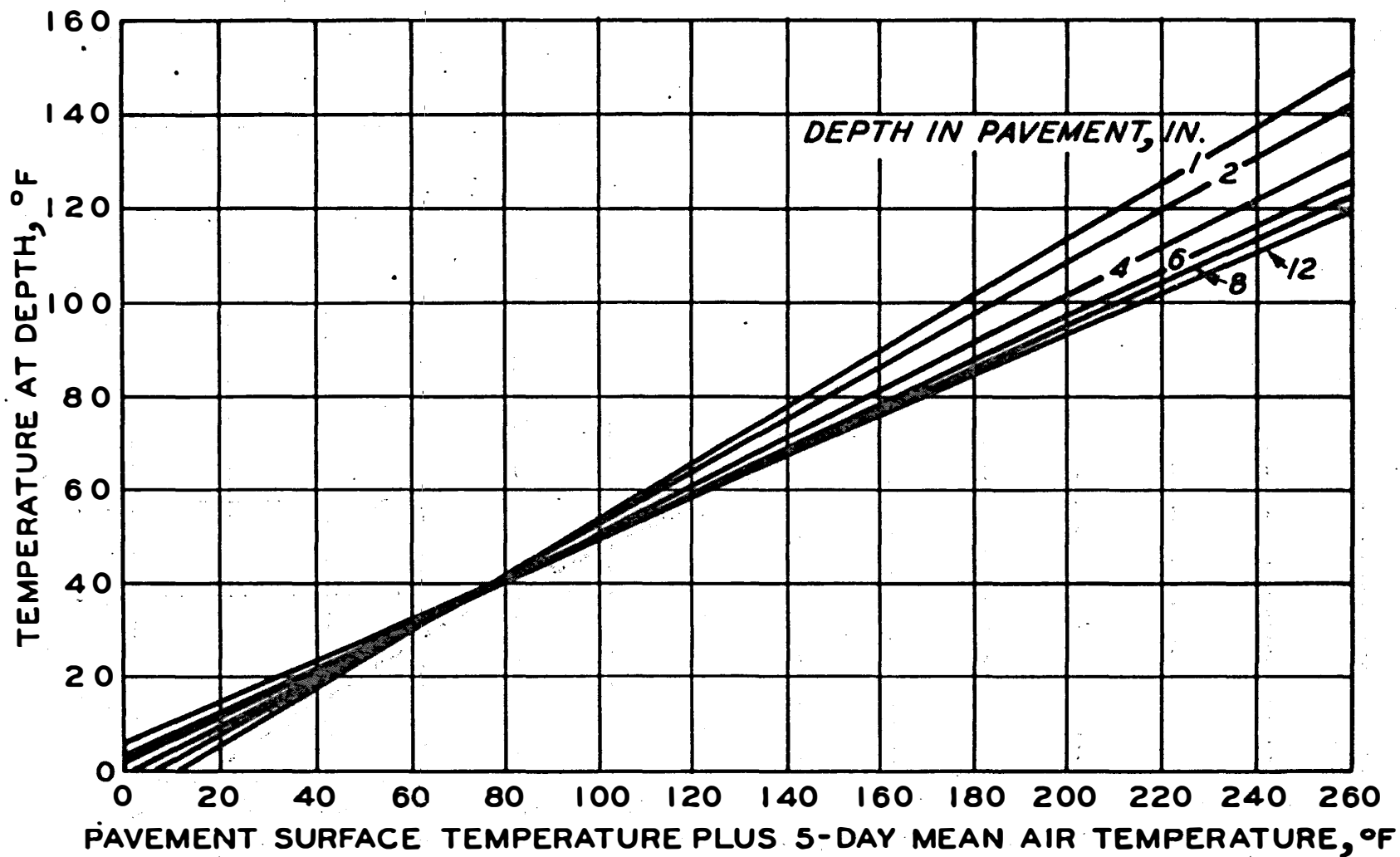


Figure 35. Prediction of flexible pavement temperatures (from Reference 17)

temperature was computed from the predicted or measured temperature. For the test sites at which data were available to compute both measured and predicted temperatures, the differences between the mean pavement temperatures ranged from 1°F (at site W2) to 6°F (at site B1). The mean pavement temperatures were used with Figure 34 to adjust the DSM data as shown in Table 12.

Effects of freeze-thaw cycles. To determine the significance of changes in the DSM of frost-susceptible pavements which take place during freeze-thaw cycles, a study was made at Truax Field in Madison, Wis., at five test sites. Three of the test sites were on flexible pavements, and the other two were on rigid pavements. A summary of pavement and subgrade data at the five test sites is given in Table 13. These data are based on borings made to depths of approximately 6 ft and laboratory soil group classifications. DSM data for the frost study were obtained with the 9-kip vibrator, which was left on the jobsite for the duration of the study. Nondestructive data for the frost study were collected during five test periods that included the freeze, thaw, and normal periods. Two DSM tests were conducted near each test site for each of the five testing times, and the average value was recorded. Pavement and subgrade temperatures were measured with electronic thermometers, the probes of which were mounted on wooden supports and installed in borings. One thermometer probe installation was in a flexible pavement, and the other was in a rigid pavement.

Results of DSM measurements, along with pavement and subgrade temperatures which were measured at the same time, are presented in Tables 14 and 15 for the rigid and flexible pavements, respectively. The DSM value for each period is shown as a percent of the DSM measured on 23 May, which was considered to be the normal period when the pavements were not being influenced by a freeze-thaw cycle. The percent values are given to show the relative differences in DSM values for the different test periods. DSM versus time for the five tests is presented graphically in Figure 36.

The data shown in Figure 36 were obtained during two different

Table 12
Temperature Adjustment of DSM Data

| Test Site No. | Location | AC Thickness in. | Mean Pavement Temperature °F | Measured DSM kips/in. | Adjusted DSM kips/in. |
|---------------|---------------|------------------|------------------------------|-----------------------|-----------------------|
| P1 | Philadelphia | 10 | 48 | 2040 | 1020 |
| P2 | ↓ | 6 | 49 | 740 | 560 |
| P5 | | 3-1/2 | 50 | 910 | 790 |
| P13 | | 14 | 73 | 2780 | 3000 |
| P14 | | 14 | 80 | 2120 | 2630 |
| N18 | NAFEC | 3-1/4 | 39 | 770 | 630 |
| N20 | NAFEC | 6 | 39 | 1860 | 1170 |
| N22 | NAFEC | 6 | 46 | 1040 | 740 |
| N23 | NAFEC | 6 | 46 | 980 | 700 |
| W1 | Wilmington | 9 | 87 | 860 | 1080 |
| W2 | Wilmington | 12 | 73 | 1940 | 2060 |
| B1 | Baltimore | 17-1/2 | 65 | 3120 | 2680 |
| B2 | Baltimore | 12 | 77 | 800 | 920 |
| B3 | Baltimore | 10-1/2 | 58 | 1630 | 1170 |
| NV1 | Nashville | 13 | 62 | 3200 | 2460 |
| NV3 | Nashville | 8 | 62 | 650 | 570 |
| NV4 | Nashville | 18 | 62 | 4160 | 3160 |
| SS1 | WES soil | 3 | 105 | 610 | 730 |
| S1 | stabilization | 15 | 92 | 360 | 520 |
| S2 | test section | 15 | 92 | 270 | 400 |
| S3 | ↓ | 24 | 91 | 480 | 710 |
| S4 | | 3 | 101 | 300 | 350 |
| S5 | | 3 | 69 | 600 | 590 |
| S6 | | 3 | 69 | 680 | 670 |
| S7 | | 3 | 70 | 570 | 570 |
| S8 | | 3 | 70 | 1140 | 1140 |
| S9 | | 3 | 102 | 750 | 900 |
| S10 | | 3 | 102 | 530 | 630 |
| S11 | | 3 | 102 | 600 | 710 |
| S12 | | 3 | 104 | 560 | 680 |
| S13 | | 3 | 104 | 610 | 740 |

Table 13

Pavement and Subgrade Data at Truax Field Test Sites

| Test Site No. | Type Pavement | Bound Pavement Thickness in. | Strata No. | | | | | | | |
|---------------|---------------|------------------------------|-------------|----------------|-------------|----------------|-------------|----------------|-------------|----------------|
| | | | 1 | | 2 | | 3 | | 4 | |
| | | | Soil Groups | Thick-ness in. | Soil Groups | Thick-ness in. | Soil Groups | Thick-ness in. | Soil Groups | Thick-ness in. |
| 1DB | PCC | 11 | E-4 (SW) | 53 | E-3 (GC-GM) | 12+ | -- | -- | -- | -- |
| 2DB | PCC | 9 | E-2 (GP-GM) | 71+ | -- | -- | -- | -- | -- | -- |
| 3DB | AC | 7 | E-2 (GP-GM) | 11 | E-5 (SP-SM) | 18 | E-9 (MH) | 12 | E-7 (ML-CL) | 30+ |
| 5DB | AC | 2 | E-5 (SP-SM) | 16 | E-7 (ML-CL) | 42+ | -- | -- | -- | -- |
| 6DB | AC | 5 | E-5 (SP-SM) | 13 | E-8 (CL) | 24 | E-4 (SW) | 18+ | -- | -- |

Table 14

Results of DSM Measurements on PCC Test Sites

| Test Site No. | PCC Thickness | 22 Feb 73 | | | 23 Feb 73 | | | 26 Feb 73 | | | 8 Mar 73 | | | 6 Apr 73 | | | 23 May 73 | |
|-----------------------------------|---------------|-------------------|----------------------|--------------------|--------------|----------------------|--------------------|--------------|----------------------|--------------------|--------------|----------------------|--------------------|--------------|----------------------|--------------------|--------------|----------------------|
| | | DSM kips/in. | Average DSM kips/in. | % of DSM on 23 May | DSM kips/in. | Average DSM kips/in. | % of DSM on 23 May | DSM kips/in. | Average DSM kips/in. | % of DSM on 23 May | DSM kips/in. | Average DSM kips/in. | % of DSM on 23 May | DSM kips/in. | Average DSM kips/in. | % of DSM on 23 May | DSM kips/in. | Average DSM kips/in. |
| 1DBA | | 2050 | | | | | | 900 | | | 1225 | | | 1350 | | | 1550 | |
| 1DBB | | 2150 | | | | | | 1200 | | | 1425 | | | 1600 | | | 1850 | |
| | 11 | | 2100 | 123 | | | | | 1050 | 61.8 | | 1320 | 77.6 | | 1480 | 87.0 | | 1700 |
| 2DBA | | | | | 2000 | | | 775 | | | 1800 | | | 1650 | | | 1700 | |
| 2DBB | | | | | 2050 | | | 800 | | | 2050 | | | 1950 | | | 1400 | |
| | 9 | | | | | 2030 | 131 | | 790 | 51.0 | | 1420 | 91.5 | | 1800 | 116.0 | | 1550 |
| Depth Below Pavement Surface, in. | | Temperature, °F / | | | | | | | | | | | | | | | | |
| 0 | | 30.8 | | | 37.2 | | | 36.0 | | | 45.5 | | | 55.0 | | | 65.0 | |
| 1 | | Below 30 | | | Below 30 | | | 31.0 | | | 37.8 | | | 46.4 | | | 62.0 | |
| 2 | | | | | Below 30 | | | 31.2 | | | 37.6 | | | 46.0 | | | 57.9 | |
| 4 | | | | | Below 30 | | | 31.0 | | | 37.0 | | | 44.6 | | | 55.7 | |
| 6 | | | | | 30.0 | | | 30.5 | | | 37.3 | | | 44.4 | | | 57.1 | |
| 8 | | | | | 30.5 | | | 30.5 | | | 37.1 | | | 44.0 | | | 55.0 | |
| 12 | | | | | 30.5 | | | 30.3 | | | 37.3 | | | 43.8 | | | 55.2 | |
| 18 | | 30.8 | | | 31.0 | | | 30.2 | | | 37.0 | | | 43.3 | | | 55.4 | |
| 24 | | 31.0 | | | 31.4 | | | 31.5 | | | 36.9 | | | 42.5 | | | 56.2 | |
| 36 | | 33.2 | | | 33.4 | | | 33.3 | | | 36.0 | | | 42.4 | | | 53.4 | |
| 48 | | 34.5 | | | 35.0 | | | 35.0 | | | 35.6 | | | 42.5 | | | 51.3 | |
| 60 | | 36.0 | | | 37.0 | | | 36.5 | | | 36.4 | | | 42.8 | | | 49.0 | |
| 72 | | 37.5 | | | 38.3 | | | 37.3 | | | 37.5 | | | 43.0 | | | 50.0 | |

Note: DSM values taken on 23 May 73 were considered not to be influenced by freeze-thaw cycles.

Table 15

Results of DSM Measurements on AC Test Sites

| Test Site No. | AC Thickness | 24 Feb 73 | | | 26 Feb 73 | | | 8 Mar 73 | | | 9 Mar 73 | | | 5 Apr 73 | | | 23 May 73 | |
|-----------------------------------|--------------|-----------------|----------------------|--------------------|--------------|----------------------|--------------------|--------------|----------------------|--------------------|--------------|----------------------|--------------------|--------------|----------------------|--------------------|--------------|----------------------|
| | | DSM kips/in. | Average DSM kips/in. | % of DSM on 23 May | DSM kips/in. | Average DSM kips/in. | % of DSM on 23 May | DSM kips/in. | Average DSM kips/in. | % of DSM on 23 May | DSM kips/in. | Average DSM kips/in. | % of DSM on 23 May | DSM kips/in. | Average DSM kips/in. | % of DSM on 23 May | DSM kips/in. | Average DSM kips/in. |
| 3DBA | | 1625 | | | 1300 | | | 70 | | | | | | 280 | | | 190 | |
| 3DBB | | 1650 | | | 1300 | | | 92 | | | | | | 280 | | | 210 | |
| | 7 | | 1640 | 820 | | 1300 | 650 | | 81 | 40.5 | | | | | 280 | 140 | | 200 |
| 5DBA | | 1100 | | | 850 | | | | | | 195 | | | 195 | | | 140 | |
| 5DBB | | 1050 | | | 850 | | | | | | 190 | | | 180 | | | 130 | |
| | 2 | | 1130 | 837 | | 850 | 630 | | | | | 192 | 142 | | 188 | 139 | | 135 |
| 6DBA | | 580 | | | 600 | | | | | | 282 | | | 200 | | | 240 | |
| 6DBB | | 600 | | | 550 | | | | | | 240 | | | 200 | | | 220 | |
| | 5 | | 590 | 256 | | 580 | 252 | | | | | 261 | 113 | | 200 | 87 | | 230 |
| Depth Below Pavement Surface, in. | | Temperature, °F | | | | | | | | | | | | | | | | |
| | 0 | 30.5 | | | 37.8 | | | 53.7 | | | | | | 61.5 | | | 86.0 | |
| | 1 | 33.0 | | | 42.0 | | | 50.2 | | | | | | 63.8 | | | 80.0 | |
| | 2 | 33.8 | | | 40.0 | | | 47.0 | | | | | | 64.3 | | | 75.3 | |
| | 4 | 33.2 | | | 36.0 | | | 43.4 | | | | | | 61.0 | | | 71.6 | |
| | 6 | 31.5 | | | 31.5 | | | 40.5 | | | | | | 55.8 | | | 69.0 | |
| | 8 | 34.5 | | | 32.5 | | | 38.2 | | | | | | 51.5 | | | 67.5 | |
| | 12 | 31.7 | | | 31.0 | | | 37.4 | | | | | | 47.5 | | | | |
| | 18 | 32.0 | | | 32.0 | | | 33.0 | | | | | | 42.6 | | | | |
| | 24 | 31.4 | | | 32.0 | | | 32.8 | | | | | | 42.2 | | | | |
| | 36 | 35.4 | | | 36.0 | | | 36.2 | | | | | | 44.3 | | | | |
| | 48 | 36.8 | | | 36.1 | | | 36.2 | | | | | | 44.1 | | | | |
| | 60 | 40.0 | | | 40.0 | | | 41.5 | | | | | | 44.1 | | | | |
| | 72 | 41.0 | | | 41.2 | | | 40.5 | | | | | | 44.5 | | | | |

Note: DSM values taken on 23 May 73 were considered not to be influenced by freeze-thaw cycles.

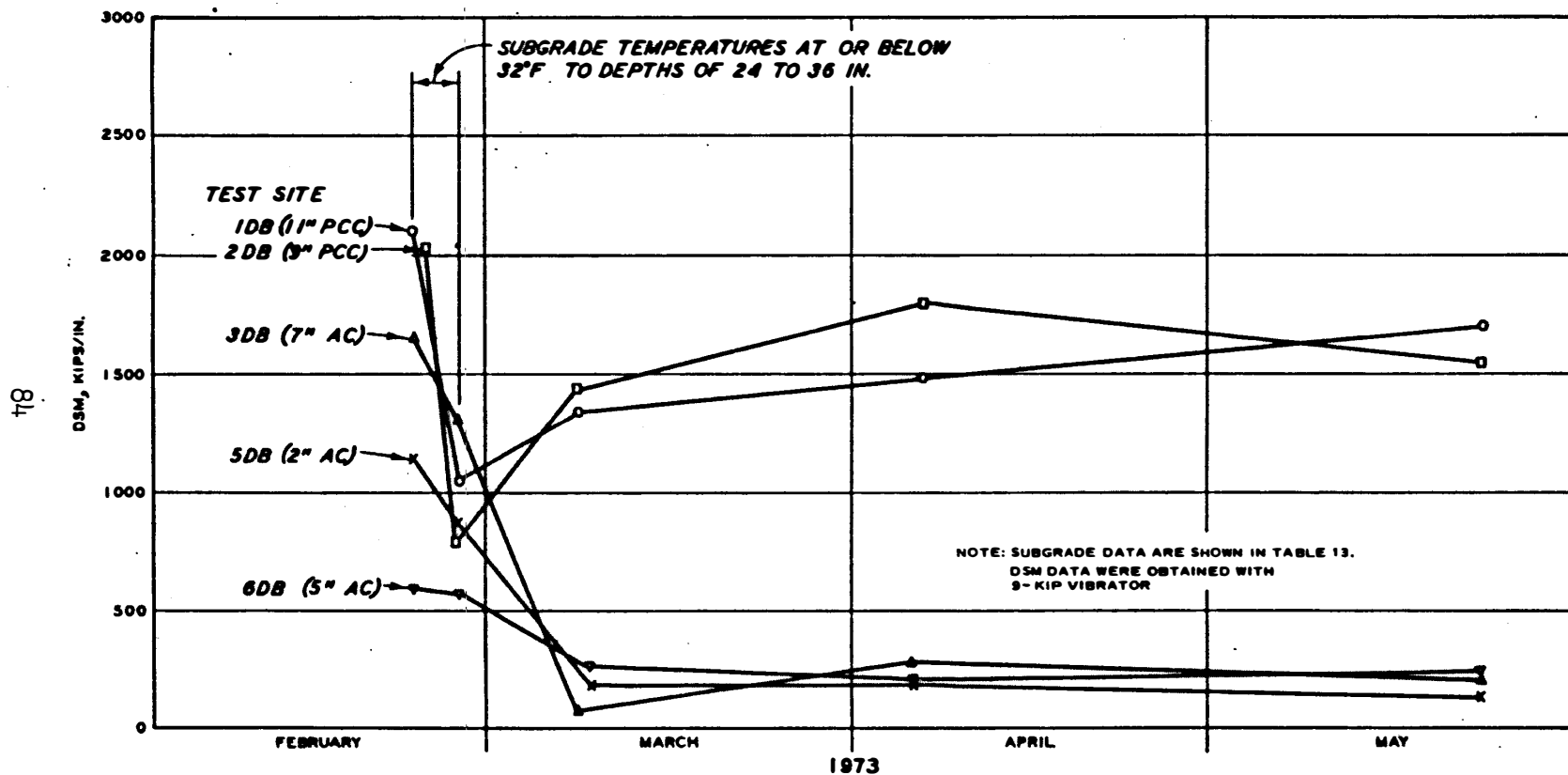


Figure 36. DSM values versus time for five test sites at Truax Field, Madison, Wis.

stages in the winter freeze and spring thaw cycles. The first series of tests in February was conducted when temperatures were below freezing to a depth of 24 in. The second series in February was conducted when temperatures were below freezing at depth of 24 in. but the top several inches had thawed. There was visible evidence that the thaw had begun, i.e., water was seeping through cracks in the pavement. The other three series of tests were all conducted under what seemed to be normal conditions for the pavement since the DSM values did not change significantly for any of the three tests. The lowest observed DSM values for the PCC pavements were recorded on 26 February when they were 61.8 and 51.0 percent of the values for the pavements in a normal condition (on 23 May). The lowest observed DSM value for the 7-in. AC pavements was on 8 March when it was 40.5 percent of the value with the pavement in the normal condition. DSM values for the 2- and 5-in. AC pavements were never observed to be significantly below their values with the pavements in the normal condition. Evidently, no observations were made during the period when the 2- and 5-in. AC pavements were weakened by the thaw. The effects of pavement temperature or fluctuations in the groundwater table on the nondestructive data obtained for the frost study have not been considered. The period during which the Truax Field pavements were significantly weakened by frost action was of short duration. From Figure 36, it can be seen that on 24 February the DSM values for PCC pavements were decreasing due to thawing action and had reached about 1400 kips/in. The DSM values remained below 1400 kips/in. until 6 March, and changes after 6 March were minor. These pavements were weakened due to a thawing period of about 14 days. Results of the studies at Truax Field indicate that the effects of frost can greatly influence DSM measurements (up to 837 percent for the flexible pavement). However, developing a correction factor to DSM values for frost effects based on data collected at Truax Field is considered impractical, particularly because of the variations in subgrade conditions and poor drainage conditions apparent in May after the effects of frost thaw should have been negligible. In areas where frost is known to be a problem, the DSM tests can be performed at periodic intervals to

include the normal and the thaw periods for evaluation purposes, which will give the variation in load-carrying capacity due to frost effects and define the length of the weak period due to thaw action.

Effects of test location. The location of the DSM test in relation to joints, free edges of pavement structures, and wheel paths of aircraft can have an effect on the results obtained. This is particularly important in rigid pavements where the edge of the slab and the joint type can influence the DSM value.

Figures 37-39 show results of DSM measurements on eight different PCC slabs, with types of joints listed where this information was available. Figure 37 shows the results of DSM measurements on two different slabs, N-F and N-N. The letter following the N-N and N-F designations represents the direction from the center of the slab of the line along which the DSM measurements were taken. For example, line N-NN was from the slab center to the north edge of the slab, and N-NE was from the slab center to the east edge of the slab. Data in Figures 38 and 39 are presented in a similar manner. The minimum DSM for each slab expressed as a percentage of the maximum DSM for each slab yields the following values:

| <u>Slab No.</u> | $\frac{\text{Minimum DSM}}{\text{Maximum DSM}} \times 100$ |
|-----------------|--|
| N-N | 25 |
| N-F | 48 |
| H-1 | 43 |
| H-2 | 41 |
| J-1 | 27 |
| J-2 | 64 |
| J-3. | 40 |
| J-4 | 45 |

These results show that considerable variations in DSM values can be obtained for the same slab depending on the location of the vibrator on the slab. The maximum DSM value does not always occur in the center of the slab, although this is generally the case. DSM data to be used in development of the nondestructive evaluation methodology were taken at the centers of the slabs. More consistent results were obtained at the slab center since the DSM at this location is least affected by the edge

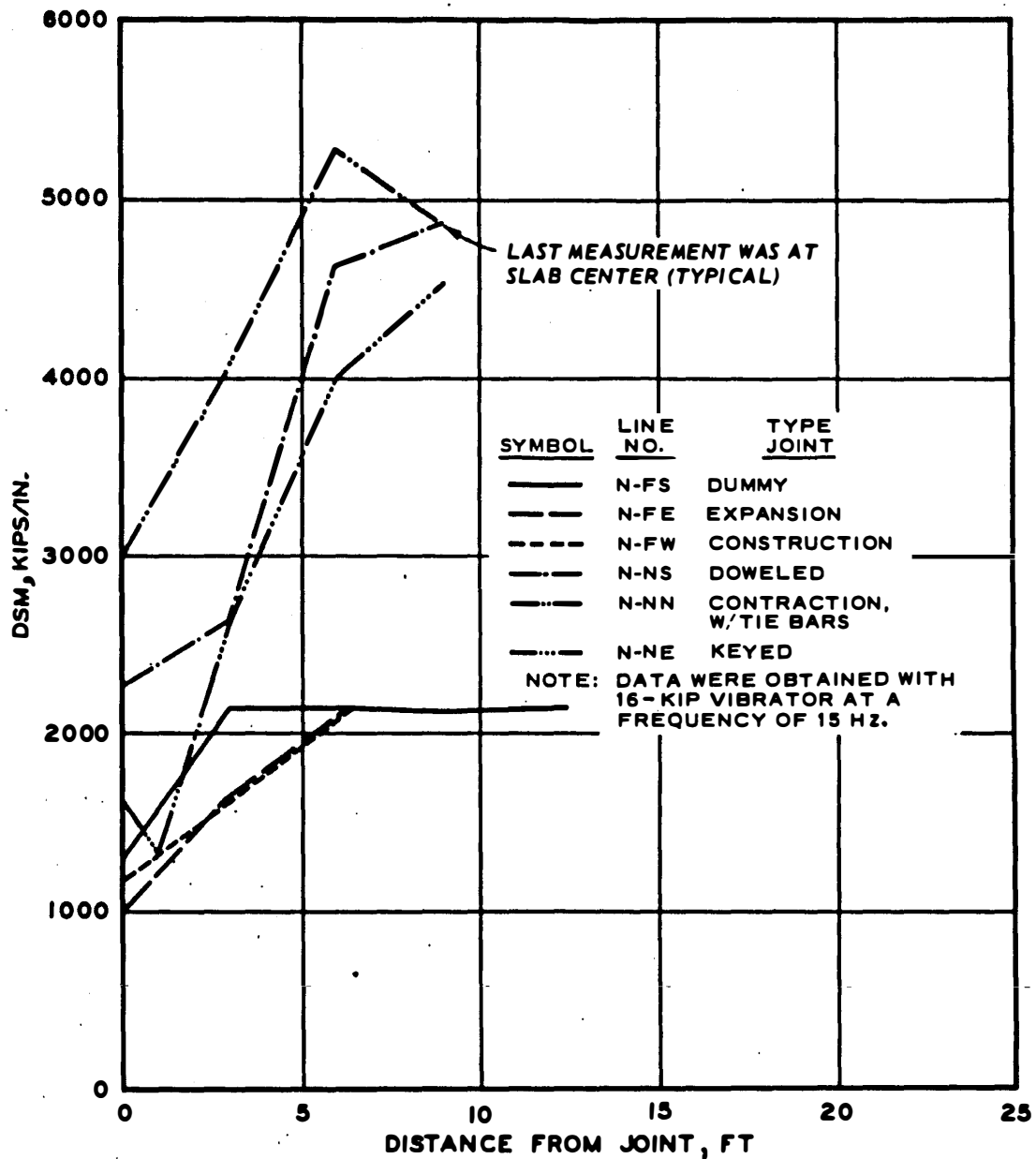


Figure 37. DSM versus distance from joint for slabs N-F and N-N at NAFEC

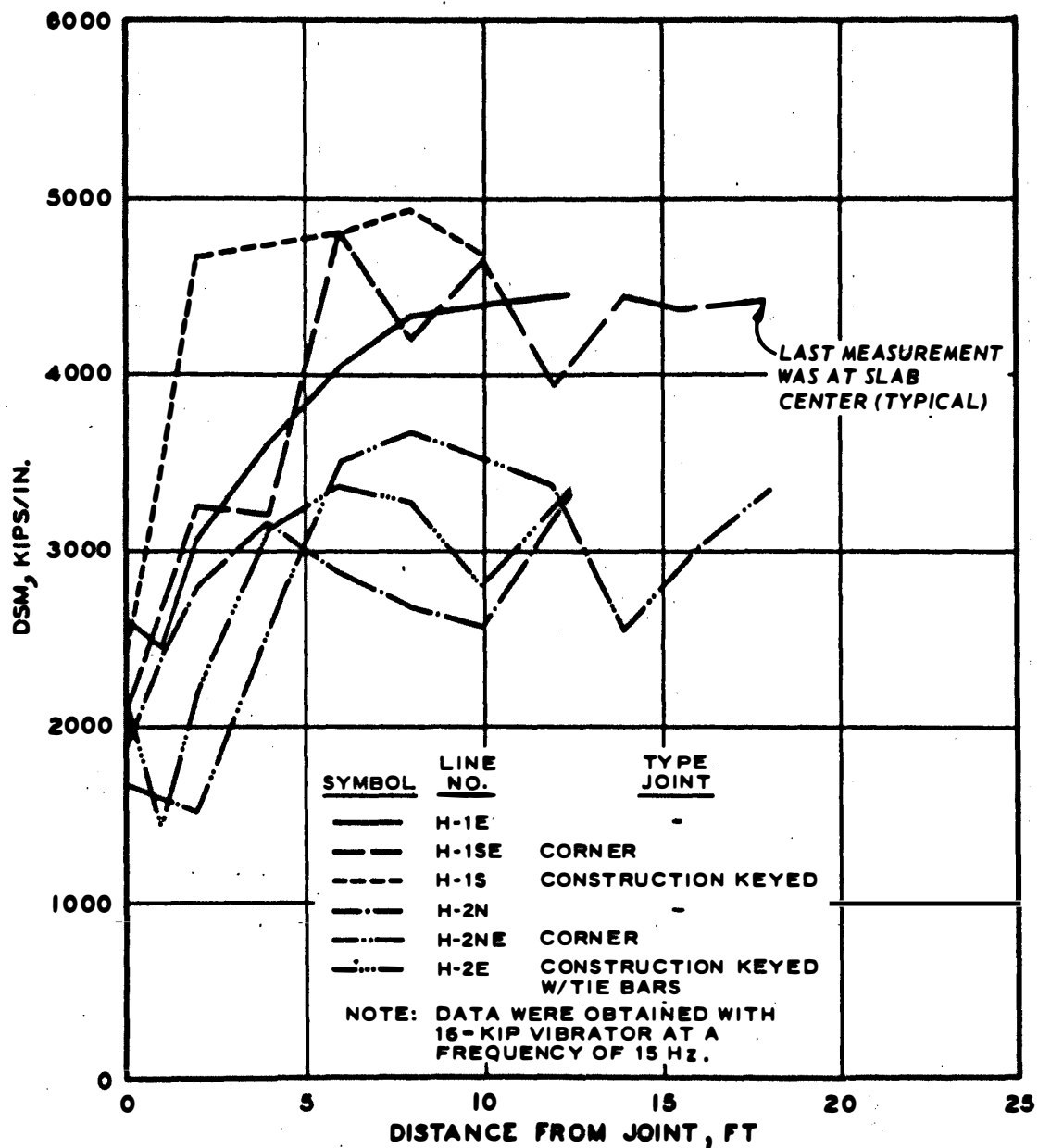


Figure 38. DSM versus distance from joint for slabs H-1 and H-2 at Houston

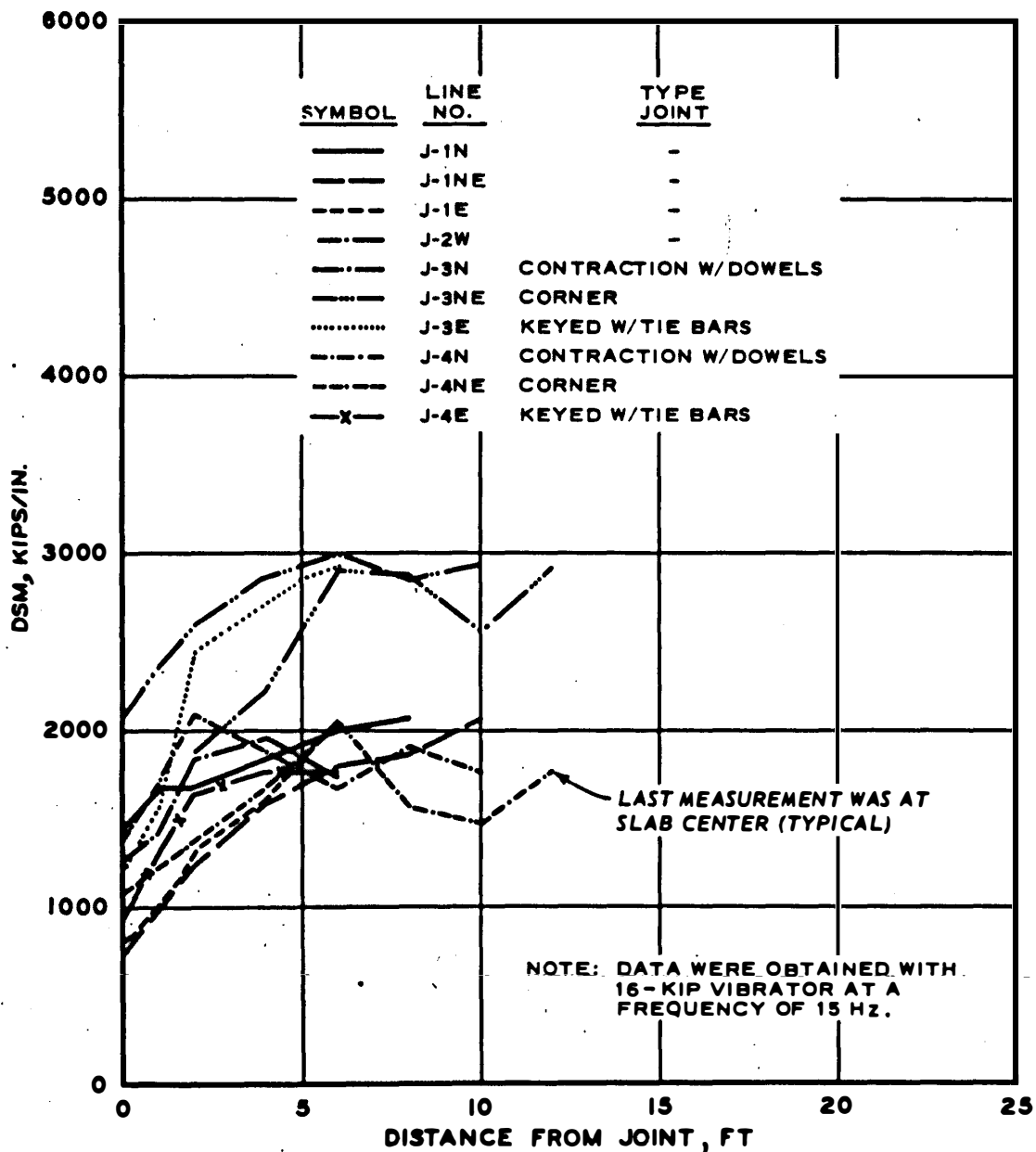


Figure 39. DSM versus distance from joint for slabs J-1, J-2, J-3, and J-4 at Jackson

condition and joint type. The allowable load for rigid pavements obtained through conventional methods considers an edge loading. The nondestructive evaluation methodology developed in this study uses a correlation between this allowable load at the slab edge and the DSM measured at the slab center. Therefore, DSM tests for evaluation should be made at the slab center. Joint and slab edge effects, however, should not be considered unimportant in a nondestructive evaluation. Future research should concentrate on procedures for evaluating the efficiency of PCC slab joints and edge effects on the DSM test results.

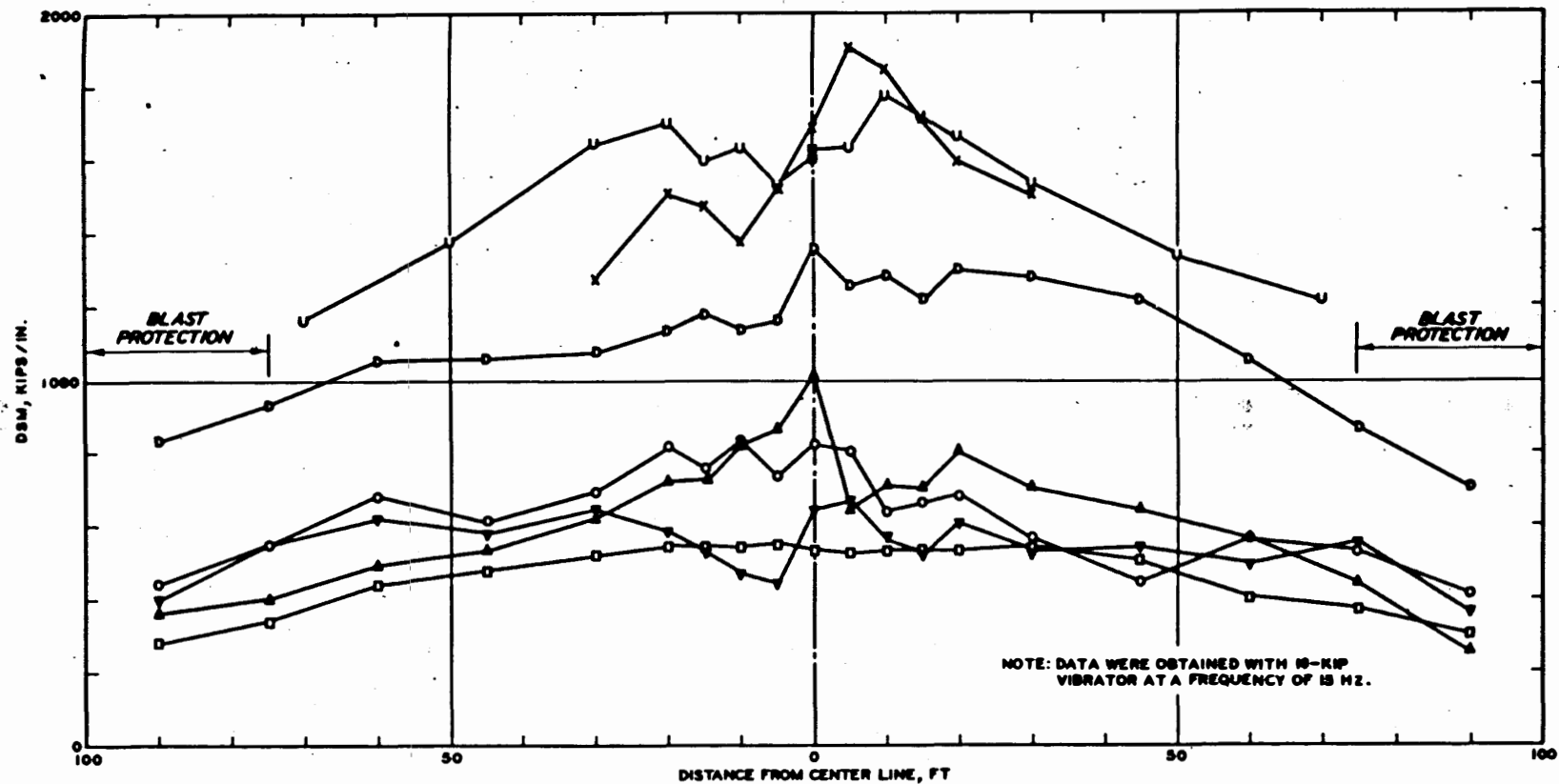
Variations in pavements are reflected in the DSM results. Figure 40 shows the variations in DSM values in the transverse direction across a typical flexible pavement runway and taxiway. It should be noted that higher DSM values were measured along the wheel paths. This tendency, of course, would be expected because of the compaction under aircraft loadings along the wheel paths. DSM tests, therefore, should be located within each area to be evaluated to reflect accurately the condition of the feature being evaluated.

NONDESTRUCTIVE EVALUATION METHODOLOGY

FLEXIBLE PAVEMENT

The methodology described in the following paragraphs is used for the structural evaluation of flexible pavement. The major parameters affecting the structural performance of flexible pavement are pavement thickness, soil strength, landing gear characteristics, and number of load repetitions. The pavement criterion to which the evaluation methodology is related has been established through accelerated traffic testing, studies of actual pavement performance, and material studies.^{13,14,15}

The nondestructive evaluation procedure for flexible pavement described in the next section of this report uses a measurement of the overall rigidity in terms of the DSM of the total pavement system and does not consider the major parameters listed above independently. However, the relative effects of the major parameters can be considered



PAYMENT DATA

| SYMBOL | LOCATION | CROSS SECTION | SURFACE | | BASE | | SUBBASE | | SUBGRADE MATERIAL |
|--------|-------------------------|---------------|----------|----------------|---------------|----------------|---------------|----------------|----------------------------------|
| | | | MATERIAL | THICKNESS, IN. | MATERIAL | THICKNESS, IN. | MATERIAL | THICKNESS, IN. | |
| O | RUNWAY 9-27, STA 38+36 | R 1-A | AC | 12 ± | AC | 2 | CRUSHED STONE | 3 | 3 FT. CINDERS OVER SAND |
| A | RUNWAY 9-27, STA 40+66 | R 3-A | AC | 12 ± | AC | 2 | CRUSHED STONE | 3 | SILT |
| □ | RUNWAY 9-27, STA 63+36 | R 5-A | AC | 12 ± | AC | 2 | CRUSHED STONE | 3 | 3 FT. CINDERS OVER SAND |
| ▽ | RUNWAY 9-27, STA 76+00 | R 7-A | AC | 12 ± | AC | 2 | CRUSHED STONE | 3 | 3 FT. CINDERS AND SILT OVER SAND |
| B | RUNWAY 9-27, STA 90+36 | R 9-A | AC | 8 ± | CRUSHED STONE | 11 | - | - | SAND |
| U | RUNWAY 9-27, STA 103+66 | R 11-A | AC | 4 ± | CRUSHED STONE | 12 | - | - | SAND |
| X | TAXIWAY A, STA 74+00 | A 2-A | AC | 12 ± | CRUSHED STONE | 3 | - | - | SAND |

Figure 40. DSM versus distance from center line for old runway 9-27 and taxiway A at Philadelphia

independently through use of direct sampling relationships established from previous research studies.

Development of the basic evaluation methodology for flexible pavements consisted of establishing a correlation between DSM and allowable single-wheel load as shown in Figure 41. This correlation was developed for a single wheel having a tire contact area of 254 sq in. and for 1200 annual departures (design life of 20 yr). (As explained previously, this area was selected because it is the area of the load plate on the 16-kip vibrator and it approximates the contact areas of tires used on many wide-bodied jet aircraft.) The correlation shown in Figure 41 was generated by performing DSM tests on several actual pavements and correlating the results with the allowable single-wheel load of the pavement structure as determined from conventional evaluation techniques using direct sampling test results. After the DSM versus allowable single-wheel load relation had been developed, the evaluation methodology for use with multiple-wheel aircraft was based on existing interrelationships between pavement thickness, load, load repetitions, soil strength, and landing gear characteristics.

The landing gear characteristics of tire spacing, arrangement, and contact area (of one tire) for multiple-wheel aircraft are considered through the development of an equivalent single-wheel load (ESWL). Curves have been established (Figures 42-44) which relate the ESWL, expressed as a percent of the load on the number of wheels used to establish the ESWL, to depth from the pavement surface. These curves were developed using the Boussinesq deflection equations, in which the ESWL is that load on a single wheel which will produce a maximum deflection equal to the maximum deflection produced by a multiple-wheel arrangement. It should be noted that the ESWL (expressed as a percent of the gross aircraft load) increases as the depth increases. This increase in ESWL with depth will cause different allowable multiple-wheel aircraft loads for two pavements, even though the pavements have the same DSM value. For example, a thin pavement on a strong subgrade and a thick pavement on a weak subgrade may have the same DSM but different evaluations (in terms of multiple-wheel aircraft load)

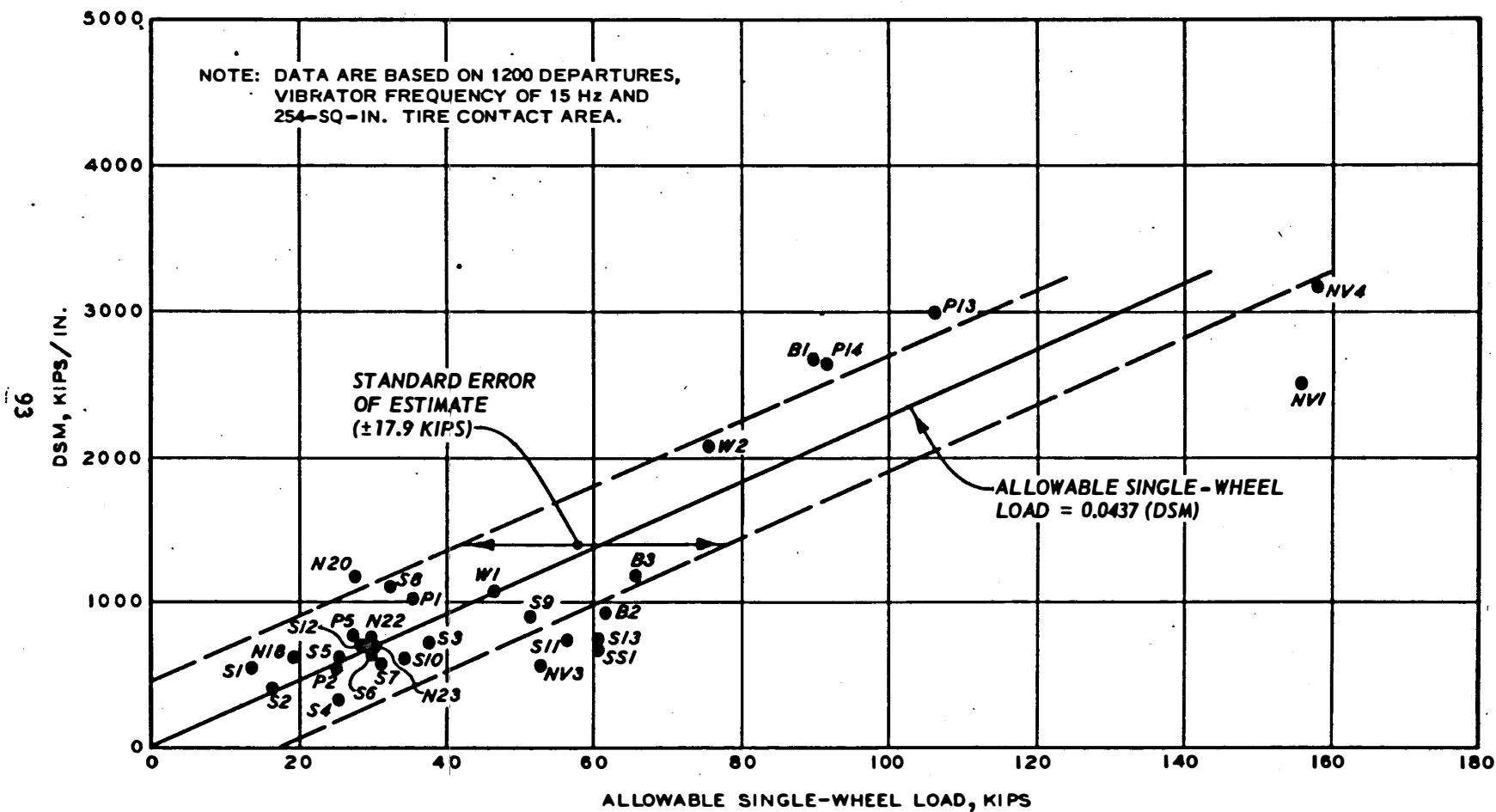


Figure 41. DSM versus allowable single-wheel load for flexible pavement

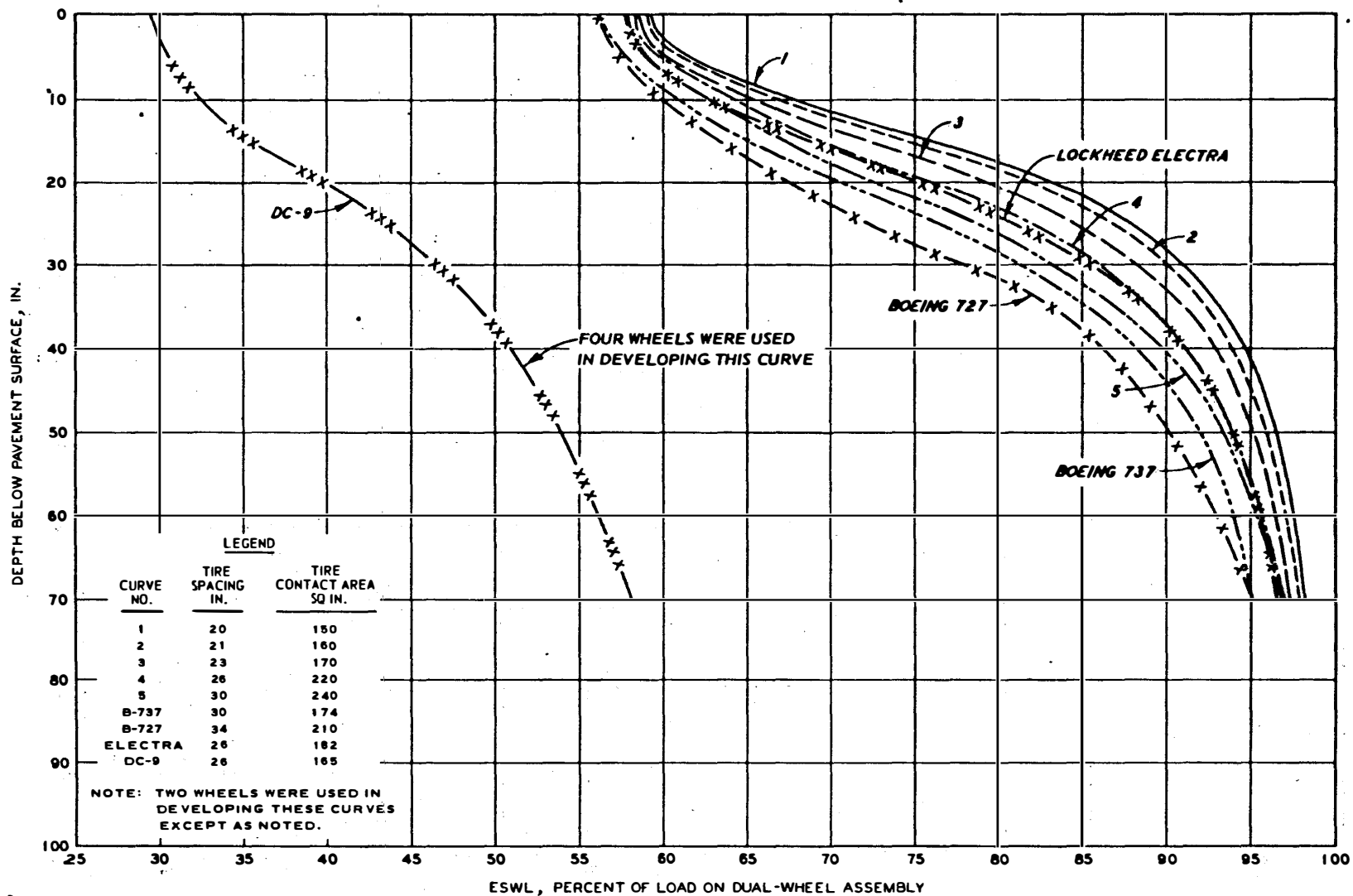


Figure 42. ESWL curves for dual-wheel aircraft on flexible pavement

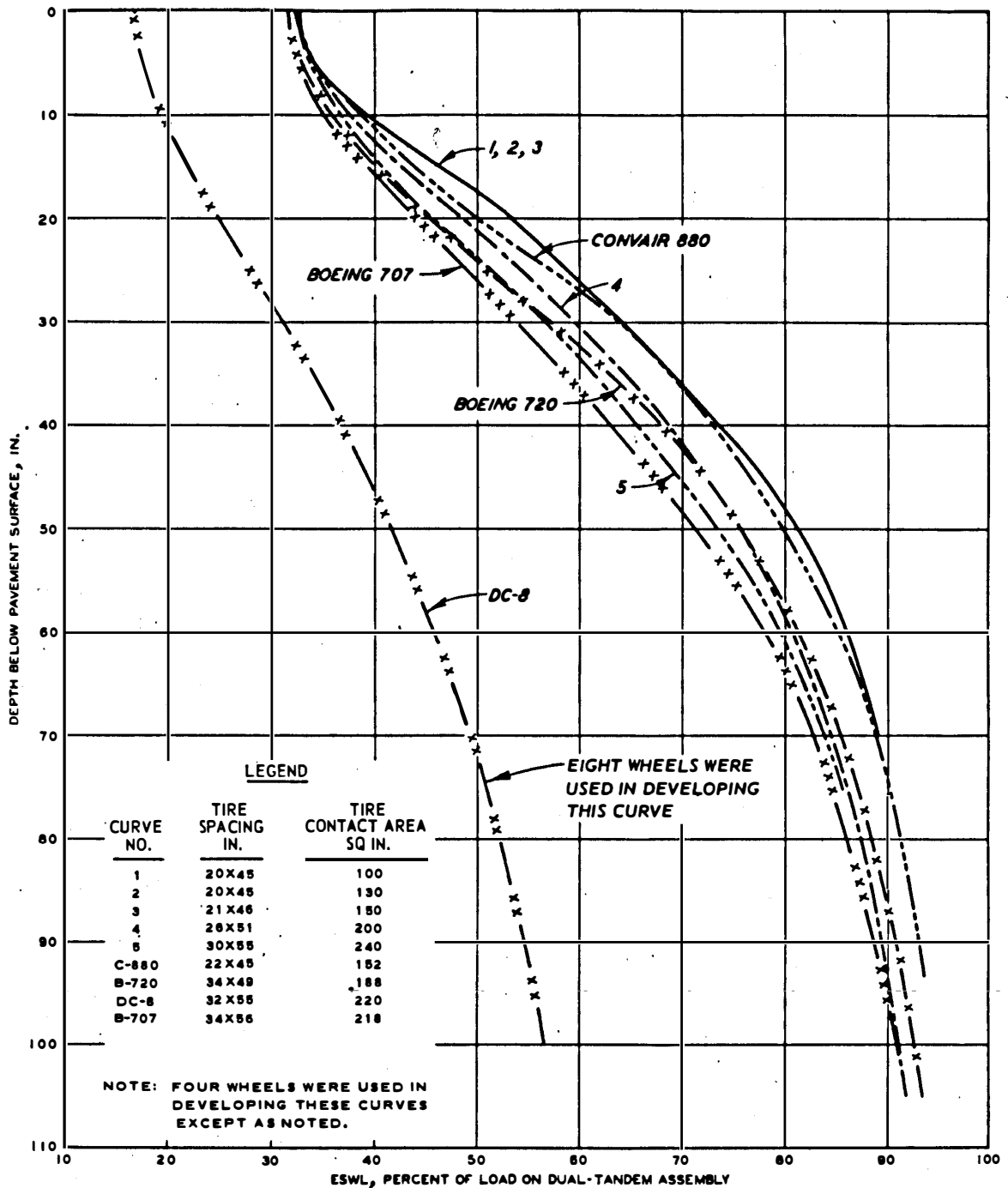


Figure 43. ESWL curves for dual-tandem aircraft on flexible pavement

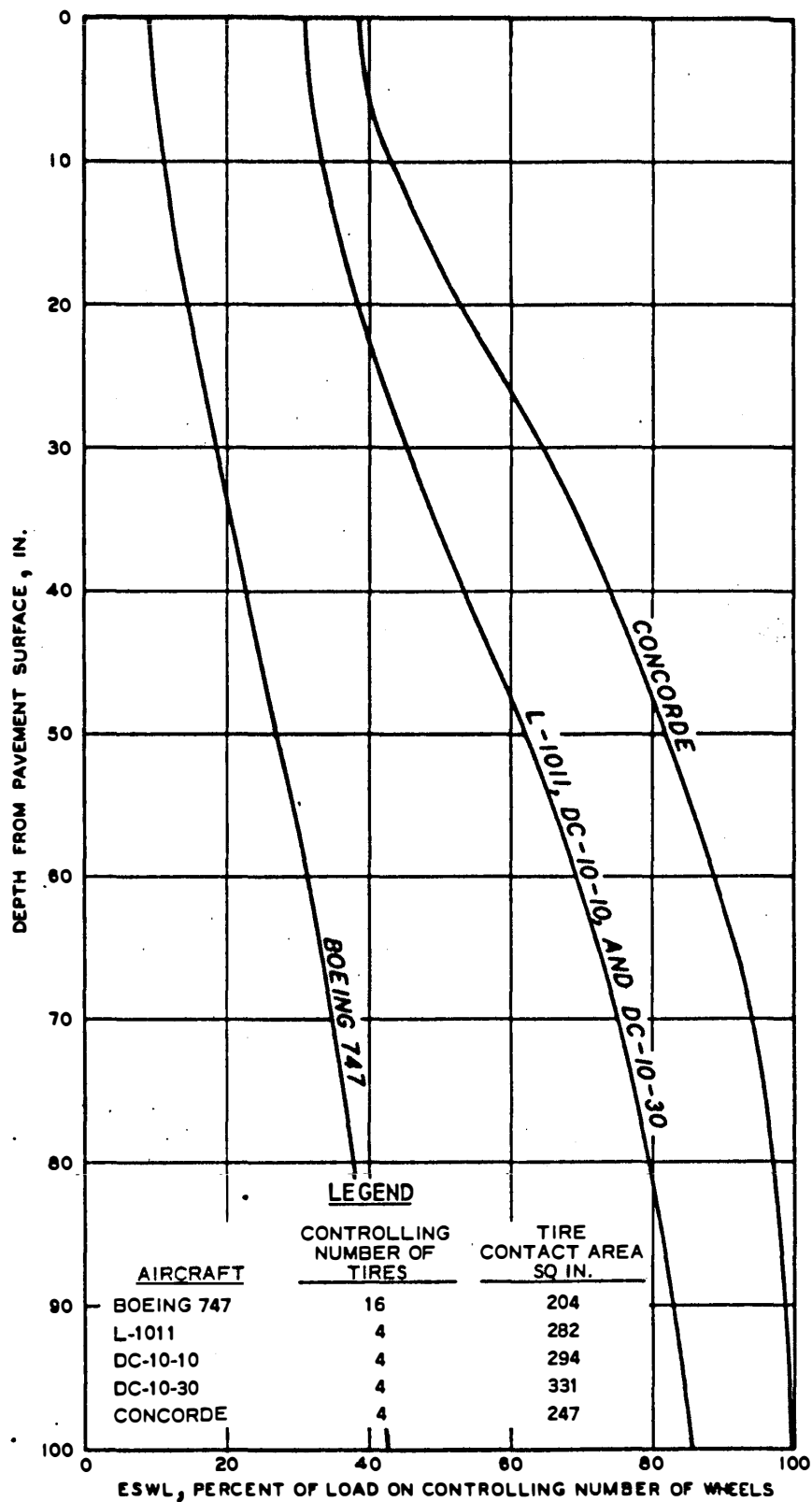


Figure 44. ESWL curves for wide-bodied jet aircraft on flexible pavement

because of the thickness variations.

The effects of load repetitions on the allowable gross aircraft load are considered using a load repetition factor α . The load repetition factor is a function of the number of aircraft departures and the number of wheels considered in establishing the ESWL. The load repetition factor has been derived from performance tests on full-scale pavement sections.^{20,21,47} The load repetition factors are independent of the pavement structure and can be determined from the curves shown in Figure 45. For simplicity in application, Table 16 presents load repetition factors that have been prepared for the annual departure levels and for the aircraft and gear arrangements presented in Reference 14.

The thickness and soil strength parameters are considered through use of the CBR/p versus $t/\alpha\sqrt{A}$ plot shown in Figure 46, in which

CBR = computed value of soil strength required under t to support the allowable single-wheel load determined from Figure 41.

p = single-wheel or equivalent single-wheel tire pressure, psi. (For single-wheel aircraft, p is determined by dividing the wheel load by the tire contact area; for multiple-wheel aircraft, p is determined by dividing the ESWL by the contact area of one tire.)

t = existing thickness of the pavement structure above the subgrade, in.

A = contact area of one tire on an aircraft, sq in.

This plot was developed from the results of numerous accelerated traffic tests and performance surveys. Data from these tests and surveys were combined and plotted in the form of CBR/p versus t/\sqrt{A} , and a best-fit curve was then drawn through the data points^{16,17,18} for a standard load repetition level. In order to make the curve applicable to any load repetition level, the load repetition factor α was added to the t/\sqrt{A} term. This addition to the relationship was technically correct since in the evaluation of a pavement, the existing thickness has to be adjusted (thickness t is divided by load repetition α) to that required for the standard load repetition level in order to use the criteria.

In using the CBR/p versus $t/\alpha\sqrt{A}$ curve, any one parameter can

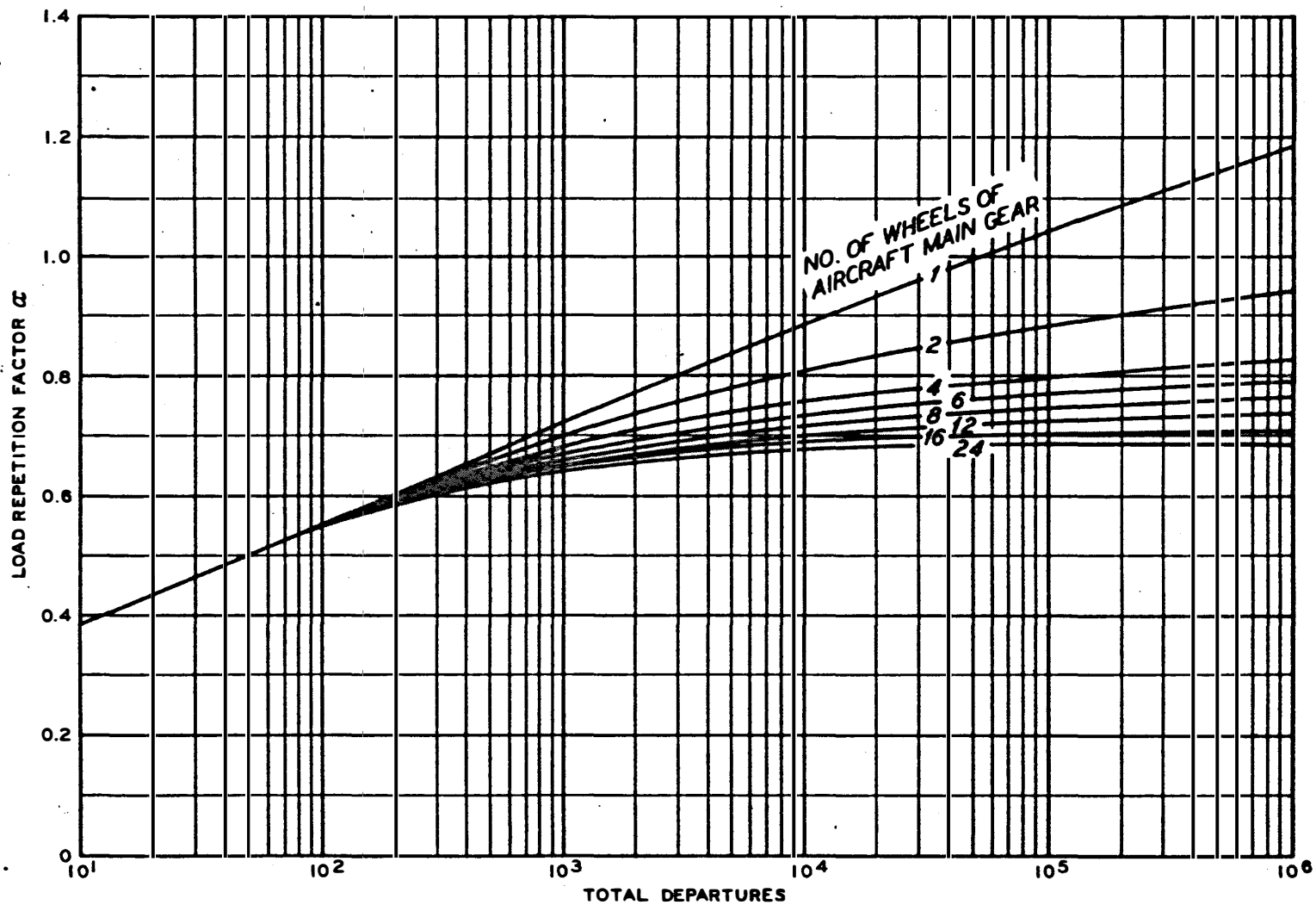


Figure 45. Load repetition factors versus total departures

Table 16

Load Repetition Factors for Flexible and Rigid Pavements

| Aircraft Gear Configuration or Model Designation | Typical Gross Weight kips | Load Repetition Factor for Cited Annual Departure Level for 20-Yr Design Life | | | | | | | | | |
|---|------------------------------------|---|-------|----------|-------|----------|-------|----------|-------|----------|-------|
| | | 1200 | | 3000 | | 6000 | | 15,000 | | 25,000 | |
| | | Flexible | Rigid | Flexible | Rigid | Flexible | Rigid | Flexible | Rigid | Flexible | Rigid |
| Single-wheel | 30 | 0.94 | 1.00 | 1.01 | 0.93 | 1.05 | 0.86 | 1.11 | 0.79 | 1.14 | 0.75 |
| Single-wheel | 45 | 0.94 | 1.00 | 1.01 | 0.92 | 1.05 | 0.85 | 1.11 | 0.78 | 1.14 | 0.75 |
| Single-wheel | 60 | 0.94 | 1.00 | 1.01 | 0.91 | 1.05 | 0.85 | 1.11 | 0.78 | 1.14 | 0.74 |
| Single-wheel | 75 | 0.94 | 1.00 | 1.01 | 0.91 | 1.05 | 0.84 | 1.11 | 0.77 | 1.14 | 0.74 |
| Dual-wheel | 50 | 0.84 | 0.97 | 0.87 | 0.88 | 0.89 | 0.82 | 0.91 | 0.75 | 0.92 | 0.72 |
| Dual-wheel | 75 | 0.84 | 0.96 | 0.87 | 0.87 | 0.89 | 0.82 | 0.91 | 0.75 | 0.92 | 0.72 |
| Dual-wheel | 100 | 0.84 | 0.96 | 0.87 | 0.87 | 0.89 | 0.81 | 0.91 | 0.75 | 0.92 | 0.72 |
| Dual-wheel | 150 | 0.84 | 0.95 | 0.87 | 0.86 | 0.89 | 0.81 | 0.91 | 0.74 | 0.92 | 0.71 |
| Dual-wheel | 200 | 0.84 | 0.95 | 0.87 | 0.86 | 0.89 | 0.81 | 0.91 | 0.74 | 0.92 | 0.71 |
| Dual-tandem | 100 | 0.78 | 0.99 | 0.79 | 0.89 | 0.80 | 0.83 | 0.81 | 0.77 | 0.82 | 0.73 |
| Dual-tandem | 150 | 0.78 | 0.98 | 0.79 | 0.88 | 0.80 | 0.82 | 0.81 | 0.76 | 0.82 | 0.73 |
| Dual-tandem | 200 | 0.78 | 0.97 | 0.79 | 0.88 | 0.80 | 0.82 | 0.81 | 0.75 | 0.82 | 0.72 |
| Dual-tandem | 300 | 0.78 | 0.95 | 0.79 | 0.87 | 0.80 | 0.81 | 0.81 | 0.75 | 0.82 | 0.72 |
| Dual-tandem | 400 | 0.78 | 0.95 | 0.79 | 0.86 | 0.80 | 0.81 | 0.81 | 0.74 | 0.82 | 0.71 |
| Boeing 727 | 173 | 0.84 | 0.95 | 0.87 | 0.87 | 0.89 | 0.81 | 0.91 | 0.75 | 0.92 | 0.71 |
| DC-8-63F | 358 | 0.78 | 0.95 | 0.79 | 0.87 | 0.80 | 0.81 | 0.81 | 0.74 | 0.82 | 0.71 |
| Boeing 747 | 778 | 0.70 | 0.97 | 0.70 | 0.88 | 0.705 | 0.82 | 0.71 | 0.75 | 0.71 | 0.72 |
| DC-10-10 | 433 | 0.78 | 0.96 | 0.79 | 0.88 | 0.80 | 0.82 | 0.81 | 0.75 | 0.82 | 0.72 |
| DC-10-30 | 558 | 0.78 | 0.96 | 0.79 | 0.87 | 0.80 | 0.82 | 0.81 | 0.75 | 0.82 | 0.72 |
| L-1011 | 428 | 0.78 | 0.96 | 0.79 | 0.88 | 0.80 | 0.82 | 0.81 | 0.75 | 0.82 | 0.72 |
| Concorde | 389 | 0.78 | 0.94 | 0.79 | 0.86 | 0.80 | 0.80 | 0.81 | 0.74 | 0.82 | 0.71 |
| Boeing 737 | 111 | 0.84 | 0.97 | 0.87 | 0.88 | 0.89 | 0.82 | 0.91 | 0.75 | 0.92 | 0.72 |
| Lockheed Electra | 113 | 0.84 | 0.96 | 0.87 | 0.87 | 0.89 | 0.81 | 0.91 | 0.75 | 0.92 | 0.72 |
| DC-9 | 115 | 0.84 | 0.97 | 0.87 | 0.88 | 0.89 | 0.82 | 0.91 | 0.75 | 0.92 | 0.72 |
| Convair 880 | 188 | 0.78 | 0.97 | 0.79 | 0.88 | 0.80 | 0.82 | 0.81 | 0.76 | 0.82 | 0.72 |
| Boeing 720 | 235 | 0.78 | 0.96 | 0.79 | 0.88 | 0.80 | 0.82 | 0.81 | 0.75 | 0.82 | 0.72 |
| Boeing 707 | 336 | 0.78 | 0.96 | 0.79 | 0.87 | 0.80 | 0.81 | 0.81 | 0.75 | 0.82 | 0.72 |

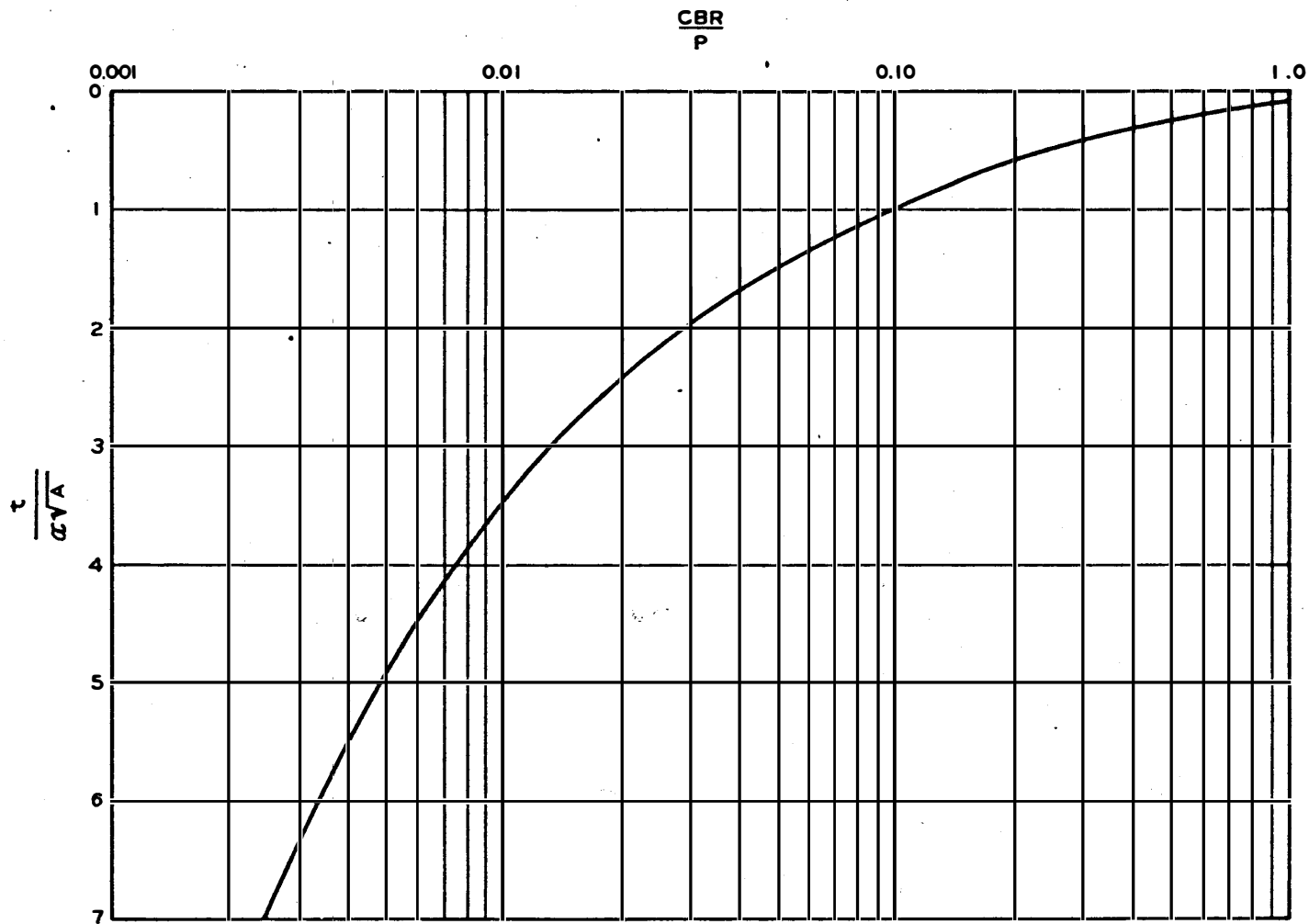


Figure 46. CBR/p versus $t/\alpha\sqrt{A}$

be determined if the other values are known. Figures 41-46 can be used with the DSM to evaluate a flexible pavement for any aircraft. The DSM is used to determine the allowable single-wheel load from Figure 41. This allowable single-wheel load is considered to be the ESWL for any multiple-wheel configuration and, when used in conjunction with the CBR/p versus $t/\alpha\sqrt{A}$ curve, can be used to calculate the theoretical value of CBR required to support the aircraft for 1200 annual departures (for a 20-yr life). This ESWL and the computed CBR value along with the pavement thickness and tire contact area can then be used to calculate the allowable gross aircraft load for the evaluated pavement for a given number of departures.

This methodology is for evaluation of critical pavement areas. For design purposes for high-speed taxiways, FAA uses 0.9 of the total pavement thickness t required for critical areas. The thickness reduction is used because these taxiways are used only by incoming aircraft, which are seldom fully loaded, and the aircraft are traveling at higher rates of speed and therefore impose less severe loadings on the pavement. Therefore, high-speed taxiway pavements can be evaluated by increasing the thickness by dividing by 0.9, i.e., the expression $t/\alpha\sqrt{A}$ becomes $t/0.9\alpha\sqrt{A}$.

The resulting nondestructive evaluation procedure given in subsequent paragraphs for flexible pavements uses the DSM to determine the pavement system strength index S_p , which is the allowable single-wheel load divided by a contact area of 254 sq in.

The term $t/\alpha\sqrt{A}$ is replaced by the term F_t in the nondestructive procedure. For a contact area of 254 sq in. and a traffic level of 1200 annual departures ($\alpha = 0.94$), the F_t factor becomes

$$F_t = \frac{t}{(0.94)(\sqrt{254})} = 0.67t$$

For high-speed taxiways, F_t becomes

$$F_t = \frac{t}{(0.9)(0.94)(\sqrt{254})} = 0.074t$$

The term CBR/p is replaced by the term SSF/S_p in the nondestructive procedure where SSF is the subgrade strength factor. Once the term SSF is obtained, then the relationship between F_t and SSF/S_p can be calculated from Figure 47 for any desired aircraft and load repetition factors using the appropriate values for A and α . The term S_p is used to calculate the allowable ESWL for the desired aircraft from:

$$ESWL = \frac{S_p}{A}$$

The percent ESWL of the main gear tires is obtained from Figures 42, 43, and 44. The allowable gross aircraft load is then obtained from the equation:

$$P_G = \frac{ESWL(W_m)}{0.95(\%ESWL)(W_c)}$$

where:

P_G = allowable gross aircraft load

W_m = total number of wheels on all main gears of the aircraft

$\%ESWL$ = value obtained from Figures 42, 43, and 44

W_c = number of controlling wheels used to determine the $\%ESWL$ from Figures 42, 43, and 44

The 0.95 factor is introduced in the above equation because 5.0 percent of the gross aircraft load is considered to be supported by the nose gear.

Flexible pavements with stabilized layers. The thickness t in the preceding discussion assumes a conventional flexible pavement consisting of an AC wearing surface and a crushed stone base course, with or without a granular subbase. Pavement structures to be evaluated must be converted to equivalent sections of conventional pavement to account for the variability in performance of different materials under traffic. Equivalency factors listed in Table 17 were developed from studies of performance of WES test sections.⁴⁸ The equivalency factors are based on a standard of 1.00 for granular subbase. For example, Table 17 shows that a layer of cement-stabilized sand-gravel in one pavement section will allow the same number of coverages to failure as a

$\frac{SSF}{S_p}$

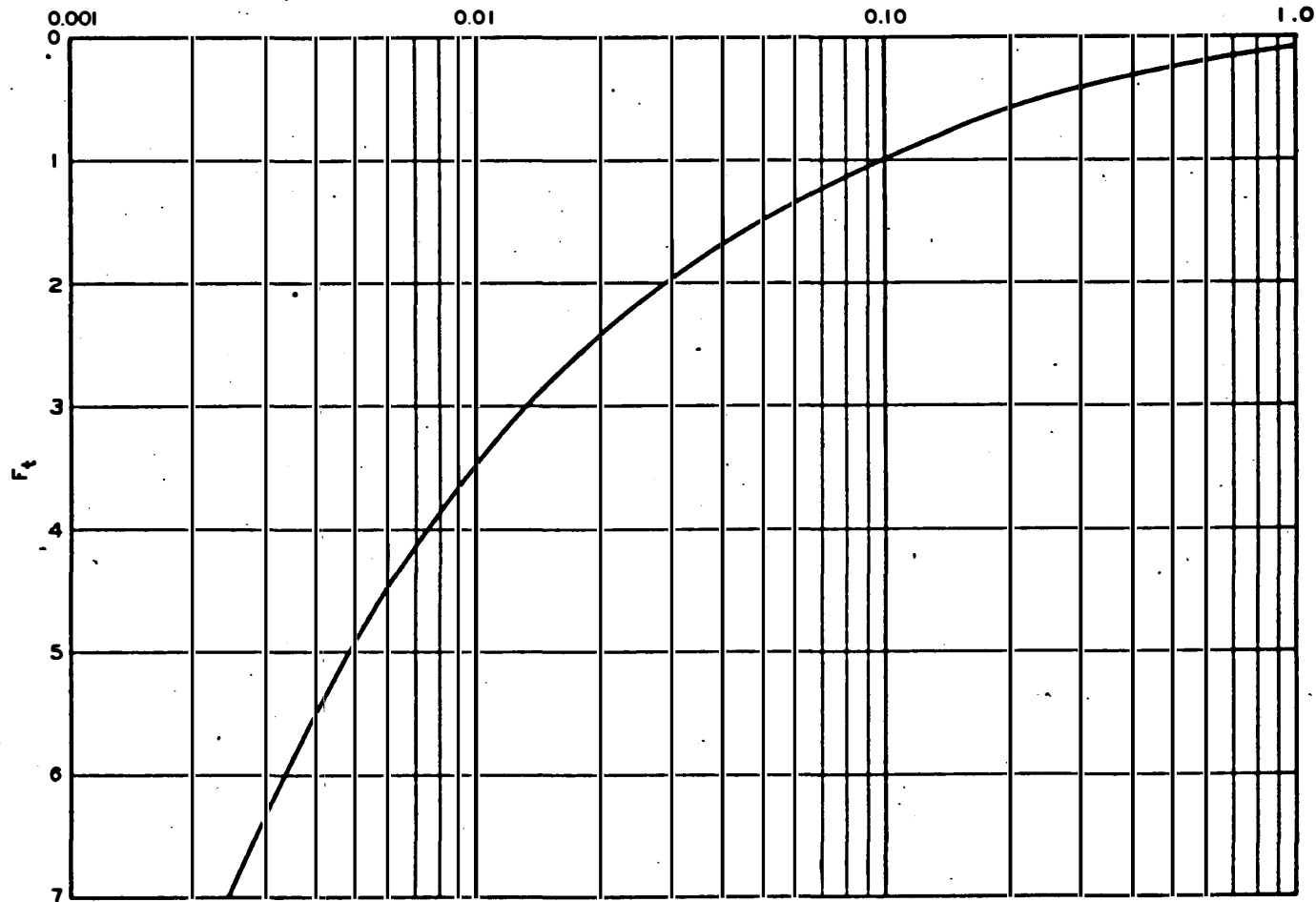


Figure 47. F_t versus $\frac{SSF}{S_p}$

Table 17

Summary Listing of Materials and Equivalency Factors

| <u>Material</u> | <u>Stabilizing Agent</u> | <u>Surface Course</u> | <u>Base Course</u> | <u>Subbase Course</u> | <u>Subgrade</u> |
|---|--------------------------|-----------------------|--------------------|-----------------------|-----------------|
| AC (P-401, P-408) | Asphalt | 1.70 | 1.70 | 1.70 | -- |
| Unbound crushed stone (P-209) | -- | -- | 1.40 | 1.40 | -- |
| Sand-gravel | Cement | -- | 1.60* | 1.60** | -- |
| Clay-gravel | Cement | -- | 1.45* | 1.45** | -- |
| Fine-grained soil | Cement | -- | 1.25* | 1.25** | -- |
| Clay-sand | Cement | -- | 1.15* | 1.15** | -- |
| Clay-sand | Fly ash | -- | -- | 1.15** | -- |
| Sand-gravel or clay-gravel (P-201, P-215, P-216)† | Asphalt | -- | 1.50 | 1.50 | -- |
| Fine-grained soil | Lime | -- | -- | 1.10†† | 1.10‡ |
| Unbound granular material (P-154) | -- | -- | -- | 1.00 | -- |

Note: Specifications for materials are taken from Reference 49.

* To use equivalency factor in evaluation, unconfined compressive strength of layer must be 1000 psi.

** To use equivalency factor in evaluation, unconfined compressive strength of layer must be 700 psi.

† Bituminous.

†† To use equivalency factor in evaluation, unconfined compressive strength of layer must be 200 psi.

‡ To use equivalency factor in evaluation, unconfined compressive strength of layer must be 100 psi.

layer of granular subbase which is 1.60 times as thick in a second pavement section provided that other layers in the two pavement sections are equal in quality and thickness.

The following examples illustrate the use of the equivalency factors for converting nonstandard pavement sections to standard sections. For these examples, a standard pavement section is defined as having a 4-in. AC (FAA specification No. P-401⁴⁹) wearing surface and a 9-in. unbound crushed stone base course (FAA specification No. P-209⁴⁹), with or without a granular subbase (FAA specification No. P-154⁴⁹), placed on a natural subgrade.

Example No. 1. Assume a pavement section to be evaluated has a 3-in. AC wearing surface, a 3-in. bituminous base, and a 6-in. granular subbase. Compute the equivalent standard pavement section by first converting the existing section to an equivalent section of granular subbase material as follows:

| <u>Layer Material</u> | <u>Layer Thickness in.</u> | <u>Layer Equivalency Factor</u> | <u>Equivalent Subbase Thickness in.</u> |
|-----------------------|--------------------------------|---|---|
| AC | 3.0 | 1.70 | 5.1 |
| Bituminous base | 3.0 | 1.50 | 4.5 |
| Granular subbase | 6.0 | 1.00 | 6.0 |

Total equivalent granular subbase thickness = 15.6

The thickness of AC required is 4 in. The amount of granular subbase material equivalent to 4.0 in. of AC is $4.0 \text{ in.} \times 1.70$ (equivalency factor for AC) = 6.8 in. This leaves $15.6 \text{ in.} - 6.8 \text{ in.} = 8.8 \text{ in.}$ of granular subbase material. The required thickness of crushed stone base course is 9.0 in. or 12.6 in. of equivalent granular subbase (equivalency factor is 1.40). For this example, the thickness of granular subbase is less than the equivalent 9.0 in. of thickness for the required crushed base, so the 8.8 in. of granular subbase will be converted to crushed stone base. The equivalent conventional pavement section thickness t to be used in the evaluation methodology is then 4.0 in. of AC plus 6.3 in. ($8.8 \div 1.40$) of crushed stone base, or 10.3 in.

Example No. 2. Assume a pavement section to be evaluated has a 5.0-in. AC wearing surface, an 8.0-in. bituminous base, an 11.0-in. crushed stone subbase, and a second subbase of 14.0-in. granular material.

| <u>Layer Material</u> | <u>Layer Thickness in.</u> | <u>Layer Equivalency Factor</u> | <u>Equivalent Subbase Thickness in.</u> |
|--------------------------|--------------------------------|---|---|
| AC | 5.0 | 1.70 | 8.5 |
| Bituminous base | 8.0 | 1.50 | 12.0 |
| Crushed stone subbase | 11.0 | 1.40 | 15.4 |
| Granular subbase | 14.0 | 1.00 | 14.0 |

Total equivalent granular subbase thickness = 49.9

The total thickness of granular subbase equivalent to a 4.0-in. layer of AC is 4.0 in. \times 1.70 in. = 6.8 in. The total thickness of granular subbase minus the thickness needed for a layer of AC = 49.9 in. - 6.8 in. = 43.1 in. The total thickness of granular subbase equivalent to 9 in. of crushed stone base = 9.0 in. \times 1.40 = 12.6 in. The remaining granular subbase = 43.1 in. - 12.6 in. = 30.5 in. The equivalent conventional pavement section thickness t to be used in the evaluation methodology is then 4.0 in. of AC plus 9.0 in. of crushed stone base (maximum allowable thickness of base course material) plus 30.5 in. of granular subbase, or 43.5 in.

DSM-allowable single-wheel load correlation. To convert sections tested in this study to equivalent sections of conventional pavement, the previously described procedure for applying the equivalency factors was used. For the correlation of DSM to allowable single-wheel load, pavement with minimum thicknesses of AC and granular base as required by FAA⁴² were used. These requirements for a single-wheel load are 3-in. AC and base course thickness varying as a function of load. Therefore, conversion of the test pavements to equivalent conventional sections became a trial-and-error process to obtain a minimum thickness of base that was required by the computed allowable load. The measured thickness of the test pavements and the equivalent conventional sections are shown in Tables 4 and 18, respectively. Also shown in Tables 4 and

Table 18

Equivalent Conventional Flexible Pavement Thicknesses

| Test Site No. | AC Thickness in. | Base Thickness in. | Subbase Thickness in. | Single- Wheel Load kips |
|---------------------|------------------------|--------------------------|-----------------------------|----------------------------------|
| N18 | 3.0 | 4.1 | 0 | 19.6 |
| N20 | | 6.6 | 0 | 27.3 |
| N22 | | 7.0 | 0.3 | 29.8 |
| N23 | | 7.0 | 0.3 | 29.4 |
| W1 | | 9.0 | 1.5 | 46.2 |
| W2 | | 11.0 | 4.6 | 76.0 |
| B1 | | 11.0 | 10.8 | 89.3 |
| B2 | | 10.0 | 7.2 | 61.9 |
| B3 | | 11.0 | 4.7 | 65.2 |
| P1 | | 8.0 | 10.7 | 35.0 |
| P2 | | 7.0 | 9.3 | 24.5 |
| P5 | | 7.0 | 1.2 | 27.4 |
| P13 | | 12.0 | 7.4 | 105.9 |
| P14 | | 12.0 | 5.6 | 91.4 |
| NV1 | | 14.0 | 19.5 | 154.4 |
| NV3 | | 10.0 | 7.1 | 52.6 |
| NV4 | | 14.0 | 20.0 | 158.4 |
| SS1 | | 10.0 | 26.6 | 60.1 |
| S1 | | 6.0 | 8.3 | 13.4 |
| S2 | | 6.0 | 10.2 | 16.2 |
| S3 | | 8.0 | 20.5 | 39.0 |
| S4 | | 7.0 | 14.6 | 25.1 |
| S5 | | 7.0 | 14.9 | 25.7 |
| S6 | | 7.0 | 17.2 | 29.8 |
| S7 | | 7.0 | 22.4 | 30.8 |
| S8 | | 8.0 | 17.7 | 32.8 |
| S9 | | 10.0 | 23.6 | 51.7 |
| S10 | | 8.0 | 18.4 | 34.2 |
| S11 | | 10.0 | 25.4 | 56.7 |
| S12 | | 7.0 | 16.3 | 28.1 |
| S13 | | 10.0 | 26.6 | 60.1 |

18 are data for pavements that were constructed at WES to study the performance of stabilized materials. These stabilized pavements are denoted by the letter "S," such as S1. The equivalent sections were then used with the subgrade CBR of each pavement to compute the allowable load for a single wheel having a 254-sq-in. contact area for a load repetition level of 1200 annual departures of a 20-yr life (24,000 departures). These allowable single-wheel loads shown in Table 18 were then plotted against the DSM measured on each pavement as shown in Figure 41. The inclusion of the stabilized pavement data in Figure 41 shows that the stabilized pavements when converted to equivalent conventional pavements tend to have the same general relationship between DSM and allowable load as do the pavements without the stabilized layers.

Equivalent section for evaluation. Minimum AC thicknesses of 3 in. for single-gear aircraft, 4 in. for dual- and dual-tandem-gear aircraft, and 5 in. for wide-body aircraft are required in critical areas by FAA criteria.⁴² Base course thickness requirements for all aircraft vary from 6 to 14 in. Subbase thickness requirements vary from zero to approximately 60 in. Base course and, consequently, subbase course thicknesses depend on gross aircraft weights as discussed earlier. Therefore, to determine the exact thickness of an equivalent section to which an existing section must be converted, the allowable aircraft load must be known. The thicknesses can be determined by a trial-and-error process, similar to that used for the DSM-single-wheel load correlation, which must be repeated for each of the gear configurations. For example, if an evaluation is to be made for a dual-gear aircraft, the material in excess of 4 in. of AC and 6 in. of equivalent crushed stone base is converted to granular subbase for the first trial section. Then, an allowable load can be computed using a measured DSM and the first trial pavement section thickness. This allowable load can be used with the section thickness to enter Figure 3-4 of AC No. 150/5320-6B⁴² to determine if the base course thickness requirements are satisfied for the calculated load. If not, the calculation of the load using different base thicknesses must be repeated until the requirements are satisfied.

Instead of this trial-and-error process which must be repeated for each gear configuration and pavement type, it is recommended that each pavement that is to be evaluated be converted to an equivalent section containing an average thickness of 4-in. AC and 9-in. crushed stone base with any remaining material converted to granular subbase. The total thickness, t , of the equivalent pavement section is then used in the expression $t/\alpha\sqrt{A}$ in the evaluation process. The nondestructive procedure is less sensitive to changes in t than to changes in DSM. A comparison of several aircraft loads computed using the total pavement section thicknesses determined by these two methods and the same DSM values for both thicknesses gave values of load which differed by a maximum of ± 2 percent.

RIGID PAVEMENTS

Many parameters affect the load-carrying capacity of rigid pavements. The major parameters affecting the structural performance that can be considered in an evaluation methodology at the present time include the pavement thickness, strength of the concrete, strength of the foundation, loading geometry, and number of load repetitions. Other factors include temperature and moisture effects, material stability and durability, and changes in material properties due to chemical and physical changes; and, while these are not considered quantitatively, they are accounted for. That is, the pavement performance criterion to which the evaluation methodology is related has been established through accelerated traffic testing on actual pavements, long-term studies of pavement performance under actual operating conditions at existing airports, and material studies, both in the laboratory and in the field. Thus, the effects of these influencing factors on the overall ability of the pavement to carry loads satisfactorily is inherent in the performance criterion. Specifically, these factors are considered by the use of a design safety factor applied in accordance with anticipated traffic usage.

The basic rigid pavement methodology involves establishing a correlation between DSM and an allowable single-wheel loading as shown in

Figure 48. The correlation was developed for a stress repetition level representative of 1200 annual departures of a single wheel having a tire contact area of 254 sq in. The correlation shown in Figure 48 was generated by performing DSM tests on several actual pavements and correlating the DSM with the allowable single-wheel loading of the pavement section determined with conventional evaluation techniques using material properties (thickness, subgrade modulus, and flexural strength) measured during direct sampling.

To determine the allowable loading for aircraft having gears with different geometries, relationships between the loads of these aircraft and a single-wheel load with a contact area of 254 sq in. were developed. These relationships are based upon the equivalency of maximum bending stress in the concrete slab. That is, relationships were developed which permit the determination of the load of any geometry that will result in the same maximum bending stress in the concrete slab as that produced by the allowable single-wheel load determined by correlation with the DSM. The bending stress is a function of load, slab thickness, modulus of elasticity and Poisson's ratio of the concrete, and foundation modulus. The radius of relative stiffness ℓ is then used to interrelate the loading geometries. The relationship of ℓ versus load factor F is shown in Figures 49-52 and was developed using the Pickett and Ray influence charts,^{32,33} which are based upon the theory of thin slabs or plates on a dense liquid or Winkler foundation as presented by Westergaard.^{22-25,30} In these figures, the radius of relative stiffness ℓ is computed as

$$\ell = \sqrt[4]{\frac{Eh^3}{12(1 - \nu^2)k}}$$

where

h = thickness of the concrete slab, in.

ν = Poisson's ratio of concrete

It is evident that properties of the concrete and foundation must be determined in order to compute ℓ . If the modulus of elasticity E and Poisson's ratio ν are assumed as 6×10^6 psi and 0.20,

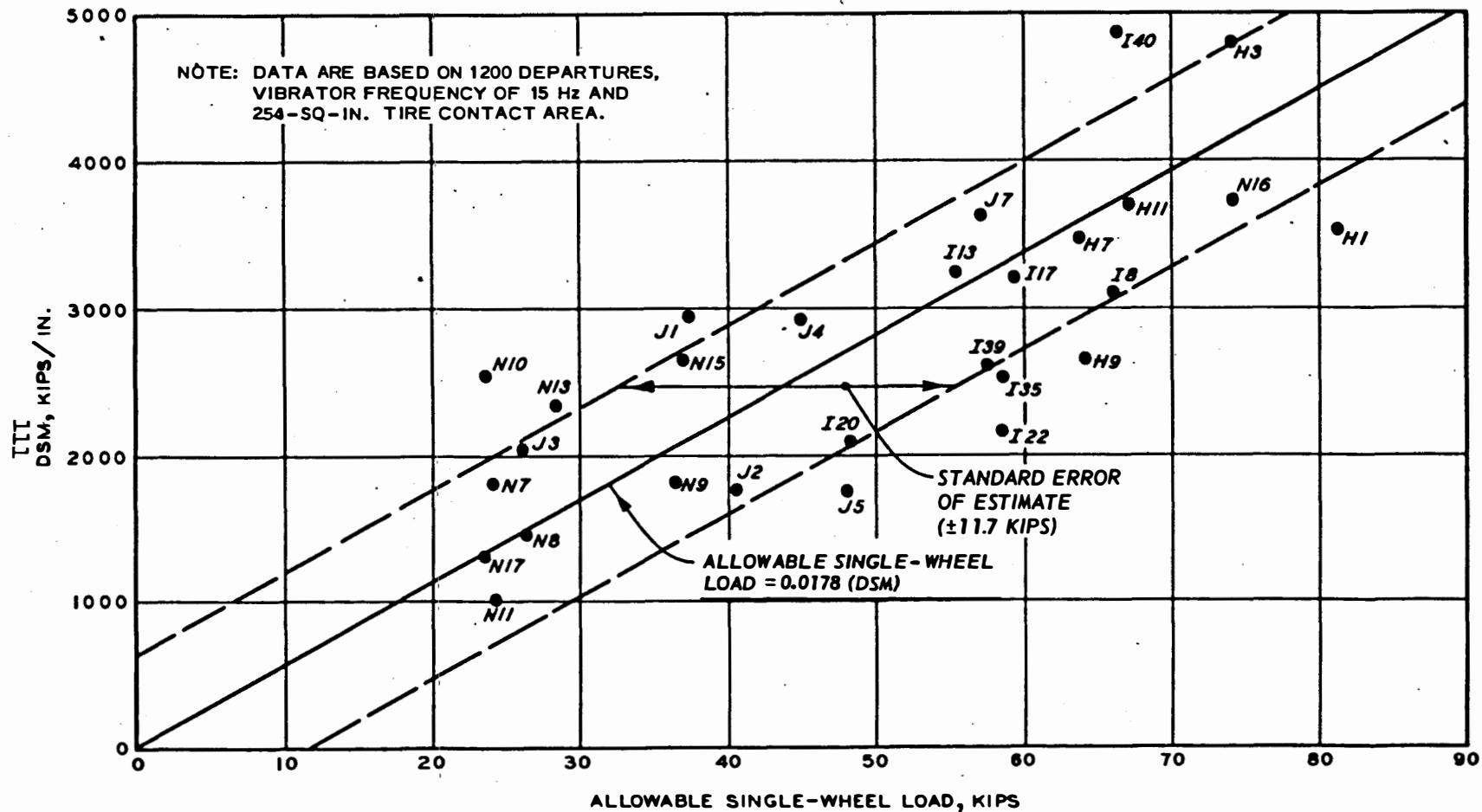


Figure 48. DSM versus allowable single-wheel load on rigid pavement

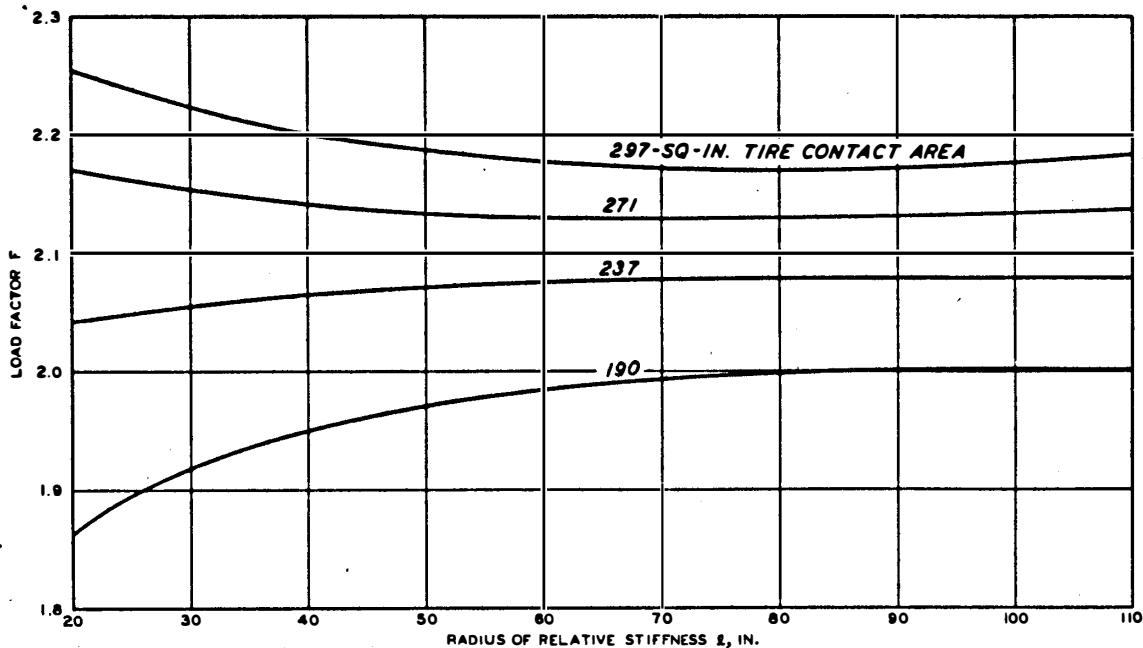


Figure 49. F versus l for single-wheel aircraft on rigid pavement

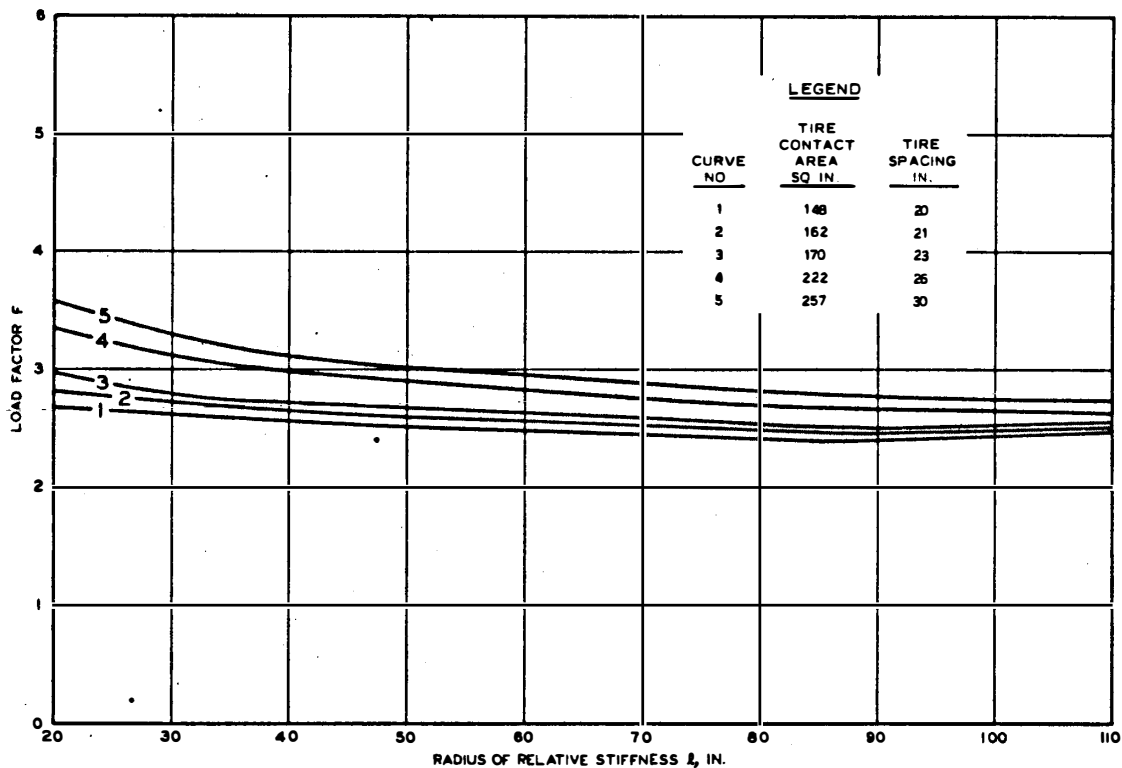


Figure 50. F versus l for dual-wheel aircraft on rigid pavement

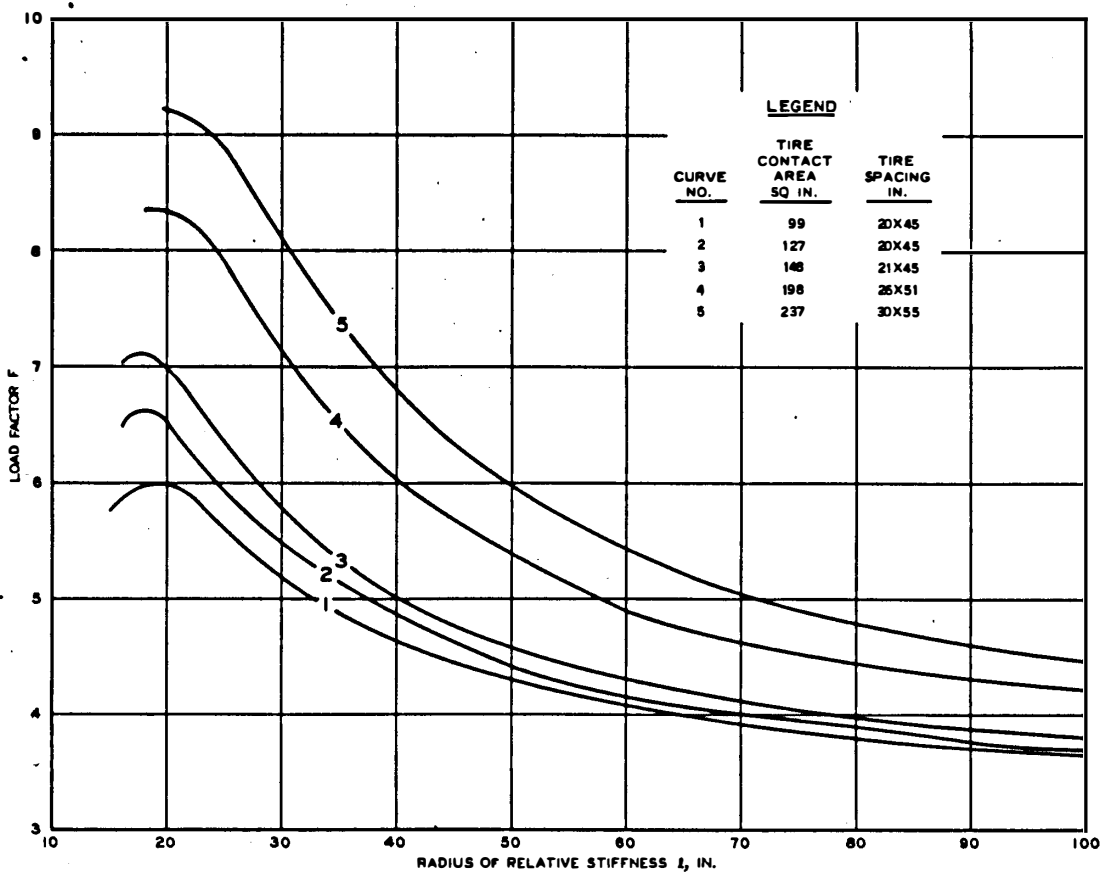


Figure 51. F versus l for dual-tandem aircraft on rigid pavement

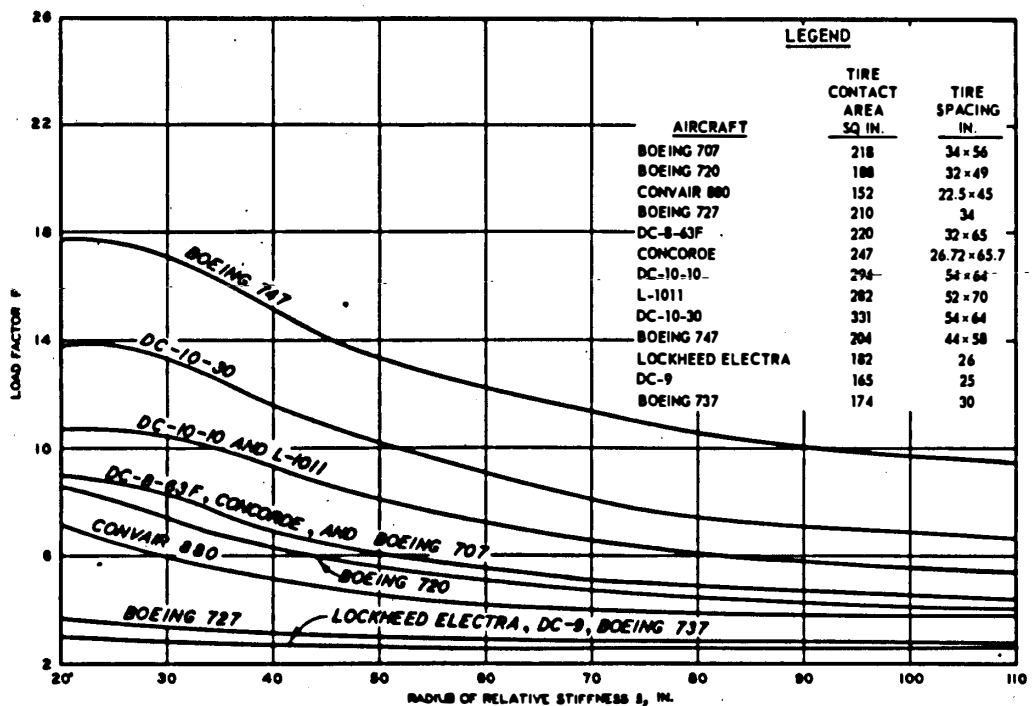


Figure 52. F versus l for various commercial jet aircraft on rigid pavement

respectively, the computation of ℓ would be reduced to

$$\ell = 26.9 \sqrt[4]{\frac{h^3}{k}}$$

If E is assumed as 4×10^6 psi, the expression becomes

$$\ell = 24.2 \sqrt[4]{\frac{h^3}{k}}$$

The difference in values of ℓ for the two different values of E is 10 percent. Therefore, the error introduced by assuming reasonable values of E is not considered significant to warrant the precise determination of E . The value of 6×10^6 psi for E was used in the development of the methodology presented here.

Although the value of ℓ is a function of $h^{3/4}$, the thickness of the slab should be determined accurately either by direct measurement or from as-built construction drawings. The ℓ value is a function of $(1/k)^{1/4}$, for which the modulus of soil reaction k , which is equal to the foundation strength factor F_f , is normally determined by a plate bearing test. However, a value can be assigned k based upon subgrade soil group (classification) without seriously affecting the accuracy of the results. Figure 53 presents the relationship between the FAA and USCS subgrade soil groups and the thickness and type of base course and yields the value of k that can be expected to occur directly beneath the concrete slab. (Approximate interrelationships of several soil classifications and bearing values are shown in Figure 54.) The relationship shown in Figure 53 is based upon actual tests and represents normal conditions (i.e., nonfrozen, normal densities; normal percent of saturation; and a fairly high quality of granular base course material).

The load factor F is the ratio of single-wheel load on a contact area of 254 sq in. to the gross aircraft load having a specified gear geometry, both of which will produce the same bending stress in the concrete slab. Stresses were computed with the gear oriented so that the maximum bending stress would be produced in the bottom of

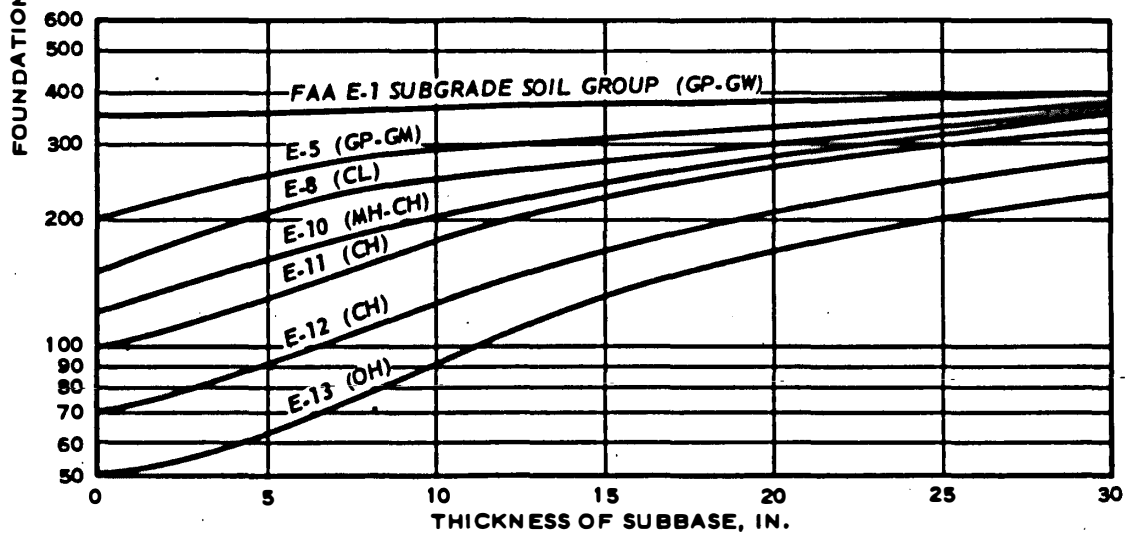
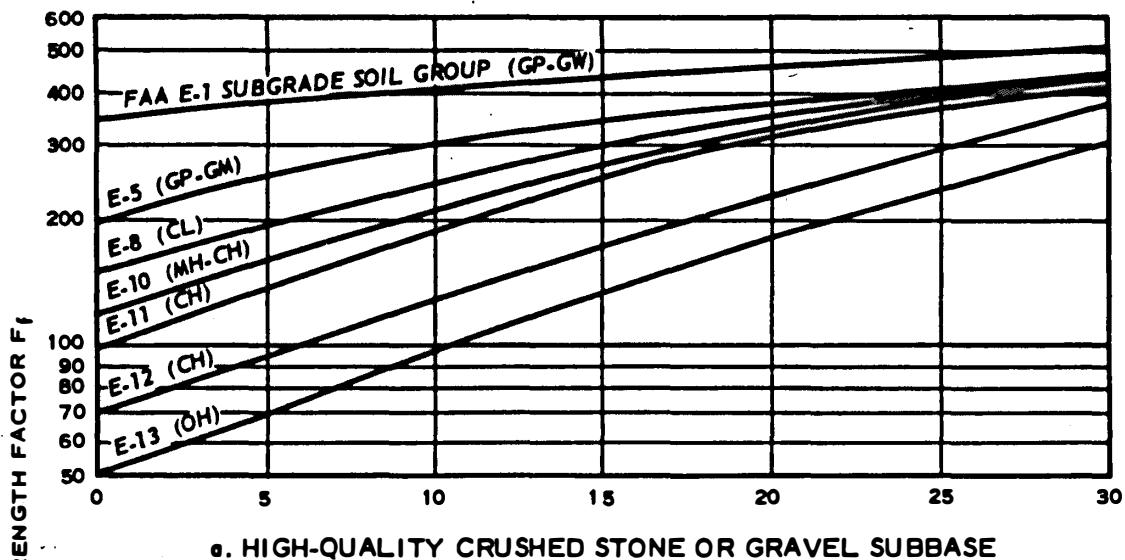


Figure 53. F_f versus subbase thickness and soil groups

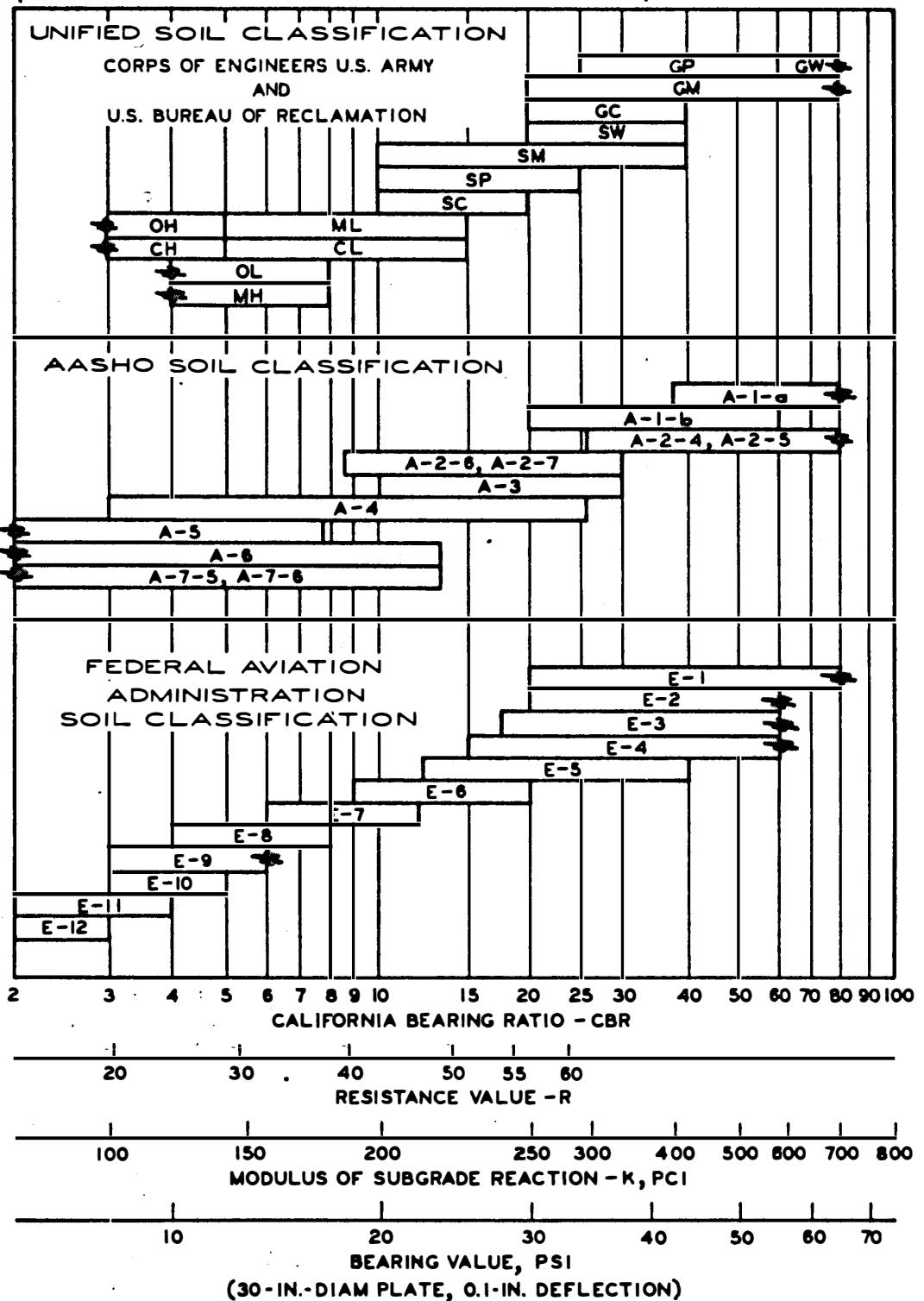


Figure 54. Approximate interrelationships of soil classifications and bearing values. Reprinted from "Design of Concrete Airport Pavement"⁵⁰ by R. G. Packard by permission of Portland Cement Association. Year of first publication 1973

the slab, at and parallel to the edge of the slab. For the aircraft considered, the nose gear and the main gears are spaced far enough apart so that the stress induced in a slab by one of the gears is independent of the stress induced by any other gear. As a consequence, the stress for an aircraft was computed by considering the effects of one main gear. It was assumed that 95 percent of the load was carried on the main gears, and the gross aircraft load was computed considering this distribution of load and the number of main gears for the particular aircraft.

The effects of stress repetition levels on the allowable gross aircraft load are considered by use of load repetition factors (Table 16). Load repetition factors are a function of the aircraft gear geometry, the lateral distribution of aircraft traffic on the pavement being evaluated, and the traffic volume, and are independent of the pavement structure. As will be seen, each gear configuration has a load repetition factor assigned based upon the number of wheels, tire contact area, and wheel spacing. In addition, the load repetition factor varies depending upon the usage of the pavement facility. For evaluation purposes, pavement usage has been considered to be that described in Reference 42: the interior width of runways and the entire width of primary taxiways are considered to be critical pavement areas receiving concentrated traffic, while high-speed taxiways are considered to receive less traffic for reasons outlined previously for flexible pavement. For design purposes for high-speed taxiways, FAA uses 0.9 of the slab thickness h required for critical areas. A ratio of 1.18 was found to exist between the evaluated loads using the full thickness and $0.9h$. Therefore, the procedure described previously for evaluation of critical pavement areas can be used for high-speed taxiways by multiplying the resulting allowable load by 1.18.

The relationship between allowable loads for various traffic volumes can be expressed mathematically by considering a pavement section having certain properties. Since the stress induced in a slab is directly proportional to the load (assuming a constant contact area), the allowable load for any stress repetition level can be found

by multiplying the load for a standard number of stress repetitions by the ratio of the safety (design) factors for the two stress repetition levels. The allowable load for any stress repetition level may be found by multiplying the allowable load at the standard stress repetition level by the ratio of the safety (design) factors for the two stress repetition levels.

The load repetition factors listed in Table 16 are the quotients of the safety (design) factors for a standard stress repetition level for 1200 annual departures (20-yr pavement life) of a single wheel having a tire contact area of 254 sq in. divided by the safety (design) factor for a stress repetition level computed for the indicated aircraft type for the indicated traffic volume and a 20-yr pavement life. The load repetition factor thus defined accounts for the differences in the factors for converting aircraft departures to stress repetitions for the single wheel with a 254-sq-in. contact area and the various aircraft. Since the safety (design) factors for particular stress repetition levels are independent of the loading producing the stress repetitions, the allowable aircraft load at the desired traffic level may be computed by multiplying the aircraft load obtained from Figures 49-52 by the appropriate load repetition factor.

It should be noted that load repetition factors were computed by assuming that only departures are critical, i.e., stress repetitions resulting from landing operations are ignored. Although the methodology can accommodate the effects of landings, these effects do not warrant the sophistication in analysis that is necessary. Normally, landing operations are only additive on the runway since en route to the apron, incoming aircraft use different taxiway systems than do departing aircraft. On runways and high-speed taxiways, the reduced loads and high speeds of landings produce stresses significantly lower than those of the more heavily loaded departing aircraft, and thus the effects on pavement life are significantly less. Aircraft departures were converted to stress repetitions (coverages) by the method suggested by Brown and Thompson⁴⁷ for taxiways and runway ends. Safety (design) factors for the various traffic levels were obtained from

curves presented by Hammitt et al.²¹

Rigid pavements with stabilized layers. The thickness h in the preceding discussion of rigid pavements assumes a conventional rigid pavement consisting of a layer of PCC with a thickness h on a granular subbase and/or a subgrade. Pavement structures to be evaluated which contain a stabilized layer beneath the layer of PCC must be converted to an equivalent thickness of PCC without a stabilized layer. This can be done by a procedure given in FAA AC 150/5320-6B⁴² from which Figure 55 is taken. The procedure requires knowledge of the modulus of elasticity of the subbase (to 1,000,000 psi for soil-cement) and the thickness of the two layers.

Example. Assume a pavement section has a concrete layer with $h_1 = 14$ in. and a subbase of soil-cement with $h_2 = 9$ in.

Equivalent thickness = $(h_1)(r)^{1.33}$ where r = relative change in pavement stiffness

$$\frac{h_1}{h_2} = \frac{14}{9} = 1.56 \text{ in.}$$

$$E_2 = 1 \times 10^6 \text{ psi}$$

From Figure 55, $r = 1.16$

$$\text{Equivalent thickness} = (14.0)(1.16)^{1.33} = 17.0 \text{ in.}$$

This procedure was used to compute equivalent pavement thicknesses for those rigid pavement test sites which contained stabilized layers. These equivalent pavement thicknesses were then used to compute the allowable single-wheel loads for the correlation with DSM shown in Figure 48. The same procedure for computing equivalent thicknesses for rigid pavements with stabilized layers should be used in the evaluation procedure.

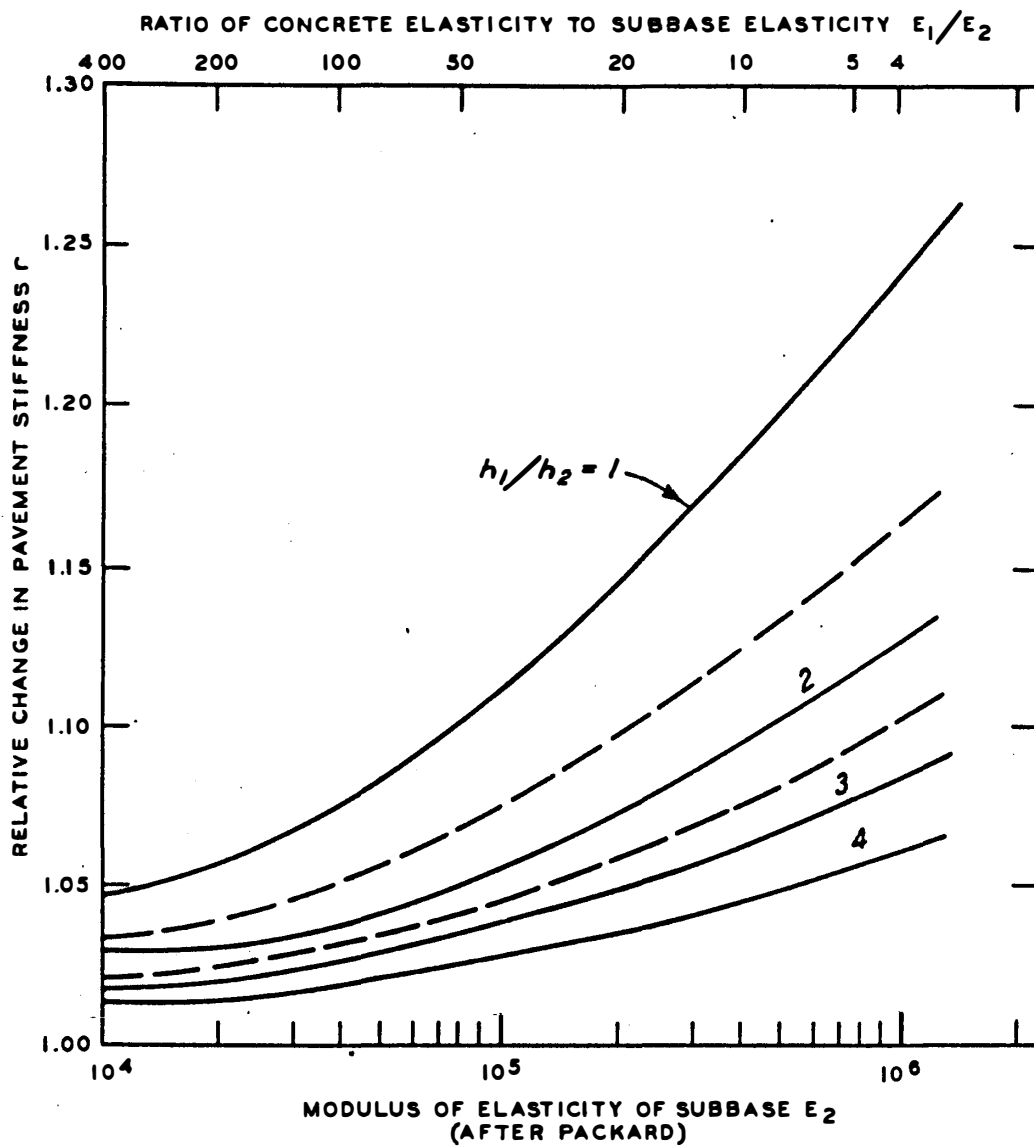


Figure 55. Effect of stabilized layer on pavement stiffness (from Reference 42)

NONDESTRUCTIVE EVALUATION PROCEDURE

The procedure presented in this section of the report is based on nondestructive testing in which a steady state vibratory loading is applied and the resulting elastic deflection is measured to determine a DSM. This procedure is designed to replace under some conditions and supplement under other conditions the existing procedure based on soil and pavement sampling and testing for the evaluation of allowable gross aircraft loads of conventional flexible and rigid pavements as defined in Reference 42. The conditions under which the nondestructive evaluation procedure replaces or supplements the existing procedure will be indicated in this section of the report. A nondestructive evaluation based on the procedure will be valid only for the conditions existing at the time of the tests and will not account for changes due to such factors as environment or moisture in the subgrade. These factors should be accounted for as deemed necessary through conventional procedures.

NONDESTRUCTIVE TESTING EQUIPMENT

Several models of transportable vibrators have already been described. These models differ in details of operation, size, and configuration, but the test methods for all of them are basically the same. The basic procedure consists of bringing a mass in contact with the pavement, exciting the mass with a steady state vibration, and monitoring the applied vibratory load and the resulting elastic deflection of the pavement surface. The evaluation procedure presented herein must be used with a vibrator with the same static weight and contact plate size as the existing 16-kip vibrator, or the vibrator described in Appendix C using the 16-kip mass. Use of vibrators other than the 16-kip size to collect data for use with the procedure may introduce errors since the evaluation methodology was developed around data collected with the 16-kip vibrator. Figures 10-13 show that all vibratory devices do not give the same results.

DATA COLLECTION

The form of nondestructive data that was selected during

development of the methodology described previously is called the DSM (dynamic stiffness modulus). "Dynamic" differentiates this data from that obtained under very slow loading conditions, normally referred to as "static loading," and implies a condition of steady state vibratory loading. "Stiffness modulus" denotes that the measurement is determined from the slope of the load-deflection plot and reflects the rigidity of the pavement being tested. Determination of the DSM for a test site requires only a few minutes, including the time for setting up equipment, recording data, and calculating the DSM. Figure 56 shows a typical deflection versus load plot measured at 15 Hz. The DSM is the slope of the deflection versus load plot, which in Figure 56 is 4550 kips/in. Many load-deflection plots are nonlinear along their lower portions and must be adjusted as discussed previously to obtain the DSM. The linear portions of the plots are used to compute DSM values because, of the various forms of nondestructive data studied, DSM values computed in this manner gave the best correlation with aircraft gross weights. Correlations are shown in Figures 41 and 48.

Determinations of allowable multiple-wheel aircraft loads using DSM values require that pavement thickness t be known for flexible pavements and that the foundation strength factor F_f and pavement (slab) thickness h be known for rigid pavements. It is not necessary that these parameters be known for each nondestructive test location. For uniform conditions, such as a critical area where the pavement thickness varies only within construction tolerances and soil conditions do not vary significantly, average values of t or F_f and h can be assumed for the entire area being evaluated. The allowable aircraft loads are not sensitive to changes in these values to a degree that the accuracy of the evaluation will be significantly affected by the use of average values. The values of t or F_f and h for each area of uniform condition to be evaluated can be determined from small aperture testing⁴⁵ or construction records, and F_f can be estimated from curves presented in this section of the report. If neither the required direct sampling data nor drawings are available, the first step in the evaluation should be to perform DSM tests on the features to be evaluated so that DSM

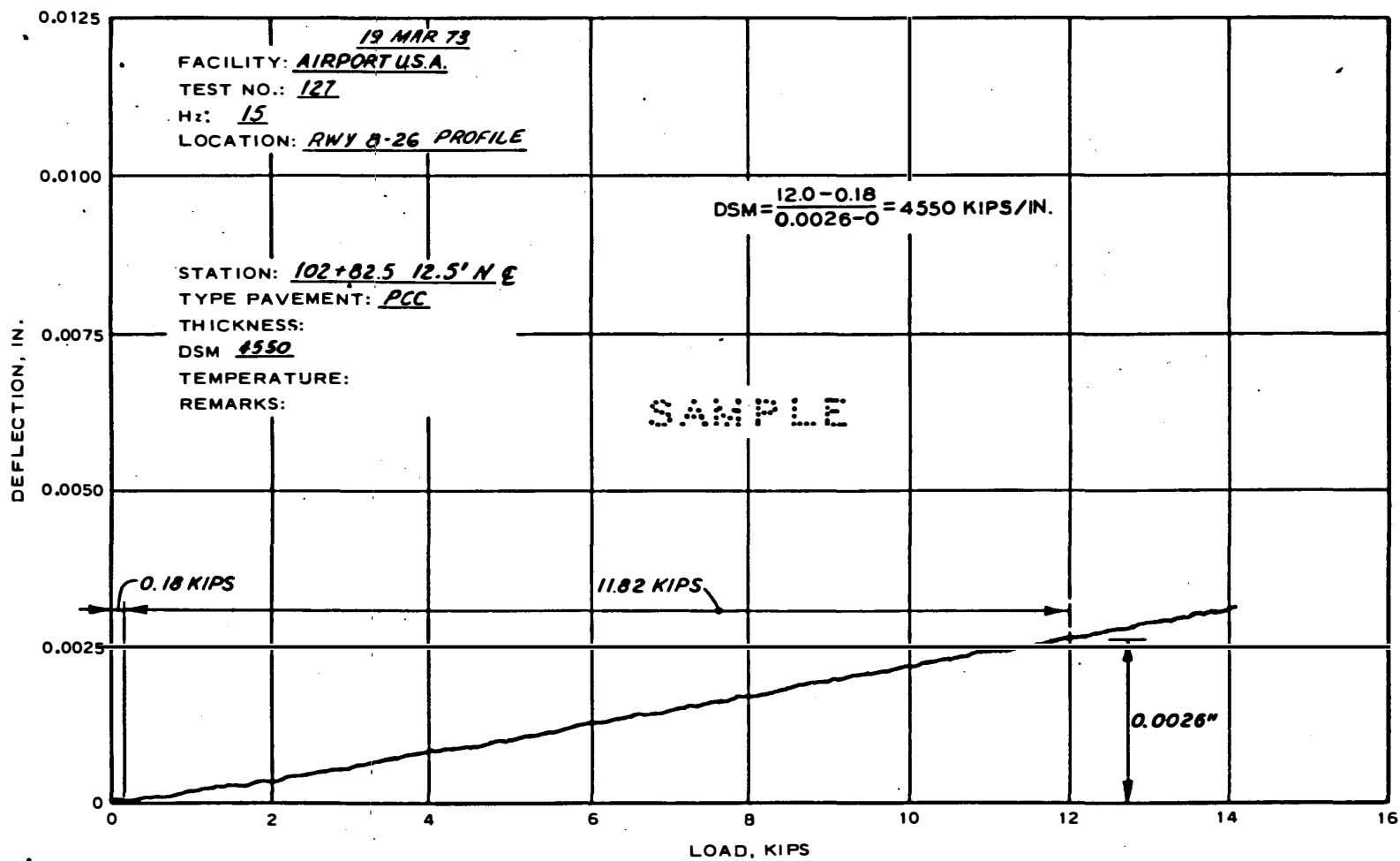


Figure 56. Deflection versus load (sample plot)

profiles of the features can be plotted. These profiles will show features for which direct sampling tests are necessary by indicating significant changes in DSM values. Such changes can be caused by variations in pavement thickness, subgrade strength, or pavement condition. Only one direct sampling test will be necessary in a particular area when there is little variability in the DSM results.

SELECTION OF TEST LOCATIONS

DSM tests are made to locate and define weak areas on a pavement facility, to provide a rational basis for selection of test pit locations for in-place tests, to rate the DSM of one pavement facility against that of another pavement, and/or to determine the allowable gross aircraft load for a pavement using the evaluation curves presented herein.

The nondestructive evaluation of a runway, taxiway, ramp, or other feature should be performed by dividing the feature into areas according to the traffic patterns, critical and noncritical areas, ages, traffic histories, and type of pavement structure. The boundaries of these areas can be drawn approximately from construction drawings and observations of airport personnel prior to obtaining the DSM measurements; however, the vibrator results can be used to locate the boundaries generally through comparisons of DSM measurements for the various areas.

The evaluating engineer may choose to perform no tests in areas which have no traffic or several hundred tests in the critical, heavy traffic, main gear path areas. DSM data from each test area should be arranged in some logical order so that they can be studied. A form, similar to Table 19, for each pavement type is suggested. Data in Table 19 are arranged in descending order of DSM values to show the extent of weak areas. In addition to DSM values, this table also shows test site locations and numbers. In determining allowable gross aircraft loads using the evaluation procedure presented herein, a representative DSM value is obtained by subtracting one standard deviation from the arithmetic mean.

Table 19
Tabulation of DSM Values (Example), Airport, USA
Runway No. 10L-200R, Critical Area No. 1, Main Gear Wheel Path

| Column 1 | Column 2 | Column 3 | Column 4 | Column 5 | Column 6 |
|----------------|--|---------------|-----------------------------|--|--|
| Runway Station | Offset to Left or Right of ℓ ft | Test Site No. | DSM _i , kips/in. | DSM _i - DSM _{MEAN} | (DSM _i - DSM _{MEAN}) ² |
| 46+00 | 10L | 24 | 1360 | 280 | 78,400 |
| 40+00 | 10R | 21 | 1320 | 240 | 57,600 |
| 42+00 | 10L | 22 | 1300 | 220 | 48,400 |
| 44+00 | 10R | 23 | 1290 | 210 | 44,100 |
| 18+00 | 10L | 18 | 1290 | 210 | 44,100 |
| 48+00 | 10R | 25 | 1240 | 160 | 25,600 |
| 64+00 | 10R | 33 | 1230 | 150 | 22,500 |
| 62+00 | 10L | 32 | 1200 | 120 | 14,400 |
| 58+00 | 10L | 30 | 1200 | 120 | 14,400 |
| 60+00 | 10R | 31 | 1180 | 100 | 10,000 |
| 38+00 | 10L | 20 | 1180 | 100 | 10,000 |
| 14+00 | 10L | 8 | 1180 | 100 | 10,000 |
| 10+00 | 10L | 6 | 1180 | 100 | 10,000 |
| 16+00 | 10R | 9 | 1170 | 90 | 8,100 |
| 36+00 | 10R | 19 | 1170 | 90 | 8,100 |
| 66+00 | 10L | 34 | 1170 | 90 | 8,100 |
| 12+00 | 10R | 7 | 1160 | 80 | 6,400 |
| 8+00 | 10R | 5 | 1140 | 60 | 3,600 |
| 30+00 | 10L | 16 | 1130 | 50 | 2,500 |
| 32+00 | 10R | 17 | 1110 | 30 | 900 |
| 34+00 | 10L | 18 | 1110 | 30 | 900 |
| 68+00 | 10R | 35 | 1080 | 00 | 0 |
| 28+00 | 10R | 15 | 1070 | -10 | 100 |
| 50+00 | 10L | 26 | 1060 | -20 | 400 |
| 6+00 | 10L | 4 | 1060 | -20 | 400 |
| 4+00 | 10R | 3 | 1060 | -20 | 400 |
| 52+00 | 10R | 27 | 1020 | -60 | 3,600 |
| 70+00 | 10L | 36 | 1000 | -80 | 6,400 |
| 24+00 | 10R | 13 | 970 | -110 | 12,100 |
| 26+00 | 10L | 14 | 950 | -130 | 16,900 |
| 2+00 | 10L | 2 | 900 | -180 | 32,400 |
| 72+00 | 10R | 37 | 880 | -200 | 40,000 |
| 0+00 | 10R | 1 | 810 | -270 | 72,900 |
| 22+00 | 10L | 12 | 800 | -280 | 78,400 |
| 74+00 | 10L | 38 | 750 | -330 | 108,900 |
| 54+00 | 10L | 28 | 750 | -330 | 108,900 |
| 56+00 | 10R | 29 | 740 | -340 | 115,600 |
| 20+00 | 10R | 11 | 740 | -340 | 115,600 |

$$\sum (DSM_i - DSM_{MEAN})^2 = 1,141,100$$

$$DSM_{MEAN} = \frac{DSM_1 + DSM_2 + DSM_3 \dots DSM_{38}}{38} = 1080 \text{ kips/in.}$$

$$S \text{ (standard deviation)} = \sqrt{\frac{1,141,100}{38}} = 173 \text{ kips/in.}$$

$$\text{Representative DSM} = 1080 - 173 = 907 \approx 910 \text{ kips/in.}$$

The standard deviation, S , can also be computed by the formula

$$S = \sqrt{\frac{\sum (DSM_i)^2}{n} - \left(\frac{\sum DSM_i}{n}\right)^2}$$

where n is the number of DSM, which is 38 in the example above, and DSM_i denotes the particular DSM value being computed.

NOTE: When the number of DSM is less than 30, the formula for the standard deviation becomes

$$S = \sqrt{\frac{\sum (DSM_i - DSM_{MEAN})^2}{n - 1}}$$

or

$$S = \sqrt{\frac{\sum (DSM_i)^2 - 2DSM_{MEAN} \sum DSM_i + n(DSM_{MEAN})^2}{n - 1}}$$

When DSM values are to be used to determine allowable gross aircraft loads using the evaluation curves presented herein, it is recommended that DSM tests be spaced at equal intervals within the areas to be evaluated. However, no fewer than 30 DSM tests should be performed within each of the areas for major features, such as primary runways and taxiways, to provide a statistically representative sampling of the DSM for that pavement feature.⁵¹ Never should fewer than 11 tests be performed in any area being evaluated. Additional tests might be desirable on certain pavements, particularly in areas where weak conditions are found. On runways and taxiways, tests should be made on alternate sides of the center line along the main gear wheel paths. Tests on parking aprons should be located in a grid pattern.

DSM tests for the determination of allowable gross aircraft loads of rigid pavements should always be performed at the slab centers. The DSM may vary considerably with location of the tests on a particular slab, as explained previously. DSM data for DSM versus gross aircraft load curves for rigid pavements contained herein were collected at the slab centers, and the evaluation methodology is based on making the tests at that location.

CORRECTIONS TO DSM VALUES

The environment or time of the year when DSM tests are performed significantly influences the results as can be seen in the discussion on temperature and in Figure 36. As the DSM value for a particular test site rises or falls during the year, so does the load-carrying capacity. It is difficult to determine what set of conditions is best representative of the "average" load-carrying capacity. DSM tests made when the pavements are under the influence of frost thaw, and probably in their weakest condition, would give conservative evaluation results. Likewise, DSM tests made in the late fall when the subgrade is normally dry and temperatures are not extreme, or tests made when subgrades are frozen, would give nonconservative results and no indication of the relatively low DSM values which would be measured during frost thaw. The relationship between the highest and lowest possible DSM values which could be

measured for a particular site has not been determined, nor has the relationship between the highest and lowest load-carrying capacities of a particular site. Therefore, a correction for the effects of frost thaw or environment has not been developed. Because of the lack of a correction factor and because there are periods of high DSM values and load-carrying capacities during the year, it is recommended that the DSM tests be performed during the period of the year when conditions are as near average as can be judged by experience. In particular, DSM measurements should be made when pavements or subgrades are not under the influence of frost or subsequent thaw, unless the evaluation is being made specifically to study frost effects on the length of time which DSM are influenced or on relative changes in DSM values.

One effect of higher temperatures on flexible pavements is to lower DSM values. This effect is magnified as the thickness of the AC layer increases. Results of tests described previously on test pavements at WES to study temperature effects were used to produce the relationship shown in Figure 34. The mean pavement temperature is determined by averaging the temperatures recorded at 1 in. below the surface, at the center, and at 1 in. above the bottom of the AC layer. Figure 34 can be used to adjust the DSM values to a common temperature, to compare values for a given pavement feature or for different features, and to correct DSM values to an adjusted temperature* for use in the allowable gross load relationships contained herein. The adjustment factor obtained from Figure 34 is multiplied times the DSM. However, the data used to develop the relationship in Figure 34 were for a particular pavement and subgrade type and therefore may not be applicable to pavements that differ greatly from it. Also, the temperature correction curves in Figure 34 were extrapolated below mean pavement temperatures of 60°F.

The mean pavement temperature at the time DSM tests are performed is determined by installing thermometers in the pavement sections. Thermometer installations in flexible pavements should consist of a minimum

* An adjustment temperature of 70°F is suggested when the DSM is to be used with the procedure contained herein because the DSM data used to develop the methodology were adjusted to 70°F.

of three thermometers in a vertical line with one at 1 in. below the surface, one at the center, and one at 1 in. above the bottom of the AC layer. If DSM tests are performed on the same location near each thermometer installation during the warmest and coolest pavement temperatures each day during the test period, then a correlation between DSM values and mean pavement temperatures can be established for the pavements. This correlation can then be used either to verify or modify the relationships shown in Figure 34 so that DSM data can be adjusted to the standard temperature of 70°F.

An alternative method in which the mean pavement temperature may be predicted from air temperature data has been developed by the Asphalt Institute.⁴⁶ Data required are the maximum and minimum air temperatures for each of the 5 days immediately prior to the date the DSM tests are made and the pavement surface temperature at the time of the DSM tests. Pavement temperatures at various depths can then be estimated from Figure 35. The estimated temperatures in the AC at 1 in. below the surface, at the center, and at 1 in. above the bottom of the AC layer can be averaged to obtain the mean pavement temperature.

DETERMINATION OF ALLOWABLE AIRCRAFT LOADING

Determination of the allowable aircraft loading for a pavement requires determination of the representative DSM value for the pavement, application of the DSM to the appropriate DSM versus allowable single-wheel load curve, and modification of the results with the proper curves and factors presented in the following paragraphs. The use of this procedure for pavement evaluation is subject to the following restrictions:

- a. The DSM must be determined using a vibrator with a static weight of 16 kips and load plate diameter of 18 in.
- b. The DSM must be computed using the slope of the linear portion of the deflection versus load curve.
- c. The DSM must be measured at 15 Hz.
- d. A temperature adjustment must be applied to the DSM on flexible pavements.
- e. The DSM for rigid pavements must be measured at the slab center.

- f. The moduli of elasticity of the respective pavement layers under investigation must decrease with depth. For example, the methodology is not applicable for pavements with an AC layer over a PCC layer or pavements with an unbound material contained between two layers of PCC.

FLEXIBLE PAVEMENT EVALUATION PROCEDURE

Step 1. Using the DSM corrected for nonlinearity and adjusted to the standard temperature, determine the pavement system strength index S_p from Figure 57.

Step 2. Using the total thickness of flexible pavement structure above the subgrade, compute the factor F_t for critical pavements as

$$F_t = 0.067t$$

and for high-speed taxiways as

$$F_t = 0.074t$$

If the pavement structure contains stabilized layers or if the AC is not equal to 4 in. in thickness and/or the crushed stone base course is not equal to 9 in. in thickness, an equivalent pavement thickness must be computed as described under the section on flexible pavements with stabilized layers. Actual thicknesses may be obtained from construction drawings, or core holes when drawings are not available. One core hole to measure thickness may suffice for several DSM tests in a given pavement feature.

Step 3. Using F_t determined in Step 2, enter Figure 47 and determine the ratio of the subgrade strength factor SSF to the pavement system strength index S_p .

Step 4. Compute the subgrade strength factor SSF by multiplying the ratio SSF/S_p by the value of S_p determined in Step 1.

Step 5. Evaluate the pavement for any aircraft desired using the following steps:

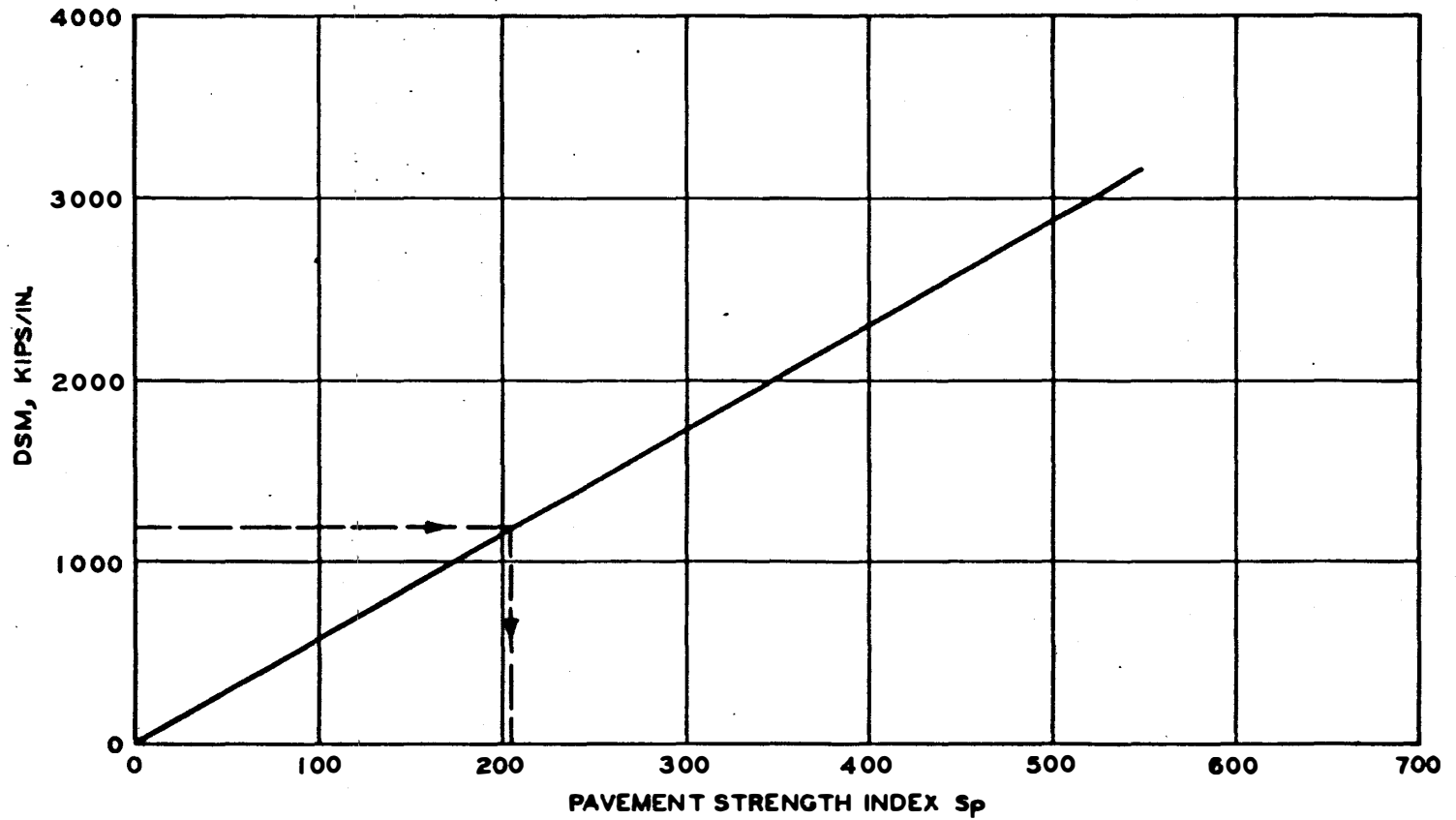


Figure 57. Evaluation curve for flexible pavement

- a. Select the aircraft or aircraft main gear configuration for which the evaluation is to be made and determine the tire contact area A of one wheel of the main landing gear from Table 20.
- b. Select the annual departure level for a 20-yr life for each aircraft for which the evaluation is being made and determine the load repetition factor for each aircraft from Table 16.
- c. Compute F_t for each aircraft for which the evaluation is being made for critical pavements as

$$F_t = \frac{t}{\alpha \sqrt{A}}$$

and for high-speed taxiways as

$$F_t = \frac{t}{0.9 \alpha \sqrt{A}}$$

- d. Enter Figure 47 with F_t and determine SSF/S_p .
- e. Compute S_p for the aircraft in question by dividing SSF determined in Step 4 into SSF/S_p determined in Step 5d. Multiply S_p by the tire contact area A from Step 5a to obtain the ESWL of the aircraft for which the evaluation is being made.
- f. Enter Figure 42, 43, or 44 with the total pavement thickness t and determine the percent ESWL for the controlling number of wheels of the aircraft for which the evaluation is being made, i.e., if the aircraft has a dual-wheel assembly with a dual spacing of 26 in., use Curve 4 in Figure 42 or, if the evaluation is for the Boeing 747 aircraft, use the Boeing 747 curve in Figure 44.
- g. The allowable gross aircraft load for the pavement being evaluated and for the traffic volume selected is then obtained by the following computation:

$$\text{Allowable gross aircraft load} = \frac{\text{ESWL}}{\% \text{ESWL}} \left(\frac{1}{W_c} \right) \left(\frac{W_m}{0.95} \right)$$

where

ESWL = determined by Step 5e

%ESWL = determined by Step 5f

W_c = number of controlling wheels used to determine the %ESWL from Figures 42, 43, or 44

Table 20

Aircraft Tire Contact Areas and Total
Number of Main Gear Wheels

| <u>Aircraft Gear Configuration or Model Designation</u> | <u>Typical Gross Weight kips</u> | <u>Tire Contact Area sq in.</u> | <u>Total No. of Main Gear Wheels</u> |
|---|--|---|--|
| Single-wheel | 30 | 190 | 2 |
| Single-wheel | 45 | 237 | 2 |
| Single-wheel | 60 | 271 | 2 |
| Single-wheel | 75 | 297 | 2 |
| Dual-wheel | 50 | 148 | 4 |
| Dual-wheel | 75 | 162 | 4 |
| Dual-wheel | 100 | 170 | 4 |
| Dual-wheel | 150 | 222 | 4 |
| Dual-wheel | 200 | 237 | 4 |
| Dual-tandem | 100 | 99 | 8 |
| Dual-tandem | 150 | 127 | 8 |
| Dual-tandem | 200 | 148 | 8 |
| Dual-tandem | 300 | 198 | 8 |
| Dual-tandem | 400 | 237 | 8 |
| Boeing 727 | 173 | 210 | 4 |
| DC-8-63F | 358 | 220 | 8 |
| Boeing 747 | 778 | 245 | 16 |
| DC-10-10 | 433 | 294 | 8 |
| DC-10-30 | 558 | 331 | 10 |
| L-1011 | 428 | 282 | 8 |
| Concorde | 389 | 247 | 8 |
| Boeing 737 | 111 | 174 | 8 |
| Lockheed Electra | 113 | 182 | 4 |
| DC-9 | 115 | 165 | 4 |
| Convair 880 | 188 | 152 | 8 |
| Boeing 720 | 235 | 188 | 8 |
| Boeing 707 | 336 | 218 | 8 |

W_m = total number of wheels on all main gears of the aircraft (i.e., wheels on the nose gear are not included) for which the evaluation is being made (see Table 20)

RIGID PAVEMENT EVALUATION PROCEDURE

Step 1. The DSM is used to enter Figure 58 and determine the allowable single-wheel load.

Step 2. The radius of relative stiffness ℓ is computed as

$$\ell = 26.9 \sqrt[4]{\frac{h^3}{F_f}}$$

If the subbase is stabilized, an equivalent pavement thickness must be computed as described beginning in the section on rigid pavement with stabilized layers. The foundation strength factor F_f is determined from Figure 53 using the subgrade soil group classification.

Step 3. Using ℓ , determine the load factor F from Figure 49, 50, 51, or 52, depending upon the gear configuration of the aircraft for which the evaluation is being made.

Step 4. Multiply the allowable single-wheel load from Step 1 by F determined from Step 3 to obtain the gross aircraft loading.

Step 5. Multiply the gross aircraft loading from Step 4 by the appropriate load repetition factor from Table 16 to obtain the allowable gross aircraft loading for critical areas for the pavement being evaluated. For the case of high-speed taxiways, the computed allowable gross load should be increased by multiplying by a factor of 1.18.

Step 6. The allowable loading obtained from Step 5 assumes that the rigid pavement being evaluated is structurally sound and functionally safe. The computed allowable loading should be reduced if one or more of the conditions outlined in the following section exist at the time of the evaluation.

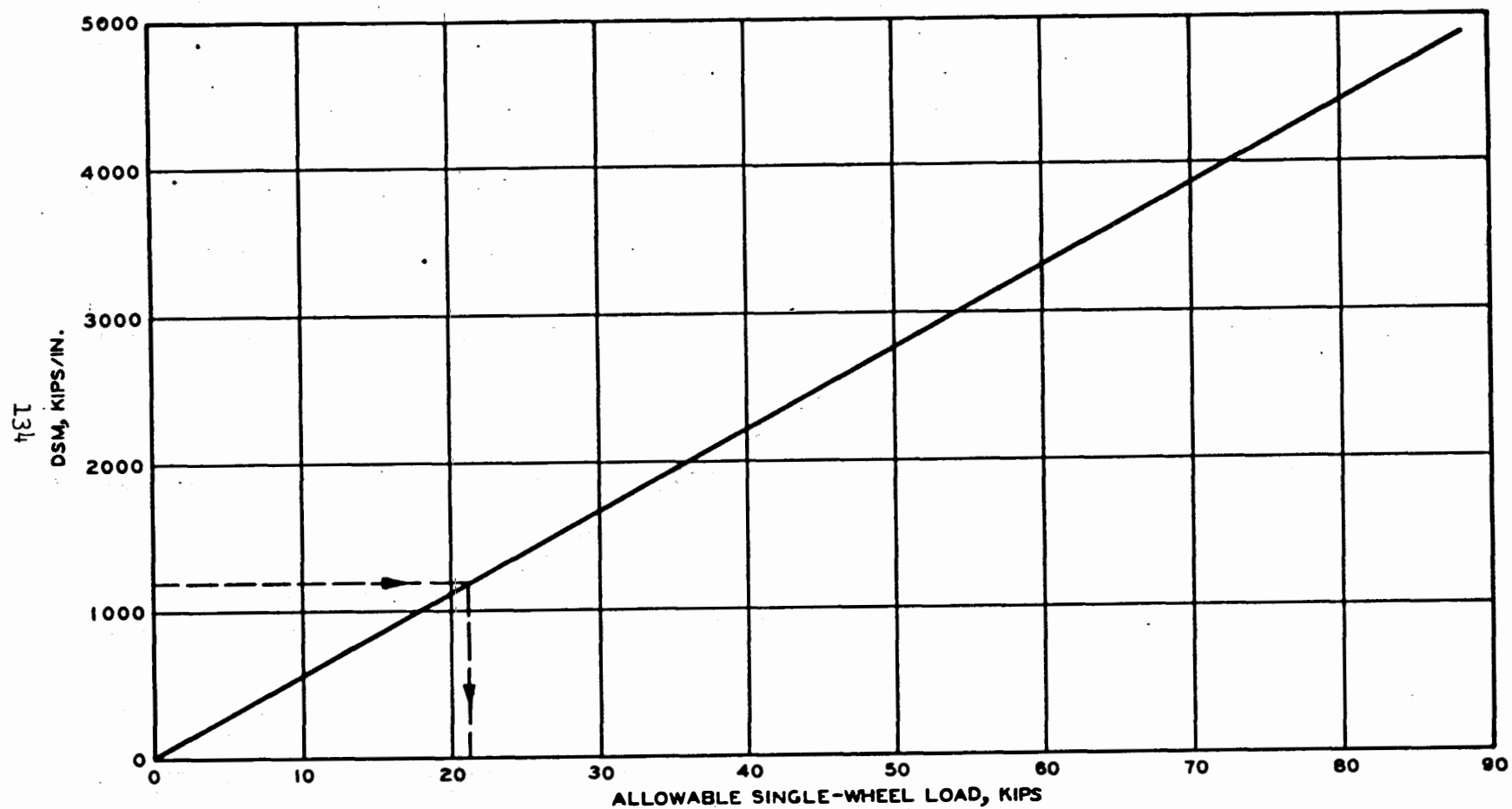


Figure 58. Evaluation curve for rigid pavement

REDUCTION OF CAPACITY OF DISTRESSED PAVEMENTS

Data used in the correlations of DSM and gross aircraft weight were collected from areas on pavements which were free of surface distress; therefore, for the evaluation curves presented herein to be valid, the DSM values used to enter the curves should be obtained from pavements that appear to be in good condition. There are many conditions of distress within pavement systems which significantly affect the DSM and, similarly, the allowable capacity; but these two factors are not necessarily affected by the same percentages of distress at a given location. The inability to treat the distressed condition accurately is inherent in the procedure presented herein and in all known direct sampling evaluation procedures, and results from the inability to describe the influencing factors accurately under all loading and environmental conditions. These conditions are recognized, however, and their effects on the pavement system can normally be accounted for by engineering judgment. Examples of the conditions caused by distress and the probable general changes which take place in DSM values as a result of these conditions are presented in Table 21 for flexible pavements and in Table 22 for rigid pavements. Most of these influencing conditions will be readily evident from a visual examination of the pavement system, and the importance of such an examination cannot be overemphasized.

For the conditions of distress for which the change in DSM is shown in Table 21 as "None," the DSM measured on a pavement which has the indicated deficiency may be used to enter the evaluation curve (Figure 57) as if no distress existed. Tests for the purpose of using the evaluation curve should not be performed on the remaining types of distressed areas; however, tests in these areas can be used as indications of relative strength. In determining the pavement system strength index of a pavement which is predominantly affected by one of the types of distress which influence the DSM, the DSM tests should be performed on pavement areas that appear to be in good condition and the extent of distressed areas should be noted in the evaluation report. Studies are under way to determine the significance of DSM in distressed areas.

Table 21

Expected Change in DSM on or near a Distressed Area of
Flexible Pavement Compared with DSM on a
Similar Area in Good Condition

| <u>Type of Distress</u> | <u>Cause*</u> | <u>Expected Change in DSM Due to Distress</u> |
|-----------------------------|--|---|
| Alligator cracks | Base failure | Decrease |
| Edge cracks | Lack of lateral or shoulder support | None |
| Joint cracks | Weak seam or poor bond | None |
| Shrinkage cracks | Volume change in as- phalt or subgrade | None |
| Slippage cracks | Lack of bond between surface and base | None |
| Channeling or depression | Consolidation or lat- eral movement of underlying layers | Increase if consolidation occurs; decrease if lateral movement occurs |
| Corrugations or shoving | Lack of stability in asphalt mixture | None |
| Upheaval | Subgrade swelling | Decrease |
| Potholes | Too little asphalt, too thin an asphalt sur- face, too many fines, or poor drainage | Decrease |

* As described in Reference 52.

Table 22

Expected Change in DSM on Distressed Slabs of Rigid
Pavement Compared with DSM on Similar
Slabs in Good Condition

| <u>Type of Distress</u> | <u>Cause</u> | <u>Expected Change in DSM Due to Distress</u> |
|---------------------------------------|---|---|
| Pumping pavement* | Subbase or subgrade failure caused by excessive moisture and/or voids created by loss of material | Decrease |
| Structural cracking** and/or spalling | Traffic greater than design | Increase if compaction of subbase or subgrade takes place; decrease if effective slab size is reduced or subgrade fails |

* Pumping may be indicated by excessive straining and/or the presence of foundation materials on the pavement surface. Pumping action can often be observed during or immediately following rains.

** Cracking may or may not be associated with such conditions as pumping, swelling soils, differential frost heave, and slab warping.

DSM tests for the purpose of using the rigid pavement evaluation curve (Figure 58) should always be run near the centers of slabs which contain no structural deficiencies. Pavements which contain slabs with distress conditions listed in Table 22 should be evaluated as described below:

- a. When evidence of pumping is present but the pavement slabs are still structurally sound, the allowable single-wheel load determined from the DSM tests should be reduced by 10 percent if over 25 percent of the slabs are pumping.
- b. If a visual examination shows that 30 to 50 percent of the slabs have structural cracking due to loading, the allowable single-wheel load determined by the DSM tests should be reduced by 25 percent. Likewise, if there is evidence of joint distress or failure, which may be characterized by excessive spalling along the joints, in 30 to 50 percent of the slabs, the allowable single-wheel load determined by DSM tests should be reduced by 25 percent.
- c. If more than 50 percent of the slabs show structural distress (i.e., cracking due to load or joint failure), the pavement should be classed as "failed" and not evaluated.

MONITORING ACCURACY OF VIBRATOR MEASUREMENTS

The accuracy of the vibrator should be established to give the evaluating engineer confidence in the measurements. Errors in the calibration and operation of the electronic equipment can be large enough to influence test results significantly. The characteristics of the vibrator determine the required checks on the accuracy of that vibrator, and a system of checks will have to be worked out by the vibrator operator or the evaluating engineer. However, a general description of checks which can be performed on the 16-kip vibrator may be helpful. The determination of DSM with the 16-kip vibrator involves the measurement of two quantities, the vibratory load and the resulting deflection of the pavement surface. As discussed previously in the section on accuracy tests with the 16-kip vibrator, two types of accuracy tests can be performed on the systems which measure these quantities. The first type of accuracy test is the laboratory test. A laboratory test can be performed on the load cells to establish calibration accuracy. A laboratory test

can also be performed on the velocity transducers to check readings against a calibrated velocity transducer. The second type of accuracy test is the field test. Repeatability of results can be periodically checked by conducting duplicate tests at a test site. Velocity transducers can be checked against one another by placing a portable velocity transducer near the load plate and comparing the resulting deflection obtained by the portable transducer with that obtained by the transducer fixed to the load plate. The load cells can be checked statically by recording the static weight of the vibrator and comparing this with the known static weight. Multiple measurements on the same test site can also be compared. In addition to laboratory and field tests, the equipment specifications should be checked to determine if the specified ranges in equipment operation are sufficient.

CONCLUSIONS AND RECOMMENDATIONS

This study has resulted in the development of a nondestructive pavement evaluation procedure for flexible and rigid civil airport pavements and complete equipment specifications for a vibratory device suitable for use with this procedure as well as for future developments in the procedure. It is recommended that the procedure be used along with other methods of evaluation as a tool for the structural evaluation of civil airport pavements.

The following specific studies are recommended to refine and verify the nondestructive evaluation procedure:

- a. Additional study of various types of vibrators should be made to determine their applicability to particular job requirements. Additional study of the effects of different vibrator static weights, vibratory loads, and load plate sizes is also suggested. The design of future vibrators should be based on the range of pavement strengths to be investigated and possibly on the characteristics of the vehicles which will be using the pavement.
- b. Relationships should be developed to allow nondestructive evaluation of composite pavements such as PCC overlaid with AC.
- c. Additional data should be collected and analyzed to refine and verify the procedure further. Pavement and subgrade properties of the test sites used in developing the DSM versus allowable single-wheel load correlations presented herein should be studied to determine which factors caused the range in gross aircraft loads for a given DSM. Attempts to develop reasonable empirical and theoretical relationships between vibrator data and allowable loads should be encouraged and reviewed in the interest of developing more accurate and universal relationships than are now available. New or untried theories or empirical relationships should be checked and verified over a sufficient time to indicate if the new methods can predict pavement performance under traffic conditions.
- d. A study should be made of the effects of PCC slab dimensions and joint types on DSM data. The load transfer across joints can be measured with the vibratory techniques, but a technique is needed to interpret these measurements.
- e. Additional effort should be made to develop further the temperature adjustment factor. A universal temperature adjustment factor should be derived which will allow deflection

data to be adjusted and thereby compared at a common temperature. Pavement sections similar to the WES temperature effects test section should be constructed on different foundation strengths for this purpose. The warping effects, if any, of PCC pavements on nondestructive data need consideration.

f. Several other items of concern which were considered during collection of the data but are not covered in the report should also be given more consideration:

- (1) A detailed study should be made of deflections measured in instrumented pavement sections at NAFEC, the Nashville Metropolitan Airport, and the WES temperature effects test section in order to relate pavement response to aircraft loadings with that to vibratory loadings. Also, the effective mass of the pavement structure being vibrated under different vibratory loadings needs to be determined. Additional data on instrumented pavements may also be needed.
- (2) Wave propagation measurements do not offer immediate promise as a pavement evaluation tool. Previous studies have shown that wave velocity measurements are greatly influenced by pavement thickness and other factors which are not fully understood. To be of practical use, the measurement techniques must be improved to provide a unique velocity for a given material; and corresponding data interpretation and application procedures must also be developed. Techniques such as recording wave velocities through probes inserted into the pavement layer to be studied may eliminate the overburden effects. A study conducted on small-scale test pavements could allow refinements and necessary improvements to the wave propagation data collection techniques. The velocity data, which are used to compute elastic constants for the pavement layers, could then possibly be used with theoretical procedures being developed, not only for evaluation but for design of pavement systems.
- (3) More thought should be given to the problem of directly relating deflection data and pavement performance. Deflection data alone can be used only to predict failure when the mode of failure is structural. For example, when the mode of failure is functional, rutting may have resulted from compaction by traffic; the pavement elements may have become stronger although the pavement may be judged as failed because the surface is rough. As the materials are compacted, deflection data will indicate a strength gain up to and beyond the point at which failure is supposed to have occurred. A system to complement deflection measurements whereby this example and similar cases can be evaluated should be developed.

- (4) Further study of the effects of pavement overlays on nondestructive testing results should be undertaken in the form of carefully constructed and controlled test sections. Three test sections on subgrades of three different strengths would probably be sufficient to determine what effects the original subgrade strength has on nondestructive data as the overlay thickness is increased.

APPENDIX A: DEFLECTION-PERFORMANCE RELATIONSHIPS AND CORRELATIONS BETWEEN DYNAMIC E-MODULUS AND CBR

DEFLECTION-PERFORMANCE RELATIONSHIPS

The U. S. Army Engineer Waterways Experiment Station (WES),⁷ the California Division of Highways,⁸ and the Transport and Road Research Laboratory⁹ have developed independently similar relationships between surface deflection (elastic rebound) and performance for flexible pavements. These deflection-performance relationships are shown in Figure A1. The California Division of Highways curve shown is for 3-in. asphaltic concrete pavements and was developed by monitoring the performance of selected California highway pavements on which deflection measurements were made. This relationship was originated in 1955 by Hveem⁵³ and has since been improved by additional data. The Transport and Road Research Laboratory curve, first published in 1972, is for a rolled asphalt surfacing over a wet-mix slag base. The WES curve was developed from data collected on several full-scale performance test pavements using aircraft loads, and also includes data collected on some highway pavement studies such as the American Association of State Highway Officials (AASHO) and the Western Association of State Highway Officials (WASHO) road tests. The aircraft loads were on single wheels with loads from 20 to 150 kips. The pavement sections consisted of varying thicknesses of asphaltic concrete surface, base, and subbase over a variety of subgrade types. This relationship was developed in 1970; however, the data on which it is based were obtained many years prior to that.

The relationships shown in Figure A1 indicate that deflection is a measure of pavement performance, although the relationship is not precise. A similar relationship has not been developed for rigid pavements because of the lack of adequate information.

CORRELATIONS BETWEEN DYNAMIC E-MODULUS AND CBR

Wave propagation measurements can be conducted on pavements to obtain dynamic E-moduli for the pavement layers. The test procedure consists of placing a vibrator on the pavement surface, generating a

steady state vibration at selected frequencies, and monitoring the wave form with velocity transducers placed on the surface at various distances from the vibrator. By use of an appropriate phase-marking circuit and an oscilloscope, the length of the wave can be determined. This is done by locating a point on the surface where the phase marker coincides with the peak (or trough) of a wave and then moving the transducer to another point where the marker coincides with the next corresponding peak (or trough). The distance measured on the surface between the points is one wavelength. The wave velocity V can be determined from

$$V = f\lambda$$

where

f = frequency, Hz

λ = wavelength, ft

The process is repeated at other frequencies to establish a relationship between wavelength and velocity. Dynamic E-moduli can then be determined from

$$E = 2(1 + \nu)\rho V^2$$

where

ν = Poisson's ratio

ρ = mass density = γ/g where γ is the wet density of the material, pcf, and g is the acceleration due to gravity, 32.2 ft/sec²

Wave propagation measurements made at the AASHO Road Test,⁴ Foss Field,⁵ and other locations showed that the effective depth of propagation through pavement layers was approximately one-half the measured wavelength. Data collected from these studies have been used to develop a correlation between E-modulus and CBR shown in Figure A2. A comparison of this relationship with the correlation developed previously by the Royal Dutch Shell Laboratory¹ is shown in Figure A3. The data in Figure A2 were obtained from vibratory measurements made at the surface of flexible pavements; the dynamic E-moduli were taken at the one-half wavelength that would place the E-moduli at depths that would correspond to base, subbase, and subgrade materials of known CBR's.

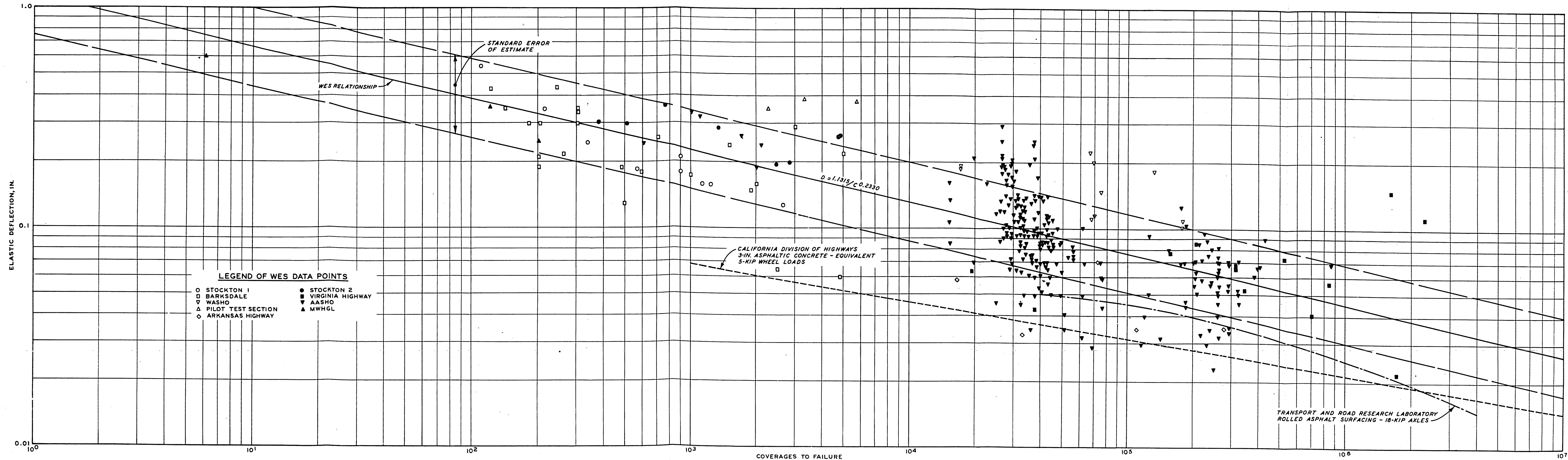


Figure A1. Elastic deflection versus coverages to failure for single- and multiple-wheel loads based on combined highway and airfield data

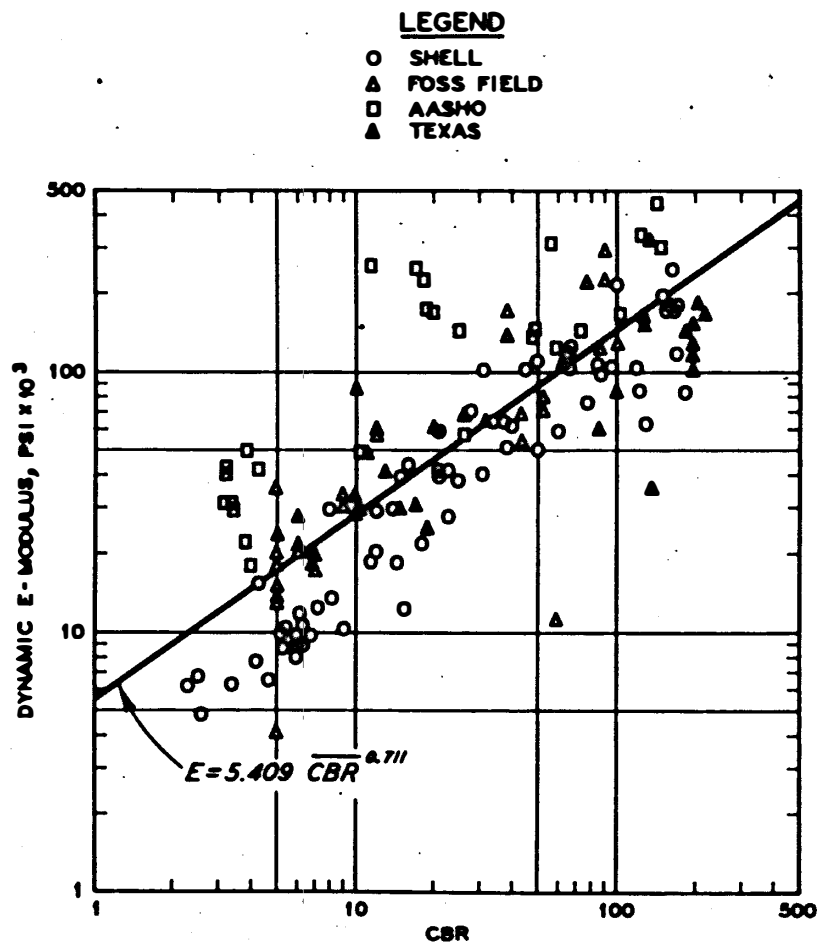


Figure A2. Dynamic E-modulus versus CBR
(WES correlation)

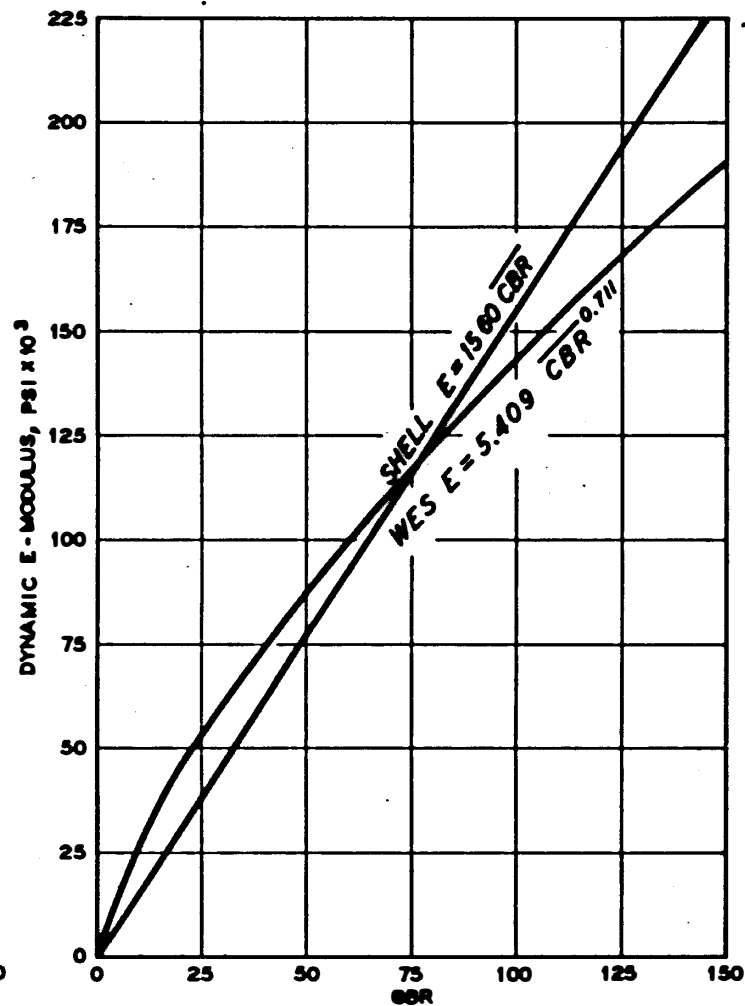


Figure A3. Dynamic E-modulus versus CBR
(comparison of Shell and WES correlations)

APPENDIX B: RELATED NONDESTRUCTIVE DATA

During this study, some information was collected that was not used as direct input to the development of the evaluation methodology; therefore, these results are presented in this appendix as a matter of record. This information consists primarily of the results of two separate studies: a pavement performance study and a study of the effect of the pavement surface layer on the nondestructive results.

PAVEMENT PERFORMANCE STUDY

The objective of the pavement performance study was to relate DSM (dynamic stiffness modulus) test results to pavement performance through studies of the performance of two soil stabilization test sections at the U. S. Army Engineer Waterways Experiment Station (WES). The soil stabilization test sections consisted of five test items each of flexible and rigid pavement construction. Traffic was applied to two traffic lanes in each test section with 200- and 240-kip twin-tandem test load carts. Layouts of the flexible and rigid pavement test sections are shown in Figures B1 and B2, respectively. To determine if the 16-kip vibrator could be used to monitor changes in pavement strength with performance, DSM data were obtained on the test items at periodic intervals during traffic testing.

FLEXIBLE PAVEMENT TEST SECTION

Table B1 presents results of DSM tests for five different periods obtained during the trafficking of the flexible pavement items. The data in Table B1 were taken at the center of each item. Table B2 shows results of tests conducted at different positions in the items during the last two test periods. Traffic was applied to the 200-kip lane first and then to the 240-kip lane. DSM values for the flexible pavement 200-kip lane showed only a slight increase during trafficking and then a decrease at the time of failure. Tests made at the same time in the 240-kip lane where no traffic had been applied showed a considerable strength increase in items 1 and 3. This increase in strength could probably be attributed to a strength gain with time in the stabilized

layers. After traffic, the DSM values of all items in the 240-kip lane had been reduced to those of the corresponding items in the 200-kip lane. It would appear from the DSM data that the strength of the stabilized sections was increasing due to the strength gain but at the same time the effects of traffic were reducing the strength. The DSM values did not relate well to the number of coverages to failure in either traffic lane. An examination of the strength of the pavement layers as indicated by the CBR values shown in Table B3 shows that many of the items had an increase in CBR. Item 4 showed a decrease in CBR of the stabilized clayey sand base after traffic. Although the test items were considered failed due to the distress of the surface layer and conditions of consolidation, the CBR data indicate that in general the pavement structures may have actually gained in strength. This development may explain the lack of correlation between DSM values and pavement performance for these test items. Although the pavements were considered failed because of the surface distress, the pavement life could have been restored with a leveling overlay.

RIGID PAVEMENT TEST SECTION

The DSM data for the rigid pavement test items, as shown in Table B4, were very limited and therefore no specific conclusions are drawn. However, the differences in performance between items 1 and 2 and between items 3 and 4 were not significant. Determination of the precise failure point was sometimes difficult. As with the flexible test section, factors other than structural support may have affected the pavement performance. Table B5 shows physical properties of the pavement items before and after traffic. Items 1 and 2 were constructed with fibrous concrete, while items 3 and 4 were constructed with plain Portland cement concrete (PCC). The performance of these materials is different; the fibrous concrete can withstand greater deflections than the plain PCC. For this reason, the DSM value may not have the same meaning on the different pavement types. The DSM values of items 3 and 4 were nearly the same, as would be expected from the similar pavement structure. The performance of items 3 and 4 were identical in the 200-kip

twin-tandem lane, but item 3 (with the bituminous base) performed better than item 4 under the 240-kip twin-tandem load. The coverage level at failure for item 3 in the 240-kip twin-tandem lane is given as a range in Table B5, which indicates that it was difficult to determine when failure actually occurred. In general, the DSM values showed that the strength of item 1 was approximately equal to that of item 2 and that item 3 had approximately the same DSM as item 4. Also, the performances of items 1 and 2 were similar, as were these of items 3 and 4.

EFFECT OF BOUND PAVEMENT ELEMENT THICKNESS ON DSM

The purpose of this study was to derive a method for the nondestructive determination of overlay pavement thickness requirements. The study was conducted at three test sites: Philadelphia International Airport, the WES temperature effects test section, and Shreveport Regional Airport. Data collected for another project at Biggs Army Airfield are also presented because of applicability to the objectives of this study. Only at Shreveport Regional Airport did circumstances allow measurements before and after pavements were overlaid. At the other sites, overlay thickness plots are based on DSM measurements on pavements of different thicknesses on the same type subgrade.

The Philadelphia International Airport pavement used in the overlay study was completed about November 1972. Tests were performed 5 December 1972 before any traffic was allowed on the runway. Pavement surface temperatures were between 40 and 52°F for all the tests. The pavement sections on which DSM measurements were made are shown in Figure B3. These bituminous sections varied in thickness from 4 in. at stations 284+75, 285+00, 305+00, 305+25, 349+75, and 350+00 at 112 ft from the runway center line to 13 in. at stations 284+75 and 285+00 at 32 ft from the center line. The subgrade beneath the test locations was in the E-1 (GP-GN) or E-2 (GM) soil group.* The results of the DSM

* The corresponding Unified Soil Classification System group is given in parentheses after each Federal Aviation Administration (FAA) soil group.

measurements on the different pavement sections are presented in Table B6 and are shown in Figure B4 in the form of a DSM versus bituminous pavement section thickness graph. If it is assumed that making DSM measurements on pavements of different thicknesses with about the same subgrade is analogous to making DSM measurements on a pavement which has been overlaid, the slope of the best-fit line through the points in Figure B4 shows that the DSM is increased by approximately 310 kips/in. for each inch of bituminous pavement added.

The WES temperature effects test section on which DSM measurements were made for this study is shown in Figure 27 of the main text. The temperature effects test section was completed in June 1973, and the tests for this study were made on 2-3 August 1973. No traffic had been allowed on the section at that time. The asphaltic concrete (AC) pavement thicknesses were 4.3, 8.2, and 14.2 in. in the section. The subgrade beneath the test locations was lean clay, which is in the FAA E-7 (ML-CL) soil group. Pavement surface temperatures were 109°F on the 4-in. item, 86°F on the 8-in. item, and 98°F on the 14-in. item. The results of DSM measurements on the different pavement sections are presented in Figure B5 in the form of a DSM versus AC pavement section thickness plot. The slope of the line through the points in Figure B5 shows that the DSM increased by 30.3 kips/in. for each inch of additional pavement thickness.

Pavement sections at Biggs Army Airfield at El Paso, Texas, on which DSM measurements were made for this study are shown in Figure B6. The pavement was several years old, and the amount of traffic on the pavement was not known; however, the surface appeared to be in excellent condition. The PCC pavement thicknesses were 9, 19, and 24 in. The subgrade under the three sections was in the FAA E-5 (SP-SM) or E-6 (SP-SC) soil group. The results of DSM measurements on the different pavement sections are shown in Figure B7 in the form of a DSM versus PCC pavement section thickness plot. The slope of the straight line through the points in Figure B7 shows that the DSM increased by 370 kips/in. for each inch of PCC pavement added.

Test sites for the overlay study at Shreveport Regional Airport

are shown in Figure B8. Tests were performed on these sites in October 1972 and March and October 1973. Pavement sections as they existed in October 1972 before the overlay are shown in Figure B9. They were of 8, 10, or 11 in. of PCC and 7 in. of subbase (FAA Specification P-154⁴⁹) or 6 in. of lime-stabilized subbase on an unknown subgrade. The original PCC pavement was constructed about 1952 and was overlaid with AC in 1973. The overlay was placed in three layers, each of which was begun at station 73+00 and carried to station 0+00 before the next layer was begun. When nondestructive tests were performed in March 1973, the first layer was complete for the entire runway length, and the second layer was complete between stations 73+00 and 55+50 except for a 25-ft strip on the west side of the runway between stations 64+00 and 55+50. When nondestructive tests were performed in October 1973, all three layers were complete. Data collected on the three dates are shown in Table B7, and overlay thickness and DSM are plotted for the three dates in Figure B10. There were 11 test sites. The data show that, as the overlay thickness was increased as compared with the DSM on the PCC, the DSM increased for both test dates at four test sites: 1(station 1+63), 4(station 3+60), 10(station 8+98), and 15(station 56+79); decreased for the first tests on the overlay and increased for the second test on the overlay at three test sites: 16(station 62+30), 30(station 67+63), and 31(station 67+63); and decreased for both test dates at two test sites: 11(station 46+24) and 17(station 67+63). At test sites 13(station 50+04) and 14(station 50+04), the first tests on the overlay showed an increase in the DSM as a result of the overlay, and the second tests on the overlay showed the DSM value to be between the value of the PCC with no overlay and the value obtained for the first tests on the overlay. Tests showed the densities of the layer of overlay at the eleven test sites to range between 133.5 and 150.6 pcf. No densities were obtained for the bottom layers at three test sites. The mean temperatures of AC overlays were approximately 57°F in March 1973 and 81°F in October 1973. Temperature corrections were not applied to the data. Average values for the data from Shreveport Regional Airport are shown in Table B8.

Table B1

Summary of DSM Values at 15 Hz and Coverages to Failure for the Flexible Pavement Test Section

| Test Item | Cover-ages to Failure | Traffic Lane | 7 Sep 72 | | | 18 Oct 73 | | | 8 Mar 73 | | | 20 Apr 73 | | | 17 May 73 | | |
|-----------|-----------------------|--------------|--------------|-----------------|------------|--------------|-----------------|------------|--------------|-----------------|------------|--------------|-----------------|------------|--------------|-----------------|------------|
| | | | DSM kips/in. | Temper-ature °F | Cover-ages | DSM kips/in. | Temper-ature °F | Cover-ages | DSM kips/in. | Temper-ature °F | Cover-ages | DSM kips/in. | Temper-ature °F | Cover-ages | DSM kips/in. | Temper-ature °F | Cover-ages |
| 1 | 3660 | 1 | 750 | 105 | 0 | 615 | 79 | 1200 | 840 | 78 | 3360 | 580 | 70 | 3660 | | | |
| 2 | 3660 | 1 | 525 | 105 | 0 | 520 | 79 | 1200 | 700 | 78 | 3360 | 625 | 70 | 3660 | | | |
| 3 | 7820 | 1 | 595 | 105 | 0 | 500 | 79 | 1200 | 840 | 78 | 3360 | 645 | 70 | 7820 | | | |
| 4 | 1240 | 1 | 560 | 107 | 0 | 460 | 79 | 1200 | -- | -- | -- | 760 | 70 | 1240 | | | |
| 5 | 2500 | 1 | 610 | 107 | 0 | 620 | 79 | 1200 | 760 | 78 | 2500 | 805 | 70 | 2500 | | | |
| 1 | 600 | 2 | 750 | 105 | 0 | 720 | 79 | 0 | 1200 | 74 | 0 | 960 | 70 | 0 | 640 | 90 | 600 |
| 2 | 400 | 2 | 525 | 105 | 0 | 610 | 79 | 0 | 740 | 74 | 0 | 720 | 70 | 0 | 520 | 90 | 400 |
| 3 | 620 | 2 | 595 | 105 | 0 | 910 | 79 | 0 | 1280 | 74 | 0 | 1280 | 70 | 0 | 540 | 90 | 620 |
| 4 | 120 | 2 | 560 | 107 | 0 | 660 | 79 | 0 | 780 | 82 | 0 | 660 | 70 | 0 | 670 | 90 | 120 |
| 5 | 40 | 2 | 610 | 107 | 0 | 770 | 79 | 0 | 800 | 82 | 0 | 760 | 70 | 0 | 840 | 90 | 340 |

Note: Temperature was measured approximately 2 in. below the pavement surface.

Table B2

DSM at 15 Hz Before and After Traffic for the Flexible Pavement Test Section

| Test Item | Location on Test Item | Lane 2 Before Traffic | | Lane 1 After Traffic | | Lane 2 After Traffic | |
|-----------|-----------------------|-----------------------|-------------------|----------------------|-------------------|----------------------|-------------------|
| | | DSM kips/in. | Temperature °F | DSM kips/in. | Temperature °F | DSM kips/in. | Temperature °F |
| 1 | West 1/4 point | 1080 | 70 | 580 (640 | 70 | -- | 90 |
| | Center point | 960 | 70 | near | -- | 640 | -- |
| | East 1/4 point | 1080 | 70 | failed area) | -- | -- | -- |
| 2 | West 1/4 point | 680 | 70 | 625 | 70 | 680 | 90 |
| | Center point | 720 | 70 | -- | -- | 520 | 90 |
| | East 1/4 point | 600 | 70 | -- | -- | 465 | 90 |
| 3 | West 1/4 point | 1580 | 70 | 680 | 70 | -- | -- |
| | Center point | 1280 | 70 | 645, 596,* 1000** | 70 | 540 | 90 |
| | East 1/4 point | 1500 | 70 | 600 | 70 | 560 | 90 |
| 4 | West 1/4 point | 800 | 70 | -- | -- | -- | -- |
| | Center point | 660 | 70 | -- | -- | 670 | 90 |
| | East 1/4 point | 750 | 70 | 760 | 70 | 580 | 90 |
| 5 | West 1/4 point | 750 | 70 | -- | -- | 810 | 90 |
| | Center point | 760 | 70 | 850 | 70 | 840 | 90 |
| | East 1/4 point | 830 | 70 | -- | -- | 950 | 90 |

Note: Temperature was measured approximately 2 in. below the pavement surface.

* Asphaltic concrete removed.

** Outside of traffic lane.

Table B3
Summary of Field Test Data on Flexible Pavement Test Section

| Test Item | Material | Depth Below Pavement Surface, in. | Construction Data | | | Traffic Coverages to Failure | After Traffic Test Data | | | | | |
|--------------------------------------|---|-----------------------------------|-------------------|-----------------------|-----------------|------------------------------|-------------------------|-----------------------|----------------------|------|-----------------------|-----------------|
| | | | CBR | Water Content percent | Dry Density pcf | | Inside Traffic Lane | | Outside Traffic Lane | | | |
| | | | | | | | CBR | Water Content percent | Dry Density pcf | CBR | Water Content percent | Dry Density pcf |
| Lane 1: 200-Kip Twin-Tandem Assembly | | | | | | | | | | | | |
| 1 | AC | 0 | -- | -- | -- | 3660 | -- | -- | -- | -- | -- | -- |
| | Crushed limestone | 4 | 110+ | 1.0 | 151.9 | | 65 | 2.3 | 154.3 | 75 | 3.3 | 147.0 |
| | Lean clay with 10% fly ash, 3% lime, 2% PC | 9 | 94 | 17.7 | 96.5 | | 123 | 20.4 | 100.1 | 97 | 23.5 | 97.4 |
| | Heavy clay subgrade | 33 | 3.3 | 30.9 | 87.3 | | 7 | 31.4 | 88.2 | 8 | 30.2 | 87.2 |
| 2 | AC | 0 | -- | -- | -- | 3660 | -- | -- | -- | -- | -- | -- |
| | Lean clay with 12% PC | 3 | 105 | 16.0 | 102.9 | | 150+ | 15.9 | 108.3 | 150+ | 14.6 | 113.4 |
| | Heavy clay subgrade | 28 | 3.6 | 30.2 | 86.5 | | 7 | 29.8 | 89.2 | 7 | 30.3 | 89.0 |
| 3 | AC | 0 | -- | -- | -- | 7820 | -- | -- | -- | -- | -- | -- |
| | Gravelly sand with 5% PC | 3 | 150+ | 3.2 | 133.4 | | 150+ | -- | -- | 150+ | -- | -- |
| | Heavy clay subgrade | 28 | 3.6 | 30.3 | 87.0 | | 5 | 30.6 | 89.0 | 3 | 32.7 | 86.7 |
| 4 | AC | 0 | -- | -- | -- | 1380 | -- | -- | -- | -- | -- | -- |
| | Clayey sand with 5% PC | 3 | 150+ | 8.9 | 116.9 | | 70 | 13.1 | 118.0 | 150+ | 11.9 | 122.6 |
| | Heavy clay subgrade | 28 | 3.7 | 30.5 | 86.9 | | 7 | 27.3 | 92.4 | 8 | 25.8 | 91.2 |
| 5 | AC | 0 | -- | -- | -- | 2500 | -- | -- | -- | -- | -- | -- |
| | Crushed limestone | 3 | 104 | 2.4 | 145.7 | | 150+ | 1.9 | 155.2 | 150+ | 1.2 | 152.2 |
| | Gravelly sand with plasticity index (PI) of 3 | 9 | 56 | 5.4 | 136.7 | | 52 | 5.2 | 141.0 | 57 | 5.1 | 140.5 |
| | Heavy clay subgrade | 42 | 4.2 | 29.9 | 89.2 | | 2.5 | 33.3 | 86.5 | 4.3 | 32.5 | 87.2 |
| Lane 2: 240-Kip Twin-Tandem Assembly | | | | | | | | | | | | |
| 1 | AC | 0 | -- | -- | -- | 600 | -- | -- | -- | -- | -- | -- |
| | Crushed limestone | 4 | 110+ | 1.0 | 151.9 | | 141 | 1.1 | 153.2 | 105 | 1.2 | 146.8 |
| | Lean clay with 10% fly ash, 3% lime, 2% PC | 9 | 94 | 17.7 | 96.5 | | 126 | 20.4 | 100.7 | 147 | 25.6 | 98.3 |
| | Heavy clay | 33 | 3.3 | 30.9 | 87.3 | | 4.2 | 32.6 | 86.7 | 4.1 | 35.4 | 83.5 |
| 2 | AC | 0 | -- | -- | -- | 400 | -- | -- | -- | -- | -- | -- |
| | Lean clay with 12% PC | 3 | 105 | 16.0 | 102.9 | | 150+ | 15.1 | 109.8 | 144 | 14.8 | 106.1 |
| | Heavy clay subgrade | 28 | 3.6 | 30.2 | 86.5 | | 5 | 31.6 | 87.4 | 3.6 | 33.9 | 84.2 |
| 3 | AC | 0 | -- | -- | -- | 620 | -- | -- | -- | -- | -- | -- |
| | Gravelly sand with 5% PC | 3 | 150+ | 3.2 | 133.4 | | 150+ | 3.3 | 137.0 | 150+ | 2.8 | 135.3 |
| | Heavy clay subgrade | 28 | 3.6 | 30.3 | 87.0 | | 1.5 | 32.9 | 85.8 | 1.8 | 34.1 | -- |
| 4 | AC | 0 | -- | -- | -- | 120 | -- | -- | -- | -- | -- | -- |
| | Clayey sand with 5% PC | 3 | 150+ | 8.9 | 116.9 | | 150+ | 14.0 | 116.4 | 150 | 14.1 | 116.4 |
| | Heavy clay subgrade | 28 | 3.7 | 30.9 | 86.9 | | 6 | 29.6 | 90.4 | 3.9 | 29.4 | 89.8 |
| 5 | AC | 0 | -- | -- | -- | 340 | -- | -- | -- | -- | -- | -- |
| | Crushed limestone | 3 | 104 | 2.4 | 145.7 | | 133 | 2.0 | 158.9 | 133 | 2.0 | 155.5 |
| | Gravelly sand with PI of 3 | 9 | 56 | 5.4 | 136.7 | | 24 | 4.4 | 138.5 | 25 | 5.1 | 143.3 |
| | Heavy clay subgrade | 42 | 4.2 | 29.9 | 89.2 | | 3.9 | 32.3 | 87.4 | 3.4 | 32.0 | 87.4 |

Note: AC = asphaltic concrete; PC = portland cement.

Table B4

DSM Values at 15 Hz and Coverages to Failure for Rigid Pavement Test Section

| Test Item | Coverages to Failure | Traffic Lane | <u>11 Jul 72.</u> | | <u>7 Sep 72</u> | | <u>9 Mar 73</u> | |
|--------------|----------------------------|-----------------|------------------------|------------------|------------------------|------------------|-------------------------|------------------|
| | | | DSM <u>kips/in.</u> | <u>Coverages</u> | DSM <u>kips/in.</u> | <u>Coverages</u> | DSM. <u>kips/in.</u> | <u>Coverages</u> |
| 1 | 3000 | 1 | | | 960 | 0 | 880 | 3000 |
| 2 | 1770 | 1 | | | 830 | 0 | | |
| 3 | 6360 | 1 | | | 2600 | 0 | | |
| 4 | 6360 | 1 | | | 2500 | 0 | | |
| 1 | 1010 | 2 | 1190 | 0 | | | | |
| 2 | 740 | 2 | 1210 | 0 | | | | |
| 3 | 1200-1500 | 2 | 3330 | 0 | | | | |
| 4 | 740 | 2 | 3400 | 0 | | | | |

Table B5

Summary of Field Test Data on Rigid Pavement Test Section

| Test Item | Material | Depth Below Pavement Surface in. | Construction Data | | | After Traffic Data | | | | | | | |
|-----------|------------------------|----------------------------------|---------------------------|-----------------------|-----------------|--------------------------|---------------------------|-----------------------|-----------------|--------------------------|---------------------------|-----------------------|-----------------|
| | | | Plate Bearing k Value pci | Water Content percent | Dry Density pcf | Lane 1: 200-Kip Assembly | | | | Lane 2: 240-Kip Assembly | | | |
| | | | | | | Coverages to Failure | Plate Bearing k Value pci | Water Content percent | Dry Density pcf | Coverages to Failure | Plate Bearing k Value pci | Water Content percent | Dry Density pcf |
| 1 | Fibrous concrete | 0 | -- | -- | -- | 3000 | -- | -- | -- | 1010 | -- | -- | -- |
| | Lean clay MESL* | 7 | 175 | 15.9 | 104.2 | | 230 | 15.2 | 100.6 | | 250 | 12.5 | 100.1 |
| | Heavy clay | 27 | 47 | 29.8 | 89.1 | | 180 | -- | -- | | 200 | 27.7 | 92.1 |
| 2 | Fibrous concrete | 0 | -- | -- | -- | 1770 | -- | -- | -- | 740 | -- | -- | -- |
| | Clay gravel with 6% PC | 4 | 545 | -- | 135.0 | | 490 | -- | -- | | 375 | -- | -- |
| | Heavy clay | 21 | 85 | 34.1 | 85.0 | | 118 | 33.1 | 85.5 | | -- | -- | -- |
| 3 | PCC | 0 | -- | -- | -- | 6360 | -- | -- | -- | 1200-1500 | -- | -- | -- |
| | Asphalt base | 15 | 99 | -- | -- | | 71 | -- | -- | | -- | -- | -- |
| | Heavy clay | 21 | 84 | 32.2 | 87.0 | | -- | -- | -- | | 164 | 33.5 | -- |
| 4 | PCC | 0 | -- | -- | -- | 6360 | -- | -- | -- | 740 | -- | -- | -- |
| | Lean clay with 12% PC | 15 | 167 | 15.8 | -- | | 200 | -- | -- | | 328 | 23.3 | -- |
| | Heavy clay | 21 | 40 | 33.1 | 86.1 | | 68.5 | 33.3 | 86.0 | | -- | -- | -- |

Note: No tests were performed on item 5; k = modulus of subgrade reaction.

* Membrane-enveloped soil layer.

Table B6
DSM Values and Bituminous Pavement Thicknesses at
Philadelphia International Airport

| <u>Taxiway or Runway</u> | <u>Distance from Center Line ft</u> | <u>Station</u> | <u>Bituminous Pavement Thickness in.</u> | <u>DSM kips/in.</u> |
|----------------------------------|---|----------------|--|-------------------------|
| 9R-27L | 112 | 284+75 | 4 | 760 |
| | | 285+00 | | 690 |
| | | 305+00 | | 680 |
| | | 305+25 | | 670 |
| | | 349+75 | | 710 |
| | | 350+00 | | 680 |
| | | | | <hr/> Average 700 |
| | 82 | 284+75 | 8 | 1940 |
| | | 285+00 | | 1800 |
| | | 305+00 | | 1960 |
| | | 305+25 | | 1960 |
| | | 349+75 | | 1700 |
| | | 350+00 | | 1760 |
| | | | | <hr/> Average 1850 |
| Tax A | 44 | 273+00 | 9 | 2120 |
| | | 273+25 | | 2160 |
| | | 284+75 | | 2000 |
| | | 285+00 | | 2040 |
| | | 349+75 | | 1860 |
| | | 350+00 | | 1920 |
| | | | | <hr/> Average 2020 |
| 9R-27L | 32 | 349+75 | 11 | 2120 |
| | | 350+00 | | 2580 |
| | | 305+00 | | 2660 |
| | | 305+25 | | 2840 |
| | | | | <hr/> Average 2550 |
| | | 284+75 | 13 | 3800 |
| | | 285+00 | | 3080 |
| | | | | <hr/> Average 3440 |

Table E7

DSM Values Before and After Overlay at Shreveport Regional Airport

| Test Site No. | Approximate PCC Thickness in. | <u>11-12 Oct 1972</u> | <u>6-7 Mar 1973</u> | | <u>9 Oct 1973</u> | | <u>Overlay Density, pcf</u> | | |
|---------------|-------------------------------|-----------------------------|-----------------------|----------------------------|-----------------------|----------------------------|-----------------------------|--------------|-----------|
| | | DSM Before Overlay kips/in. | Overlay Thickness in. | DSM After Overlay kips/in. | Overlay Thickness in. | DSM After Overlay kips/in. | Bottom Layer | Middle Layer | Top Layer |
| 1 | 10 | 1960 | 3.5 | 2320 | 8.25 | 2580 | 145.1 | 147.4 | 150.4 |
| 4 | 10 | 1620 | 2.75 | 2160 | 7.0 | 2420 | 147.5 | 147.6 | 148.8 |
| 10 | 8 | 820 | 4.25 | 1460 | 8.25 | 1780 | 150.6 | 149.6 | 146.3 |
| 11 | 10 | 2180 | 1.75 | 2120 | 6.25 | 2040 | Crumbled | 144.4 | 147.3 |
| 13 | 8 | 1340 | 2.75 | 1820 | 6.75 | 1680 | 143.3 | 145.1 | 148.2 |
| | Averages* | 1580 | 3.0 | 1980 | | | | | |
| 14 | 8 | 1480 | Not measured | 1880 | 7.5 | 1720 | Could not separate layers | | 149.4 |
| 15 | 8 | 1160 | 6.5 | 2000 | 8.75 | 2100 | 144.4 | 150.3 | 149.2 |
| 16 | 10 | 2640 | 7.25 | 2200 | 8.75 | 3340 | Crumbled | 149.3 | 148.0 |
| 17 | 11 | 3040 | 6.5 | 2140 | 9.0 | 1740 | 140.3 | 149.9 | 146.6 |
| 30 | 8 | 1760 | 6.0 | 1280 | 9.0 | 1880 | 139.2 | 149.4 | 145.0 |
| 31 | 8 | 1900 | 7.25 | 1300 | 8.75 | 2460 | 133.5 | 146.5 | 142.3 |
| | Averages** | 2100 | 6.7 | 1780 | | | | | |
| | Averages† | 1810 | | | 8.0 | 2160 | | | |

* For approximately 3 in. of overlay (tests on 1 layer of overlay) in place 6-7 March 1973.

** For approximately 6 in. of overlay (tests on 2 layers of overlay) in place 6-7 March 1973.

† For approximately 9 in. of overlay (tests on 3 layers of overlay) in place 9 October 1973.

Table B8
Average Thickness and DSM Values for
Shreveport Regional Airport Overlay

| <u>Date</u> | <u>Number of Test Sites</u> | <u>Average Overlay Thickness in.</u> | <u>Average DSM kips/in.</u> | <u>Change in DSM After Overlay kips/in.</u> | <u>Change per Inch of Overlay kips/in.</u> |
|--------------|---|--|-------------------------------------|---|--|
| 11-12 Oct 72 | 5 | 0 | 1580 | | |
| 6-7 Mar 73 | 5 | 3.0 | 1980 | +400 | +133 |
| 11-12 Oct 72 | 5 | 0 | 2100 | | |
| 6-7 Mar 73 | 5 | 6.7 | 1780 | -320 | -48 |
| 11-12 Oct 72 | 11 | 0 | 1810 | | |
| 9 Oct 73 | 11 | 8.0 | 2160 | +350 | +44 |

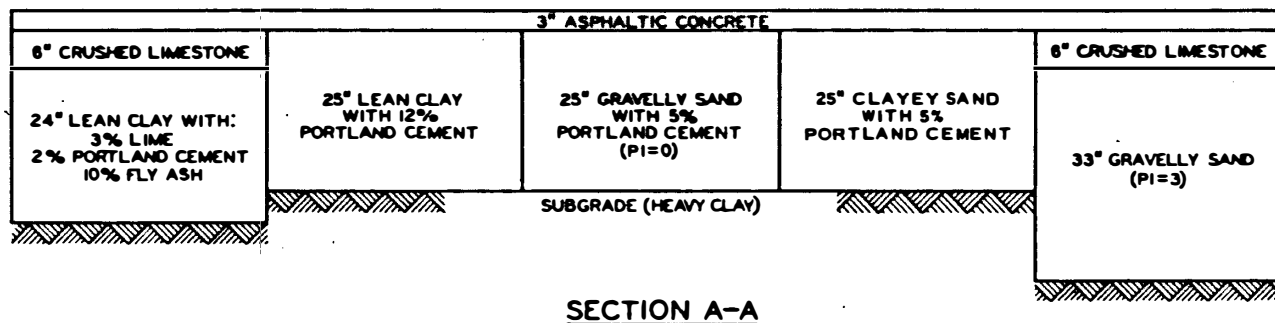


Figure B1. Plan and section of WES soil stabilization test section (flexible pavement)

The diagram illustrates a cross-section of a road structure with the following layers and materials:

- Top Layer:** 7" FIBROUS CONCRETE
- Second Layer:** 4" FIBROUS CONCRETE
- Third Layer:** 15" PORTLAND CEMENT CONCRETE
- Fourth Layer:** 6" BITUMINOUS BASE
- Fifth Layer:** 15" PORTLAND CEMENT CONCRETE
- Sixth Layer:** 6" LEAN CLAY WITH 12% PORTLAND CEMENT
- Subgrade:** SUBGRADE (HEAVY CLAY)

Additional details include:

- TRANSITION ZONE:** Indicated between the 4" fibrous concrete and 15" portland cement concrete layers.
- 20" MEMBRANE-ENCASED LEAN CLAY:** Located beneath the 7" fibrous concrete layer.
- 17" CLAY GRAVEL WITH 6% PORTLAND CEMENT:** Located beneath the 4" fibrous concrete layer.
- Dimensions:** 3" and 9" are marked for specific sections of the structure.

LEGEND





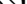

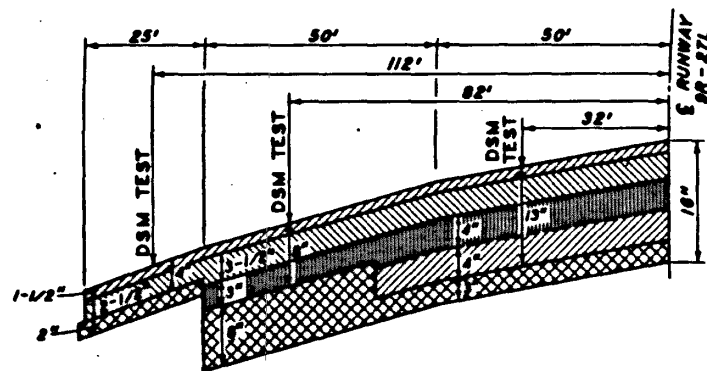
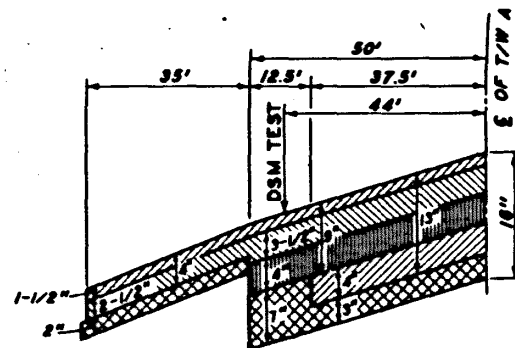
-  35-PSI POLYSTYRENE PANELS
 120-PSI POLYSTYRENE PANELS
 38-PCF LIGHTWEIGHT CONCRETE
 CONSTRUCTION JOINTS
 WEAKENED PLANE JOINTS
 TRAFFIC LANE BOUNDARY

Figure B2. Plan and section of WES soil stabilization test section (rigid pavement)



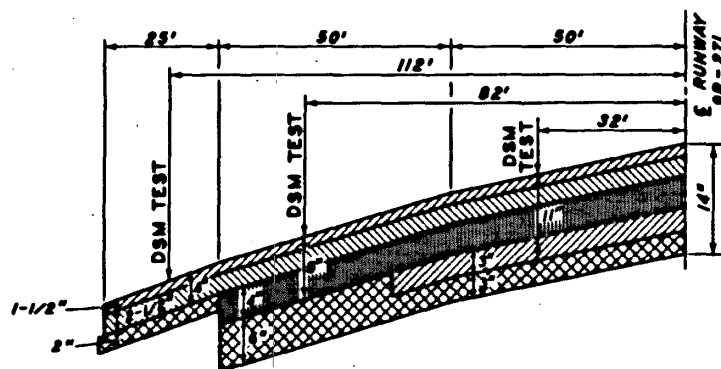
RUNWAY (CRITICAL)

TEST STATIONS: 284 + 75
285 + 00



TAXIWAY A

TEST STATIONS: 273 + 00
273 + 25
284 + 75
285 + 00
348 + 75
350 + 00



RUNWAY (NONCRITICAL)

TEST STATIONS: 305 + 00
305 + 25
348 + 75
350 + 00

| <u>LEGEND</u> | |
|---------------|-------------------------------|
| <u>SYMBOL</u> | <u>ITEM</u> |
| DSM TEST | DENOTES LOCATION OF DSM TEST. |
| | BITUMINOUS SURFACE COURSE |
| | BITUMINOUS BINDER COURSE |
| | BITUMINOUS BASE COURSE |
| | SUBBASE |

NOTE: SUBGRADES UNDER ALL TEST SITES WERE IN THE FAA SOIL GROUPS E-1 (GP-GW) OR E-2 (GM).

Figure B3. DSM test locations and pavement sections for Philadelphia International Airport

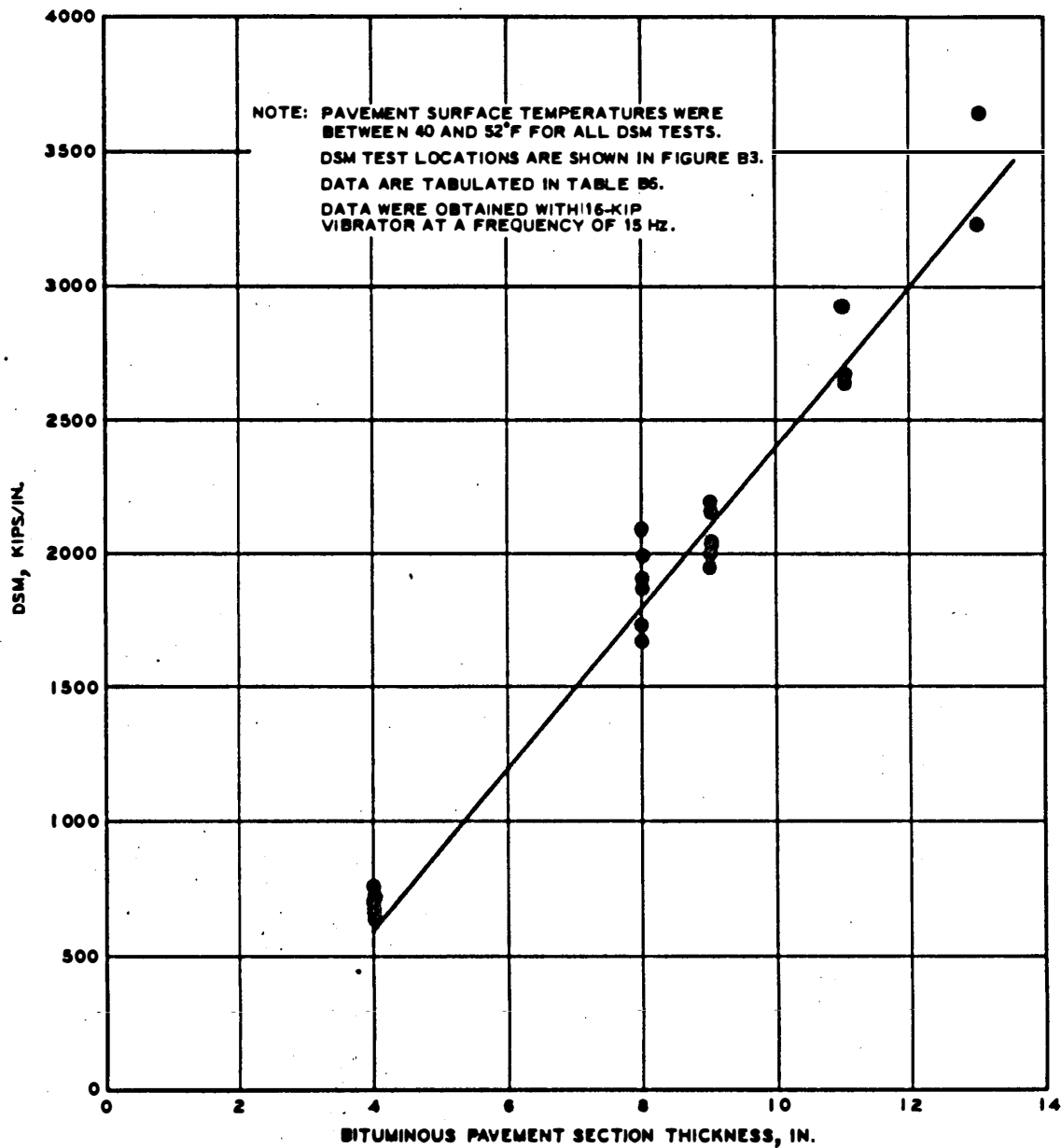


Figure B4. DSM versus bituminous pavement section thickness at Philadelphia International Airport

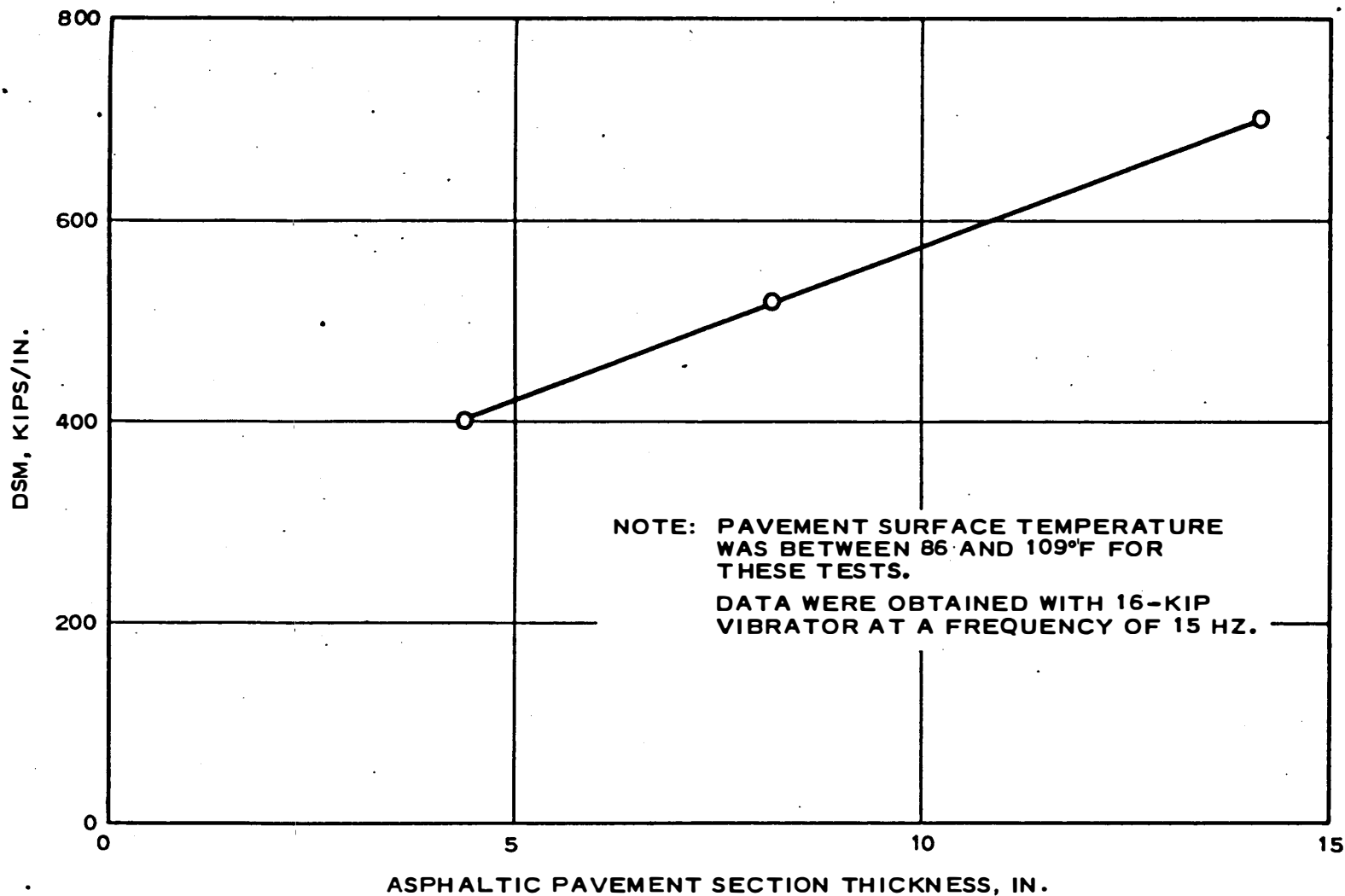
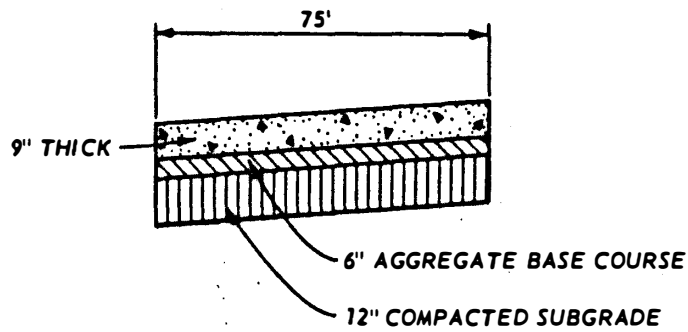
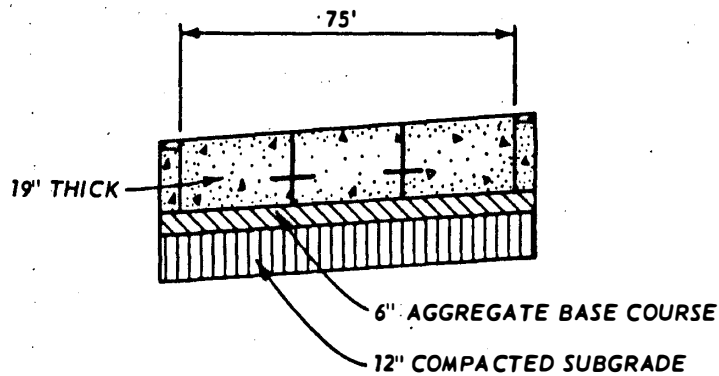


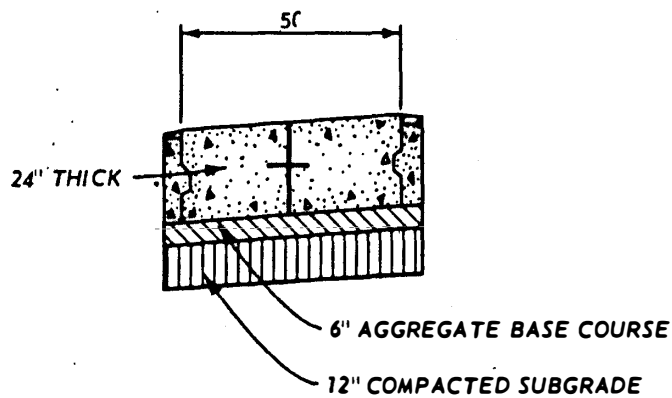
Figure B5. DSM versus asphaltic pavement section thickness for the WES temperature effects test section



PRESTRESSED CONCRETE



REINFORCED CONCRETE



PLAIN CONCRETE

Figure B6. Pavement cross section of taxiway T-3 at Biggs Army Airfield

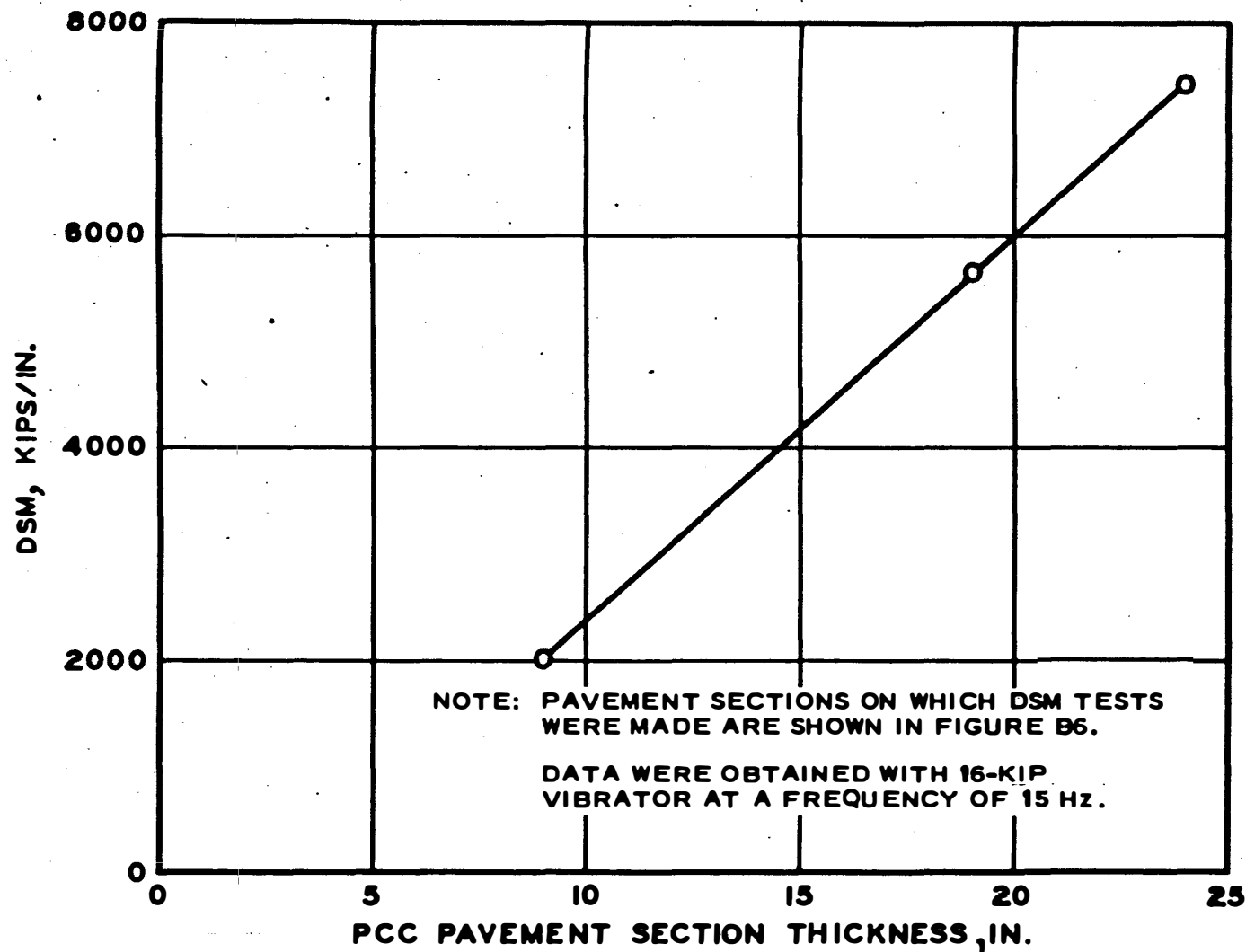
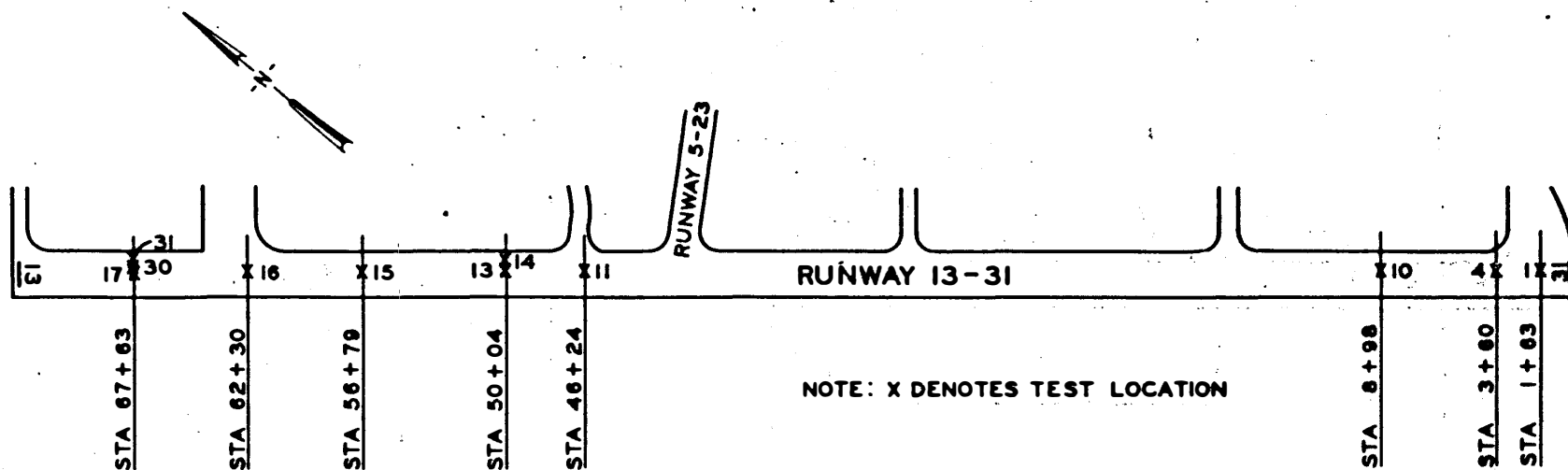


Figure B7. DSM versus PCC pavement section thickness for Biggs Army Airfield



PLAN

| TEST NUMBER | DISTANCE FROM CENTER LINE OF RUNWAY, FT (TO NORTHEAST) |
|--------------------------|---|
| 1, 4, 10, 11, 15, 16, 17 | 6 |
| 30 | 18 |
| 13 | 31 |
| 31 | 42 |
| 14 | 70 |

Figure B8. DSM test locations at Shreveport Regional Airport

| PCC THICKNESS, IN. | DSM TEST STATION | TEST NUMBERS |
|-----------------------|------------------------|-----------------|
| 8 | 8+28 | 10 |
| | 50+04 | 13, 14 |
| | 56+79 | 15 |
| | 67+63 | 30, 31 |
| 10 | 1+63 | 1 |
| | 3+60 | 4 |
| | 46+24 | 11 |
| | 62+30 | 16 |
| 11 | 67+63 | 17 |

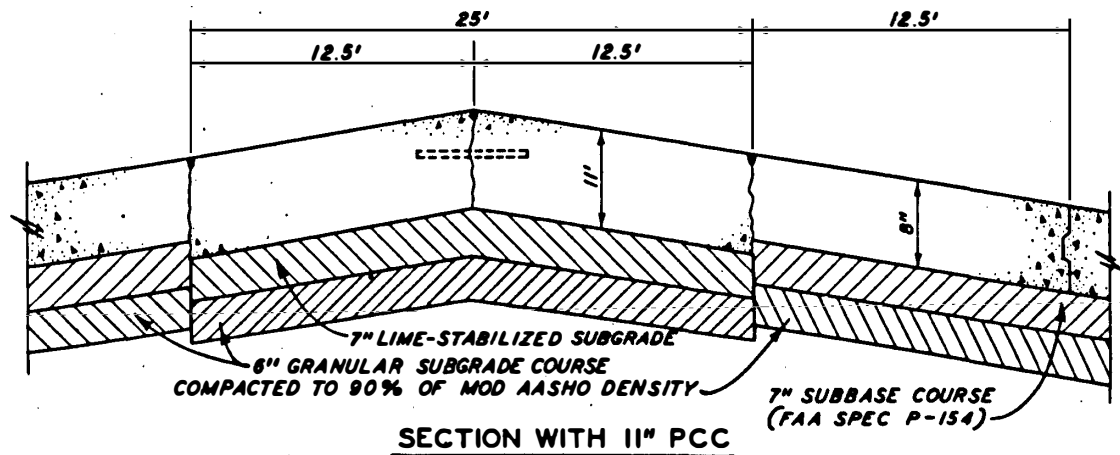
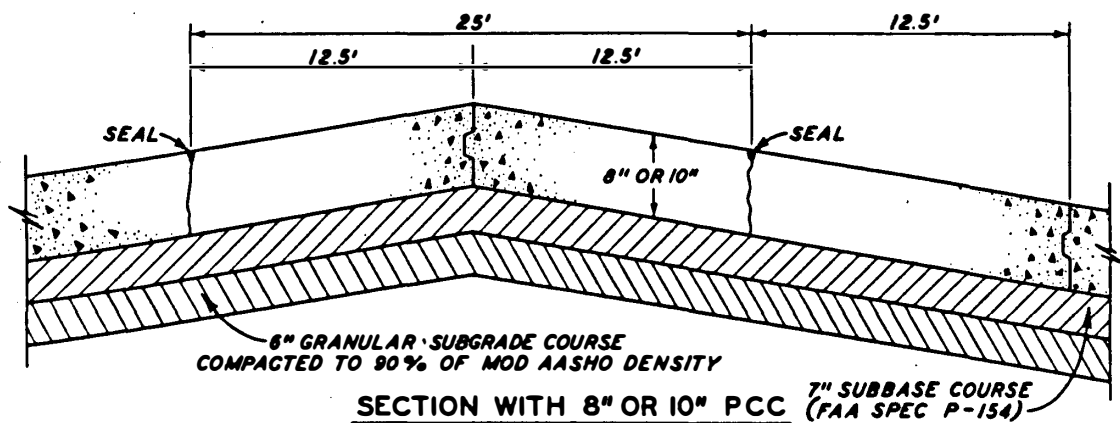
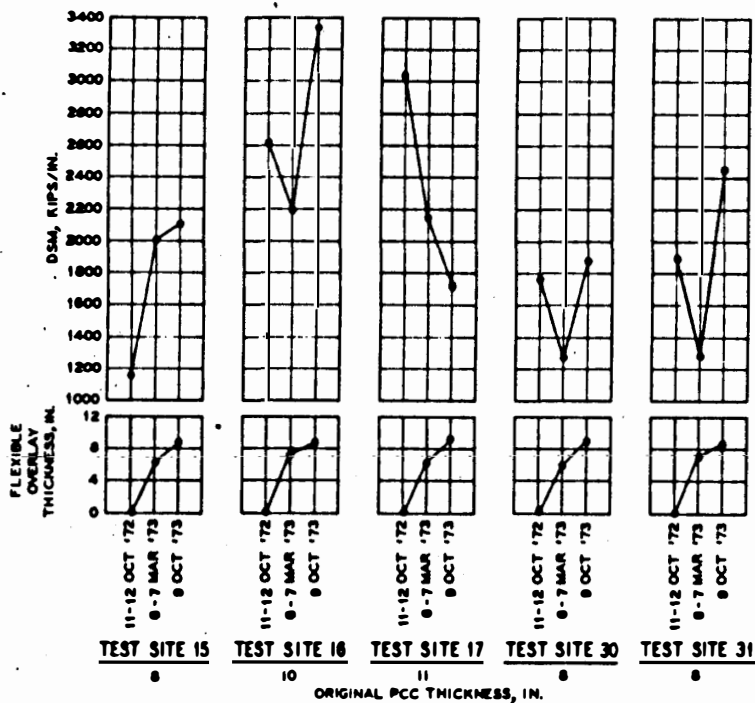
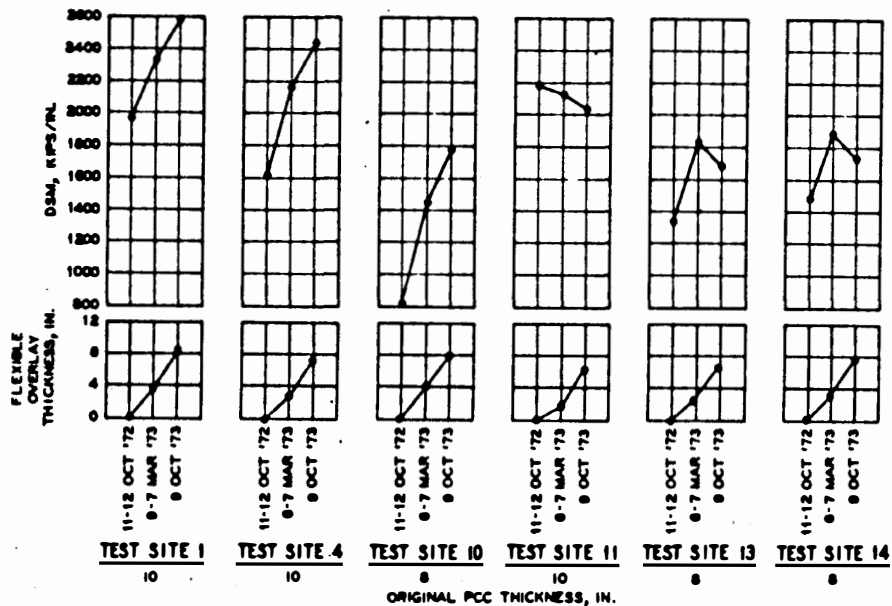


Figure B9. Pavement sections before overlay at Shreveport Regional Airport



NOTE: TEST SITES ARE SHOWN IN PLAN IN FIGURE B0.
 PAVEMENT SECTIONS BEFORE OVERLAY ARE SHOWN IN FIGURE B0.
 DATA ARE TABULATED IN TABLE B7.
 DATA WERE OBTAINED WITH 16-KIP VIBRATOR AT A
 FREQUENCY OF 15 Hz.

Figure B10. Flexible overlay thickness and plots of
 DSM versus time for Shreveport Regional Airport

APPENDIX C: EQUIPMENT SPECIFICATIONS

INTRODUCTION

Basically, three types of tests are used to obtain input for non-destructive pavement evaluation: dynamic stiffness modulus (DSM), frequency response, and wave propagation tests. Although the evaluation methodology presented in this report uses only the DSM test, future refinements and expansion of the technology will no doubt require all of the measurements that will be described below. The objective of this appendix is to provide procurement specifications and general operating procedures for nondestructive testing equipment recommended for use in evaluating the load-carrying capacity of airport pavements. The recommended machine will be capable of performing the load-deflection and wave propagation tests used for input to the nondestructive pavement evaluation methodology discussed in the main text of this report. The equipment design provides for rapid testing and quick removal of the machine from the pavement facility for emergency aircraft operations, direct test results for on-site analysis, and mobility for transfer of the equipment to any airport within the United States.

DSM TEST

DSM is the ratio of vibratory load to deflection and is obtained by a sweep of dynamic force at a constant frequency. The DSM is a value representative of the overall strength of the composite pavement structure. Since the mass of pavement affected during a DSM determination is dependent on both the vibrator static weight and the vibratory load, a variable mass (static weight) vibrator is recommended. The size of the vibrator should probably be dictated by the type aircraft for which a pavement is evaluated, and the static weight of the vibrator should be proportional to the gross aircraft weight, although this was not proven in the main text.

FREQUENCY RESPONSE TEST

The frequency response is also developed from load-deflection

data by a sweep of frequency (range of 5 to 100 Hz) at a constant vibratory load. The frequency response shows how a pavement structure reacts to the dynamic force at different frequencies, and may become important in evaluating pavements for different aircraft speeds.

WAVE PROPAGATION TEST

The wave propagation test uses a 50-lb electrodynamic vibrator in conjunction with the larger vibrator to measure the velocity of shear waves propagated through various layers of a pavement structure. The wave velocities are used with elastic theory to compute a dynamic E-modulus, modulus of elasticity, for each pavement layer.

SPECIFICATIONS

A general description of each component of the nondestructive testing (NDT) system is given in the following paragraphs and is followed by a set of specifications for each component.

TRUCK-TRAILER UNIT

The large vibrator, power supplies, and electronic equipment are contained in a semitrailer as shown in Figure C1. The 36-ft semitrailer is towed by a tandem-axle tractor unit. An alternate system in which the generator and hydraulic power supply were mounted on the single unit truck that tows a small four-wheel trailer containing the vibrator was also studied, but there appeared to be no advantage to that system. The semitrailer unit is recommended because it is easier to maneuver over test locations and all equipment is contained in the one trailer, which simplifies maintenance. Specifications will be listed later in this appendix for the tractor-truck unit and a semitrailer suitable for modifying into an NDT trailer.

VIBRATOR UNIT

The vibrator is lowered to the pavement surface, and a steady state vibratory load is generated by the electronically controlled double-action hydraulic piston. The hydraulic piston is oriented with the rod end attached to the load plate on the pavement, and the reaction

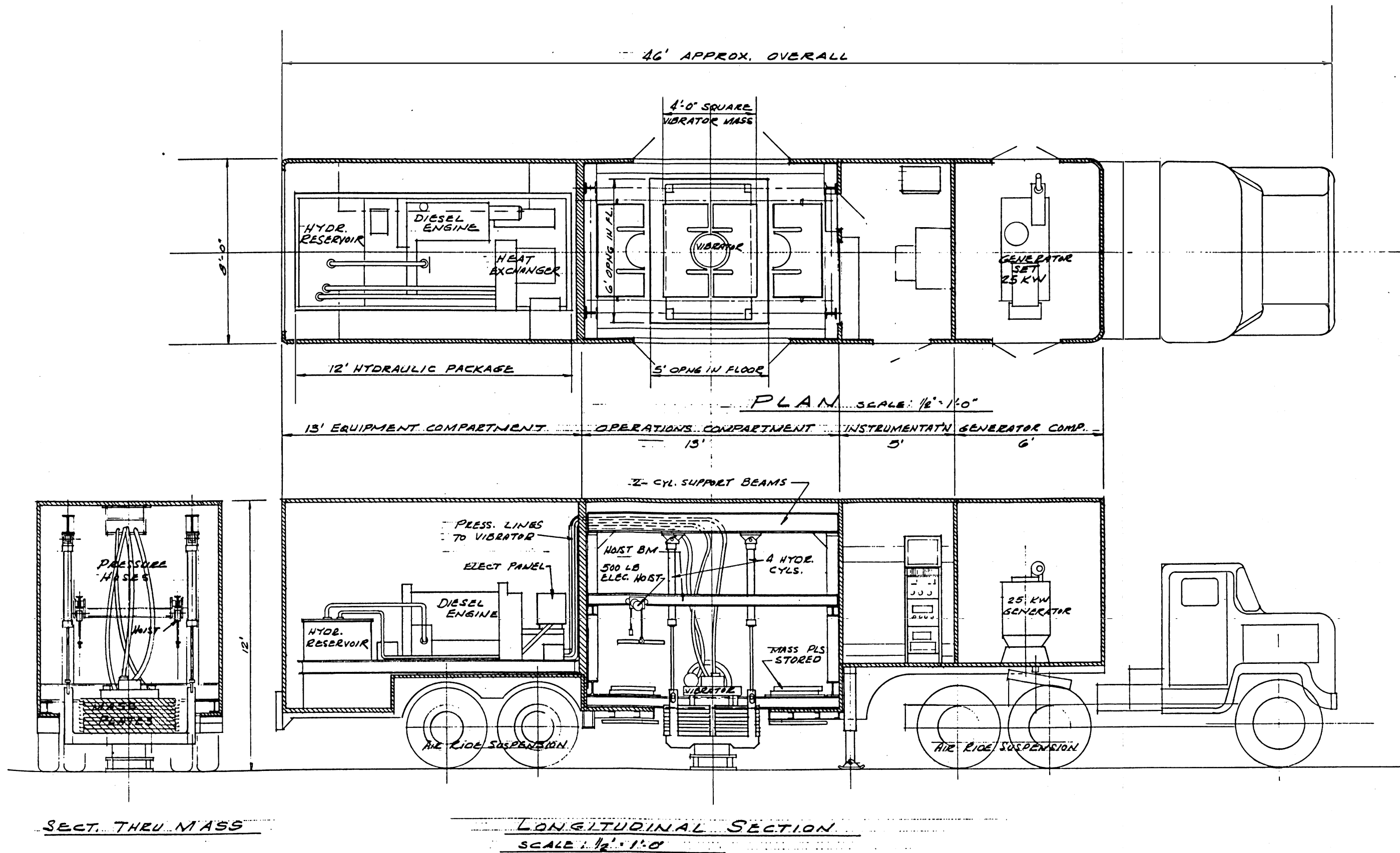


Figure C1. Truck-trailer unit with details of actuator system

mass is mounted to the body of the piston. The reaction mass is oscillated vertically (raised and lowered) at the specified frequency and with a magnitude to produce the desired dynamic force level. Either force or frequency can be held constant while the other quantity is automatically varied at a specified sweep rate.

The fixed static weight of the vibrator being used in the Federal Aviation Administration research study is 16 kips. Results of the study show the DSM to be dependent on the vibrator static weight, vibratory load, and load plate size. The vibrator weight and the vibratory load should probably be determined by the pavement type and the aircraft for which the pavement is to be evaluated. Therefore, the proposed vibrator is one of variable mass and can range from 5 to 16 kips. A "stacked-mass" concept (shown in Figure C1) is used to allow the static weight of the vibrator to be changed easily. The vibrator load plate size can be varied with interchangeable plates of 12, 18, and 30 in. in diameter.

Although the vibrator can be varied from a small unit to a large one, the hydraulic power supply must be designed for the maximum force output. The 38-gpm pump similar to that used with the existing 16-kip vibrator is therefore required. A 25-kw electric generator is recommended to provide ample electric power. These units are specified in detail in this appendix.

INSTRUMENTATION

Load-deflection measurements. The existing data recording package was designed for measuring peak values of vibratory load and deflection at the load plate. The proposed system allows for recording peak values of vibratory load and dynamic deflection, as well as frequency of vibration, on a set of X-Y recorders. Load-deflection data at constant frequency or deflection-frequency data at constant load can be displayed on these recorders, and the test results can be inspected and checked as the field tests are performed. Specifications for the load-deflection instrumentation will be presented subsequently.

- a. DSM. Figure C2 is a block diagram showing the overall sequence of the NDT process using a dynamic load-deflection

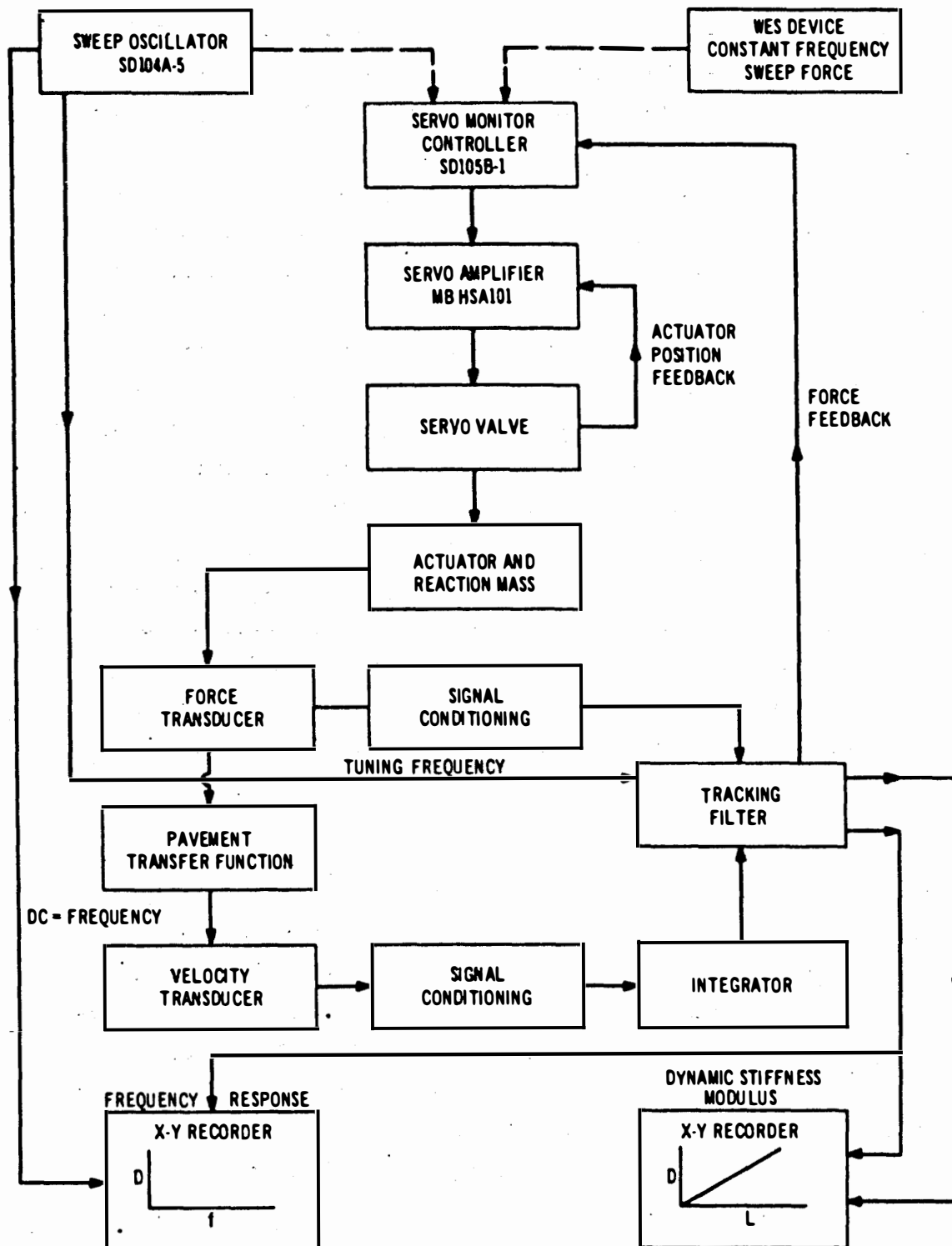


Figure C2. Block diagram of the NDT process using a dynamic load-deflection response

response. A steady state vibratory load is applied to the pavement through an 18-in.-diam steel plate. Three load cells mounted on the plate record the vibratory load and provide feedback for control of the electrohydraulic vibrator. The load cell signals are electronically summed and conditioned for input into the X-Y recorder. A velocity transducer also mounted on the load plate produces a signal that is electronically integrated and input to the plotter. With the vibratory load and deflection connected to the axes of the plotter, the load can be increased at a constant frequency from zero to maximum force and thus provide a load-deflection relationship of a pavement. This load-deflection curve is used to obtain the DSM.

- b. Frequency response. In the second type of dynamic load-deflection test, the vibratory load on the recorder is replaced with the frequency of loading. The frequency is then varied through a range of approximately 5 to 100 Hz while maintaining a constant load magnitude. The results of this second type of test show the pavement response at different rates of loading, and it is therefore termed a frequency response test.
- c. Other measurements. The instrumentation for recording other measurements, such as deflection basin shape and phase difference, can be added to the system in the future if desired. A digital printer or magnetic tape could also be added; one or the other would be needed to record deflection basin shapes.

Wave propagation measurements. In order to determine an E-modulus for individual pavement layers, the velocity of shear waves propagated from steady state vibration is measured. The equipment for performing this test includes a 50-lb electrodynamic vibrator, velocity transducers for monitoring the wave output, a phase meter for measuring the phase change between wave signal peaks, and related amplifiers and filters. A block diagram of the equipment is shown in Figure C3. The electrohydraulic vibrator is used for the vibration source in the low-frequency range (below 500 Hz), which provides velocity data for the subgrade material. The electrodynamic vibrator is used for obtaining velocity data for the other pavement layers, which generally require frequencies to about 3000 Hz for the surface layer. Velocity transducers are used for monitoring the propagated waves up to frequencies of about 600 Hz, above which frequency accelerometers are required. The change in phase

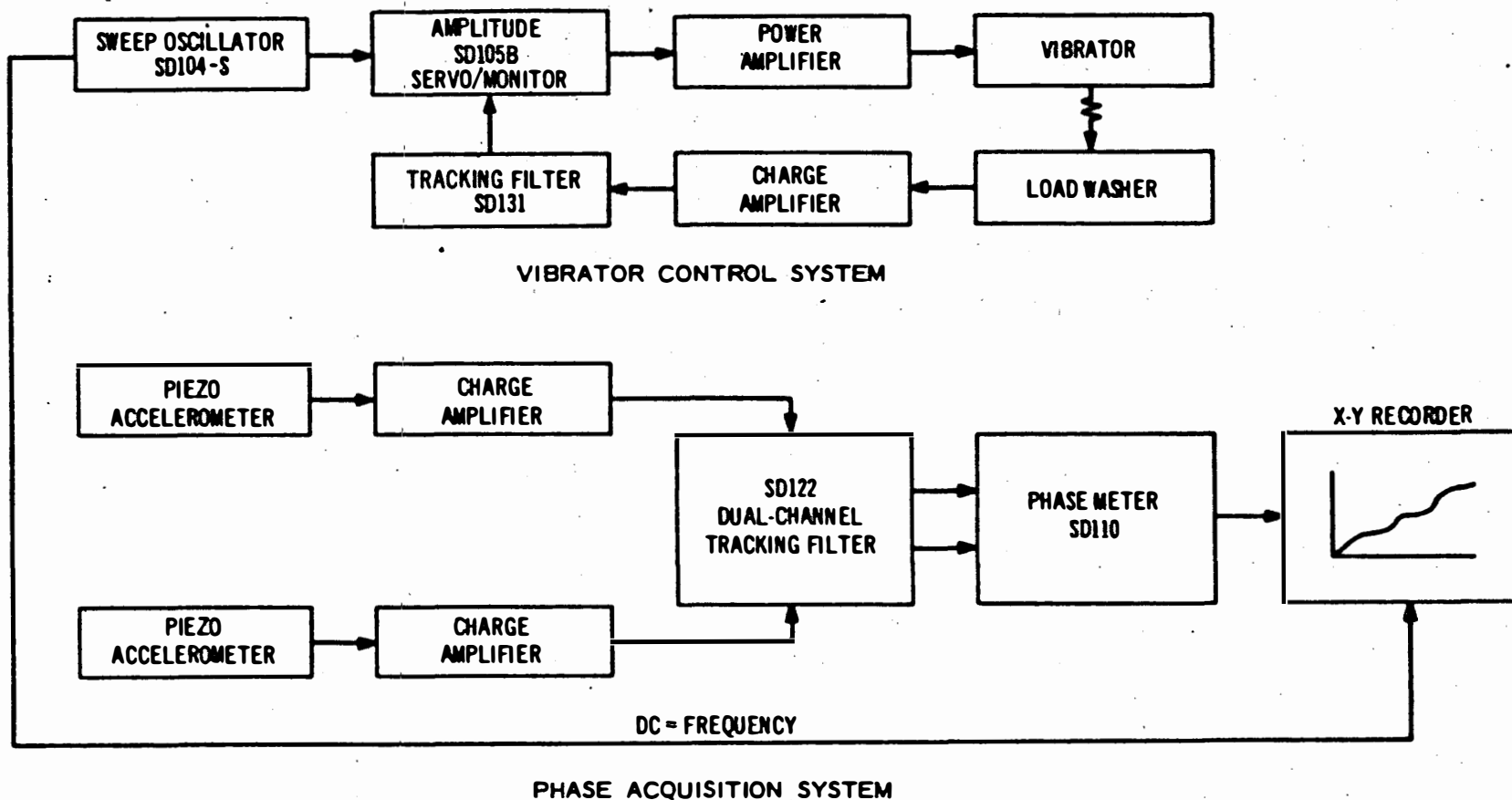


Figure C3. Block diagram of equipment for wave-propagation measurements

with change in frequency is recorded on the X-Y recorder for the full frequency range. With the transducers positioned a known distance apart, the wavelength and therefore the velocity of propagation can be computed for any frequency within the data range. The shear wave velocity can then be used to produce values of shear modulus and elastic modulus using elastic theory. These elastic constants are useful for theoretical analysis of pavements. Specifications for the wave-velocity instrumentation will be presented in this appendix.

ESTIMATED COSTS

Estimation of costs for the construction of an NDT machine such as the one described in this appendix is difficult. The costs of the component parts, especially the electronic components, vary with different suppliers and have been steadily increasing for some time. The estimate given below is within approximately 20 percent error based on 1974 costs.

| Item | Estimated Cost |
|---|----------------|
| Tractor | \$ 25,000.00 |
| Trailer | 8,000.00 |
| Generator (25 kw) | 5,000.00 |
| Vibration unit (electrohydraulic vibrator, power package, and controls) | 50,000.00 |
| Vibrator reaction mass | 10,000.00 |
| Instrumentation packages: | |
| Load-deflection measurements | 40,000.00 |
| Wave velocity measurements | 15,000.00 |
| Labor for assembly of system | 25,000.00 |
| TOTAL | \$178,000.00 |

SPECIFICATIONS FOR TRACTOR-TRUCK UNIT AND SEMITRAILER

TRACTOR-TRUCK UNIT

Cab. The cab shall be of the cab-over-engine type with a hydraulic tilt system. The cab shall be furnished with, but not limited to,

the following: adjustable driver's seat, windshield wiper and washer, padded vinyl upholstery, heater, air horn, seat belts, and all lights required by Federal regulations.

Chassis. The front axle shall be rated at not less than 9,000 lb, and the rear shall be a dual-tandem axle rated at not less than 38,000 lb. The rear axle suspension shall be an air-ride assembly. The wheelbase of the vehicle shall be not greater than 160 in., and the wheels shall be of steel or aluminum with not less than 10:00x20, 12-ply tires. The vehicle shall be fitted with dual fuel tanks with a combined capacity of not less than 80 gal, an emergency air tank, and a fifth wheel assembly.

Engine transmission. The engine shall be not less than a six-cylinder with two- or four-stroke cycle, and shall develop not less than 800 lb-ft of torque at 1200 rpm, and not less than 230-brake horsepower at 2100 rpm. The engine shall be equipped with, but not limited to, an oil bath air cleaner, full-flow oil filter, air compressor, fuel filter, and any other equipment that is standard with the manufacturer. The transmission shall be of the manual type and provide a minimum shift range of 8.5:1, with the lowest gear ratio such that, with an engine speed of 2100 rpm, a road speed of not less than 65 mph will be possible.

Ecological requirements. The noise level shall be less than 86 db when tested in accordance with Federal requirements and shall also meet the recommended inside-cab noise level. Smoke shall not be visible from the exhaust while the engine is in operation, except during the process of shifting gears.

SEMITRAILER UNIT.

The van trailer to be furnished under this specification shall be the product of a manufacturer who is normally engaged in the fabrication of standard trailers. The trailer shall be a tandem-axle, dual-wheel, drop frame capable of carrying a payload of 40,000 lb. It shall have a king pin designed for tow by a tandem-axle truck with a standard fifth wheel. Features not described or specified herein shall be to manufacturer's standard.

The length of the trailer shall be nominal 26 ft from the drop to the rear. Length ahead of the drop shall accommodate a tandem-axle truck and shall not be less than 10 ft.

The height shall not exceed 11 ft 6 in. overall.

The width shall not exceed 8 ft (outside).

The exterior finish shall be smooth aluminum sheet or steel sheet with manufacturer's standard paint application.

The interior shall be unfinished, without insulation.

Flooring shall be wood, tongue and groove, with the bottom surface treated to prevent wood from being soaked by road spray.

The rear door shall be roll-up garage type, maximum opening. Door shall have manufacturer's standard locking device.

Five side doors as shown in the plan view of Figure C1 shall be centered in their respective compartments. The operations compartment shall have a 5-ft double door on each side. The instrumentation compartment shall have a 30-in. door. The generator compartment shall have a 3-ft double door on each side. Height of all doors shall be maximum allowable.

Axles shall be tandem, 18,000-lb minimum rating per axle, and shall have an air-ride suspension.

Brakes shall be air powered, 16-1/2- by 7-in. minimum surface area.

Wheels shall be dual, demountable rims with 10:00x20, 12-ply tires. A spare wheel shall be furnished and stored in a wheel carrier. Mud flaps shall be installed at rear wheels.

The landing gear shall be a two-speed vertical screw type.

Lights and wiring shall be a 12-v system and shall comply with current Interstate Commerce Commission Safety Code. Lights shall include, but not be limited to, turn signals, tail lights, dual stop lights, license light, and clearance and identification lights.

The van trailer shall be weathertight and doors shall have door seals (weatherproofing).

SPECIFICATIONS FOR VIBRATION UNIT AND POWER SUPPLIES

PAVEMENT VIBRATION UNIT

The pavement vibration unit consists of the actuator with servo valve, accumulators, and reaction mass; hydraulic power supply; and electronic controls. The vibration unit described herein shall be capable of producing a maximum vibratory load of 15,000 lb and maintaining the maximum load through a frequency range of 10 to 100 Hz. The unit shall be designed and constructed to perform in an ambient environment of 0 to 120°F and 10 to 90 percent relative humidity. The block diagram of Figure C3 shows the vibration unit control system. A fuel tank shall be provided in the semitrailer to supply diesel fuel to the engines on the hydraulic power package and the generator set for at least one full day's operation.

HYDRODYNAMIC ACTUATOR UNIT

The hydrodynamic actuator shall be a double-acting piston-cylinder device to convert hydraulic energy into a controllable mechanical energy. This unit shall be so designed and constructed as to eliminate any resonances within the operating frequency range. The unit shall be capable of providing a 2-in. double-amplitude stroke through a force range of 0 to 15,000 lb and a frequency range of 5 to 100 Hz with a velocity capability of up to 9 in./sec. The hydraulic actuator shall have an integral manifold with the servo valve and accumulator directly mounted to the manifold as shown in Figure Clb. The actuator shall have a steel baseplate for vertical inverted mounting, 30 in. square and 4 in. thick. The retracted height of the actuator shall be not less than 18 in., and the extended height shall be not greater than 24 in. including the 4-in.-thick baseplate. The actuator rod diameter shall be not less than 5 in. The actuator shall be so designed and constructed as to allow continuous operation throughout the performance spectrum specified and withstand a 5000-lb side load on the rod end. There shall be a d-c-type displacement transducer with an external core positioning adjustment contained in the actuator body. Full-flow 10-μ line

filters shall be provided complete with a remote pressure drop indicator and not less than one change of filter elements. All hydraulic connections between the actuator and power supply shall be of the quick-connect type with all hose ends permanently identified as to their respective ports. All electrical cables and connectors shall be oil- and vibration-resistant with all ends permanently identified.

The servo valve shall be a high-performance single-stage type mounted directly to the actuator as shown in Figure C1 with a minimum amount of plumbing between the actuator ports and the power ports of the servo valve. The servo valve driver assembly shall consist of a permanent magnet assembly and a movable driver coil suspended in an air gap within the magnet structure. The servo valve shall have a moving coil directly coupled to the spool. The valve spool and moving coil shall be located between two helical-wound springs to minimize null drift as specified below. The servo valve shall have the capability of obtaining different flow ratings by interchanging springs. The flow ratings shall have a range from a minimum of not more than 8 gpm to a maximum of not less than 50 gpm at a 2500-psi valve drop and a corresponding 6 gpm to a maximum of 31 gpm at 1000-psi valve drop. The spool shall be flow-compensated to reduce the effect of fluid flow force on the spool. Convenient, externally adjustable hydraulic load damping and null adjustment shall be provided. The servo valve shall be furnished with a d-c-type linear displacement transducer so designed and constructed that no moving parts are in contact with each other. The output of this transducer will be inserted into the servo amplifier in order to stabilize the electro-hydraulic system. The null leakage at 1000 psi shall be not greater than 0.8 gpm. The full-flow frequency range shall be 0 to 500 Hz at the low-flow rating and 0 to 170 Hz at a high-flow range. A 25- μ filter shall be mounted at the input of the servo valve to eliminate foreign matter from entering the chamber. The hysteresis shall not be more than 0.25 percent of the stroke.

An accumulator package with a force stroke rating of not less than 100,000 lb/in. which provides peak system flow requirements and reduction of line-pressure fluctuations shall be supplied with all

necessary hoses and fittings for connection to the servo valve. The accumulator package shall be mounted with the servo valve at the base of the actuator as shown in Figure C1. Figure C1 shows the package at the top of the actuator.

HYDRAULIC POWER PACKAGE

The power package shall be skid-mounted and forced-air cooled and provide sufficient hydraulic energy to drive the actuator unit on a continuous basis for 10-hr intervals at any given set of performance conditions within the specified performance spectrum. Mounted directly to the package for local operation shall be start and stop buttons, reservoir oil temperature gage, oil level sight gage, hydraulic pressure output adjustment with pressure gage, and any other items standard with the manufacturer. Remote controls required are covered in a separate section. The main hydraulic pressure pump shall be driven by a diesel engine with continuous net brake horsepower of not less than 75 at 1800 rpm or greater as required for the performance specified. The main pressure pump shall be a pressure-compensated axial-piston pump with a manually variable displacement and shall be capable of supplying not less than 38 gpm at 3000 psi. The pressure compensator shall be electrically operated with provisions for local and remote adjustment of operating pressure from 500 to 3000 psi with local and remote pressure readout devices at the adjustment stations. There shall be a pressure relief bypass or equivalent device to prevent system pressure from exceeding a 3000-psi maximum operating limit and no adjustable relief device to maintain pressure on return line to prevent cavitation.

The diesel engine, the hydraulic pump, air-cooling system, and hydraulic oil reservoir shall be mounted as one unit and shall be not more than 12 ft. long or 5 ft wide. The oil reservoir shall be at least 100 gal and shall have a low-level shutoff device to shut the system down if the oil level falls below design level, and a thermostatically controlled electric immersion heater(s) of sufficient size to maintain a 40°F oil temperature in a 0°F environment. A thermostatically controlled forced-air cooling system shall be provided to maintain the oil

temperature within allowable limits while the system is operating under full load throughout the ambient temperature range specified. The system shall be provided with controls for starting the engine at a pump pressure of 0 psi.

All hydraulic connections between actuator unit and power package shall be of the quick-connect type and shall be permanently marked to correspond to the proper hose ends. All hydraulic hoses shall be furnished for connecting the components and shall have corresponding quick connections and identification code. All electrical cables and connections shall be oil- and vibration-resistant with ends properly marked.

ELECTRONIC CONTROL UNIT

The control console shall contain all the remote controls necessary for the operation of the vibration system. The control racks in which the equipment is mounted shall contain a rear door, side panels, a louvered top panel, and blank filler panels where no equipment is placed. The console shall contain blowers necessary to cool adequately the equipment mounted in it throughout the 0-120°F range. The console shall have all the input/output connectors and terminals identified to correspond to the proper interconnecting cables to be attached. The console shall have a wiring harness(es) in which all interconnecting cables are routed from one component to other components. The console shall contain, but not be limited to, the following items.

Pump control module. The pump control panel shall include, but not be limited to, the following: a "master off" switch to deenergize the entire control network, a pressure pump "ready" and "on" switch, a pressure "increase" and "decrease" switch with pressure indicator, a low oil level indicator, a high oil temperature indicator, a pressure drop through filter indicator, and a resettable running-time indicator. All switches shall be the illuminated push-button type. The pump controls shall have a built-in interlock system to prevent misoperation of the hydraulic power supply. The power requirements for the control system shall be 95 to 120 v, 60 Hz, single phase.

Servo controller. The servo controller shall contain an electronic amplifier for use in closed-loop control applications. It shall include a main frame with the central electronics, metering, power supplies for internal circuits, and power to drive external transducers that complete the closed-loop system. The controller shall be capable of receiving and controlling two inputs, one of which shall be a feedback voltage (actuator position control) and a command signal. The input sensitivity shall be 0.25 to 10 v RMS. A span shall be on the front panel for adjusting the command signal from 1 to 100 percent of maximum with an accuracy of 0.5 percent. The span control shall be a continuously variable 10-turn potentiometer with a microdial knob. There shall be an input gain control to set the gain of the command signal for proper system calibration. There shall be a feedback control which sets the feedback gain level for the system and shall be the primary calibration between output response and input command level. There shall be a switch to select an input to a panel meter to monitor the input command feedback and power supply levels. There shall be a connector available to monitor continuously the output of the feedback channel. There shall be a control to balance the feedback. This control shall be the primary zero system centering control.

There shall be a switch to calibrate the servo system. This switch shall provide a positive signal peak, a negative signal peak, or the maximum peak of the signal being calibrated at the system comparator. There shall be a switch to select either the input command signal or the feedback, whichever is being calibrated. While the system is in operation, the switch should be in the operate mode. The calibration standard shall be ± 0.5 percent of full scale. The calibration accuracy shall be 1 percent of full scale. The feedback system shall be any type: random, sine, periodic, or mixed.

There shall be a floating d-c power supply for any transducer used in the system. The voltage output of the power supply shall be two fixed values of 10 and 24 v DC, and a continuously variable output of 5 to 25 v DC. A 10-turn potentiometer with a calibrated microdial read-out shall be mounted on the front panel to optimize the closed-loop

system. The span of the adjustment shall be 2 to 102 percent or 50 to 1. A set point control shall be provided to supply a d-c command signal used primarily to set the initial static actuator position. A secondary function of this control is its use in system calibration, at which time it shall provide the primary reference against which all other system signal levels are compared. A toggle switch shall be on the front panel to set the direction in which the set point is applied to the load. There shall be a zero control to trim the servo loop so that changes in gain setting do not cause variations in the set point level. This control shall be used for system zero centering. A limiter control shall be used to hard-clip the error signal amplitude for use as a limit on system frequency response. This control shall be supplied with an uncalibrated looking dial, but shall be used for uncalibrated reference reading only. The feedback selector shall be a switch suitable to select a system feedback signal from either input or both inputs, depending on project requirements. A stability control shall control the gain or slope of the servo loop response at lower levels. At the center, the system response shall be flat, while to the right of center, it shall produce an increase. There shall be a stability gain control to set the range over which the stability control shall be effective for the correction of low-level system nonlinearity. An overload indicator shall provide a visual indication if the maximum signal levels are exceeded. There shall be an illuminated power switch to give an indication that the servo controller is energized from the power line. There shall be an INT CAL switch to provide a cycled d-c square wave command signal corresponding to ± 10 on the SET POINT control in the "0-db" position, and in the "-20-db" position, a similar signal corresponding to ± 1 on the SET POINT control. The repetition frequency of the calibrate signal shall be variable by an internal control.

The output unit shall have a Master Dither control to set the dither level to be used to reduce the effects of spool binding the servo valve. In the full counterclockwise position, the dither level shall be zero. There shall be an internal switch available to select between the internally originating dither and the externally originating dither.

The maximum dither amplitude derived from the internal dither oscillator shall be approximately 50 percent of full scale as indicated on the servo controller. A dither frequency control shall be supplied so that when internally derived dither is selected, the dither frequency control shall provide continuous frequencies from 400 and 2000 cycles. A lock-type phase switch level shall be provided with two positions: plus and minus. This switch, when reversed, shall in turn reverse the current direction applied to the servo valve coil. A three-position range switch shall be supplied to select a full-scale current range from 8 to 40 ma. This switch shall be set to agree with the full-scale range of the servo valve current requirements. A valve balance control shall provide an independent d-c balancing current which shall be used generally to fine-trim any slight mechanical offset which might occur in the valve spool during the time of no signal input conditions. A test switch shall be supplied for setting the valve balance control, which momentarily removes the input signal so that balancing may be conducted on the valve itself free of any other system unbalances. A monitor output connector (BNC type) shall be provided to provide a voltage proportional to the output current level. It shall be short-circuit-proof and shall not be capable of being inadvertently switched.

Sweep oscillator. The control unit shall contain a Spectral Dynamics Model SD 104A-5 sweep oscillator, or equivalent.

Amplitude servo monitor. The control unit shall contain a Spectral Dynamics Model SD 105B-1 servo monitor, or equivalent.

25-kw GENERATOR SET

The generator set shall be powered by a diesel engine that provides sufficient horsepower at 1800 rpm to give the specified performance of the generator set. The engine shall be provided with a 12-v electric starting system and a 12-v negative ground alternator. The engine shall be water cooled and provided with radiator, blower fan, and positive action gear-driven centrifugal water pump for continuous operation in an ambient temperature of 125°F. The engine shall have a hydraulic

governor capable of regulating the voltage within ± 2 percent. The engine shall be lubricated with a gear-driven oil pump and shall have an easy-to-change oil filter that filters particles as small as 15μ . The system shall include an oil cooler that will maintain oil viscosity and lubricating qualities in an ambient temperature of 125°F . The engine shall be supplied with a residential exhaust silencer for minimized noise and shall have the necessary flexible exhaust fittings. The engine shall have an instrument panel consisting of an engine start-and-stop switch, tachometer, water temperature gage, oil pressure gage, and battery-charging ammeter.

The generator shall be a revolving field, a-c generator with built-in, statically regulated, statically excited system and shall conform to National Electrical Manufacturers Association standards. The generator shall provide single-phase, 115-/230-v, 60-Hz power through a wye connection with a continuous rating of not less than 25 kw at 0.80 power factor and shall have a standby rating of not less than 30 kw. The generator shall have provisions to adjust the terminal voltage within ± 5 percent of the rated voltage. The system shall be provided with Class B insulation in the stator and Class F insulation in the rotor. The generator shall be directly connected to the engine crankshaft. A solid-state voltage regulator shall automatically maintain ± 2 percent voltage regulation from no load to full load. A wall-mounted generator control panel equipped with ammeter, voltmeter, frequency meter, phase selector switches, and breakers shall be provided.

SPECIFICATIONS FOR INSTRUMENTATION FOR LOAD-DEFLECTION TESTS

The purpose of the instrumentation package is to measure the response of pavements when subjected to dynamic steady state sinusoidal loading conditions. The various components are shown in the block diagram of Figure C2 and are described below. The specifications given here specify particular models and part numbers. The proposed system should contain these or equivalent components.

FORCE TRANSDUCERS (LOAD CELLS)

The force transducers in the design are BLH Electronics Model U3L1 20,000-lb load cells. This load cell was selected because of its high natural frequency, physical height, low deflection, and high accuracy under application of side and eccentric loads. The strain gage load cell was selected over the crystal type so that a static load could be measured. Weighing the reaction mass is an excellent means to verify the load cell calibration. Three of these load cells spaced 120 deg apart are used to measure the total force of 31,000 lb (static weight of 16,000 lb plus maximum vibratory load of 15,000 lb) in the proposed machine.

The signal conditioning for the load cells includes bridge balance, single shunt calibration, and scale valve (gain) control capabilities. The amplifier frequency response shall be flat from 1 to 1000. All the above capabilities are included on a printed circuit board fabricated at the U. S. Army Engineer Waterways Experiment Station. The Burr-Brown Model 3061/25 instrumentation amplifier is used. An operational amplifier is used to sum the output of the three load cell amplifiers.

VELOCITY TRANSDUCERS

The dynamic deflection of the pavement is sensed with a velocity transducer. The velocity transducer was selected for several reasons, the major reason being that a seismic mass displacement transducer that would measure the maximum anticipated deflection (approximately 0.025 in.) would be unreasonably large and heavy. The velocity transducer shall have a low natural frequency and a high sensitivity to measure extremely small deflections (0.0005 in.) in strong pavement systems. A Mark Product Model L-1-U velocity transducer has a high sensitivity and good natural frequency-size relationship. The size of the velocity transducer is usually inversely proportional to its natural frequency. However, an extremely low natural frequency increases the fragility of the transducer. A 1-Hz velocity transducer could not survive in the environment of the pavement vibration system.

The signal conditioning for the velocity transducer shall have

amplification continuously variable from 10 to 1000 and a means for inserting a sine wave voltage into the input of the amplifier to simulate a known velocity. A printed circuit board employing a Burr-Brown Model 3061/25 amplifier provides these requirements. An operational amplifier integrator printed circuit is used to operate between 2 and 100 Hz and to convert velocity to deflection.

DATA RECORDER

An X-Y recorder is used to plot a load versus deflection or frequency versus deflection curve. A rack-mounted Hewlett Packard Model 135 X-Y recorder was selected because the electrostatic paper hold-down is a favorable feature for field work.

Equipment for the constant frequency with load variation capability is a simple circuit consisting of a multiplier, an integrator, and an oscillator, which were designed and used. The sine wave input from the oscillator is connected to the X-input of the multiplier. The output of the integrator is attached to the Y-input of the multiplier. The sine wave voltage is held constant in both amplitude and frequency.

The load variations are controlled by changing inputs and parameters of the integrator circuit. With proper controls the force can be made to increase, hold, decrease, or reset to zero.

SPECIFICATIONS

The instrumentation for the load-deflection tests shall conform to the following specifications:

I. Force transducer

| | |
|--|-----------------|
| A. Full scale | 20,000 lb |
| B. Performance: | |
| 1. Rated output (RO) | 3 mv/v |
| 2. Calibration accuracy in compression | 0.25 percent RO |
| 3. Nonlinearity | 0.10 percent RO |
| 4. Hysteresis | 0.10 percent RO |
| 5. Repeatability | 0.02 percent RO |

| | |
|---|---|
| 6. Creep | 0.05 percent RO |
| 7. Output variance between tension and compression load | 0.30 percent RO |
| C. Electrical: | |
| 1. Excitation, recommended maximum | 12-v AC or DC |
| 2. Zero balance | 1.0 percent RO |
| 3. Terminal resistance: | |
| a. Input | 350 \pm 5 ohms |
| b. Output | 350 \pm 3.5 ohms |
| 4. Electrical connections | Bendix connector (PC 02C-12-100) |
| 5. One bridge | |
| 6. Insulation resistance: | |
| a. Bridge to ground | 5 \times 10 ⁹ ohms |
| b. Shield to ground | 2 \times 10 ⁹ ohms |
| D. Temperature: | |
| 1. Range: | |
| a. Compensated | +15 to 115°F |
| b. Safe | -65 to 200°F |
| 2. Effect on span | 0.0025 %/°F |
| 3. Effect on zero balance | 0.0025 %/°F |
| E. Overload and adverse load ratings: | |
| 1. Safe overload | 150 percent rated capacity |
| 2. Ultimate overload | 300 percent rated capacity |
| 3. Maximum side load without damage | 100 percent axial load capacity |
| 4. Maximum bending moment without damage | 50 percent axial load capacity in inch-pounds |
| 5. Maximum torque applied to center thread without damage | 30 percent axial load capacity in inch-pounds |

6. Fatigue rating:
 - a. 3-mv/v full-scale capacity 1×10^6 cycles
 - b. 1.5-mv/v full-scale capacity 1×10^8 cycles
- F. Natural frequency Greater than 5 kHz
- G. Deflection at rated capacity 2×10^{-3} to 5×10^{-3} in.
- H. Dimensions:
 1. Height, maximum 2 in.
 2. Maximum horizontal dimension 5-9/16 in.
 3. Mounting bolt 3/8-16
 4. Center bolt 1-14 NF-2

II. Signal conditioning (load cells)

- A. Power supply:
 1. Amplifier power supply, dual output ± 15 -v DC at 1.4 amp
 2. Bridge excitation, dual output 5 v at 2.7 amp
 3. Regulation:
 - a. Line $0.01\% + 1$ mv
 - b. Load $0.01\% + 1$ mv
 - c. Ripple and noise 250 μ v
 - d. Remote program resistance 1000 ohms, v, nominal
 - e. Remote program voltage Volt/volt
 - f. Temperature coefficient $0.01\% + 300 \mu\text{v}/^\circ\text{C}$ with external programming resistor
 $0.015\% + 300 \mu\text{v}/^\circ\text{C}$ with internal programming resistor
 4. a-c input 105- to 132-v AC
 5. Power:
 - a. Amplifier supply 125 w
 - b. Bridge excitation 80 w

- | | |
|---|--|
| 6. Overshoot | No overshoot on power turn-on, turn-off, or power failure |
| 7. Temperature: | |
| a. Operating range | -20 to 71°C |
| b. Storage range | -55 to 85°C |
| 8. Overload protection: | |
| a. Thermal | Thermostat: automatic reset when over-temp condition is eliminated |
| b. Electrical | External overload protection: automatic electronic current-limiting circuit limits the output current to a preset value, thereby providing protection for the load as well as power supply |
| 9. Input and output | On terminal strip at rear of chassis |
| 10. Convection cooled | |
| 11. Current limit: | |
| a. Amplifier supply | 110% of 40-C rating |
| b. Bridge supply | 140% of 40-C rating |
| 12. Physical: | |
| a. Weight: | |
| Amplifier supply | 8 lb |
| Bridge supply | 6 lb |
| b. Size: | |
| Amplifier supply | 4-29/32 by 4-29/32 by 5 in. |
| Bridge supply | 3-3/16 by 3-3/4 by 6-1/2 in. |
| B. <u>Bridge balance.</u> The bridge balance shall be capable of adjusting the output voltage of the bridge to 0 v while the load cell is under a one-half scale load (1.5 mv/v). | |

The potentiometer shall be a film type for stability and continuous operation. The limiting resistor shall be of either wire or metal film construction so that a minimum unbalance will occur with changes in temperature.

- C. Shunt calibration. The load cell bridge should be capable of being single-shunted with five resistors having the following resistance: 320, 160, 80, 40, and 20 kilohms. The resistors shall be connected to a rotary switch in such a manner to be able to simulate both tension and compression loads. The resistors shall be wirewound, with 0.25 percent tolerance and a temperature coefficient of ± 0.00002 ohms/ohm/ $^{\circ}\text{C}$. The wattage rating shall be nominally $1/4$ w.

D. Amplifier:

- | | |
|--|--------------------------------|
| 1. Gain: | Continuous 10 to 1000 |
| a. Nonlinearity at gain = 100 | $\pm 0.02\%$ |
| b. Temperature coef- ficient at gain = 100 | $0.001\%/^{\circ}\text{C}$ |
| 2. Output: | |
| a. Rated voltage | ± 10 v |
| b. Rated output current | ± 10 ma |
| c. Impedance DC -1 kHz | 0.1 ohm |
| 3. Input: | |
| a. Impedance differential | 50 megohms |
| b. Impedance common mode | 10 megohms |
| c. Voltage range | ± 10 v |
| d. Common mode rejection: | |
| at $G = 10$ min | 74 db |
| at $G = 1000$ bal source | 100 db |
| 4. Offsets and noise: | |
| a. Input max | ± 1 mv |
| b. Output $G = 1000$: | |
| vs temperature | ± 3 mv/ $^{\circ}\text{C}$ |

- vs supply ± 50 mv/v
 - vs time ± 10 mv/month
- c. Output $G = 1$:
 - vs temperature ± 20 μ v/ $^{\circ}$ C
 - vs supply ± 200 μ v/v
 - vs time 50 μ v/month
- d. Bias current each input:
 - at 25° C ± 20 na
 - vs temperature ± 1.0 na/ $^{\circ}$ C
- e. Input noise $G = 100$:
 - 0.01 to 10 Hz:
 - Voltage P-P 5 μ v
 - Current P-P 200 Pa
 - 10 Hz to 10 kHz:
 - Voltage RMS 5 μ v
 - Current RMS 50 Pa
- f. Output noise, $G = 1$:
 - Volts, RMS 10 Hz to 10 kHz 8 μ v
- 5. Dynamic response:
 - a. Small signal frequency:
 - For $\pm 1\%$ flatness, minimum 15 kHz
 - For 3-db flatness, minimum 50 kHz
 - b. Settling time to within ± 10 mv of final output 100 μ sec
 - c. Slew rate 1.2 v/ μ sec
 - d. Full power $G = 10$ 20 kHz
- 6. Power requirements:
 - a. Rated voltage ± 15 -v DC
 - b. Voltage range ± 12 - to ± 18 -v DC
 - c. Quiescent supply current, maximum ± 14 ma
- 7. Temperature range:
 - a. Specification 0 to 70° C

III. X-Y recorder

A. Input ranges:

1. 0.5, 1, 5, 10, and 50 mv/in.
2. 0.1, 0.5, 1, 5, and 10 v/in.
3. Continuous vernier between ranges

B. Input:

1. Floating
2. Maximum voltage 500-v DC or AC
3. Polarity reversal switch on front panel
4. Parallel front and rear connectors
5. Resistance, all ranges 1 megohm
6. Common mode:
 - a. 110 db DC
 - b. 90 db at 50 Hz and above

C. Slewing speed:

1. Fast response 30 in./sec
2. Slow response 15 in./sec

D. Acceleration:

1. Y-axis 3000 in./sec²
2. X-axis 2000 in./sec²

E. Accuracy

±0.2 percent full
scale (FS)
(±0.01%/°C)

F. Linearity (terminal based)

±0.1 percent FS

G. Resettability

±0.1 percent FS

H. Overshoot, maximum

1 percent FS

I. Zero set may be placed anywhere on the writing areas or electrically off scale up to one full scale from zero index.

J. Environmental:

1. Temperature operating 0 to 55°C

2. Humidity at 40°C Less than 95 percent

K. Miscellaneous:

1. Writing:

- a. Servo-actuated ink pen
- b. Area, 10 by 15 in.

2. Electrostatic holddown. Vacuum holddown not acceptable. Special paper not required.

3. Electric pen lift

4. Dimensions: 15-3/4 in. high, 19 in. wide,
6-1/2 in. deep

5. Rackmount structure integral with unit

6. Power: 120-v AC ± 10 percent, 50 to 400 Hz
at 175-v AC

7. Weight: 30 lb

IV. Signal conditioning (velocity transducer)

A. Shall use same power supply as load cell amplifiers.

B. Amplifier same type specified in II-D.

C. Calibration:

1. The system shall have a calibration potentiometer where a preselected voltage can be set with a voltmeter to less than 1 percent accuracy. The potentiometer shall be a 20-turn (nominal) film element potentiometer for each channel of signal conditioning. The voltmeter used shall be a John Fluke Model 887AB or equal.

2. The system shall contain a calibration switch (Double-pole, double-throw) which shall switch both the high and low sides of the input amplifier from the transducer to the calibrated potentiometer for the calibration of the system and then back to the velocity transducer for operation.

3. The calibration voltage set is based on the calibration sensitivity (volts/inch/second) of the particular velocity used on that channel. It should be set as accurately as possible because it is the standard for the entire system.

V. Velocity transducer (L-1-U)

- A. Natural frequency ± 0.75 Hz 4.5 Hz
- B. Coil resistance 500 ohms
- C. Output voltage sensitivity 1.5 v/in./sec
(nominal)

| | |
|--|---|
| D. Coil inductance (henries) | 0.127 |
| E. Damping | 0.7 of critical |
| F. Natural frequency change with tilt | Less than 0.25 Hz at 15 deg |
| G. Stroke (travel) | 1/16 in. |
| H. Weight | 22 oz |
| I. Without base | 2-1/2 in. high, 2-7/8 in. in diameter |

VI. Tracking filter, Spectral Dynamics Model SD122

The Spectral Dynamics equipment and X-Y recorders can be used in both the wave velocity measurements and the DSM tests.

.SPECIFICATIONS FOR INSTRUMENTA-
TION FOR WAVE VELOCITY MEASUREMENTS

The vibrator for use in wave velocity determinations shall be an electrodynamic type and shall have a minimum full-scale output of 50-lb force peak and be force-limited at low frequencies by only the displacement of its armature. The vibrator shall be capable of generating a sine wave force over a frequency range of 5 to 10,000 Hz. The vibrator shall be light (weight) enough to be easily moved about by one man.

The control system for the vibrator shall be compatible with the electrohydraulic system used in the load-deflection tests. The control system shall consist of a sweep frequency oscillator, amplitude servo monitor, tracking filter, power amplifier, piezoelectric load washer, and charge amplifier. The oscillator shall generate a sine wave output from 1 to 10,000 Hz at a constant voltage level and a d-c voltage linearly proportional to frequency. The constant sine wave voltage shall drive the amplitude servo monitor. The amplitude servo monitor shall automatically adjust the input to the power amplifier, as corrected by the load washer feedback, to keep the output of the vibrator at a constant load level while the system is being swept through the desired frequency range. This feedback loop is necessary so that damage of the vibrator suspension will not occur at some resonant or antiresonant frequency. The power amplifier shall have a power output large enough

to drive the vibrator to full scale without damage. A piezoelectric accelerometer can be used on a feedback element to keep a constant acceleration, or a piezoelectric load washer can be used as a force control device. The latter is desirable since this would be a protective device for the vibrator, since an electrodynamic vibrator is quite easily destroyed by excessive power applied to its input. The tracking filter in the feedback circuit is there to clean up the feedback signal from the load washer so that only the frequency generated by the oscillator shall be input to the amplitude servo monitor for force control. This reduces the total system noise and adds stability in the system.

The modulated 100-kHz output of two identical channels consisting of accelerometers, charge amplifiers, and tracking filters is applied to the reference and signal input of a phase meter. The tracking filters and phase meter shall be part of a system. This is the only acceptable way to measure the phase angle between two signals where the signal amplitude is subject to radical changes as the frequency is being swept. The modulated 100-kHz output allows the phase meter to see a constant frequency and amplitude. The direct current proportional to phase is inserted into the ordinate of the X-Y recorder and the linear direct current proportional to frequency (from the oscillator) is inserted into the abscissa. The vibrator is preset to vibrate at a given force level and then is swept over the desired frequency range. A plot of phase versus frequency is generated on the X-Y plotter.

The following equipment is suggested for the vibrator and its control system:

| <u>Number Required</u> | <u>Item</u> |
|----------------------------|---|
| 3 | Accelerometer, Edevco Model 2219E |
| 3 | Charge amplifier, Kistler Model 503D |
| 1 | Tracking filter, dual channel, Spectral Dynamics Model SD122 |
| 1 | Phase meter, Spectral Dynamics Model SD110 |
| 1 | X-Y recorder, Hewlett Packard |

(Continued)

Number
Required

Item (Concluded)

| | |
|---|---|
| 1 | Oscillator, Spectral Dynamics Model SD104A-5 |
| 1 | Amplitude servo monitor, Spectral Dynamics Model SD105B |
| 1 | Tracking filter, Spectral Dynamics Model SD131S |
| 1 | Load washer, Kistler Model 901A |
| 1 | Vibrator and amplifier, Ling or MB/Gilmore |

REFERENCES

1. Heukelom, W. and Foster, C. R., "Dynamic Testing of Pavements," Journal, Soil Mechanics and Foundations Division, American Society of Civil Engineers, Vol 86, No. SMI, Part 1, Feb 1960, pp 1-28.
2. Maxwell, A. A., "Nondestructive Testing of Pavements," Miscellaneous Paper No. 4-373, Jan 1960, U. S. Army Engineer Waterways Experiment Station, CE, Vicksburg, Miss.
3. _____, "Non-Destructive Testing of Pavements," Non-Destructive Dynamic Testing of Soils and Highway Pavements, Highway Research Board Bulletin No. 277, pp 30-36, 1960, National Academy of Sciences--National Research Council, Washington, D. C.
4. U. S. Army Engineer Waterways Experiment Station, CE, "Analysis of Data, Non-Destructive Dynamic Soil Tests at AASHO Road Test," Contract Report No. 4-79, Sep 1963, Vicksburg, Miss.; prepared by Eustis Engineering Company under Contract No. DA-22-079-eng-349.
5. _____, "Analysis of Data, Non-Destructive Dynamic Soil Tests, Foss Field, Sioux Falls, South Dakota," Contract Report No. 4-85, Jan 1964, Vicksburg, Miss.; prepared by Eustis Engineering Company under Contract No. DA-22-079-eng-349.
6. Maxwell, A. A. and Joseph, A. H., "Vibratory Study of Stabilized Layers of Pavement in Runway at Randolph Air Force Base," Proceedings, Second International Conference on the Structural Design of Asphalt Pavements, 1967, University of Michigan, Ann Arbor, Mich.
7. Joseph, A. H. and Hall, J. W., Jr., "Deflection-Coverage Relationship for Flexible Pavements," Miscellaneous Paper S-71-18, Jun 1971, U. S. Army Engineer Waterways Experiment Station, CE, Vicksburg, Miss.
8. Sherman, G. B. and Hannon, J. B., "Overlay Design Under Deflections," paper presented at Western Summer Meeting of the Highway Research Board, Aug 1970.
9. Lister, N. W., "Deflection Criteria for Flexible Pavements," TRRL Report RRL 375, 1972, Transport and Road Research Laboratory, Crowthorne, Berkshire, England.
10. Hall, J. W., Jr., "Nondestructive Testing of Flexible Pavements - A Literature Review," Technical Report No. AFWL-TR-68-147, May 1970, Air Force Weapons Laboratory, Kirtland Air Force Base, N. Mex.
11. _____, "Nondestructive Testing of Pavements; Tests on Multiple-Wheel Heavy Gear Load Sections at Eglin and Hurlburt Airfields," Technical Report No. AFWL-TR-71-64, Mar 1972, Air Force Weapons Laboratory, Albuquerque, N. Mex.
12. _____, "Nondestructive Testing of Pavements; Final Test Results and Evaluation Procedure," Technical Report No. AFWL-TR-72-151, Jun 1973, Air Force Weapons Laboratory, Albuquerque, N. Mex.

13. U. S. Army Engineer Waterways Experiment Station, CE, "Flexible Pavement Behavior Studies," Interim Report 2, May 1947, Vicksburg, Miss.
14. U. S. Army Engineer District, Sacramento, "Accelerated Traffic Test at Stockton Airfield, Stockton, California (Stockton Test No. 2)," May 1948, Sacramento, Calif.
15. U. S. Army Engineer Waterways Experiment Station, CE, "Collection of Letter Reports on Flexible Pavement Design Curves," Miscellaneous Paper No. 4-61, Jun 1951, Vicksburg, Miss.
16. _____, "Design of Flexible Airfield Pavements for Multiple-Wheel Landing Gear Assemblies; Analysis of Existing Data," Technical Memorandum No. 3-349, Report 2, Jun 1955, Vicksburg, Miss.
17. _____, "Mathematical Expression of the CBR Relations," Technical Report No. 3-441, Nov 1956, Vicksburg, Miss.
18. _____, "Combined CBR Criteria," Technical Report No. 3-495, Mar 1959, Vicksburg, Miss.
19. _____, "Developing a Set of CBR Design Curves," Instruction Report No. 4, Nov 1959, Vicksburg, Miss.
20. Cooksey, D. L. and Ladd, D. M., "Pavement Design for Various Levels of Traffic Volume," Technical Report AFWL-TR-70-133, Mar 1971, Air Force Weapons Laboratory, Albuquerque, N. Mex.
21. Hammitt, G. M., II, et al., "Multiple-Wheel Heavy Gear Load Pavement Tests; Analysis of Behavior Under Traffic," Technical Report S-71-17, Vol IV, Nov 1971, U. S. Army Engineer Waterways Experiment Station, CE, Vicksburg, Miss.
22. Westergaard, H. M., "Stresses in Concrete Pavements Computed by Theoretical Analyses," Public Roads, Vol 7, No. 2, Apr 1926, pp 25-35.
23. _____, "Analytical Tools for Judging Results of Structural Tests of Concrete Pavements," Public Roads, Vol 14, No. 10, Dec 1933, pp 185-188.
24. _____, "Stresses in Concrete Runways of Airports," Proceedings, Highway Research Board, Vol 19, Dec 1939, pp 197-202.
25. _____, "Stress Concentrations in Plates Loaded Over Small Areas," Transactions, American Society of Civil Engineers, Vol 108, No. 2197, 1943, pp 831-856.
26. U. S. Army Engineer District, Cincinnati, "Wright Field Slab Tests," May 1942, Cincinnati Testing Laboratories, Cincinnati, Ohio.
27. U. S. Army Engineer Division, Ohio River, "Final Report on the Dynamic Loading of Concrete Test Slabs--Wright Field Slab Tests," Aug 1943, Ohio River Division Laboratories, Rigid Pavement Laboratory, Mariemont, Ohio.

28. Phillippe, R. R., "Structural Behavior of Concrete Airfields Pavements, the Test Program," Proceedings, Highway Research Board, Vol 25, Dec 1944, pp 129-146.
29. U. S. Army Engineer Division, Ohio River, "Lockbourne No. 1; Test Track, Final Report, Mar 1946, Ohio River Division Laboratories, Mariemont, Ohio.
30. Westergaard, H. M., "New Formulas for Stresses in Concrete Pavements of Airfields," Transactions, American Society of Civil Engineers, Vol 113, No. 2340, 1948, pp 425-444.
31. U. S. Army Engineer Division, Ohio River, "Final Report, Lockbourne No. 2; Modification, Multiple-Wheel Study," Jun 1950, Ohio River Division Laboratories, Rigid Pavement Laboratory, Mariemont, Ohio.
32. Pickett, G. and Ray, G. K., "Influence Charts for Concrete Pavements," Transactions, American Society of Civil Engineers, Vol 116, No. 2425, 1951, pp 49-73.
33. Pickett, G., et al., "Deflections, Moments, and Reactive Pressures for Concrete Pavements," Bulletin No. 65, Oct 1951, Kansas State College, Manhattan, Kansas.
34. Mellinger, F. M. and Phillippe, R. R., "Structural Behavior of Heavy-Duty Concrete Airfield Pavements," Proceedings, Highway Research Board, Vol 33, Jan 1952, pp 87-100.
35. U. S. Army Engineer Division, Ohio River, "A Model Study of the Effect of High-Contact Pressures on Stresses in Rigid Pavements," Oct 1954, Ohio River Division Laboratories, Rigid Pavement Laboratory, Mariemont, Ohio.
36. Behrmann, R. M. and Carlton, P. F., "A Model Study of Rigid Pavement Behavior Under Corner and Edge Loadings," Proceedings, Highway Research Board, Vol 35, Jan 1956, pp 139-146.
37. U. S. Army Engineer Waterways Experiment Station, CE, "Study of Channelized Traffic," Technical Memorandum No. 3-426, Feb 1956, Vicksburg, Miss.
38. Mellinger, F. M., Sale, J. P., and Wathen, T. R., "Heavy Wheel Load Traffic on Concrete Airfield Pavements," Proceedings, Highway Research Board, 1957.
39. U. S. Army Engineer Division, Ohio River, "A Model Study of the Load-Distributing Characteristics of Twin, Twin-Tandem, and Twin-Twin Gear Configurations for Rigid Pavements," Technical Report 4-8, Oct 1958, Ohio River Division Laboratories, Rigid Pavement Laboratories, Mariemont, Ohio.
40. Hutchinson, R. L., "A Method of Estimating the Life of Rigid Airfield Pavements," Technical Report 4-23, Mar 1962, U. S. Army Engineer Division, Ohio River, Ohio River Division Laboratories, Cincinnati, Ohio.

41. Weiss, R. A., "Nondestructive Vibratory Testing of Airport Pavements, Theoretical Study of the Dynamic Stiffness and Its Application to the Vibratory Nondestructive Method of Testing Pavements," Report No. FAA-RD-73-205-II, Vol II (in preparation), Federal Aviation Administration, Washington, D. C.
42. U. S. Federal Aviation Administration, "Airport Pavement Design and Evaluation," Advisory Circular AC 150/5320-6B, 28 Mar 1974, Department of Transportation, Washington, D. C.
43. Office, Chief of Engineers, Department of the Army, "Unified Soil Classification System for Roads, Airfields, Embankments, and Foundations," Military Standard MIL-STD-619B, 12 Jun 1968, Washington, D. C.
44. Geswein, A. J. and Rice, J. L., "Nondestructive Testing of Concrete Pavements: Equipment Evaluation," Technical Report S-12, Jan 1973, U. S. Army Construction Engineering Research Laboratory, CE, Champaign, Ill.
45. Hall, J. W., Jr., and Elsea, D. R., "Small Aperture Testing for Airfield Pavement Evaluation," Miscellaneous Paper S-74-3, Feb 1974, U. S. Army Engineer Waterways Experiment Station, CE, Vicksburg, Miss.
46. The Asphalt Institute, "Asphalt Overlays and Pavement Rehabilitation," Manual Series No. 17, Nov 1969, College Park, Md.
47. Brown, D. N. and Thompson, O. O., "Lateral Distribution of Aircraft Traffic," Miscellaneous Paper S-73-56, Jul 1973, U. S. Army Engineer Waterways Experiment Station, CE, Vicksburg, Miss.
48. Hammitt, G. M., II, Barber, W. R., and Rone, C. L., "Comparative Performance of Structural Layers in Pavement Systems; Analysis of Test Section Data and Presentation of Design and Construction Procedures," Report No. FAA-RD-73-198, Vol II (in preparation), Federal Aviation Administration, Washington, D. C.
49. U. S. Federal Aviation Administration, "Standard Specifications for Construction of Airports," AC 150/5370-1, May 1968, Department of Transportation, Washington, D. C.
50. Packard, R. G., "Design of Concrete Airport Pavement," Engineering Bulletin, 1973, Portland Cement Association, Skokie, Ill.
51. Sadar, D. J. and Strange, J. N., "Basic Statistical Definitions and Procedures," Miscellaneous Paper No. 2-250, Jan 1958, U. S. Army Engineer Waterways Experiment Station, CE, Vicksburg, Miss.
52. The Asphalt Institute, "Asphalt Technology and Construction, Instructor's Guide," Educational Series No. 1, 1971, College Park, Md.
53. Hveem, F. N., "Pavement Deflections and Fatigue Failures," Design and Testing of Flexible Pavement, Bulletin No. 114, pp 43-73, 1955, Highway Research Board, National Academy of Sciences--National Research Council, Washington, D. C.